

# **A Study on Nucleic Acids with Metal-Mediated Base Pairs**

DISSERTATION

zur

Erlangung der naturwissenschaftlichen Doktorwürde

(Dr. sc. nat.)

vorgelegt der

Mathematisch-naturwissenschaftlichen Fakultät

der

Universität Zürich

von

Silke Johannsen

aus

Deutschland

Promotionskomitee

Prof. Dr. Roland K. O. Sigel (Vorsitz, Leitung der Dissertation)

Prof. Dr. Heinz Berke

Prof. Dr. Jens Müller

Zürich 2010



*Where Nature finishes producing its own species,  
man begins, using natural things and with the help of this  
nature, to create an infinity of species.*

Leonardo da Vinci

Für Martin, Sebastian und Merle





My very special thanks go to my Ph.D. advisor

Prof. Dr. Roland K. O. Sigel

for giving me the opportunity to work on this interdisciplinary and fascinating project, for continuous support, endless enthusiasm and the manifold scientific advice over the last years. Thank you so much for your kindness to arrange the Ph.D. work with the beautiful task to be a mom.

and to the members of my PhD committee

Prof. Dr. Heinz Berke from the University of Zürich  
for kindly acting as referee.

and

Prof. Dr. Jens Müller from the Westfälische Wilhelms-Universität Münster  
for the fruitful collaboration on the synthetic part of my project.

I would like to thank all the people who supported me during my Ph.D. time in Zürich:

Thanks to all past and present members of the SF-group for the nice atmosphere and daily support. Special thanks go to SUSANN PAULUS for all the technical advises, the production of the *T7* polymerase and all the other things that have to be done to keep the lab running. My labmates CINZIA FINAZZO, MARIA PECHLANER, DANIELA DONGHI as well as BERND KNOBLOCH, who joined me in the office for some time, for a wonderful atmosphere with great scientific and personal discussions. DANIELA DONGHI, MICHÈLE ERAT, CINZIA FINAZZO, MAXIMILANE KORTH, DANIELA KRUSCHEL, MARIA PECHLANER, and VERONIKA ZELENAY for their help and support within the NMR subgroup of the Sigel lab. BERND KNOBLOCH, the SF-brain, for the help with the potentiometric titrations and numerous discussions about everything. Now we know the story about Pandora's box! My project students STEFAN MARKOVIC and MARCO FETZ for their efforts and a lot of fun. Professor Dr. EVA FREISINGER for great help with the DLS and sharing the experience to be a mom. DANIELA KRUSCHEL and SUSANN PAULUS for their friendship and support in all areas of my life. AUGUSTO DOS SANTOS CABRAL, PALLAVI CHOUDRY and JOACHIM SCHNABL for good discussions and fun during the breaks.

The group of Prof. Dr. JENS MÜLLER from the Westfälische Wilhelms-Universität for clean and high yield oligonucleotide samples, especially DOMINIK BÖHME, NICOLE MEGGER, DOMINIK MEGGER and KRISTOF SEUBERT. Special thanks go to NICOLE MEGGER for a nice time during her two stays in Zürich and her continuous enthusiasm to prepare good samples.

The group of Prof. Dr. LARS B. HEMMINGSEN from the University of Copenhagen for the PAC-measurements. In particular, HANS WERNER, MARIANNE, MONIKA, PETER and SØREN for a nice week in CERN with lot of fun during the long breaks while waiting for the beam line.

Prof. Dr. OLIVER ZERBE and the NMR team NADJA BROSS and SIMON JURT, as well as THOMAS FOX for setting up and running the NMR facilities, for all the help, tips and tricks. Special thanks go to HELENA KOVACS from Bruker Biospin for showing us the NMR world from the technical side and for a lot of help.

All members of the Institute of Inorganic Chemistry at the University of Zürich, especially NATHALIE FICHTER, SUSANNA SPROKKEREERF, PATRIZIA ALLEGRO, BEATRICE SPICHTIG and TANJA SPÖRRI for administrative services. MANFRED JÖHRI, MARIA PECHLANER, JOACHIM SCHNABL, BERNHARD SPINGLER and THORSTEN STEENBOCK for computer and software support. Prof. Dr. HELMUT SIGEL for his huge support in the evaluation of the potentiometric data and the NMR chemical shift change data. I learned a lot and I was strongly impressed by your precise working style.

Special thanks go to SOFIA GALLO, MAXIMILANE KORTH, SUSANN PAULUS, and my parents for carefully reading and correcting my thesis.

Finally, I would like to thank my family and friends who supported me outside the lab. My volleyball team VBC Kanti Oerlikon for a lot of fun and sharing my love for volleyball. DANIELA, IRIS, JULIANE, MIRIAM, MONI, SUSANN, and YVETTE, thanks for being my friends. My parents and my brother KRISTOF for their continuous love and support. Last but not least I thank MARTIN and SEBASTIAN, my big and my little sunshine, for making me laugh every day. Without you this work would not have been possible.



# Content

<b>List of Abbreviations .....</b>	<b>V</b>
<b>1 Introduction .....</b>	<b>1</b>
<b>1.1 Nucleic acids – highly versatile building blocks .....</b>	<b>1</b>
1.1.1 Basic structural features of nucleic acids.....	1
1.1.2 Modifications of nucleic acids.....	4
1.1.2.1 Metal-mediated base pairs .....	5
1.1.3 Electron transfer in nucleic acids.....	6
<b>1.2 Nuclear magnetic resonance (NMR) spectroscopy of nucleic acids .....</b>	<b>8</b>
1.2.1 Determination of nucleic acid structures by NMR.....	8
1.2.2 Exploring metal ion coordination by NMR.....	11
<b>1.3 Thesis outline .....</b>	<b>13</b>
<b>2 <i>In vitro</i> construction of nucleic acids as scaffolds for one-dimensional arrays of mercuric ions.....</b>	<b>15</b>
<b>2.1 Introduction .....</b>	<b>15</b>
<b>2.2 Results and discussion.....</b>	<b>18</b>
2.2.1 Formation of consecutive uracil-mercury-uracil base pairs .....	18
2.2.1.1 <i>In vitro</i> transcription of RNA with long stretches of uracil residues .....	18
2.2.1.2 NMR-spectroscopic characterization of the transition to Hg <sup>2+</sup> -based molecular RNA wire .....	20
2.2.1.3 Determination of the hydrodynamic radii .....	25
2.2.1.4 UV-VIS and CD spectra of the transition to Hg <sup>2+</sup> -modified RNA duplexes .....	28
2.2.2 Incorporation of thymine instead of uracil into RNA sequences .....	31
2.2.2.1 Wild-type <i>T7</i> RNA polymerase discriminates deoxyribonucleotides.....	31
2.2.2.2 Incorporation of up to 20 consecutive dTTPs into RNA using a double mutant <i>T7</i> polymerase .....	35
2.2.2.3 Spectroscopic characterization of PM01(T) and PM03(T).....	36
2.2.3 Using <sup>199m</sup> Hg PAC spectroscopy to investigate Hg <sup>2+</sup> binding of nucleic acids	38
2.2.3.1 <sup>199m</sup> Hg perturbed angular correlation (PAC) spectroscopy .....	38
2.2.3.2 For the first time <sup>199m</sup> Hg PAC spectroscopy is applied on nucleic acids....	39
<b>2.3 Conclusions and outlook.....</b>	<b>43</b>

<b>3</b>	<b>Using artificial imidazole nucleobases to construct consecutive metal-mediated base pairs in DNA .....</b>	<b>45</b>
<b>3.1</b>	<b>Introduction .....</b>	<b>45</b>
<b>3.2</b>	<b>Results and discussion.....</b>	<b>47</b>
3.2.1	The 1-(2'-Deoxy- $\beta$ -D-ribofuranosyl)imidazole 5'-monophosphate (dImMP <sup>2-</sup> )	47
3.2.1.1	Potentiometric pH Titrations of H <sub>2</sub> (dImMP) <sup>±</sup> .....	47
3.2.1.2	Microconstant Scheme for H <sub>2</sub> (dImMP) <sup>±</sup> .....	51
3.2.1.3	<sup>31</sup> P-NMR shift studies of dImMP <sup>2-</sup> .....	54
3.2.1.4	<sup>1</sup> H-NMR shift studies of dImMP <sup>2-</sup> .....	56
3.2.2	The hairpin structure of an oligonucleotide containing artificial imidazole nucleobases is strongly influenced by pH .....	60
3.2.2.1	The modified DNA adopts a hairpin in solution.....	60
3.2.2.2	<sup>1</sup> H NMR shift experiments.....	63
3.2.2.3	Spectral features of the hairpin at different pH conditions .....	67
3.2.2.4	The structure of the hairpins at pD 4.7 and pD 10.2 .....	69
3.2.2.5	The loop conformation is dependent on pH.....	72
3.2.3	Structure conversion from hairpin to duplex upon addition of silver(I) ions ...	75
3.2.3.1	The oligonucleotide adopts a duplex structure in the presence of silver(I)	75
3.2.3.2	Silver(I)-mediated base pairs are formed in the DNA double helix .....	76
3.2.3.3	Solution structure of the DNA double helix .....	80
<b>3.3</b>	<b>Conclusion and outlook .....</b>	<b>86</b>
<b>4</b>	<b>Materials and methods.....</b>	<b>89</b>
<b>4.1</b>	<b>Materials and chemicals .....</b>	<b>89</b>
<b>4.2</b>	<b>Instrumentation .....</b>	<b>90</b>
<b>4.3</b>	<b>Methods chapter 2 .....</b>	<b>91</b>
4.3.1	Sample preparation .....	91
4.3.2	NMR spectroscopy .....	93
4.3.3	UV melting studies .....	94
4.3.4	Circular dichroism .....	95
4.3.5	Dynamic light scattering.....	95
4.3.6	Perturbed angular correlation of gamma rays (PAC) .....	95
<b>4.4</b>	<b>Methods chapter 3 .....</b>	<b>97</b>
4.4.1	Sample preparation .....	97

4.4.2	NMR spectroscopy .....	97
4.4.3	Structure calculation .....	98
4.4.3.1	Insertion of new residues in the parameter and topology files .....	98
4.4.3.2	Structure calculation of the hairpin .....	101
4.4.3.3	Structure calculation of the duplex .....	102
4.4.3.4	Visualisation and analysis of the structures .....	102
4.4.4	Determination of the acidity constants of $\text{H}_2(\text{ImMP})^\pm$ with potentiometric pH titrations .....	103
4.4.5	Dynamic light scattering .....	103
<b>5</b>	<b>Summary .....</b>	<b>105</b>
<b>6</b>	<b>Zusammenfassung .....</b>	<b>113</b>
<b>7</b>	<b>Appendices .....</b>	<b>121</b>
<b>8</b>	<b>Literature.....</b>	<b>193</b>
	<b>Curriculum Vitae.....</b>	<b>203</b>





# List of Abbreviations

A	adenine
C	cytosine
CD	circular dichroism
DLS	dynamic light scattering
dNTP	deoxyribonucleoside 5'-triphosphate
DOSY	diffusion ordered spectroscopy
DTT	(2 <i>S</i> ,3 <i>S</i> )-1,4-bis-sulfanylbuthane-2,3-diol
G	guanine
GNA	glycol nucleic acid
HSQC	heteronuclear single quantum coherence
INEPT	insensitive nuclei enhancement by polarisation transfer
MOPS	[3-( <i>N</i> -morpholino)propane-sulfonic acid]
NMR	nuclear magnetic resonance
NOE	nuclear overhauser effect
NOESY	nuclear overhauser effect spectroscopy
NTP	ribonucleoside 5'-triphosphate
PAGE	polyacrylamide gel electrophoresis
PNA	peptide nucleic acid
ppm	parts per million
r.m.s.d.	root-mean-square deviation
dNTP	nucleoside 5'-triphosphate
sw	sweep width
T	thymine
TOCSY	total correlation spectroscopy
tris	2-amino-2-hydroxymethyl-propane-1,3-diol
U	uracil
wt	wildtype



# 1 Introduction

## 1.1 Nucleic acids – highly versatile building blocks

Small ... smaller ... smallest

In the world of electronics everything is oriented to increase the speed and complexity of electronic devices by becoming smaller and smaller, because smaller size means cheaper cost and better performance. Nowadays, the task of miniaturization derived from the famous dictum known as Moore's law – the doubling of transistor density on integrated circuits every 18-24 month<sup>[1]</sup> can hardly be achieved by conventional “top-down” approaches such as photolithography. Hence, the “bottom-up” technology, a fundamentally different approach, is a promising way to produce nanometer-sized electronic devices. In this approach small molecular building blocks are arranged into more complex elements due to their self-assembling properties.<sup>[2]</sup> Biomolecules, and in particular nucleic acids, possess such superb self-assembly features that have been optimized by evolution over billions of years. Therefore nucleic acids are of great interest for the application as nanomaterial.

### 1.1.1 Basic structural features of nucleic acids

The basic repeating motif in DNA (deoxyribonucleic acid) is the nucleotide that consists of three components: a nitrogenous heterocyclic base, which is either a purine (adenine (A) or guanine (G)) or a pyrimidine (cytosine (C) or thymine (T)), a deoxyribose sugar, and a phosphate group (Figure 1-1). RNA (ribonucleic acid) is a structural analog of DNA, but differs in that it incorporates an unmethylated form of thymine called uracil (U) as a building block and has an additional 2'-hydroxyl group on the sugar subunit (Figure 1-1). To generate oligonucleotides, DNA and RNA polymerases have evolved, that catalyze the polymerization reaction of single nucleoside triphosphates upon release of pyrophosphate (PP<sub>i</sub>) (see also Section 2.2.2). Nowadays, the synthesis of oligonucleotides by both chemical and biochemical methods is well-established, allowing easy access to reasonable amounts of short and long oligonucleotides with defined length and sequence for biochemical, chemical, and physical studies.

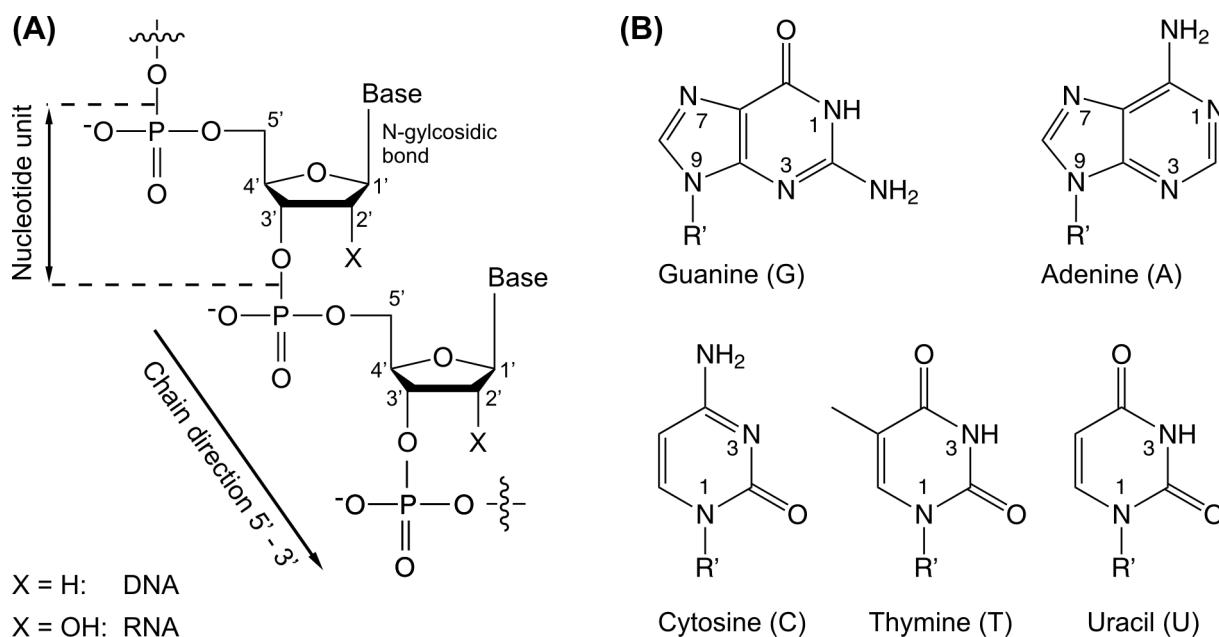


**Figure 1-1** General structure of nucleic acids. **(A)** Section of a DNA (Y = H) or a RNA (Y = OH) strand, respectively. The individual nucleotides are linked by 3', 5'-phosphodiester bonds. **(B)** Chemical structure of the nucleobases guanine, adenine, cytosine, thymine (only present in DNA), and uracil (only present in RNA) including the numbering scheme.

One special feature of nucleic acids is to form hydrogen bonds between the bases which are essential for information storage and retrieval in organisms. Certainly the canonical Watson-Crick base pairs between guanine and cytosine as well as adenine and thymine (only present in DNA) or adenine and uracil (only present in RNA) are the most famous and by far the most abundant ones (Figure 1-2).<sup>[3]</sup> Besides, in RNA, also other base pairing schemes like the GU wobble or the (reverse) Hoogsteen base pairs are found regularly and are important for the formation of complex three dimensional structures. Hydrogen bonding increases the stability of the macromolecules and generates double strands of paired nucleotides, in which the sequence of one strand implies the complementary sequence of the opposite one. DNA

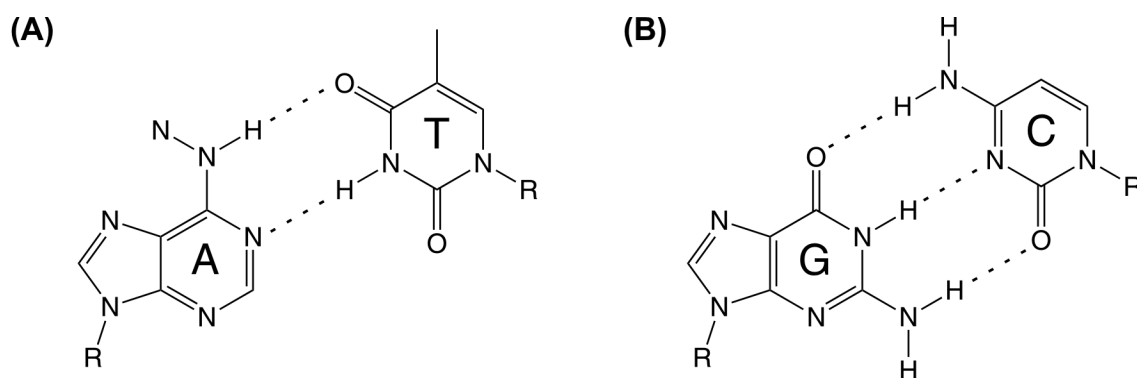


**Figure 1-2** The classical Watson-Crick base pairs. **(A)** Adenine pairs with thymine (in RNA thymine is exchanged by uracil) and **(B)** guanine with cytosine.

**Table 1-1** Parameters for the A-helical and the B-helical form of polynucleotide helices.<sup>[5]</sup>

	A-helical form	B-helical form
Direction of helix rotation	Right	Right
Number of residues / turn	11	10
Pitch	30 Å	33.8 Å
Turn angle / nucleotide residue	32.7°	36°
Axial rise / nucleotide residue	2.9 Å	3.38 Å
Diameter	26 Å	20 Å

molecules are usually double stranded (ds), whereas RNA secondary structure includes single-stranded regions, hairpins, duplexes, internal loop or bulges, and junctions all within one single polymer chain.<sup>[4]</sup>

Double stranded DNA usually adopts the B-form helix described by Watson and Crick,<sup>[3]</sup> however, the double-stranded RNA regions generally form an A-form helix (Figure 1-3). Table 1-1 summarizes the parameters for the A-form RNA and the B-form DNA revealing several differences in the structure of the helices. In the B-form helix the major and the minor groove are of similar depth but different widths (Figure 1-3A). By contrast, the A-form helix has a deep, narrow major groove and a shallow, wide minor groove (Figure 1-3B). The latter one is ideally suited for metal ion interactions with various partners. Additionally, the

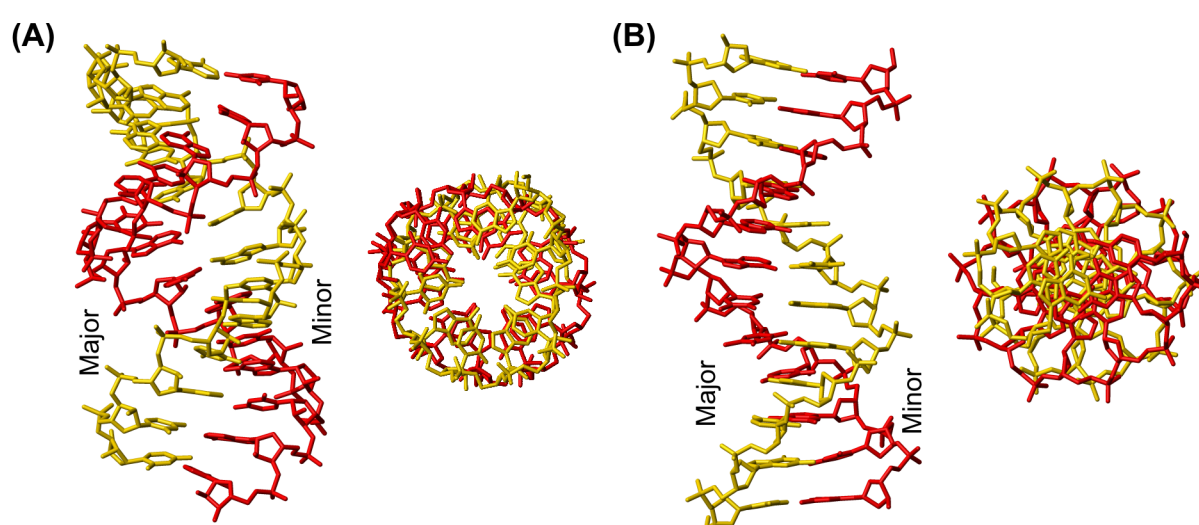


**Figure 1-3** Nucleic acid helices formed by hydrogen bonding. The two separate strands are shown in red and yellow. **(A)** Front (left) and top (right) view of the A-form RNA helix. The base pairs are aligned around the z-axis of the helix causing a cylindrical hole in the center. **(B)** Front (left) and top (right) view of the B-form DNA helix. The base pairs are aligned in the center of the helix. The Figures were prepared with MOLMOL<sup>[6]</sup> based on the PDB files 1RNA,<sup>[7]</sup> and 1BNA,<sup>[8]</sup> respectively.

nucleobase pairs in A-RNA are tilted with respect to the helix axis of about  $17^\circ$ ,<sup>[5]</sup> which gives rise to the typical hole in the middle of the double helix when looking along the helix axis (Figure 1-3A, left).

### 1.1.2 Modifications of nucleic acids

Beside the eminent role of nucleic acids as the carrier of genetic information, these molecules gain more and more importance in nanoscience due to their appealing structural features.<sup>[9,10]</sup> Especially, the self-assembly by highly specific interstrand recognition of two complementary oligonucleotides is a remarkable property to utilize nucleic acids as versatile building blocks in the “bottom-up” approach. In particular, the sequences of nucleic acids can be engineered in a way that complex and large nanoarchitectures are assembled.<sup>[9-13]</sup> Moreover, specifically inserted modifications can increase their functionalities even further. Thus, the development of automated phosphoramidite chemistry<sup>[14,15]</sup> makes the chemical synthesis of small oligonucleotides not only trivial, but also provides an excellent tool for the incorporation of nucleic acid modifications of all kinds. Longer nucleic acids strands carrying modifications can be prepared using methods of molecular biology like the ligation<sup>[16]</sup> or the polymerase chain reaction (PCR).<sup>[17]</sup>

In principle, all three building blocks of the nucleic acids, namely the phosphate, the sugar and the nucleobases, are equally amenable to chemical modifications. The strongest motives for the design and synthesis of oligonucleotides mimics have been the search for antisense and antigene activities<sup>[18-20]</sup> and to the question about the origin of nucleic acids.<sup>[21]</sup> In the beginning, the research was mainly dedicated to changes of the sugar-phosphate backbone. Such modifications can range from simple substitutions at the 2'-hydroxyl group up to the entire replacements of the sugar-phosphat backbone by completely different structural scaffolds such as in PNA (peptide nucleic acids).<sup>[22-26]</sup> By contrast, research on the generation of artificial base pairs is a newer field initiated with the main goal to expand the four letter code of nucleic acids.<sup>[27,28]</sup> In the pioneering work of Benner and co-workers several unnatural nucleosides with altered hydrogen-bonding scheme were established.<sup>[29,30]</sup> They also successfully demonstrated that oligonucleotides containing such altered nucleobases can be replicated<sup>[29-31]</sup> as well as translated into proteins with unnatural amino acids *in vitro*.<sup>[32]</sup> Moreover, also other artificial base pairing schemes were developed mediated for example by hydrophobic interaction,<sup>[33]</sup> shape complementarity,<sup>[34]</sup> and charge complementarity.<sup>[35]</sup> In the last ten years, a new generation of such nucleoside mimics were reported in which the hydrogen-bonding pattern was replaced by metal-mediated base-pairing.

### 1.1.2.1 Metal-mediated base pairs

In 1999, Tanaka and Shionoya reported the first example of an artificial ligand that is potentially suitable for the incorporation of metal ions between the strands.<sup>[36]</sup> In such a base pair, the natural nucleobases are replaced by mimics with a high affinity towards metal ions,<sup>[37-41]</sup> which should fulfil several requirements in order to successfully accomplish metal-mediated base pairing.<sup>[42]</sup>

- (I) The artificial nucleoside can be introduced into nucleic acid by standard automated nucleic acid synthesis.
- (II) The coordinating part of the artificial nucleoside has a higher affinity than the natural bases towards metal ions.
- (III) The artificial base pair forms planar complexes with the metal ions that are of similar dimension as the natural base pairs.

Only one year later, the first effective introduction of a metal-mediated base pair inside a DNA duplex was successfully achieved by Meggers, Romesberg and Schultz.<sup>[43]</sup> In the following years plenty of metal-mediated base pairs were not only introduced into DNA,<sup>[44-62]</sup> but also into GNA (glycol nucleic acid),<sup>[63]</sup> and PNA (peptide nucleic acid)<sup>[64-69]</sup> generating oligonucleotides with up to three, four, five, ten, or even 19 consecutive metal-ion-mediated base pairs.<sup>[46,51,53-55,62]</sup> Even different metal ions were incorporated at the same time using a set of at least two different orthogonal base pairs with sufficient selectivity for different metal ions.<sup>[54]</sup> In addition, also natural nucleosides can be used to form metal-ion-mediated base pairs typically applying mismatched bases pairs like TT and CC.<sup>[41,50]</sup>

Metal-mediated base pairs represent a powerful tool for the site-specific functionalization of nucleic acids with metal ions. The oligonucleotides serve as scaffolds to linearly array the metal ions along the helical axis. Thus, various additional applications for nucleic acids are conceivable such as metal ion sensors, nanomagnets, molecular wires or the application in the catalysis of enantioselective reactions.

### 1.1.3 Electron transfer in nucleic acids

Already in 1962, about ten years after the first molecular structure of double helical DNA was revealed, Eley and Spivey suggested that the DNA  $\pi$ -stack might serve as pathway for charge transfer processes.<sup>[70]</sup> In the 1990s Barton and co-workers pioneered this research field through remarkable contributions on photoactivated charge transfer in DNA.<sup>[71]</sup> Since then, the fundamental question whether DNA is a conducting or non-conducting biopolymer has been subject in a highly controversial scientific dispute. Interestingly, DNA has been considered as anything from molecular wire,<sup>[72-74]</sup> superconductor,<sup>[75]</sup> conductor,<sup>[76,77]</sup> semiconductor<sup>[78]</sup> or insulator.<sup>[79-81]</sup> Such controversy demonstrates that the result are strongly affected by DNA sequence, DNA length, DNA surface interaction, sample preparation, measuring technique, and the nature of the electrical contacts between DNA and the macroscopic electrodes. In principle, DNA-mediated charge transfer can be divided into oxidative hole hopping<sup>[82]</sup> or reductive electron transfer.<sup>[83]</sup> The research, originally motivated by the biological relevance to oxidative or other DNA damage,<sup>[84-87]</sup> demonstrates that DNA is a promising candidate for the creation of nanoscale electronic devices. Nevertheless, it is undoubted that the electron transport through longer DNA molecules ( $> 20$  nm) requires more research effort in order to use DNA as a molecular wire. Therefore, it is necessary to develop DNA-inspired materials which contain the typical structural features but exhibit improved electron transport capabilities. One promising way to enhance the conducting properties is the coordination of metal ions to DNA. There are mainly three possibilities to achieve metalized DNA.<sup>[88-90]</sup>

(i) Metals coating the DNA duplex: In this approach the natural counter ions of the backbone are exchanged by other metal ions such as  $\text{Ag}^+$ , that are subsequently reduced to form potentially conducting metal-wires.<sup>[91-99]</sup> The complete metallization of DNA causes a significant increase in conductivity.<sup>[89]</sup> However, this method leads to the formation of non-specifically coated nucleic acids. Therefore a protocol has been developed that allows the sequence-specific metalation of DNA.<sup>[100,101]</sup>

(ii) Metals complexed by the DNA duplex: The so-called M-DNA is formed from natural DNA at elevated pH values in the presence of divalent metal ions such as  $\text{Zn}^{2+}$ ,  $\text{Co}^{2+}$  or  $\text{Ni}^{2+}$ .<sup>[102-104]</sup> The exact position of the metals is currently not clear and is still discussed controversially.<sup>[105]</sup> Based on NMR data it was proposed that the imino protons of the base pairs were substituted by the metal ions,<sup>[102]</sup> but it is also possible that the metal ions are located in the grooves of the DNA double strand.<sup>[88]</sup> Conductivity studies revealed that the efficiency of the electron transport could be enhanced significantly upon coordination of the



divalent metal ions.<sup>[104]</sup> However, M-DNA is poorly soluble, and its precise structure has not been determined yet.

(iii) Metal-mediated base pairing: The hydrogen-bonding interactions of the natural nucleobases are replaced by metal-mediated base pairing using artificial nucleotides. The advantage of this modification strategy is that it allows to place the metal ions in the interior of the DNA duplex and confines the metalation to predefined sites which is important for the construction of nucleic acid based electronic devices. However, until now, no comprehensive conductivity study of such modified DNA strands has been performed. To obtain a meaningful characterization of their electric conductivity, DNA duplexes with long continuous stretches of metal ion mediated base pairs of a well-defined geometry are prerequisite.

## 1.2 Nuclear magnetic resonance (NMR) spectroscopy of nucleic acids

### 1.2.1 Determination of nucleic acid structures by NMR

Apart from single crystal X-ray diffraction, NMR is the only method that allows the determination of three-dimensional nucleic acids structures. Many different types of information can be gained from NMR: (i) distances between protons by the NUCLEAR OVERHAUSER EFFECTS (NOE), (ii) scalar couplings (iii) chemical shifts, (vi) relaxation times, and (v) diffusion coefficients. Thus, NMR spectroscopy provides not only precise structural data but also information about dynamics in nucleic acids.

The elucidation of the three-dimensional structure of nucleic acids can be subdivided into several steps.<sup>[106]</sup> First a series of NMR experiments are performed in 100 % D<sub>2</sub>O and in 10 % D<sub>2</sub>O / 90 % H<sub>2</sub>O to observe the non-exchangeable and the exchangeable protons, respectively. The 2D [<sup>1</sup>H,<sup>1</sup>H]-NOESY spectra in D<sub>2</sub>O including the so-called "*sequential walk*" region give the most valuable first hand structural information. In NOESY experiments, the Nuclear Overhauser effect (NOE) between nuclear spins is used to transfer magnetization through magnetic dipole-dipole coupling. Hence nuclei that are close in space (up to 5-6 Å)

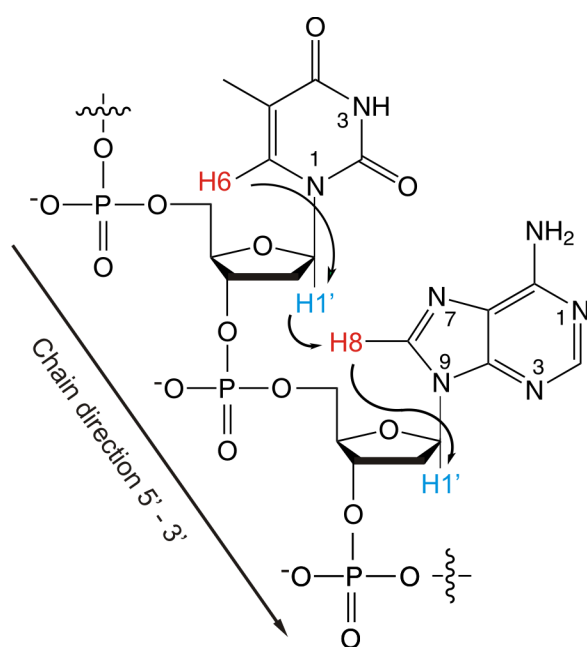


**Figure 1-4** The "*sequential walk*". Through-space connectivities of nucleobase and sugar protons are indicated by black arrows. The protons, which are of great importance for structure determination by NMR, are highlighted in blue (H8/H6) and red (H1').

give cross-peaks in the resulting two-dimensional spectrum. The intensity of these cross-peaks is proportional on the interatomic distance by  $r^{-6}$  and therefore the approximate distances of nuclei can be derived.<sup>[107]</sup> The aromatic nucleobase protons H6 and H8 are spatially close to their intraresidue ribose H1', but also to the H1' of the upstream 5' nucleotide (Figure 1-4). Thus the connectivity of nucleotides along a nucleic acid strand can be established (*sequential-walk*). By walking along the sequence, it is possible to assign the entire spectrum and to extract distance information on the protons. In addition to the *sequential walk* region,

NOESY spectra include information about base-stacking and also about sugar-sugar interactions. Therefore, these spectra are the major source for structural restraints containing the non-exchangeable protons. Nevertheless, other multidimensional NMR experiments like [ $^1\text{H}, ^1\text{H}$ ]-TOCSY and [ $^{13}\text{C}, ^1\text{H}$ ]-HSQC serve to cross-validate the assignments. Exchangeable proton resonances obtained from 2D [ $^1\text{H}, ^1\text{H}$ ]-NOESY spectra in  $\text{H}_2\text{O}$  provide information regarding base pairing and give rise to the majority of cross-strand interactions. Imino proton resonances and many amino resonances are found downfield well separated from the other proton resonances. Only exchangeable protons which are included in base pairs are observable in NMR spectra due to the decreased exchange rate of free protons with the bulk solvent.<sup>[108]</sup> If the protons are not involved in base pairs, the exchange with the solvent is in the range of milliseconds or even faster. Thus, base pairs at the end of helical stems often have broadened exchangeable proton resonances due to the rapid exchange with the water.<sup>[109]</sup> Once all cross-peaks are assigned and integrated they are classified into three different ranges as strong, medium and weak and will then be included as distance restraints into the structure calculation.

It is not only important to know the identity of the nucleobases, but also the backbone and sugar pucker conformation to fully describe the structure of nucleic acids. The backbone torsion angles  $\alpha$ ,  $\beta$ ,  $\gamma$ ,  $\delta$ ,  $\epsilon$ , and  $\zeta$  describe the backbone conformation of every nucleotide linkage, the endocyclic torsion angles  $\nu_0$ - $\nu_4$  determine the furanose ring conformation, and the glycosidic torsion angle  $\chi$  defines the orientation between the base and the sugar ring (Figure 1-5).

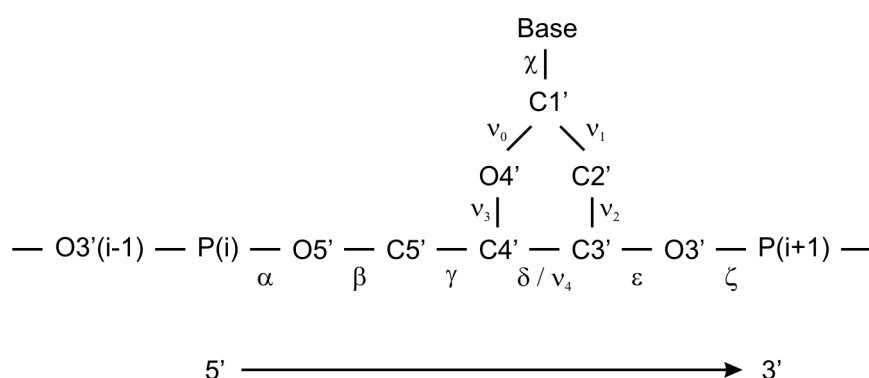


**Figure 1-5** Definition of the torsion angles in the sugar phosphate backbone:  $\alpha$ ,  $\beta$ ,  $\gamma$ ,  $\delta$ ,  $\epsilon$ , and  $\zeta$ , the glycosidic torsion angle  $\chi$ , and the endocyclic torsion angles  $\nu_0$ - $\nu_4$  in the sugar ring.

With the help of certain NMR experiment almost all angles can be determined. However, of special interest is thereby the glycosidic bond, which can either adopt a *syn* or an *anti* conformation. Typically, the *anti* conformation is found in nucleic acids since it allows to

maximize hydrogen bonding and base stacking in the secondary structure and minimizes the electrostatic repulsion of the phosphate groups. The *syn* conformation appears less frequently, e.g. at guanosines in the (dC-dG)<sub>3</sub> DNA, which forms left-handed Z-DNA.<sup>[8]</sup> The intraresidue H1' – H6/H8 distance in an *anti* conformation is about 3.7 Å while in an *syn* conformation a distance of about 2.2 Å is observed.<sup>[107,110]</sup> Therefore, a weak or intermediate cross-peak is expected for an *anti* conformation, whereas for a *syn* conformation a very strong cross-peak will occur.

Another important feature of nucleic acid structures is the sugar pucker conformation (Figure 1-6). The most prominent conformations are C2'-endo (or South) in B-DNA and C3'-endo (or North) in A-RNA. The atom termed *endo* describes the atom, which points towards the same side as C5' with respect to the plane of the ribose (Figure 1-6). RNA usually exists in the A-form because the C2'-endo conformation sterically hinders the B-form

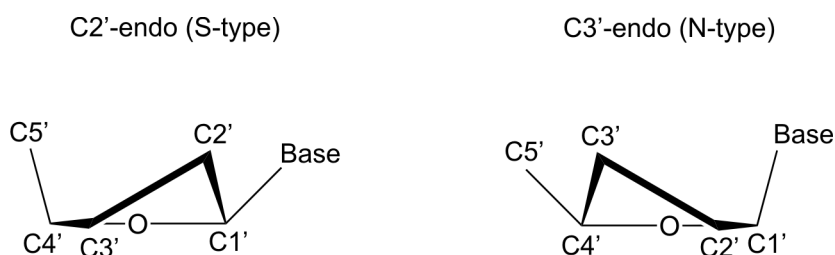


**Figure 1-6** The sugar pucker conformations of deoxyribose and ribose found in nucleotides are depicted. The C2'-endo (S-type) conformation is typical present in B-form DNA and the C3'-endo (N-type) conformation is usually found in A-form RNA.

helix due to the additional 2'-OH group.<sup>[111]</sup>

With the help of [<sup>1</sup>H, <sup>1</sup>H]-TOCSY experiments it is possible to distinguish between a C3'-endo and a C2'-endo conformation.

Compared to the NOESY experiments in TOCSY experiments the magnetization transfer occurs through bonds. In a C3'-endo sugar pucker the angle between H1' and H2' is about 90° and thus no coupling can be detected in the TOCSY spectra. By contrast, the angle between H1' and H2' in a C2'-endo conformation is about 180° and therefore, a coupling is observable.<sup>[107]</sup>

Having a set of distance and conformational restraints collected, structure calculation can be performed using a molecular dynamics simulated annealing protocol.<sup>[112-114]</sup> Starting from an extended structure, molecular dynamics simulations shift slightly the positions of the atoms in order to minimize their overall energy. Contributions to this energy can derive from bonding, torsional movement, repulsion, van-der-Waals attraction, and electrostatics.<sup>[109]</sup> In a first step of simulated annealing, the nucleic acids are heated to high temperatures to obtain single unstructured strands. At this high temperature, experimental restraints are gradually applied as quadratic, square-well energy functions. After the protocol is completed a first set of structures is obtained. These output structures are analyzed for distance and conformational

violations, the input files corrected, and supplemented with further restraints before a next round of simulated annealing is performed. This cycle is repeated until at least 10 % of the output structures are converged (e.g. 20 out of 200 calculated structures).

After the final structure is obtained, it is of great importance to judge the quality of the NMR structure. Criteria which reflect how well the structure is defined are the number of restraints used in the calculation, the statistics of final restraint violations as well as the superposition of the final structures. However, it has been shown that standard NMR methods can precisely determine local conformational parameters like sugar pucker and glycosidic torsion angle, but long-range parameters like helical twist, helical rise, and backbone torsion angles are less well defined.<sup>[115]</sup> Moreover, the definition of the global conformation becomes increasingly difficult as the molecular size increases. Nevertheless, especially for RNA sequences that can be *in vitro* transcribed with  $^{13}\text{C}$ ,  $^{15}\text{N}$ -labeled nucleotides,<sup>[116]</sup>  $^{13}\text{C}$ ,  $^1\text{H}$ -HSQC and  $^{15}\text{N}$ ,  $^1\text{H}$ -HSQC spectra experiments can be recorded to extract residual dipolar couplings (RDC) which provide long-range orientational information. These additional orientation restraints can then be inserted into the simulated annealing protocol for further refinement of the NMR structures.

### 1.2.2 Exploring metal ion coordination by NMR

Metal ions are essential for charge compensation, proper folding and function of large nucleic acids. Nucleic acids and their building blocks offer a multitude of donor atoms to coordinate metal ions.<sup>[117,118]</sup> The most prominent sites for metal ions are the two non-bridging oxygen atoms of the negatively charged phosphate sugar backbone. However, aside from these negatively charged residues, also the nucleoside moieties offer coordinating atoms: the ring nitrogens, the carbonyl oxygens and in some cases even the sugar oxygens. The purine N7 position is certainly the most prominent one due to the well-known coordination of *cisplatin* to this site.<sup>[119]</sup> The interaction with the nucleic acid is not always direct (inner sphere coordination) but can also be mediated through water ligands of the solvated metal ions (outer sphere coordination).

The detection of the metal ions that are naturally associated with nucleic acids (e.g.  $\text{Na}^+$ ,  $\text{K}^+$ ,  $\text{Ca}^{2+}$  and  $\text{Mg}^{2+}$ ), is a challenging task as they are spectroscopically silent and can thus not be observed directly in an NMR experiment. However, over the last years new strategies have been developed to detect metal binding sites and to elucidate their specific coordination sphere in nucleic acids by NMR. Certainly the easiest way is the exchange of the NMR-silent isotopes by NMR-active isotopes, but unfortunately, only a few of these isotopes exist ( $^{23}\text{Na}$ ,

$^{113}\text{Cd}$ ). Therefore other metal ions are commonly used to mimic the naturally associated ones. For example, inner sphere binding of  $\text{Mg}^{2+}$  towards oxygen ligands can be studied using  $\text{Cd}^{2+}$  in so-called thio-rescue studies.<sup>[120,121]</sup> A further mimic for the diamagnetic  $\text{Mg}^{2+}$  is the paramagnetic  $\text{Mn}^{2+}$  ion that induces a significant line broadening of the resonances in close vicinity.<sup>[122-124]</sup> Thus,  $\text{Mn}^{2+}$  can be used as a qualitative probe for direct metal ion coordination to nucleic acids as shown by different examples in the literature.<sup>[125-128]</sup> Moreover, to investigate outer sphere binding of  $\text{Mg}^{2+}$  ions,  $[\text{Co}(\text{NH}_3)_6]^{3+}$  can be used to mimic the spectroscopically silent  $[\text{Mg}(\text{H}_2\text{O})_6]^{2+}$ .<sup>[124,126-132]</sup> Coordination of  $[\text{Co}(\text{NH}_3)_6]^{3+}$  to nucleic acids can then be studied either by chemical shift mapping or by observation of NOE contacts between the ammonia protons of the Co(III) complex and protons of the nucleic acids. In addition, it is also possible to observe directly  $\text{Mg}^{2+}$  coordination by NMR because the chemical shifts as well as the resonance line widths of the nucleic acid protons are affected by a coordinating  $\text{Mg}^{2+}$ .<sup>[123,133-135]</sup> A change of the chemical shift can be caused by  $\text{Mg}^{2+}$ -coordination in close vicinity of the observed proton or by a structural change in the local geometry that is induced by the metal ion. Furthermore,  $\text{Ti}^+$  and  $\text{NH}_4^+$  are well known substitutes for the monovalent  $\text{K}^+$  ion. The  $\text{Ti}^+$ -ion which has a similar ionic radius and metal-ligand bond length as  $\text{Mg}^{2+}$  can be directly detected by  $^{205}\text{Ti}$ -NMR,<sup>[136]</sup> whereas  $\text{NH}_4^+$  allows the observation of NOE cross peaks between the ammonium ion and the nucleic acid protons similar to the situation with  $[\text{Co}(\text{NH}_3)_6]^{3+}$ .<sup>[137]</sup>

Chemical shift studies and line broadening analysis are two approaches to determine metal ion binding sites qualitatively. To assess the metal ion binding sites quantitatively, affinity constants of  $\text{M}^{n+}$  to the nucleic acids can be calculated from the NMR chemical shift change data. Recently, *ISTARv2.2*, a MATLAB script, has been developed to automate this extensive calculation using an iterative procedure to calculate the intrinsic metal ion affinity for each metal binding site.<sup>[133]</sup> Thereby, for the first time, also the binding of  $\text{M}^{n+}$  to all the other sites is taken into account, when calculating the affinity for one binding site.

Besides the studies on metal ion interaction with DNA and RNA in naturally occurring systems, investigations on artificially metal-modified nucleic acids become important, as these molecules are promising candidates for nanodevices and can be employed as tools in biotechnology. Although the development and investigation of these artificial systems is currently a popular research field only few NMR studies are known in which direct nucleic acid-metal contacts or metal induced structural changes could be observed. Already in 1963 Katz proposed that  $\text{Hg}^{2+}$  ions bind specifically to thymine-thymine mismatches in a linear fashion to form metal-ion mediated base pairs.<sup>[138]</sup> The N3 protons are replaced by  $\text{Hg}^{2+}$  to

coordinate the oppositely located nitrogen atoms. However, only recently Tanaka et al. were able to directly prove the proposed bond formation by [ $^{15}\text{N}$ ]-NMR experiments revealing a  $^{15}\text{N}$ - $^{15}\text{N}$   $J$ -coupling across the  $\text{Hg}^{2+}$  ion.<sup>[57]</sup> Moreover, all N3 resonances assigned exhibit large downfield shifts of about 30 ppm upon addition of  $\text{Hg}^{2+}$  that can only be explained by a proton-metal exchange.

The above mentioned examples nicely show that NMR is a powerful tool to determine nucleic acid structures and to elucidate their metal binding properties. Therefore NMR was the method of choice in this work to characterize the structural properties of several metal modified nucleic acids.

### 1.3 Thesis outline

This work deals with the investigation of several oligonucleotides that are specifically functionalized by metal ions and therefore are highly interesting candidates for the use as nanomaterial. In the first part of the work a new approach is applied to obtain long stretches of successively metal-modified base pairs by *in vitro* transcription. The structure and the metal ion binding properties of the synthesized RNA and RNA/DNA sequences were subsequently characterized by various spectroscopic methods. In the second part, an oligonucleotide containing three consecutive imidazole nucleobases is extensively studied by NMR upon addition of metal ions. This first deep structural insight into such metal-modified nucleic acids is established that is a prerequisite to further improve these systems and to expedite the development of DNA-inspired nanomaterial.



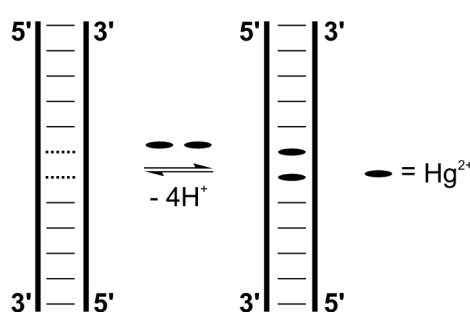


## 2 *In vitro* construction of nucleic acids as scaffolds for one-dimensional arrays of mercuric ions

### 2.1 Introduction

One major problem in the synthesis of nucleic acids containing multiple metal ions is the tiring, expensive and time-consuming chemical synthesis of the modified nucleobases and the subsequent phosphoramidites. The latter being the building blocks for automated chemical DNA strand synthesis. A first step to circumvent elegantly the "problem" of chemical synthesis of the artificial nucleobases has recently been made by adding  $\text{Hg}^{2+}$  ions to a

(A)



(B)

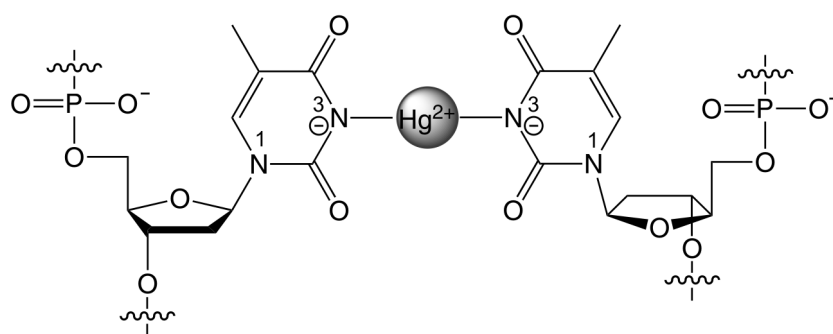


**Figure 2-1** Metal-modified DNA duplex as potential molecular wire. (A) Schematic depiction of the conversion from a DNA strand to a metal-modified DNA duplex upon addition of  $\text{Hg}^{2+}$ . (B) Two thymines of a T-T mismatch base pair are deprotonated at the N3 position thus coordinating the  $\text{Hg}^{2+}$  ion in between.

DNA solution.<sup>[57]</sup> The oligonucleotides are palindromic, but complementary at the two ends and contain a central continuous stretch of thymidine residues.<sup>[57,139-141]</sup> Metal ions like platinum(II),<sup>[142,143]</sup> or mercury(II) are well-known to replace protons within hydrogen bonds and thereby coordinate to the oppositely located nitrogen atoms.<sup>[144-146]</sup>

In the above mentioned case,  $\text{Hg}^{2+}$  replaces both N3H protons of two thymine residues

located opposite to each other, by linking the nucleobases,<sup>[138,147,148]</sup> and at the same time getting lined up in the middle of the DNA helix (Figure 2-1).

The chemical coupling of the phosphoramidites to build up longer DNA strands is well established and straightforward.<sup>[14,15]</sup> Nevertheless, despite the high yield of each coupling step, the overall yield rapidly decreases with increasing lengths and the costs rise fast with the demand of large amounts, which are needed for either a detailed analytical characterisation or possible future large-scale synthesis.

All of these drawbacks prompted us to look for alternative ways to build up such nucleic acid duplexes capable of aligning metal ions along their helical axis. Nature has evolved DNA and RNA polymerases to synthesize oligonucleotides fast, efficiently, in large amounts, and of defined and theoretically indefinite lengths, by using the nucleoside triphosphates as building blocks. Although being highly similar enzymes, DNA and RNA polymerases exhibit some distinct requirements for the construction of long nucleic acids strands. Both types of polymerases need a template strand to build up a new complementary strand. A DNA polymerase needs a primer to elongate a new nucleic acid chain. In contrast, a RNA polymerase starts transcription by binding a double stranded promoter region and begins with a single nucleotide, typically a guanosine 5'-triphosphate. Both kinds of polymerases are very distinct with respect to the incorporation of either NTPs or dNTPs and have found wide application in the (bio)chemical laboratory. DNA polymerases are mostly applied in molecular biology, i.e. for PCR to amplify small amounts of double-stranded DNA. Thereby the maximal yield is theoretically determined by the amount of primer added and the number of cycles used by PCR. By contrast, RNA polymerases are used to synthesize single-stranded RNA utilizing only very small amounts of template strands because they are recycled and can be used almost indefinitely. Moreover, compared to PCR, which requires a rather expensive PCR machine and can be used for only small volumes, the easy handling of RNA polymerases also in large scale approaches is a further big advantage. Thus, RNA polymerase is in theory an ideal molecular machine to synthesize custom-designed single-stranded nucleic acids with high fidelity and in large quantities. However, in the present context of metal-modified nucleic acids and their potential use as molecular wires, it is unclear if it is possible to incorporate long stretches of the same nucleotide, irrespective of whether it is a natural or a synthetic one, and still maintain fidelity and processivity of the polymerase reaction.

To the best of our knowledge, so far metal-modified nucleic acids have been built up from DNA<sup>[36,43-62]</sup> or PNA<sup>[64-69]</sup> monomers only, i.e. yielding DNA or PNA strands, rather than being based on RNA. However, also RNA can coordinate metal ions not only in high numbers<sup>[133,135]</sup> but also site specifically and in close neighbourhood to each other.<sup>[117,118,134,149]</sup> Nevertheless, the reason for DNA being the nucleic acid of choice so far

certainly lies in the higher stability of the 2'-deoxy form of nucleic acids against hydrolytic decomposition. In addition, RNA is often considered not to be double-stranded, but rather being seen as a three-dimensional complex, which is mostly single-stranded but structured with some double-helical regions and many bulges. While naturally occurring RNAs indeed form such complex three-dimensional structures, the formation of regular duplexes is only dependent on the right design and sequence. A RNA duplex is much less prone to hydrolytic decomposition than the corresponding single strands, even in the presence of di- or trivalent metal ions, as the 2'-OH is not in the correct geometrical position to undergo a nucleophilic in-line attack at the adjacent bridging phosphodiester bridge.<sup>[150,151]</sup> It follows that regular A-form RNA duplexes should not be discarded in general from serving as a scaffold to align metal ions in a one-dimensional way.

## 2.2 Results and discussion

### 2.2.1 Formation of consecutive uracil-mercury-uracil base pairs

#### 2.2.1.1 *In vitro* transcription of RNA with long stretches of uracil residues

In order to test the capability of *T7* RNA polymerase to insert long stretches of a single kind of nucleotides, i.e. uracil in the present case, we designed several constructs with a central line-up of an increasing number of consecutive uracil nucleotides. As a starting point we used the sequence of Tanaka et al.,<sup>[57]</sup> which has two TT mismatched base pairs flanked on each side by four regular Watson-Crick base pairs (Figure 2-2).

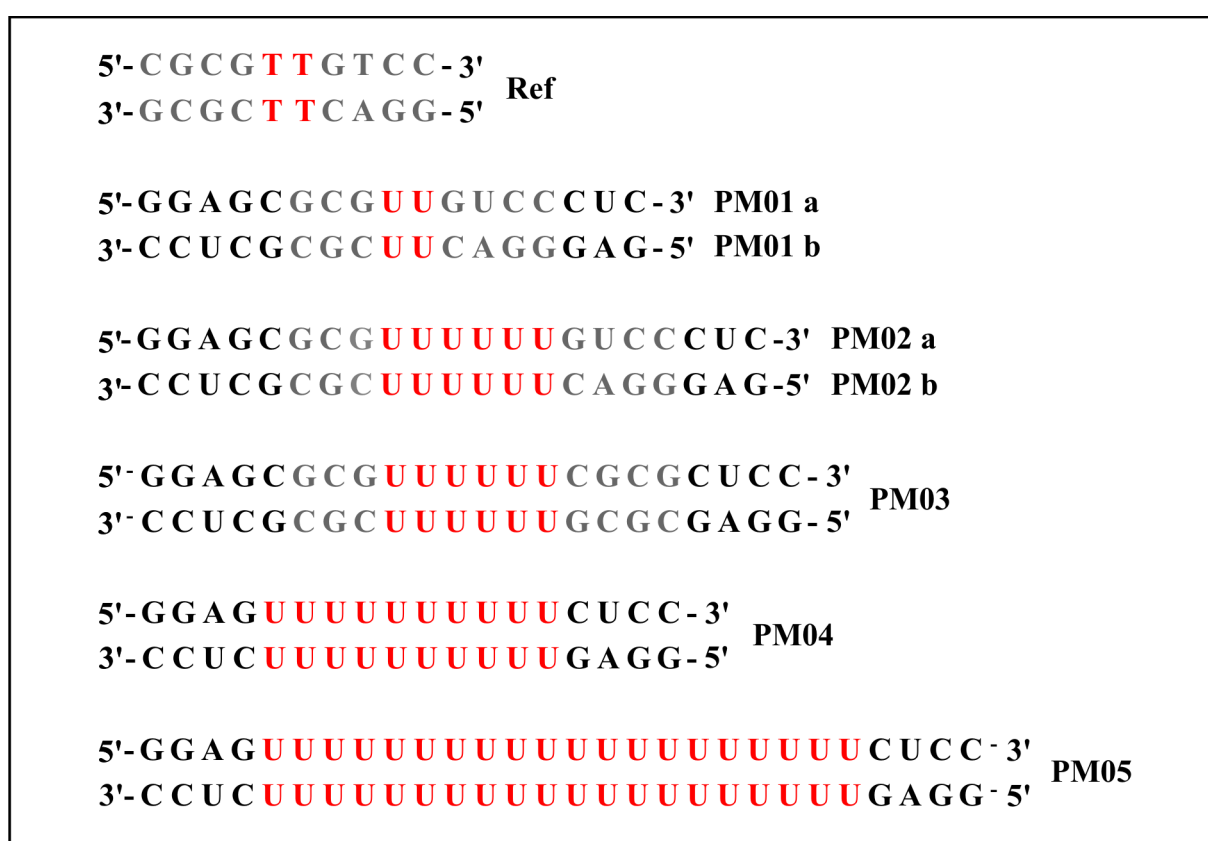


**Figure 2-2** The DNA construct used by Tanaka et al.<sup>[57]</sup> as well as the RNA constructs **PM01** - **PM05**. Red indicates the continuous stretches of thymine or uracil residues, and grey displays the Tanaka sequence.

Naturally, as we are working with RNA, all deoxyribonucleotides were replaced by the corresponding ribonucleotides in comparison to this previous work,<sup>[57]</sup> and therefore also the thymine nucleobases were substituted by uracil residues. The initiation of the transcription by the *T7* RNA polymerase has the strict requirement of a 5'-G as a first nucleotide and the subsequent two to five nucleotides determine to a large part the yield of transcription.<sup>[116,152]</sup> Hence, we added three or four base pairs, respectively, to the two ends of the helix giving the duplex **PM01** (Figure 2-2), 5'-GGAG being known to be an excellent sequence for high yield transcriptions.<sup>[116,123]</sup>

*In vitro* transcription of the two strands giving **PM01** (as well as of all other RNAs) was performed following standard protocols for high yield transcription as, e.g., needed for NMR experiments.<sup>[116,123]</sup> **PM01 a** transcribed slightly better than **PM01 b** (Figure 2-2), giving yields of 10 nmol/mL and 7.3 nmol/mL, respectively (Table 1-1). With both strands, rather intense so-called n<sup>+</sup> bands were observed, stemming from the run-off transcription of *T7* RNA polymerase adding extra nucleotides at the 3'-end of a fresh transcript. With only 17 nucleotides each, these strands are on the short side for *in vitro* transcription, and both the moderate yields as well as the pronounced n<sup>+</sup> bands are actually expected for a transcript of this size.

**Table 2-1** Conditions and yields of the purified RNA strands **PM01** - **PM05** (in nmol/mL transcription solution) after *in vitro* transcription by *T7* RNA polymerase.

	<b>PM01 a</b>	<b>PM01 b</b>	<b>PM02 a</b>	<b>PM02 b</b>	<b>PM03</b>	<b>PM04</b>	<b>PM05</b>
[RNA]/nmol/mL	10	7.3	14	30	27	11	3.0
[NTP]/mM	5	5	7.5	5	5	5	5
[UTP]/mM	5	5	7.5	5	5	15	30
[MgCl <sub>2</sub> ]/mM	20	45	45	45	45	30	30

In a second step we increased the number of uracil nucleotides in each RNA strand from two to six in total, giving the two constructs **PM02** and **PM03** (Figure 2-2). In both duplexes, six Hg<sup>2+</sup> ions can be insert into the UU base pairs without disrupting the duplex structure, assuming a conversion from *cis*-UU-wobble pairs to the Hg<sup>2+</sup>-mediated U-Hg-U base pairs (Figure 2-3). **PM02** and **PM03** differ in that respect that the latter is a palindromic sequence,

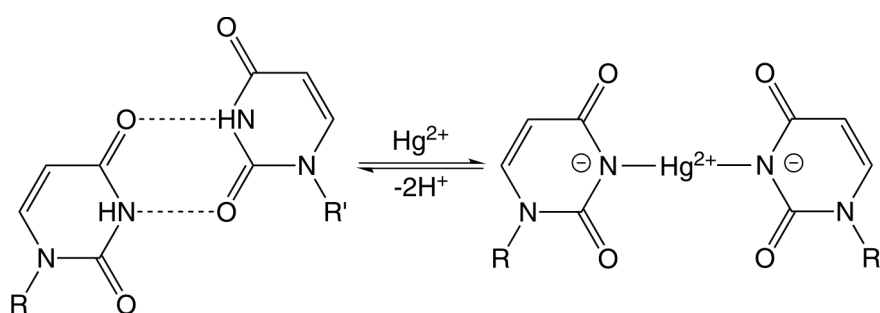


**Figure 2-3** Proposed formation of the Hg<sup>2+</sup>-mediated U-Hg-U base pair from a *cis*-UU-wobble pair.

which makes the interpretation of its NMR spectra much easier: In the absence of Hg<sup>2+</sup> the formation of a hairpin structure is feasible with a loop comprising six uracil residues whereas

upon addition of Hg<sup>2+</sup> duplex formation is expected. This hairpin-duplex transition should enable a clear distinction of the two forms based on their hydrodynamic radii. For symmetry

reasons, in the case of a duplex, only about half of the number of resonances (compared to a non-palindromic sequence such as **PM02**) should be observed in the NMR spectra. The increased lengths of **PM02** and **PM03** are readily reflected in the transcription yield, which is considerably higher compared to that of the two strands of **PM01**. The transcription of **PM02 b** actually gives a very good yield of 30 nmol/mL and **PM03** was transcribed almost as well (27 nmol/mL). In addition, we obtained transcripts of precisely defined lengths with only very little run-off transcription products. This clearly indicates that a stretch of six consecutive nucleotides of the same kind poses no problem for *T7* RNA polymerase to keep a high level of transcription fidelity.

To test how far one can push the system, we designed the two palindromic constructs **PM04** and **PM05** with 10 and 20 uracil nucleotides in a row, respectively. Both duplexes represent oligonucleotides towards "real" nanowires with only short helix ends and a large number of uracil residues in between. Compared to **PM03**, the transcription yield was distinctly decreased with **PM04** and even more with **PM05**. Furthermore, in both cases an increasing number of additional bands were found on the denaturing gels. By comparison their lengths with RNAs of comparable but known lengths on 18 % denatured PAGE (polyacrylamide gel electrophoresis), not only the typical additional nucleotides of the 3'-terminus<sup>[152]</sup> were observed but also shorter abortion products. However, for **PM04** and **PM05** the two bands of highest intensity belong to the full-length transcript and the n-1 band which probably misses one uracile residue. It seems as if the *T7* RNA polymerase loses partially its fidelity of advancing along the DNA template strand, when too many nucleotides of the same kind are lined up in one row. One reason for these extraordinary abortions could be that the long stretch of uracil residues stops transcription because it is also known to be a signal for termination.<sup>[153-155]</sup> Moreover, it is also possible that the early incorporation of the uracil stretch, already after insertion of four NTPs, causes further problems, because the transcription is still in the not stable initiation phase.<sup>[156]</sup> Nevertheless, as the bands are well-separated on the denaturing PAGE, we extracted and further investigated only the full-length transcripts **PM04** and **PM05**, respectively.

#### 2.2.1.2 NMR-spectroscopic characterization of the transition to Hg<sup>2+</sup>-based molecular RNA wire

NMR provides a good tool to investigate structural changes within biomolecules. Hence, a series of NMR experiments was run in order to gain more structural information on the Hg<sup>2+</sup>-free as well as Hg<sup>2+</sup>-bound state of **PM03**. We choose **PM03**, as this palindromic construct with a length of 22 bases is still in a size range well accessible for NMR studies and

at the same time can incorporate six  $\text{Hg}^{2+}$  ions. In addition, a restructuring from hairpin to duplex form is likely to occur upon addition of  $\text{Hg}^{2+}$ , which should result in distinct changes of chemical shifts as well as size.

The  $[\text{}^1\text{H}, \text{}^1\text{H}]$ -NOESY spectrum in 100 %  $\text{D}_2\text{O}$  displays well resolved and dispersed peaks, indicating that indeed a distinct conformation is present in solution (Figure 2-4). Starting at the 5'-end, the *sequential walk* can be followed all the way through the Watson-Crick base-paired region into the stretch of uracil residues and back out to the 3'-end. The presence of the expected A-form helix in the flanking Watson-Crick sequence was thereby verified by the observation of the stacking peaks between the aromatic nucleobase protons as well as the backward peaks between the pyrimidine H5 and the H8/H6 of the 3'-positioned nucleotide (see also CD-spectra in Section 2.2.1.4).

It is well known that specific sequences, like GNRA or UNCG (N represents any nucleotide, and R a guanosine or adenosine), adopt highly stable loops with all nucleotides stacking on each other thereby closing a hairpin. Additional pyrimidines inserted into these short sequences are then often flipped out into solution and due to dynamics difficult to observe by NMR spectroscopy. The fact that the *sequential walk* of **PM03** can be fully followed through the stretch of six uracil nucleobases is therefore rather surprising. This indicates that these central six uracil residues form a well structured loop without any display of imminent dynamics. Such a stable and rigid hairpin structure with a closing U6-loop and not a duplex structure is corroborated by the below described DOSY and DLS data (Section 2.2.1.3). The formation of the linear array of  $\text{Hg}^{2+}$  ions was induced by the addition of 1.2 equivalents of  $\text{Hg}(\text{ClO}_4)_2$  to each of the

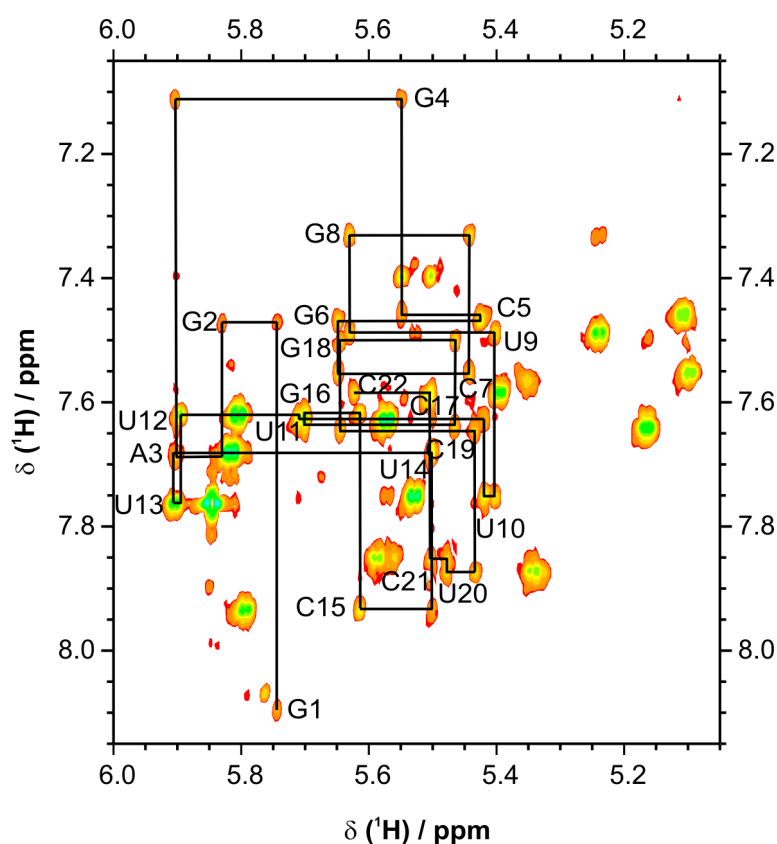


**Figure 2-4** 2D  $[\text{}^1\text{H}, \text{}^1\text{H}]$ -NOESY spectrum of **PM03** acquired in 100 %  $\text{D}_2\text{O}$  (100 mM  $\text{NaClO}_4$ ,  $\text{pD} = 7.2$ ) at 298 K. The *sequential walk* is indicated by a black solid line and can be followed from the 5'-end all the way through to the 3'-end.

constructs **PM01-PM05** to obtain the metalated duplexes **PM01·Hg**, **PM02·Hg**, etc.. One equivalent is defined as the amount of  $\text{Hg}^{2+}$  needed to form the complete set of U-Hg-U base pairs in a given duplex, e.g. if a solution of **PM03** contains 1 mM double helix, 6 mM  $\text{Hg}(\text{ClO}_4)_2$  are required to reach one equivalent. Every sample was heated up to 70 °C and slowly cooled down to room temperature to enable the formation of the U-Hg-U base pairs. The excess of  $\text{Hg}^{2+}$  was then removed by the addition of CHELEX 100<sup>®</sup> resin as it was described before<sup>[57]</sup> for the DNA sequence that corresponds to the central part of **PM01**. We

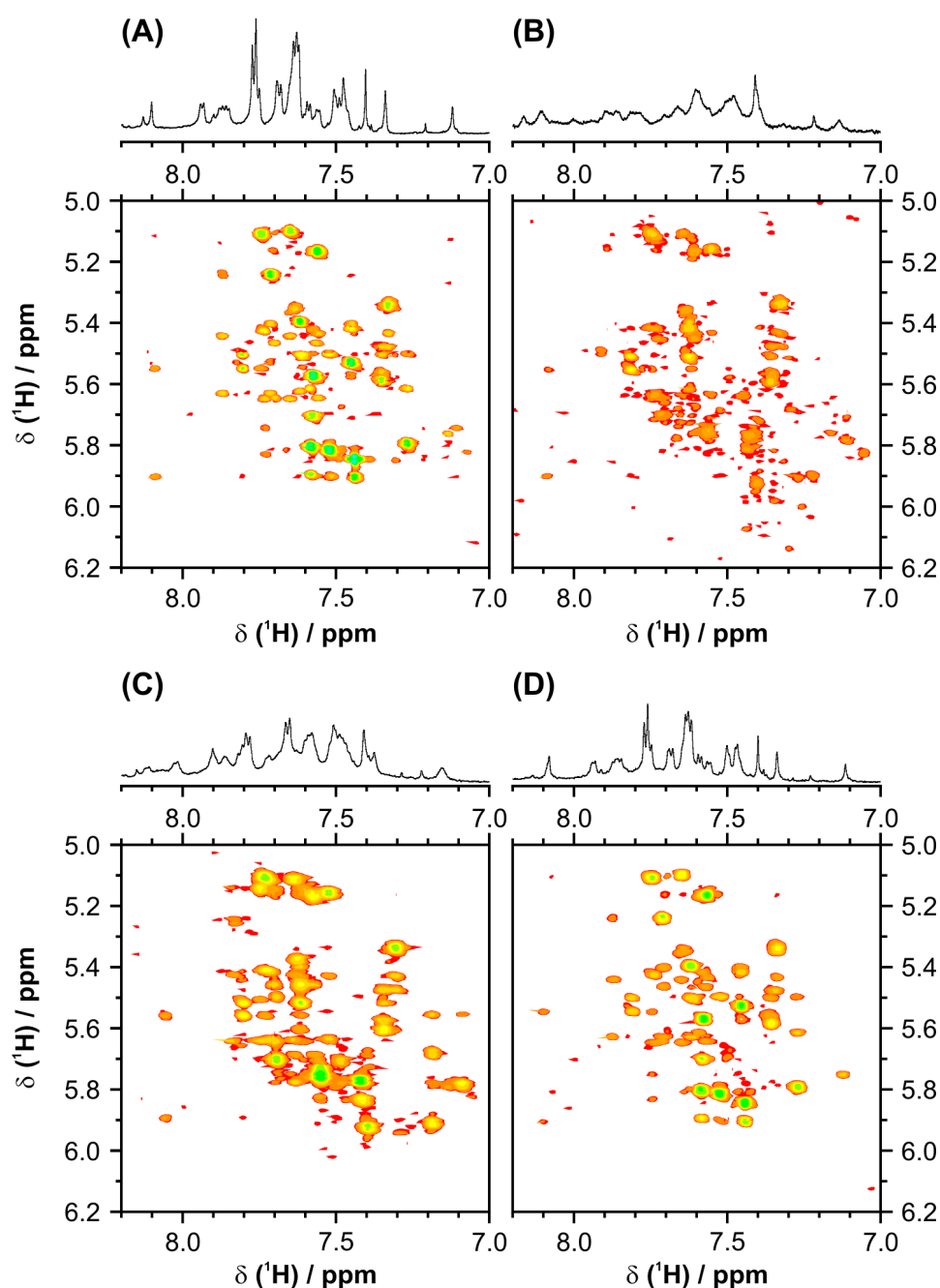


**Figure 2-5** Formation of the  $\text{Hg}^{2+}$ -mediated RNA duplex **PM03·Hg**.  $^1\text{H}$ -NMR spectra and 2D  $^1\text{H}$ ,  $^1\text{H}$ -NOESY spectra (100 %  $\text{D}_2\text{O}$ , 100 mM  $\text{NaClO}_4$ , pD = 7.2, 298 K) of the aromatic region before (A), after addition of 1.2 eq.  $\text{Hg}^{2+}$  (B), after subsequent treatment with CHELEX 100<sup>®</sup> for two hours (C), and after additional treatment with CHELEX 100<sup>®</sup> over night (D).



followed the transition from non-metalated RNA to RNA with metal-ion mediated base pairs by several spectroscopic methods in order to characterize the resulting metal-modified nucleic acids.

[ $^1\text{H}$ ]-NMR spectra of each construct were recorded in 100 %  $\text{D}_2\text{O}$  (Figure 2-5) to follow the changes in chemical shifts upon formation of the metal-ion mediated base pairs. All five samples behaved identically during the corresponding steps: Upon addition of 1.2 eq. of mercury(II) salt, a severe line broadening was observed (Figure 2-5B), which hampered our efforts to obtain detailed information on any of the five metalated duplexes. As the line broadening can very well be caused by the slight excess of  $\text{Hg}^{2+}$ , we subsequently gently treated each sample with CHELEX 100<sup>®</sup> in order to remove any excess  $\text{Hg}^{2+}$ . CHELEX 100<sup>®</sup> treatment for two hours resulted in a sharpening of the resonances, indicating the removal of at least some of the  $\text{Hg}^{2+}$  by CHELEX 100<sup>®</sup> (Figure 2-5C). As these spectra still did not allow a detailed assignment of resonances, we subsequently treated each sample with CHELEX 100<sup>®</sup> over night. To our surprise, after this additional treatment the resulting spectra looked

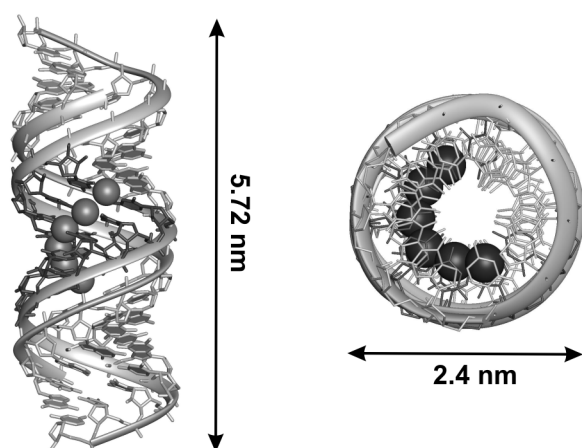


**Figure 2-6** Side and top view of an A-form model of **PM03·Hg** illustrating that the  $\text{Hg}^{2+}$  ions are in close neighborhood and lined up in a helical fashion. This panel has been prepared by MOLMOL.<sup>[6]</sup>

identical to the ones recorded in the absence of  $\text{Hg}^{2+}$  (Figure 2-5D). This clearly indicates that the binding of  $\text{Hg}^{2+}$  between two uracil base pairs is not that strong and that the metal ion can thus be removed by CHELEX 100<sup>®</sup>. CHELEX 100<sup>®</sup> is known to be a very strong binding agent for  $\text{Hg}^{2+}$ , but these findings are in contrast to a previous report, where  $\text{Hg}^{2+}$  was incorporated into two adjacent TT base pairs in a DNA double helix and where only excess of  $\text{Hg}^{2+}$  was removed by CHELEX 100<sup>®</sup>.<sup>[57]</sup> There are several possible reasons for this apparent

discrepancy: It is feasible that uracil residues do not coordinate  $\text{Hg}^{2+}$  as strongly as thymine nucleobases. A further reason could lie in the different helical structures, as A-form RNA is clearly distinct from B-form DNA. Either such metal-mediated U-Hg-U base pairs are unfavourable or the wider A-form helix allows for a facilitated attack of CHELEX 100<sup>®</sup> compared to B-DNA, leading to removal of the  $\text{Hg}^{2+}$  from the double helix. Indeed, the model of such a metalated A-RNA shows that the ions are twisted around the helical axis and thus

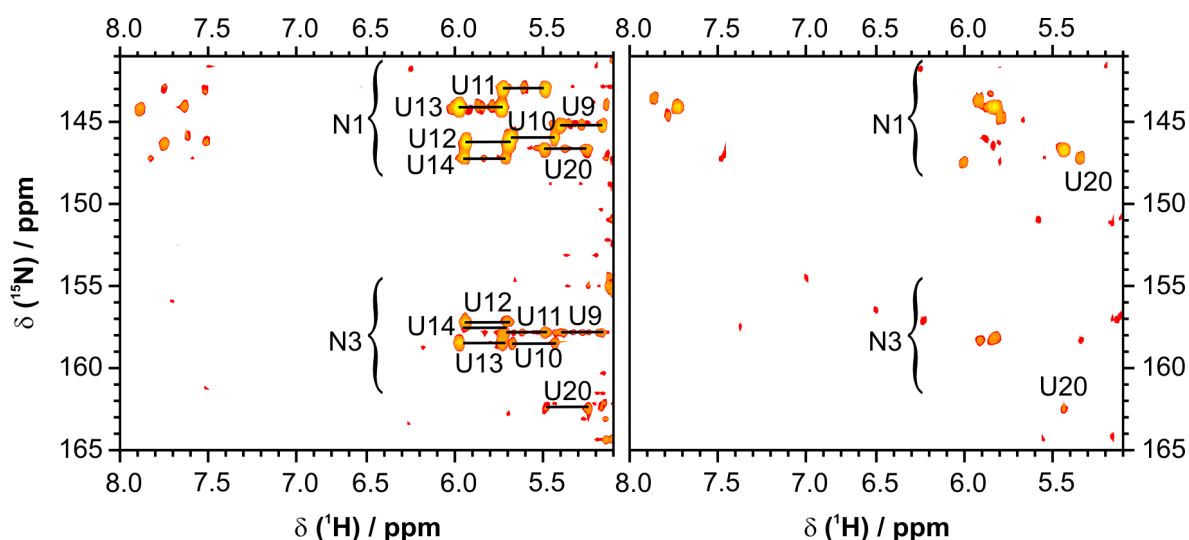


**Figure 2-7** Comparison of sections of the  $[\text{}^{15}\text{N}, \text{}^1\text{H}]$ -HSQC spectra of **PM03** (90 %  $\text{H}_2\text{O}$  / 10 %  $\text{D}_2\text{O}$ , 100 mM  $\text{NaClO}_4$ , pH = 7.2, 298 K) in the absence of  $\text{Hg}^{2+}$  (left) and after addition of  $\text{Hg}^{2+}$  and subsequent treatment with CHELEX for two hours (right).

located at the minor groove edge (Figure 2-6). Therefore, care has to be taken, when applying CHELEX 100<sup>®</sup> to remove excess of metal ions.

In order to investigate if the mercuric ions are really incorporated between two oppositely located uracil nucleobases, we performed a series of  $[\text{}^{199}\text{Hg}]$  and  $[\text{}^{15}\text{N}]$ -NMR experiments, to observe the metal ion and the coordinating N3 positions directly. No resonance other than that of the free mercuric(II) ions was observed in a  $[\text{}^{199}\text{Hg}]$ -NMR spectrum of **PM03·Hg**. This is not surprising, as first,  $\text{Hg}^{2+}$  is a kinetically labile metal ion, and second, it has recently been calculated that the nitrogen coordination leads to a strong broadening of the resonance of coordinated metal ions like  $^{199}\text{Hg}$ .<sup>[157]</sup> We therefore concentrated on the  $^{15}\text{N}$  resonances and

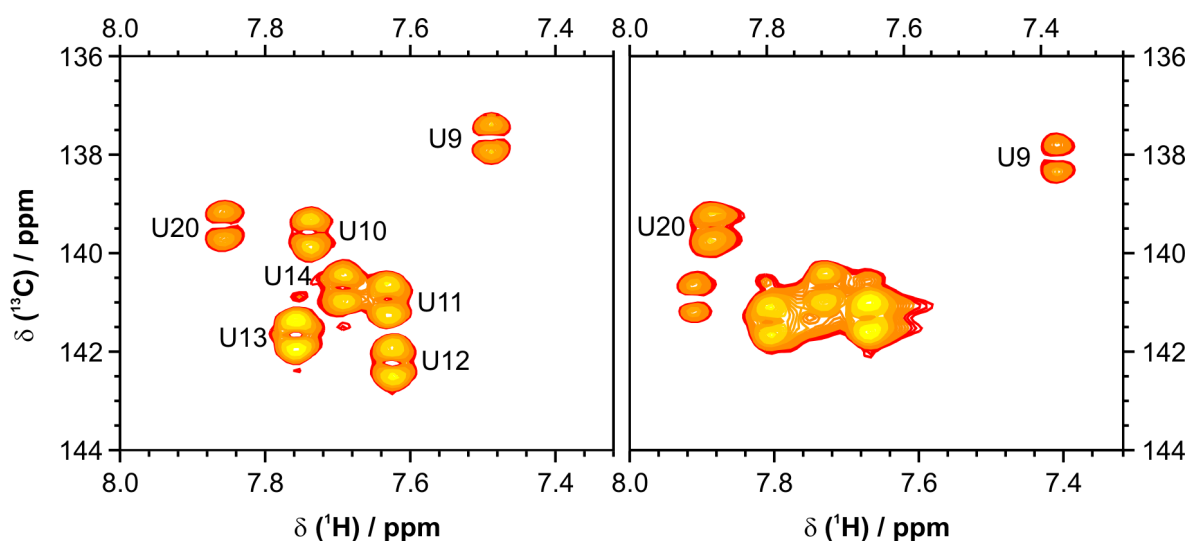


**Figure 2-8** Section of the  $^1J_{\text{HC}}$ -HSQC spectra of **PM03** (left) and **PM03·Hg** (right) showing the  $^1J$  correlation between H6 and C6 of all uracil residues. H6-C6 of U20 being located in a Watson-Crick base pair is least affected by the addition of  $\text{Hg}^{2+}$ .

recorded a  $^3J_{\text{HN}}$ -HSQC spectrum of  $^{13}\text{C}$ ,  $^{15}\text{N}$ -**PM03** correlating the H5 protons of the uracil to the endocyclic nitrogen atoms N1 and N3 (Figure 2-7). By comparison with the *sequential walk* (Figure 2-4), all N1 and N3 resonances of the seven uracil residues present in **PM03**, could be unambiguously assigned. After addition of  $\text{Hg}^{2+}$  and subsequent treatment with CHELEX for two hours, the N3 resonances of the six central pyrimidines were completely broadened out, whereas the N3 resonance of U20 were still detectable.

In addition to the  $^3J_{\text{HN}}$ -HSQC spectrum, also  $^1J_{\text{HC}}$ -HSQC spectra were recorded. Comparison of the H6-C6 cross-peaks showed that the ones of U20 and U9 are more or less unaffected by the addition of  $\text{Hg}^{2+}$ , whereas the resonances of the other five central uracil residues are strongly shifted (Figure 2-8). Taken together, these NMR spectra provide a further piece of evidence that  $\text{Hg}^{2+}$  inserts itself between two opposite uracil nucleobases leading in **PM03·Hg** to a continuous stretch of six metal-ion mediated base pairs.

### 2.2.1.3 Determination of the hydrodynamic radii

For further investigation of the formation of  $\text{Hg}^{2+}$ -mediated RNA duplexes, we determined the size of the molecules in solution by diffusion-ordered spectroscopy (DOSY) and dynamic light scattering (DLS). Both methods provide independently an accurate measure of the hydrodynamic radius  $r_H$  and taken together should give a clear picture not only of the size of the molecules, but also of the uniformity of the sample (Table 3-1). DOSY (Figure 2-9) and DLS experiments were measured with identical samples, i.e. under identical conditions.

To determine whether the helix under investigation can be modelled as a spherical particle, the ratio  $q$  of its theoretical length  $L$  and its diameter  $d$  ( $q = L / d$ ) needs to be known. The theoretical length  $L$  can be estimated based on the number of base pairs, assuming an average distance of 0.26 nm between individual base pairs along the helix axis (Table 3-1). For the diameter  $d$ , a value of 2.4 nm typical for an A-RNA double helix was used. It is obvious

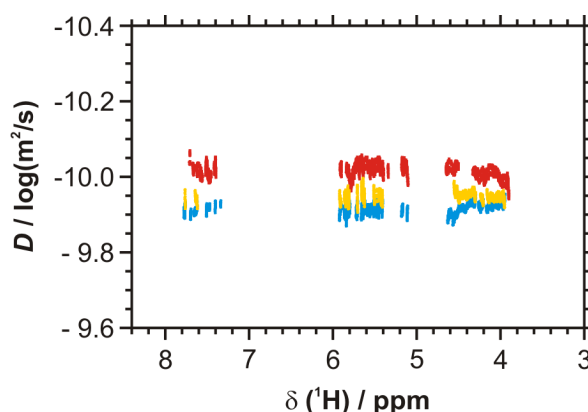


**Figure 2-9** Overlay of DOSY spectra of **PM03** in the absence of  $\text{Hg}^{2+}$  (blue), in the presence of 1.2 eq.  $\text{Hg}^{2+}$  (red) and after subsequent treatment with CHELEX for two hours (yellow).

that RNA (and DNA) molecules cannot necessarily be considered spherical because the length usually exceeds the RNA helix diameter of 2.4 nm. While for length-to-diameter ratios

$q < 2$  a spherical model according to the following equation

$$r_H = \frac{L}{2} \quad (1)$$

can still be successfully applied in the calculation of the apparent hydrodynamic radius, the use of a symmetrical cylinder model (equation 2) is recommended for molecules with  $2 < q < 30$ .<sup>[158,159]</sup>

$$r_H = \frac{L}{2(1 + 0.3 + 0.5 q^{1.6} - 0.1 q^{-2})} \quad (2)$$

**Table 2-2** Hydrodynamic radii  $r_H$  of **PM01** – **PM05** as determined by DLS ( $r_{H,DLS}$ ) and DOSY ( $r_{H,DOSY}$ ) experiments before and after the addition of  $\text{Hg}^{2+}$  and subsequent treatment with CHELEX 100<sup>®</sup>. Shown are also the theoretical length  $L$  of the respective RNA based on an average distance between base pairs of 0.26 nm along the helix axis, the ratio  $q = L/d$  (with  $d = 2.4$  nm being the diameter of A-RNA), and the theoretical hydrodynamic radius  $r_H$ . The latter was calculated according to a spherical model for  $q < 2$  (equation 1) or to a symmetrical cylinder model for  $q > 2$  (equation 2). If the sequence is able to form a hairpin or a duplex structure, theoretical values are given for both conformations.

		PM01	PM02	PM03	PM04	PM05
		Theoretical				
Hairpin	$L$			2.86	2.34	3.64
	$q$			1.19	0.98	1.52
	$r_H$			1.43	1.17	1.82
Duplex	$L$	4.42	5.46	5.72	4.68	7.28
	$q$	1.84	2.28	2.38	1.95	3.03
	$r_H$	2.21	2.00 <sup>[c]</sup>	2.04 <sup>[c]</sup>	2.34	2.28 <sup>[c]</sup>
		Experimental				
0.0 eq $\text{Hg}^{2+}$	$r_{H,DOSY}$ <sup>[a]</sup>	2.06±0.12	2.26±0.11	1.63±0.10	1.51±0.35	1.82±0.10
	$r_{H,DLS}$ <sup>[a,b]</sup>	2.13±0.02	2.00±0.02	1.56±0.02	1.74±0.04	2.40±0.05
1.2 eq $\text{Hg}^{2+}$	$r_{H,DOSY}$ <sup>[a]</sup>	2.18±0.33	2.36±0.16	2.06±0.17	2.18±0.38	2.81±0.90
	$r_{H,DLS}$ <sup>[a,b]</sup>	2.23±0.02	1.69±0.02	2.26±0.05	2.08±0.05	2.65±0.06 <sup>[d]</sup>
1.2 eq $\text{Hg}^{2+}$ / CHELEX	$r_{H,DOSY}$ <sup>[a]</sup>	2.26±0.18	2.11±0.17	1.75±0.11	1.44±0.27	1.34±0.20
	$r_{H,DLS}$ <sup>[a,b]</sup>	2.11±0.04	1.71±0.03 <sup>[d]</sup>	1.81±0.10 <sup>[d]</sup>	1.47±0.04 <sup>[d]</sup>	1.75±0.07 <sup>[d]</sup>

<sup>[a]</sup> All values are average values of at least five measurements. Error limits correspond to one standard deviation.

<sup>[b]</sup> The  $r_{H,DLS}$  values have been converted to D<sub>2</sub>O as solvent by applying the factor 0.8122<sup>[159]</sup> (see also Materials and methods sections 4.3.2 and 4.3.5). <sup>[c]</sup>  $r_H$  values corresponding to the apparent hydrodynamic radii calculated according to the symmetrical cylinder model ( $2 < q < 30$ ). See also Materials and methods 4.3.2. <sup>[d]</sup> These samples showed a high polydispersity in the DLS measurements.

Table 2-2 lists a comparison of the apparent hydrodynamic radii calculated according to equations 1 or 2, respectively, and the experimental values. In the absence of  $\text{Hg}^{2+}$ , **PM01** and **PM02** form stable duplex structures as can be judged from the relatively good agreement between calculated and experimental  $r_H$ . Of the three palindromic sequences, **PM03** clearly forms a hairpin structure with an experimental  $r_H$  of about 1.6 nm. In the case of **PM04** and **PM05**, a clear prediction of the structure cannot be made. The DOSY measurements hint in both cases that structures smaller than that of an extended double helix are formed, although the error in the case of **PM04** is rather large. Actually, for **PM05**, the hydrodynamic radius obtained by the DOSY measurements perfectly fits the value calculated for a hairpin structure. On the other hand, the DLS measurements give slightly larger values, suggesting the presence of a duplex. Most probably, none of the two constructs **PM04** and **PM05** are present in a distinct form. Hence, the diverging experimental values of  $r_H$  can be explained by the long non-Watson-Crick region of consecutive uracil nucleobases, giving rise to the coexistence of different structural conformations.

Upon addition of  $\text{Hg}^{2+}$ , the hydrodynamic radii of the non-palindromic double helices **PM01** and **PM02** do not change within the error limits. At most, a slight increase in size can be observed. While this is by no means proof for the formation of metal-ion mediated base pairs, it can very well be interpreted in this way: When substituting the amide protons of two oppositely located uracil residues by one central metal ion, no overall change of size of the helical molecule is expected. Additional UV spectroscopic measurements indeed showed that metal-modified nucleic acids with uracil-mercury-uracil base pairs are formed in the case of **PM01** and **PM02** (see Section 2.2.1.4). In the case of **PM03** that adopts a hairpin structure in the absence of  $\text{Hg}^{2+}$  ions with six uracil nucleotides in the loop, the addition of  $\text{Hg}^{2+}$  leads to a conformational change towards a regular double helix as can be seen from the 30 % increase of the hydrodynamic radius from about 1.6 to about 2.1 nm (Table 2-2). A logical explanation why the duplex becomes more stable than the hairpin in the presence of  $\text{Hg}^{2+}$  is its stabilization by metal-ion mediated U-Hg-U base pairs. A similar hairpin to duplex transition, also accompanied by an increase of  $r_H$  of about 30 %, has recently been reported by us for a DNA oligonucleotide containing artificial triazole base pairs that are capable of forming  $\text{Ag}^+$ -mediated base pairs.<sup>[45]</sup> Interestingly, previous work on thymine-mercury-thymine base pairs in DNA had shown that hairpins comprising  $T_2$  and  $T_3$  loops rearrange to form double helices with two and three metal-ion mediated base pairs, respectively, whereas a hairpin with a  $T_4$  loop does not rearrange but forms a metal cross-link between the first and the fourth thymine residue.<sup>[148]</sup> As we could show here, hairpins with larger loops such as the  $U_6$  loop in **PM03**

are able to form duplexes with consecutive metal-ion mediated base pairs. Presumably, intrastrand cross-links within a hairpin loop can only be formed if the nucleosides happen to be prearranged in the geometrically correct fashion. The structural changes that take place upon addition of  $\text{Hg}^{2+}$  to **PM04** and **PM05** cannot easily be derived from their hydrodynamic radii. The increase in size of both constructs in the presence of  $\text{Hg}^{2+}$  clearly suggests that long double helices are formed. However, the relatively high polydispersity as found particularly in the case of **PM05** points towards the formation of a complex mixture of duplexes, probably including partially overlapping oligonucleotides with bulges and mispaired bases.

Once the metal-modified oligonucleotides are treated with CHELEX 100<sup>®</sup> resin overnight to remove excess  $\text{Hg}^{2+}$ , the hydrodynamic radii of **PM01** – **PM05** return to approximately their respective values prior to the addition of  $\text{Hg}^{2+}$  (Table 2-2). Going along with the above mentioned observation that the  $^1\text{H}$ -NMR spectra of the constructs without  $\text{Hg}^{2+}$  and after CHELEX 100<sup>®</sup> treatment look identical, this suggests that the affinity of the chelator CHELEX 100<sup>®</sup> towards  $\text{Hg}^{2+}$  is too high to remove only excess metal ions. Instead,  $\text{Hg}^{2+}$  appears to be also removed from within the metal-ion mediated base pairs. While this can clearly be stated for the palindromic sequences **PM03** - **PM05**, the facts are not so clear for the non-palindromic sequences **PM01** - **PM02**, as they adopt regular double helix structures both in the absence and in the presence of  $\text{Hg}^{2+}$ . Indeed, Tanaka et al. have been able to use NMR spectroscopy to observe directly a thymine-Hg-thymine base pair in a DNA duplex after treating their sample with CHELEX 100<sup>®</sup>.<sup>[57]</sup> It therefore appears that a precise sequence design is necessary to obtain metal-modified nucleic acids with long continuous stretches of  $\text{Hg}^{2+}$ -mediated base pairs.

#### 2.2.1.4 UV-VIS and CD spectra of the transition to $\text{Hg}^{2+}$ -modified RNA duplexes

To further characterize the formation of the  $\text{Hg}^{2+}$ -mediated RNA duplexes, we followed the incorporation of the  $\text{Hg}^{2+}$  ions into different RNA constructs by UV-VIS and CD spectroscopy. (Figure 2-10 and Appendix 1 – Appendix 5). In a first step we examined the effect of  $\text{Hg}^{2+}$  on the melting behaviour of our RNA (0.5  $\mu\text{M}$  duplex form). **PM01**, **PM02**, and **PM03** all display a clear melting transition in the absence of  $\text{Hg}^{2+}$  being in accordance with the DOSY and DLS data (see Section 2.2.1.3), which showed that these constructs adopt distinct duplex or hairpin structures, respectively. The melting curve of **PM02** exhibits two melting transitions, whereby the first one at around 40°C probably stems from the pre-melting of the UU-wobble base pairs (Figure 2-10B). In contrast to **PM01** - **PM03**, **PM04** and especially **PM05** do not show a clear melting transition in the absence of  $\text{Hg}^{2+}$ , which is most

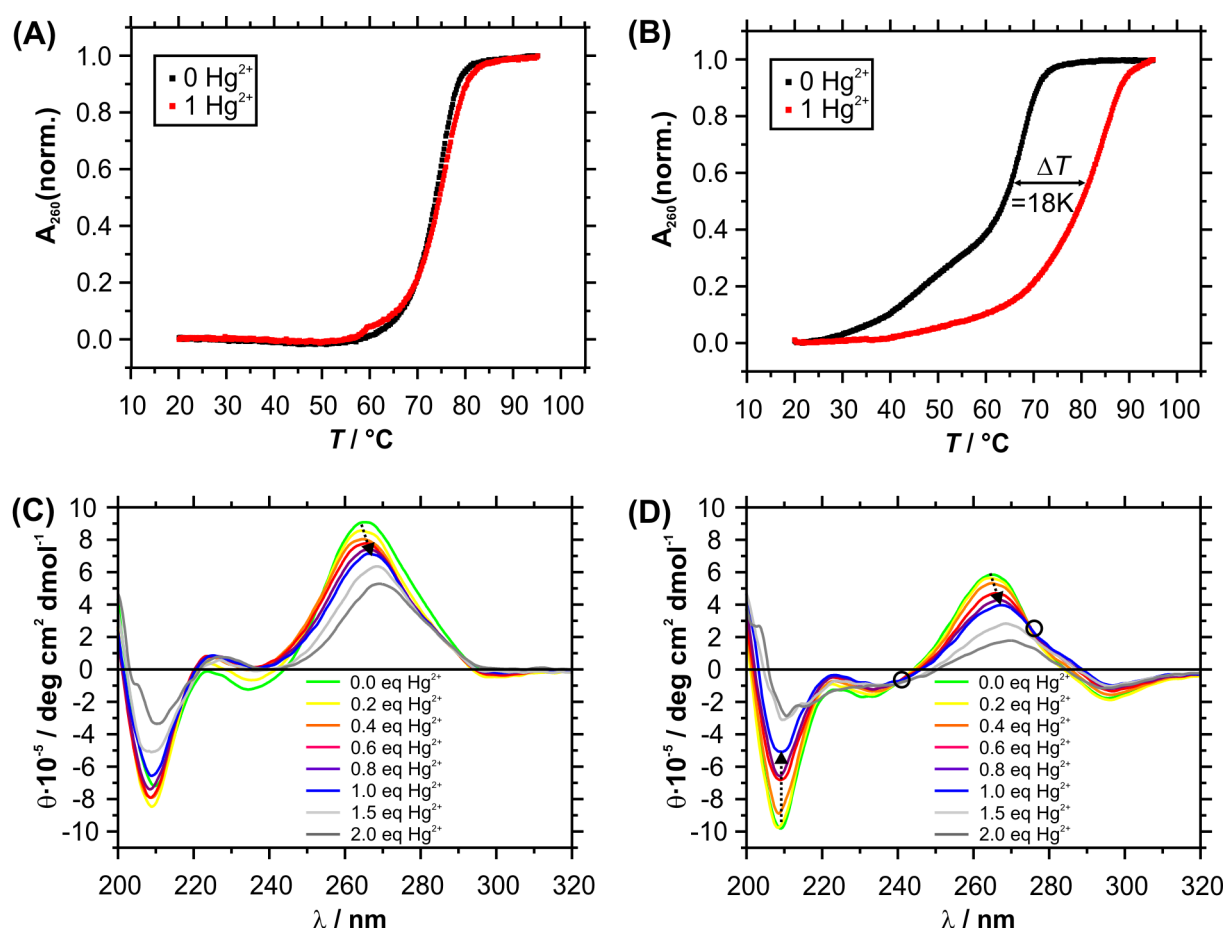


**Figure 2-10** Changes in CD spectra and melting temperature upon addition of  $\text{Hg}^{2+}$ . **(A)** Melting curve of **PM01** (0.5  $\mu\text{M}$  duplex) shows an increase in  $T_m$  of 1  $^\circ\text{C}$  upon addition of 1 eq.  $\text{Hg}^{2+}$  giving **PM01·Hg**. **(B)** For **PM02** (0.5  $\mu\text{M}$  duplex) an increase in  $T_m$  from 67  $^\circ\text{C}$  to 85  $^\circ\text{C}$  is observed upon addition of 1 eq.  $\text{Hg}^{2+}$  giving **PM02·Hg**. **(C)** CD spectra of **PM02** showing a continuous decrease and slight red shift of the maximum at 260 nm upon stepwise addition of  $\text{Hg}^{2+}$ . **(D)** CD spectra of **PM03** showing the same trend in spectral change as observed for **PM02**. In addition two isosbestic points at 240 nm and 275 nm (black circles) are observed up to the addition of 1 eq of  $\text{Hg}^{2+}$ .

likely due to the small number of Watson-Crick base pairs in a potential double helix. The addition of one equivalent of  $\text{Hg}^{2+}$  leads in all cases to an increase in melting temperature  $T_m$ : Whereas the increase in  $T_m$  is very modest in the case of **PM01** (1 K), **PM02** having six U-Hg-U metal modified base pairs, shows already a substantial rise from 67  $^\circ\text{C}$  to 85  $^\circ\text{C}$ . Parallel to the increasing number of uracil residues also the  $\Delta T_m$  values further rise to at least 23  $^\circ\text{C}$  for **PM04** and 50  $^\circ\text{C}$  for **PM05**. Although in the latter cases, the  $T_m$  of the non-metalated RNAs is rather ill-defined due to lack of defined structures, the trend is clear being a strong indication that  $\text{Hg}^{2+}$  is inserted into the UU pairs thereby stabilizing the duplex structures. In the case of **PM03**, a comparison of the melting temperatures before and after addition of  $\text{Hg}^{2+}$  is not meaningful, as this construct adopts different conformations under these conditions (hairpin vs. double helix). In principle, the addition of divalent metal ions generally has a stabilizing effect on a duplex due to better charge compensation. However, as

our measurements were carried out at a background of 100 mM NaClO<sub>4</sub>, the ionic strengths did change by less than 0.04 % upon addition of Hg(ClO<sub>4</sub>)<sub>2</sub> making it highly unlikely that such large effects are brought about by unspecific and random binding of metal ions.

Circular dichroism provides a good method to follow structural changes not only of proteins but also of nucleic acids. All three structure families of nucleic acids (A, B and Z-helical form) have a characteristic CD spectrum, whereas the A-helical RNA has a large positive ellipticity at 260 nm and a negative one at 210 nm.<sup>[160,161]</sup> Changes in the characteristic band at 260 nm correspond to hyperchromism of nucleobases as a result of helical stacking<sup>[162]</sup> and the band at 210 nm is associated with changes in loop structures.<sup>[163]</sup> Thus, changes in the shape of the CD spectrum can be directly related to structural changes in the RNA. To investigate structural changes of the RNAs upon addition of Hg<sup>2+</sup> ions, Hg(ClO<sub>4</sub>)<sub>2</sub> was added in steps of 0.2 equivalents and after each addition, the sample was heated to 70 °C and slowly cooled down to room temperature before recording of the spectrum. **PM01 - PM04** all displayed a minimum in ellipticity at 210 nm and a maximum at around 260 nm (Figure 2-10, Appendix 1, and Appendix 4) clearly indicating A-form helical regions in all constructs already in the absence of Hg<sup>2+</sup>. However, in the case of **PM04** a very high ellipticity was observed at 220 nm, rendering the maximum intensity change at 260 nm very small. Nevertheless, upon stepwise addition of Hg<sup>2+</sup> to obtain the metal modified RNAs **PM01·Hg - PM04·Hg** the same trends in spectral change were observed with all RNAs. Whereas the maximum at 260 nm decreased continuously, the opposite effect is observed at the minimum at 210 nm, meaning that the curve is somewhat flattening (Figure 2-10C, D). Two isosbestic points are thereby observed at 240 and 275 nm together with a slight red shift of the maximum by about 8 nm. Considering that the four building blocks of nucleic acids all provide very good binding sites for metal ions, it was now interesting to see the effect of the addition of excess Hg<sup>2+</sup>. Indeed, further binding was observed as exhibited by the accelerated red shift of the maximum absorbance and the fact that the two isosbestic points are no longer observed. Taken together, this is a clear indication that the first equivalent of Hg<sup>2+</sup> binds to the RNA strands in a way that does not disrupt the natural A-form helix. In contrast, an excess of metal ions show different binding properties. This finding can be explained if at first an incorporation of Hg<sup>2+</sup> ions into the UU base pairs takes place, which is followed by a more random coordination to additional sites like the N7 of purines or further nitrogen ligands.



## 2.2.2 Incorporation of thymine instead of uracil into RNA sequences

The previous results reveal that  $\text{Hg}^{2+}$  indeed replaces the protons of the uracil nucleobases, inserting itself in-between two such bases, but also show a less strong binding of  $\text{Hg}^{2+}$  ions to RNA as to DNA. At this point it remains to be determined whether this is a result of the exchange from dTTP by UTP or if it is due the different helical structure of B-DNA and A-RNA, respectively. Therefore, in a next step RNA sequences containing central dTs instead of Us were prepared and characterized by NMR, UV-VIS, and CD spectroscopy.

### 2.2.2.1 Wild-type *T7* RNA polymerase discriminates deoxyribonucleotides

More than ten independent crystal structures of the RNA polymerase from *enterobacterio phage T7*<sup>[164-173]</sup> give not only a precise view of the structural basis but also allow a detailed description of the transcription process (Figure 2-11). In general, polymerases are categorized into four classes on the basis of template (DNA or RNA) and sugar (deoxyribosenucleotides dNTPs or ribosenucleotides rNTPs) specificity. The *T7* RNA polymerase is a 99 kDa single polypeptide encoded in the *T7 bacteriophage* genome and catalyzes the processive polymerization of messenger RNA from nucleoside triphosphate precursors by using one strand of DNA as a template. The enzyme consists of a polymerase domain and an N-terminal domain whereas the polymerase domain is further been divided into a palm, thumb, and a fingers domain (Figure 2-11). The palm, thumb, and fingers domains of the *T7* RNA polymerase define the DNA binding and RNA synthesis catalytic site. The mechanism of

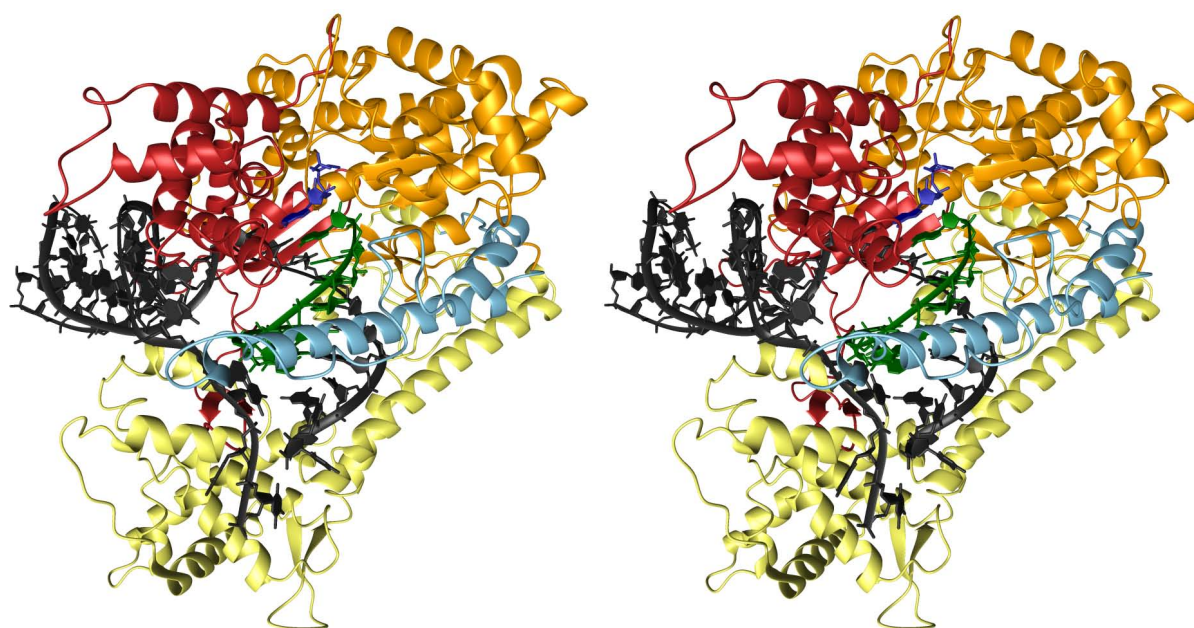


**Figure 2-11** Stereo view of the RNA polymerase elongation complex from *enterobacterio phage T7*. The enzyme is divided into N-terminal (yellow), palm (orange) thumb (pale blue), and fingers (red) domain and encloses the most parts of the DNA template (black), the RNA transcript (green) as well as the incoming rATP (blue). The figure has been prepared with MOLMOL<sup>[6]</sup> based on the PDB file 1S76.

transcription can be divided in three main stages: initiation, elongation and termination. In the initiation phase the *T7* RNA polymerase binds to a DNA specific promoter sequence, opens the double-stranded DNA at the

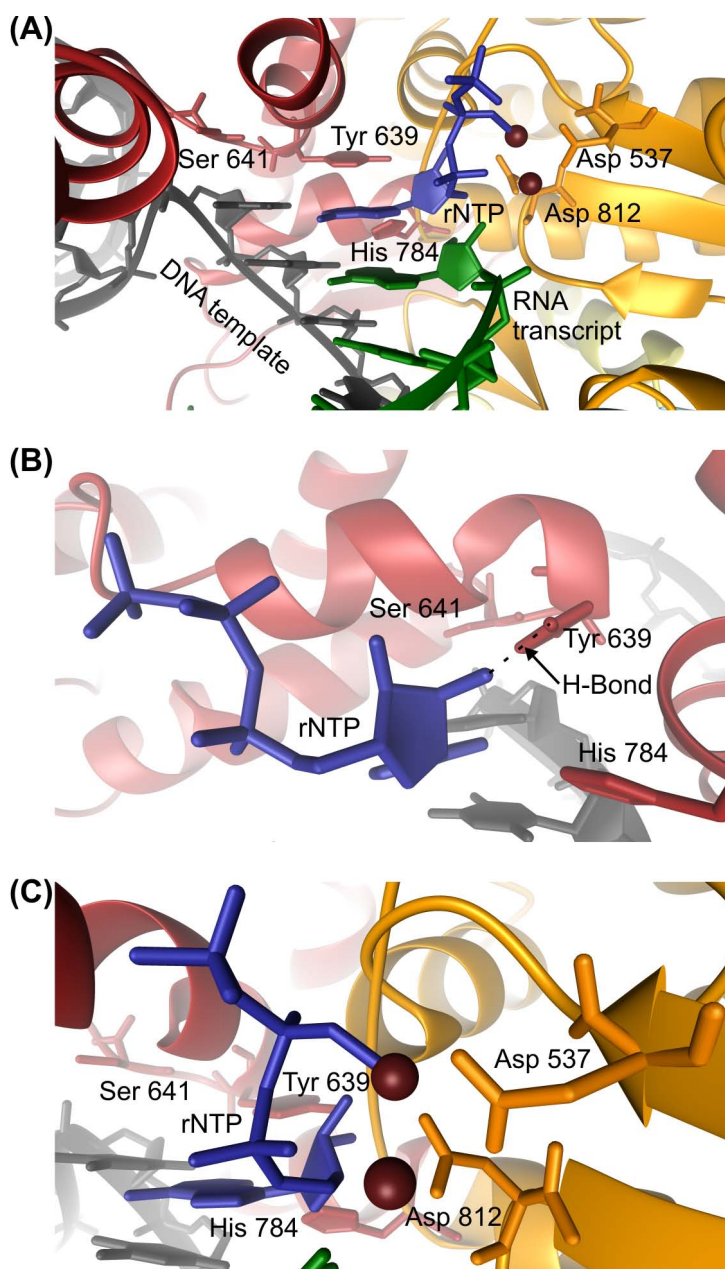


**Figure 2-12** Magnification of Figure 2-11 showing the active-site of elongation complex from *enterobacterio phage T7*. The palm domain is colored orange, the fingers domain red, the DNA template black, the RNA transcript green, the incoming ATP blue, and the magnesium ions involved in the catalytic reaction brown. (A) Close view of the catalytic center showing the amino acids probably involved in sugar discrimination as well as the aspartate residues that are conserved in every nucleic acid polymerase and are most critical for the catalytic process. (B) The amino acids Tyr 639 makes hydrogen-bonding interaction with the 2'-OH group of the incoming NTP, thus is essential for the discrimination of dNTPs. Further, influence on this activity by His 784 and Ser 641 is discussed controversial. (C) Asp 537 and Asp 812 are directly involved in catalysis via the interaction with the two magnesium ions. The figure has been prepared with MOLMOL<sup>[6]</sup> based on the PDB file 1S76.

the double-stranded DNA at the transcription start site to form and stabilize the transcription bubble and initiates RNA synthesis *de novo* starting preferentially with a purine base. This early stage of transcription is characterised by repeated abort of the initiation process leading to short RNA fragments 2-6 nucleotides in length.<sup>[174,175]</sup> After synthesis of a 10-12 long oligonucleotide, the polymerase has reached the elongation phase processively transcribing the entire RNA transcript without dissociation until termination. Upon termination, the transcribing complex dissociates and releases the single stranded RNA product.

The RNA synthesis, namely the repeated incorporation of rNTPs, requires the translocation of the product heteroduplex and the separation of the down-stream DNA duplex. Based on X-ray crystallographic (Figure 2-12) and biochemical studies a two-metal-ion mechanism similar to DNA polymerases is proposed (Figure 2-13).<sup>[156,176]</sup> Each addition of a single nucleotide can

be divided into four steps. First, the substrate NTP binds to the polymerase in a pre-insertion mode, followed by a second step in which the NTP occupies the NTP-binding site (N-site) and is base paired to the DNA template. The NTP is placed in a way that its electrophilic  $\alpha$ -phosphate is in close proximity to the 3'-OH group of the growing RNA that acts as the nucleophile and to the two magnesium ions. The 3' end of the RNA is in the priming site (P-site). In step three, the phosphoryl transfer reaction takes place producing the pyrophosphate ( $\text{PP}_i$ ) and extending the RNA transcript by one nucleotide. The reaction is catalyzed by two divalent metal ions typical  $\text{Mg}^{2+}$  ions that coordinate a pair of conserved aspartates (Asp 537 and Asp 812) of the palm domain (Figure 3-1). One of the metal ions coordinates to the 3'-OH group of the RNA, thus lowering the affinity of the 3'-OH for the hydrogen and facilitating the 3'-O-attack on the  $\alpha$ -phosphate. The other metal ion alleviates the release of the pyrophosphate group by coordinating one of the bridging oxygens. Furthermore, both metal

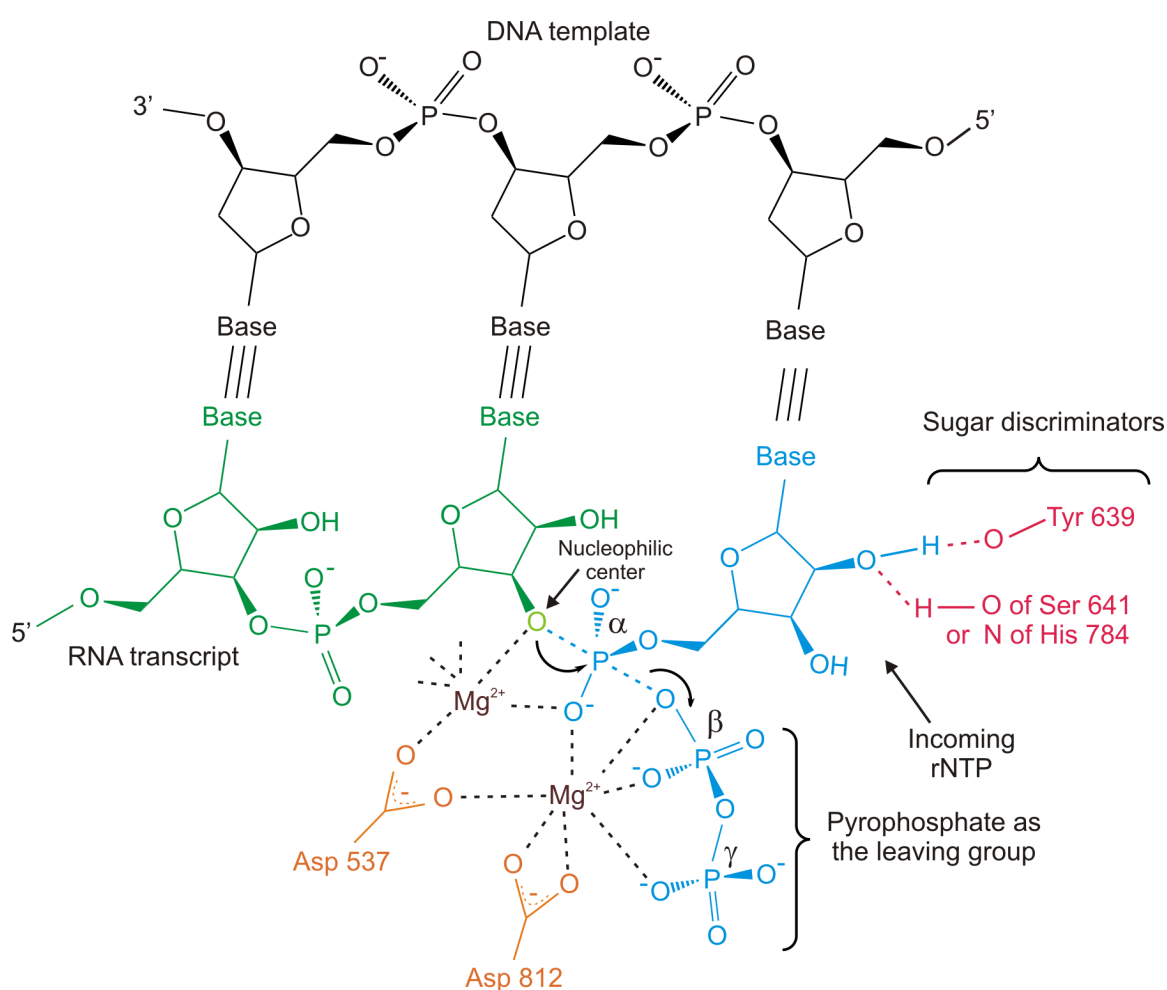


**Figure 2-13** Suggested reaction mechanism for T7 RNA polymerase phosphoryl transfer. The position of the two catalytic aspartate residues is arbitrary.

ions also stabilize the structure and charge of the expected pentacovalent transition state. In the final step, the elongated primer-template relocates relative to the active site metal ions and thereby the 3' end of the RNA moves from the N-site to the P-site, vacating the N-site for the next cycle of nucleotide addition.<sup>[156,176,177]</sup>

Structural analysis of different polymerases reveals that the active sites are closely related and similarly positioned within the active cleft even beyond the arbitrary assignment into classes on the basis of the use of DNA or RNA templates and dNTPs or NTPs. Thus, it appears that the basic mechanism of phosphoryl transfer is the same throughout the polymerase super-family, and only subtle modifications achieve the substrate specificity that is unique for each polymerase class.<sup>[178-180]</sup> However, the mechanism of substrate discrimination differs totally from each other. The substrate discrimination of DNA polymerases is mainly achieved through a "steric gate" mechanism. For example the *Klenow* fragment and the *HIV*-reverse transcriptase discriminate against ribose sugar because of bulky amino acid residues that make steric interaction with the 2'-OH group of the incoming nucleotide.<sup>[179]</sup> In contrast, RNA polymerases interact with NTPs in ways that are not possible for the smaller dNTPs.<sup>[179]</sup> In case of *T7* RNA polymerase the crystal structures reveal that the amino acid tyrosine at position 639 (Tyr 639) forms a hydrogen bond with the 2'-OH group of the incoming ribonucleoside triphosphate. Thus, mutagenesis studies have demonstrated that the mutation of Tyr 639 to phenylalanine lowers the specificity for NTPs by making the dNTPs a better substrate.<sup>[179,181-183]</sup> Furthermore, based on crystallographic studies obtained from the *T7* RNA polymerase initiation complex, it was also proposed that a histidine at position 784 (His 784) forms hydrogen-bonding interaction with the 2'-OH group, and therefore also could act as a sugar discriminator.<sup>[165]</sup> Nevertheless, the mutation of histidine 784 to alanine demonstrates that although this mutation significantly reduces the activity of the polymerase, it does not significantly reduce the level of ribose discrimination. Moreover, based on mutagenesis studies<sup>[184,185]</sup> it was also discussed if serin at position 641 (Ser 641) is actively involved in sugar discrimination. However, recent crystal structures as well as further mutagenesis studies do not support this assumption.<sup>[164-173,186]</sup> Despite numerous crystal structures of *T7* RNA polymerases the discrimination of dNTPs is still not fully understood. Besides, a further curiosity is that all DNA-dependent polymerases with regardless of their sugar specificity have a tyrosine in the sequence position corresponding to Tyr 639 of *T7* RNA polymerase. Although until now the discrimination of *T7* RNA polymerase against dNTPs cannot reverse completely, mutations of single amino acids can lower the substrate specificity substantially. Additionally, replacement of  $Mg^{2+}$  by  $Mn^{2+}$  can

further relax the sugar discrimination,<sup>[179,186]</sup> and thus allowing the incorporation of single dNTPs into RNA strands.

### 2.2.2.2 Incorporation of up to 20 consecutive dTTPs into RNA using a double mutant *T7* polymerase

Transcription trials of a well transcribing sequence incorporating dTTP instead of UTP were performed to check which polymerase is the best for our demand. We used three different polymerases, the wild-type, the single mutant Y639F (tyrosine was exchanged by phenylalanine) as well as the double mutant Y639F / S641A (for the second mutation serine was replaced by alanine) *T7* RNA polymerase. As expected no full-length transcript was obtained using the wild-type polymerase. The transcription stopped directly when the polymerase tried to incorporate the first dNTP. In contrast, with both mutated polymerases the

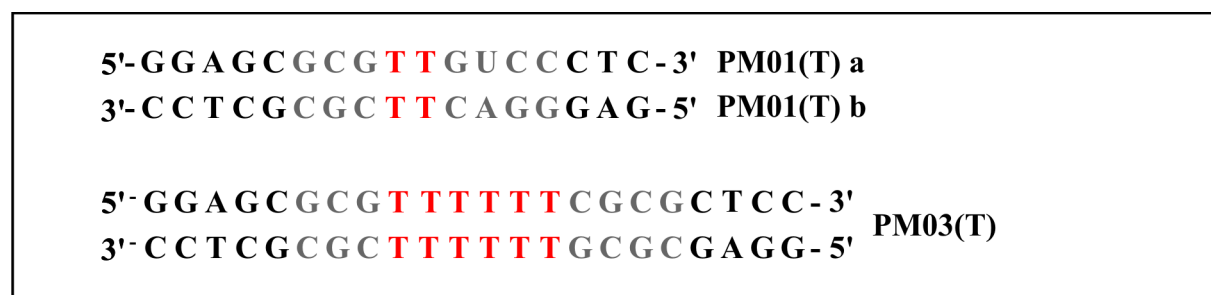


**Figure 2-14** The following constructs **PM01(T)** and **PM03(T)** correspond to the RNA constructs **PM01** and **PM03** (Figure 2-2). The UTPs are just replaced by dTTPs. Red indicates the continuous stretch of thymine and grey displays the Tanaka sequence.<sup>[57]</sup>

full transcript with similar yields could be achieved. However, slightly better yields were obtained with double mutant polymerase, thus in the following only the double mutant polymerase was used.

The first transcription was performed with **PM01(T)** (Figure 2-14) following the standard protocols for high yield transcription. **PM01(T)** corresponds to the RNA sequence **PM01** (Figure 2-2) containing dTTP instead of rUTP. The transcription yields of 5.1 nmol/mL for **PM01(T) a** as well as for **PM01(T) b** were a little bit lower than for the corresponding pure RNA sequences. Nevertheless, these yields are promising results to further increase the number of consecutive dTTPs. Therefore, in a next step **PM03(T)** (Figure 2-14) the pendant to **PM03** was transcribed giving a yield of 9 nmol/mL. The 18 % PAGE showed two main transcription bands due to the full-length transcript and an additional n+1 band. It is well known that *T7* RNA polymerase tends to add random nucleotides to the 3'-terminus of “run-off” transcripts.<sup>[152]</sup> By running the complete transcription solution on a 18 % PAGE, it was



possible to separate the  $n+1$  band from the 22 nucleotide long intended transcript. Moreover, additional transcription trials of the equivalent sequences of **PM04** and **PM05** (Figure 2-14) still showed distinct full-length bands. This nicely demonstrates that even up to 20 successive dNTPs, usually ignored by *T7* RNA polymerase, can be inserted using the double-mutant Y639F / S641A polymerase.

### 2.2.2.3 Spectroscopic characterization of PM01(T) and PM03(T)

To directly prove if indeed dTTP and not other NTPs were inserted into the sequence NMR experiments were performed with the palindromic construct **PM03(T)**. NMR is an excellent method to distinguish between dNTPs and NTPs due to the differences in chemical shift of the sugar moieties. The sugar protons resonances of the ribose nucleotides are all in the same chemical shift range of 3.8 - 4.8 ppm, except H1' that resonates between 4.8 and 6.0 ppm. By contrast, the sugar protons of the deoxyribose nucleotides show a different distribution of the chemical shifts. While the H1', H3', H4', H5', and H5'' protons have almost identical chemical shifts as the ones of NTPs, the H2' and H2'' protons resonate in a completely different range between 1.8 - 3.0 ppm due to the absence of the 2'OH group. Furthermore the incorporated dTs possess with the CH<sub>3</sub> group (0.8 - 2.0 ppm) a special feature that strongly simplifies the identification of the inserted thymines. The [<sup>1</sup>H,<sup>1</sup>H]-NOESY spectrum of **PM03(T)** (Figure 2-15) is nicely resolved even in the part of the thymine

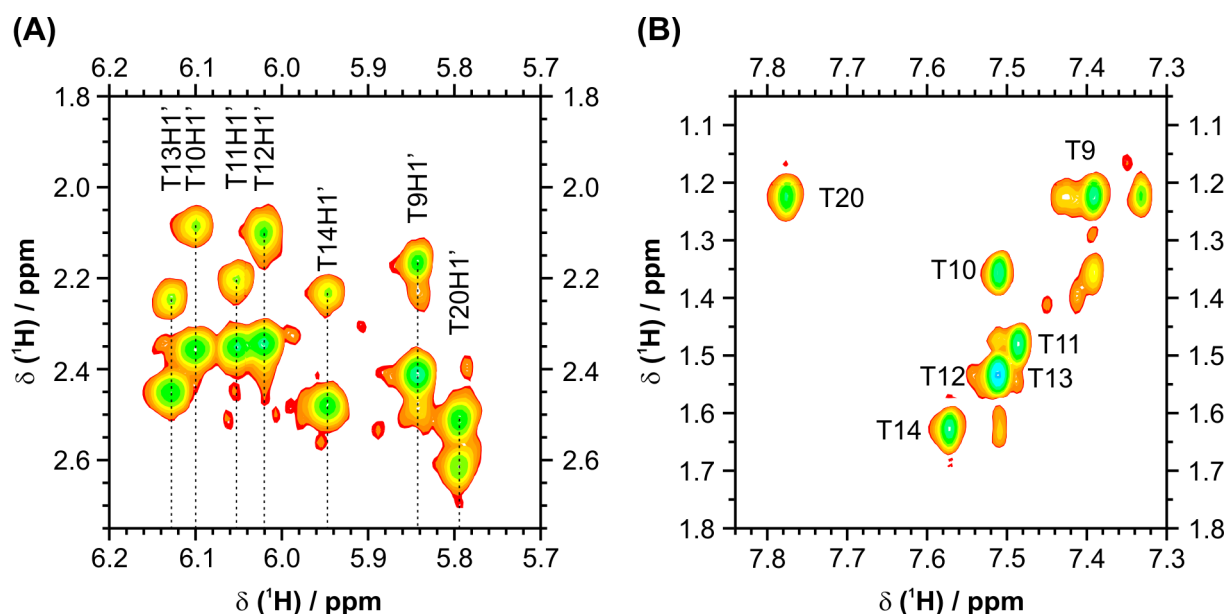


**Figure 2-15** 2D [<sup>1</sup>H,<sup>1</sup>H]-NOESY spectrum of **PM03(T)** acquired in 100 % D<sub>2</sub>O (100 mM NaClO<sub>4</sub>, pD = 7.2) at 298 K clearly shows that indeed seven thymines were incorporated. (Figure 2-8A). **(A)** The H1' - H2'/H2'' region of the NOESY spectra is depicted. It can be nicely seen that seven H1' (perpendicular) and H2'/H2'' (horizontal) resonances were observed. **(B)** The H6 - CH<sub>3</sub> region reveals also exactly seven crosspeaks. Six H6 protons show very similar resonances whereas the one belonging to T20 is slightly shifted just like U20 in **PM03**.

stretch. Moreover, especially the thymine resonances are very intense and sharp indicating a very well structured loop similar to the one of **PM03** (Figure 2-4). Seven different H2'/H2'' and CH<sub>3</sub> resonances, respectively, were observed clearly demonstrating that indeed seven dTTPs were incorporated. The chemical shifts of the six consecutive thymines are very similar, but still distinguishable and T20 is also like U20 in **PM03** slightly separated from the others.

To further investigate how the inserted dTs influence the RNA typical A-helical structure, CD spectra as well as UV melting curves of **PM01(T)** were recorded. Overlay of CD spectra from **PM01(T)** and **PM01** (Figure 2-16) shows that the general shape of the CD curves is the same. However, a small decrease as well as a slight red shift of the maximum at 260 nm can

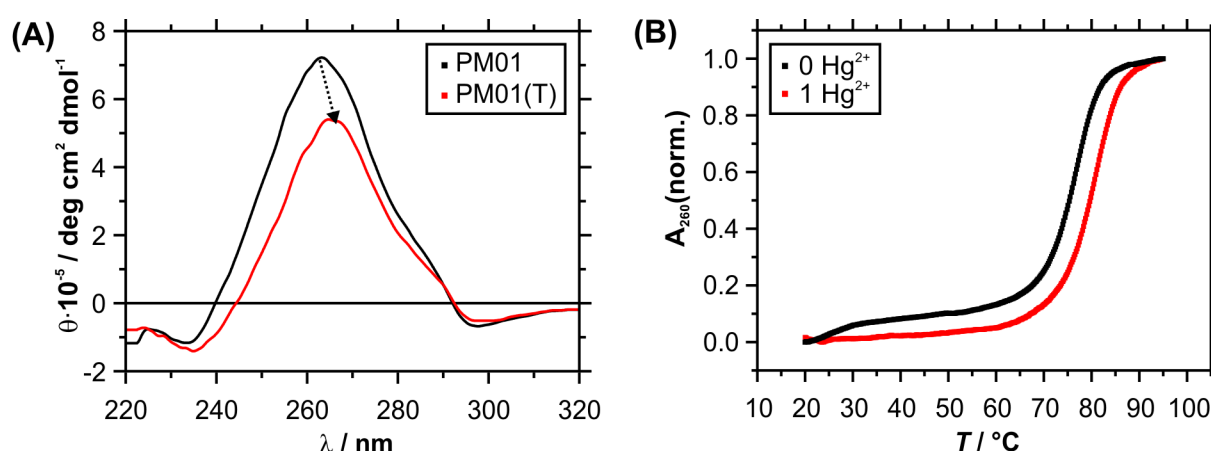


**Figure 2-16** CD spectra and UV melting studies of **PM01(T)**. **(A)** Change in the CD signal upon exchange of rUTPs by dTTPs. **(B)** Melting curve of **PM01(T)** (2  $\mu\text{M}$  duplex) shows an increase in  $T_m$  of 6  $^\circ\text{C}$  upon addition of 1 eq.  $\text{Hg}^{2+}$  giving **PM01-Hg(T)**.

be observed which is most likely due to marginal differences between A-helical RNA and A-helical DNA having the maximum ellipticity at 260 nm and 270 nm, respectively.<sup>[160]</sup> These results clearly demonstrate that RNA maintains in the A-helical form rather than undergoing a conversion to a different secondary structure. This is also supported by the UV melting studies of **PM01(T)** in the absence and in the presence of 1 eq of  $\text{Hg}^{2+}$  (Figure 2-16B) showing a very similar melting behaviour like **PM01** (Figure 2-10A). To accomplish equilibrium,  $\text{Hg}^{2+}$  was added thereby at least one week before acquisition (for further details see Materials and methods sections 4.3.3). Since the melting temperature of duplexes is generally concentration dependent,<sup>[187]</sup> additional melting curves of 2  $\mu\text{M}$  **PM01** (Appendix 6) were recorded, thus allowing a comparison of the melting temperatures. In the absence of  $\text{Hg}^{2+}$ , **PM01(T)** as well as **PM01** display a clear melting transition with a melting temperature of 76  $^\circ\text{C}$  and 80  $^\circ\text{C}$ , respectively. Upon addition of  $\text{Hg}^{2+}$  the melting temperatures of **PM01(T)** and **PM01** increase up to 82  $^\circ\text{C}$  and accordingly to 87  $^\circ\text{C}$  revealing an almost

identical  $\Delta T_m$ . Both, CD and UV melting studies reveal a very similar behaviour of **PM01(T)** and **PM01** indicating that the exchange of Us by dTs has almost no influence on the secondary structure. Even upon addition of 1 eq of  $\text{Hg}^{2+}$  no distinct difference in  $\Delta T_m$  was observed.

## 2.2.3 Using $^{199\text{m}}\text{Hg}$ PAC spectroscopy to investigate $\text{Hg}^{2+}$ -binding of nucleic acids

### 2.2.3.1 $^{199\text{m}}\text{Hg}$ perturbed angular correlation (PAC) spectroscopy

Perturbed angular correlation (PAC) spectroscopy is based on radioactive nuclei emitting two  $\gamma$ -rays, in our case the isotope  $^{199\text{m}}\text{Hg}$  (Figure 2-17). A property of this nuclear decay is that there is an angular correlation between the two  $\gamma$ -rays i.e., they are not emitted in random directions with respect to each other. However, if the nucleus interacts with its surrounding during decay, the angular correlation is perturbed. This is due to the interaction of the nucleus with the electrical field gradient (EFG)  $\neq 0$  created by the electrical charge distribution of the environment (hyperfine interaction). In PAC spectroscopy this perturbed angular correlation is measured providing a “fingerprint” of the local structure and dynamics. Therefore, the coordination geometry at the site of the PAC isotope (e.g., a metal ion binding site in nucleic acids) can be investigated in terms of possible coordinating ligands, ligand positions, and metal ion binding site flexibility.<sup>[188]</sup>

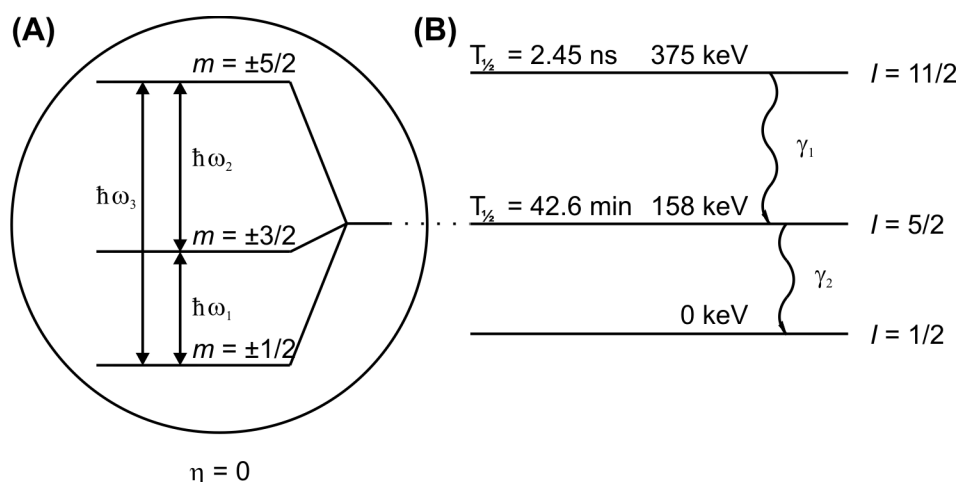


**Figure 2-17** Energy splitting of the PAC relevant nuclear level for  $^{199\text{m}}\text{Hg}$  due to the electric interaction (NQI) of the nuclear quadrupole moment ( $Q$ ) with the electric field gradient (EFG) originating from the surrounding charge distribution. In PAC spectroscopy, the hyperfine splitting of the intermediate nuclear level is measured, in a decay where two  $\gamma$ -rays are emitted successively. For a NQI and the intermediate state of  $^{199\text{m}}\text{Hg}$  with spin  $I = 5/2$ , this causes to a splitting into three doubly degenerate levels. **(A)** Schematic presentation of the decay of the 375 keV state of  $^{199\text{m}}\text{Hg}$ . **(B)** The energy splitting of the intermediate level in an axially symmetric EFG ( $\eta = 0$ ;  $\omega_2 = 2\omega_1$ ;  $\omega_3 = \omega_1 + \omega_2$ ). The figure was adapted from reference<sup>[188]</sup> and modified for the  $^{199\text{m}}\text{Hg}$  isotope.



$^{199}\text{mHg}$  PAC spectroscopy has been applied only to a limited number of biological systems, but promises to be an extremely powerful probe of  $\text{Hg}^{2+}$  structure and dynamics in biological environments.<sup>[188-190]</sup> Especially when used in conjunction with  $^{199}\text{Hg}$ -NMR the different timescale of these techniques can generate information that can be crucial for understanding the kinetics of conversion between different species in solution.<sup>[189]</sup>

### 2.2.3.2 For the first time $^{199}\text{mHg}$ PAC spectroscopy is applied on nucleic acids

As already mentioned  $^{199}\text{mHg}$  PAC spectroscopy in combination with other spectroscopic methods is an effective way to study and determine the  $\text{Hg}^{2+}$  coordination and geometry. Therefore PAC measurement of several RNA and DNA sequences (Figure 2-18) were performed to gain structural information of  $\text{Hg}^{2+}$  when bound between two uracils or two thymines, respectively. Of special interest is thereby if the less strong binding of  $\text{Hg}^{2+}$  ions to RNA compared to DNA can be explained by differences in coordination properties. The

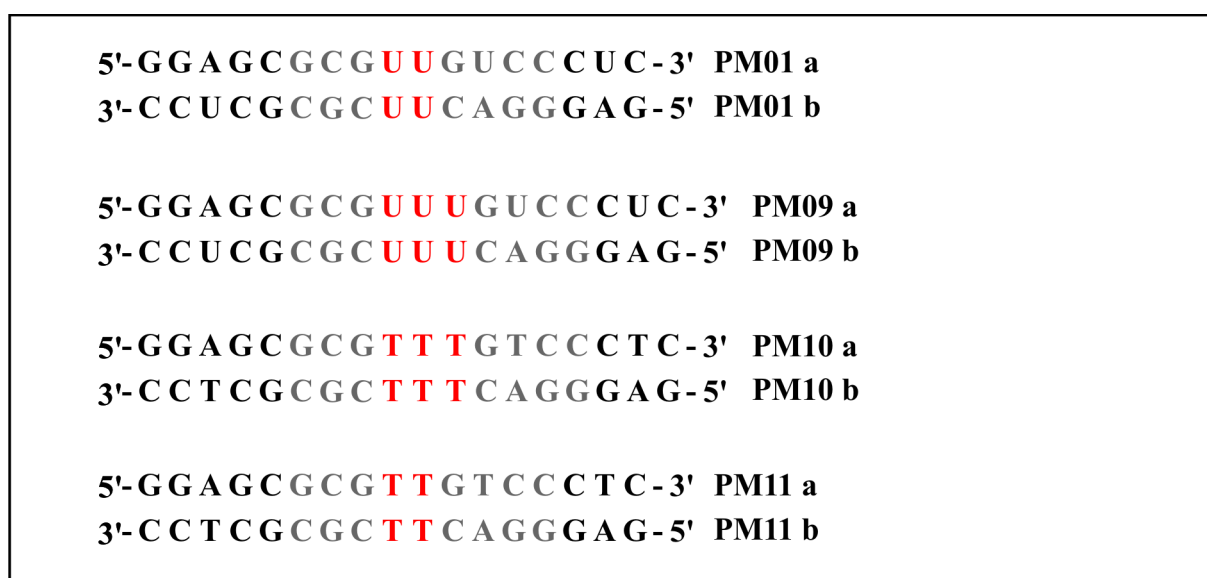


**Figure 2-18** RNA and DNA sequences used in PAC spectroscopy. **PM10** and **PM11** are the corresponding DNA sequences of the RNA constructs **PM01** and **PM09**. **PM01** and **PM09** and accordingly **PM10** and **PM11** differ only by one additional UU or TT mismatch, respectively.

applied sequences differ only in that respect that **PM09** has one additional UU-mismatch compared to **PM01**, and **PM11** and **PM10** are the corresponding DNA sequences of **PM01** and **PM09**, respectively.

To prove if the new RNA construct **PM09** behaves similar than **PM01**, CD spectra and UV melting studies of **PM09** (Figure 2-19) were performed in the same manner as mentioned for **PM01**. Both, CD spectra and UV melting studies reveal the same trend as already observed for **PM01** showing a decrease and slight red shift of the maximum in CD and an increase in melting temperature from 76 °C to 87 °C upon addition of  $\text{Hg}^{2+}$ . Furthermore,

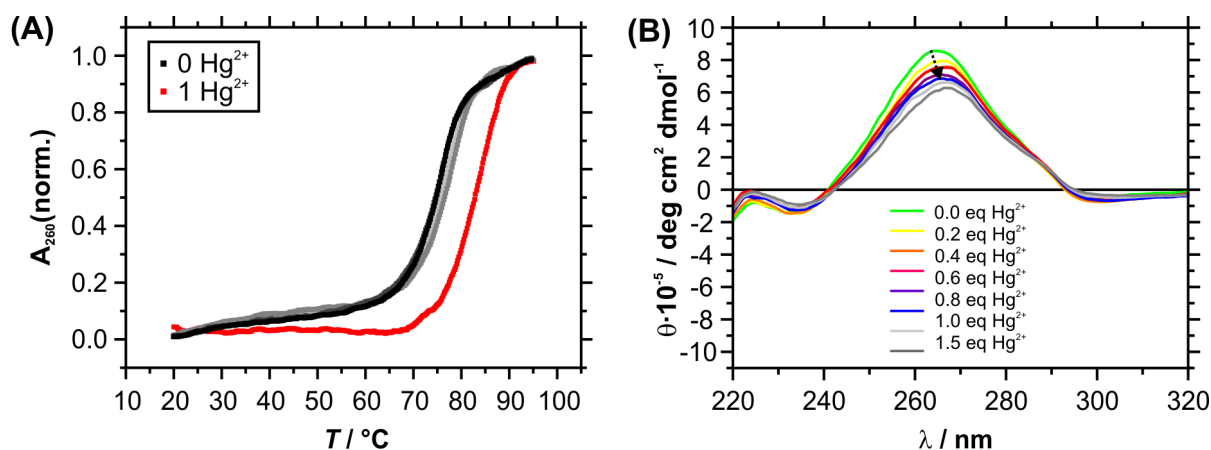


**Figure 2-19** Changes in melting temperature and CD spectra of **PM09** upon addition of  $\text{Hg}^{2+}$ . **(A)** The addition of 1 eq  $\text{Hg}^{2+}$  causes an increase in melting temperature from 76  $^\circ\text{C}$  (black) to 87  $^\circ\text{C}$  (red). However, in the presence of 1 eq  $\text{Hg}^{2+}$  the first cooling (light grey), the second heating (grey), and the second cooling curve (dark grey) display the same melting behavior as in the absence of  $\text{Hg}^{2+}$ . **(B)** Similar to all RNA sequences characterized above, the CD spectra of **PM09** reveal a decrease and slight red shift of the maximum at 260 nm upon stepwise addition of  $\text{Hg}^{2+}$ .

$\Delta T_m = 7 \text{ K}$  of **PM01** (section 2.2.2.3) as well as  $\Delta T_m = 11 \text{ K}$  of **PM09** display the same increase of 3 to 4  $^\circ\text{C}$  per uracil-uracil base pair upon addition of 1 eq of  $\text{Hg}^{2+}$ . However, also the results of **PM09** indicate that mercury binding between the UU-mismatches is not so strong. In particular an additional melting cycle (Figure 2-19A) of **PM09** demonstrates that denaturation of the metal-modified RNA duplex leads to the loss of  $\text{Hg}^{2+}$  ions. Moreover, the  $\text{Hg}^{2+}$  ions were not reassembled anymore during an equilibration time of 30 minutes between the cooling and the heating cycle.

The PAC experiments were carried out with the radioactive  $^{199\text{m}}\text{Hg}$  isotope at the ISOLDE facility in CERN in collaboration with the group of Prof. Lars Hemmingsen (Copenhagen, Denmark). with a total volume of 350  $\mu\text{L}$ . The  $^{199\text{m}}\text{Hg}$  as well as nonradioactive  $\text{Hg}(\text{ClO}_4)_2$  giving a total of 0.91 equivalents  $\text{Hg}^{2+}$  was added to 25  $\mu\text{M}$  RNA solution of **PM01**, **PM09**, **PM10**, and **PM11** (for details see Materials and methods section 4.3.6).

Figure 2-20 shows the FOURIER transforms of the  $^{199\text{m}}\text{Hg}$  PAC spectra

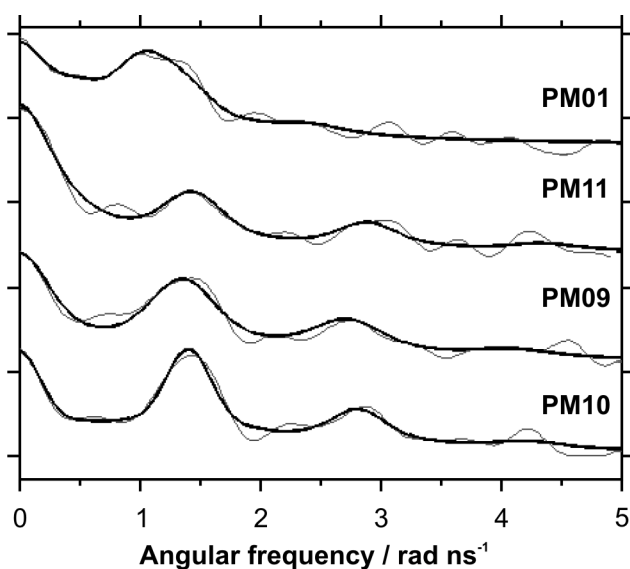


**Figure 2-20**  $^{199\text{m}}\text{Hg}$  PAC spectra of **PM01**, **PM11**, **PM09**, and **PM10**. All solutions contained 25  $\mu\text{M}$  RNA or DNA, 100 mM  $\text{NaClO}_4$ , 5 mM MOPS pH 6.8 and 0.91 eq of  $\text{Hg}^{2+}$ . The thin lines represent the FOURIER transform of the experimental data and the bold lines represent the fit.

**Table 2-3** Parameters used to the PAC data.<sup>[a]</sup>

	$\nu_Q$ [GHz]	$\eta$	$\delta \times 100$	$1/\tau_c$ [ $\mu\text{s}^{-1}$ ]	$A \times 100$	$\chi_r^2$
<b>PM01</b>	0.78(3)	0.68(8)	12(9)	0(39) 1000(450)	6(3) 8(4)	0.80
<b>PM11</b>	1.53(3)	0(1)	0(4)	240(100) 450(100)	9(2) 3.9(8)	0.72
<b>PM09</b>	1.44(2)	0(1)	3(3)	255(45)	16(1)	0.92
<b>PM10</b>	1.47(2)	0(1)	5(2)	135(30)	15(1)	0.80

<sup>[a]</sup> The numbers in parenthesis are the standard deviations of the fitted parameters.

corresponding to these RNA sequences. All four spectra were fit with two nuclear quadrupole interactions (NQIs) and each NQI was modeled by using a separate set of parameters that includes  $\nu_Q$ ,  $\eta$ ,  $\delta$ ,  $1/\tau_c$ , and  $A$ . The parameters used to these PAC data are reported in Table 2-3. However, fitting the spectra was difficult, and there may be other fits as good as those presented. It should be noted that for a spin 5/2 nucleus, which is the case for the nuclear level of  $^{199}\text{Hg}$ , one NQI manifests itself as three peaks in the FOURIER transform of the PAC data. In solution the molecules are randomly oriented, and thus the intensity distribution of the three peaks from each signal is such that the lowest frequency peak has highest intensity, the second intermediate intensity and the third lowest intensity.

Already at the first glance it is obvious that all spectra look somewhat similar, but with slightly different frequencies and intensities. The PAC spectrum of **PM10** displays the most intense signal belonging to one relatively clear NQI. This NQI falls in the range of linear  $\text{HgS}_2$  structures, but more interestingly, it is also quite similar to the NQI observed for the bis(benzamido) $\text{Hg(II)}$  coordination compound.<sup>[191]</sup> Thereby the linear N-Hg-N coordination is the dominant interaction. Nevertheless, the structure might also be viewed as an irregular four coordinate geometry with two additional oxygens, although the Hg-O distances are somewhat larger than the Hg-N bonds. For **PM09** a PAC spectrum akin to that of **PM10** was observed, thus indicating a similar structure. However, the PAC signal appears to be more affected by dynamics on the ns time scale, that is maybe due to ligand exchange dynamics or internal dynamics in the double helix. For **PM01** and **PM11** the picture is somewhat similar, but with some complications. There is a fraction of the signal that is highly similar to that observed for **PM10**, and thus also to the PAC signal from bis(benzamido) $\text{Hg(II)}$ . But, there is an additional

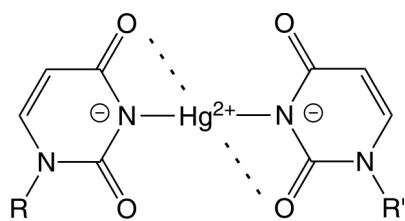


**Figure 2-21** Schematic depiction of an uracil-mercury-uracil base pair. The PAC results indicate that beside the linear coordination between two nitrogens an additional coordination to oxygens (either belonging to the own bases or to the adjacent ones) is reasonable.

signal either with very low frequency or significantly affected by dynamics. If the latter is the case it may be unbound or unspecifically bound  $\text{Hg}^{2+}$ .

Here, we have presented the first  $^{199\text{m}}\text{Hg}$  PAC measurements applied in nucleic acids. Unfortunately, repetition of some PAC spectra (results are not shown) reveal that the results were not reproducible. Moreover, no general trend could be observed to draw a logical conclusion. Nevertheless, the signals found so far clearly indicate that  $\text{Hg}^{2+}$  is bound between two nitrogens and

also additional coordination to oxygens can be assumed (Figure 2-21). These results are well in line with a recent crystal structures of N1-(3-hydroxypropyl)-5-fluoro-uracilate-mercury(II)<sup>[192]</sup> that in contrast to the crystal structure of 1-methylthymine-mercury(II) (2:1 complex)<sup>[147]</sup> also shows additional coordination to oxygen.

However, it appears that most likely the sample preparation is the critical point. As described in Materials and methods section 4.3.6,  $\text{Hg}^{2+}$  was added just 10 minutes before acquisition and apparently it was not enough time to insert the entire  $\text{Hg}^{2+}$  into the duplexes. In particular, the UV melting studies of **PM09** (Figure 2-19A) show that even half an hour was not enough to reassemble  $\text{Hg}^{2+}$ . Therefore further investigation of these systems is needed. On the hand the preparation has to be optimized to achieve the fully occupied duplex form in a reproducible manner. Besides, for the PAC measurements it is necessary to simplify the system using just one UU or TT mismatch to get a more precise picture of the  $\text{Hg}^{2+}$ -binding properties to DNA and RNA, respectively.

## 2.3 Conclusions and outlook

Here we have shown that potential molecular wires made from nucleic acids with metal-ion mediated base pairs can be synthesized by *in vitro* transcription using *T7* RNA polymerase. This is a simple and straightforward approach to obtain wires of distinct length and sequence, which can be easily defined by the template strand. *T7* RNA polymerase thereby shows the capability to insert long stretches of the same nucleotide, i.e. uracil in our case, without much loss of processivity. Moreover, just by mutating two amino acids (Y639F / S641A) of the *T7* RNA polymerase also the corresponding sequences could be achieved with similar transcription yields containing the thymine deoxynucleotide instead of the uracil nucleotide. However, in the case of continuous stretches of more than ten identical residues, not only the full-length transcript and the typical  $n+1$  band are observed, but also some shorter abortion products. It seems that the *T7* RNA polymerase loses partially its precision, when too many nucleotides of the same kind are lined up in a row. Nevertheless, these different transcription products can be well separated by denaturing 18 % PAGE. It is feasible that optimization of the transcription conditions, or further mutations of the polymerase might enhance the capability of *T7* RNA polymerase to build up such special nucleic acid strands.

By NMR, UV-VIS, and CD spectroscopy as well as DLS we could also demonstrate that all RNA constructs described above indeed incorporate  $\text{Hg}^{2+}$  ions into the helix. Thereby  $\text{Hg}^{2+}$  replaces the protons of the uracil nucleobases and inserts itself in-between two such bases. As was shown by DOSY and DLS measurements, the double helices **PM01·Hg**, **PM02·Hg**, and **PM03·Hg** are of defined size and length corresponding to well-defined metal-modified duplexes with properly base-paired ends. These RNA helices comprise continuous stacks of up to six metal-ion mediated base pairs. In the case of **PM04·Hg** and **PM05·Hg** with ten and twenty consecutive uracil residues, respectively, not only single products of defined size were obtained. This indicates that a precise design of the nucleic acid sequence is necessary to obtain long stretches of consecutive metal-mediated base pairs. Besides, to proof the incorporation of thymine deoxynucleotides into RNA, NMR experiments of **PM03(T)** were performed, clearly demonstrating that indeed thymine deoxynucleotides were inserted. Moreover, CD and UV melting studies reveal that the sequences retain their RNA typical A-helical form and that they behave like their corresponding pure RNA sequences upon addition of  $\text{Hg}^{2+}$  ions. However, in both cases the  $\text{Hg}^{2+}$ -binding was not that strong as recently observed for DNA.<sup>[57]</sup> Therefore  $^{199\text{m}}\text{Hg}$  PAC measurements were performed to elucidate possible differences of  $\text{Hg}^{2+}$ -coordination in RNA and DNA, respectively. This method was

applied for the first time on nucleic acids but unfortunately, no distinct geometry could be observed. Nevertheless, the results proof the linear coordination between two nitrogens but also indicate an additional coordination to oxygens that is well in line with recent crystal structures.

These first examples of metal-mediated RNA double helices demonstrate that RNA appears to be a viable candidate for the generation of metal-modified nucleic acids. First, RNA duplexes are less susceptible to hydrolysis than the respective single strands due to a positioning of the 2'-OH group in the minor groove of the double helix. Therefore the 2'-OH group cannot easily attack by the adjacent phosphodiester bond. Indeed, no sign of degradation was detected for any of the metalated RNA duplexes during the course of our experiments. Secondly, and more importantly, the divalent metal ions are confined to the interior of the duplex; hence they cannot participate catalytically in any potential hydrolysis step. In the near future, the capability of *T7* RNA polymerase to generate even longer continuous stretches of identical nucleobases without the emergence of too much "frame shifting" certainly needs to be investigated. Further improvement of the sample preparation is also required to obtain metal-mediated RNA duplexes in a reproducible manner. Once such longer constructs are at hand, they could be used to determine experimentally the extent to which the incorporation of metal-ion mediated base pairs modifies the electrical properties of the respective nucleic acids.

### 3 Using artificial imidazole nucleobases to construct consecutive metal-mediated base pairs in DNA

#### 3.1 Introduction

Metal-mediated base pairs can either be formed by natural nucleosides as described in the previous chapter or by artificial nucleosides that provide even more combinations. Although plenty of metal-mediated base pairs have been generated in DNA,<sup>[43-62]</sup> RNA,<sup>[193]</sup> GNA (glycol nucleic acid),<sup>[63]</sup> and also PNA (peptide nucleic acid),<sup>[64-69]</sup> structural information on such metal modified nucleic acids is very scarce. Only one DNA double helix comprising two non-neighbouring metal-mediated base pair has been structurally characterized to date.<sup>[44]</sup> In addition, the structure of one metal-containing GNA duplex is known.<sup>[194]</sup> Neither of these contains a continuous stretch of metalated base pairs despite the enormous interest in this type of modification. Interestingly, in neither of the known structures, the helices adopt the canonical B-type structure. The DNA duplex containing two pyridine-2,6-dicarboxylate-Cu<sup>2+</sup>-pyridine base pairs crystallizes in a Z-conformation, probably as a result of the propensity of Cu<sup>2+</sup> ions to bind additional axial ligands.<sup>[44]</sup> The structural distortion that is necessary to place these ligands above and below the square planar Cu<sup>2+</sup> coordination environment provided by the artificial nucleosides leads to a destabilization of the B-conformation and a concomitant stabilization of the Z-conformation. The GNA duplex on the other hand, adopts a conformation that is entirely different from the canonical A-, B- or Z-form and is largely a result of the unnatural backbone.<sup>[194]</sup>

To fill in the gap and gain structural insight into a nucleic acid double helix that contains metal ions along a stretch of its helical axis we investigated a self-complementary oligonucleotide with three consecutive artificial imidazole nucleosides in its centre (Figure 3-1). The oligonucleotide was prepared by members of the collaborating group of Prof. Jens Müller (Münster, Germany) using DNA solid phase synthesis. It was previously shown that in the absence of transition metal ions such a type of sequence adopts a hairpin structure with the artificial nucleosides located in the loop. A rearrangement to form a regular double helix with consecutive metal-mediated base pairs takes place in the presence of Ag<sup>+</sup> ions.<sup>[45]</sup> Based on this observation, which has also been reported for other nucleic acids, other nucleobases and other metal ions,<sup>[193]</sup> we substituted the 1,2,4-triazole nucleosides used in

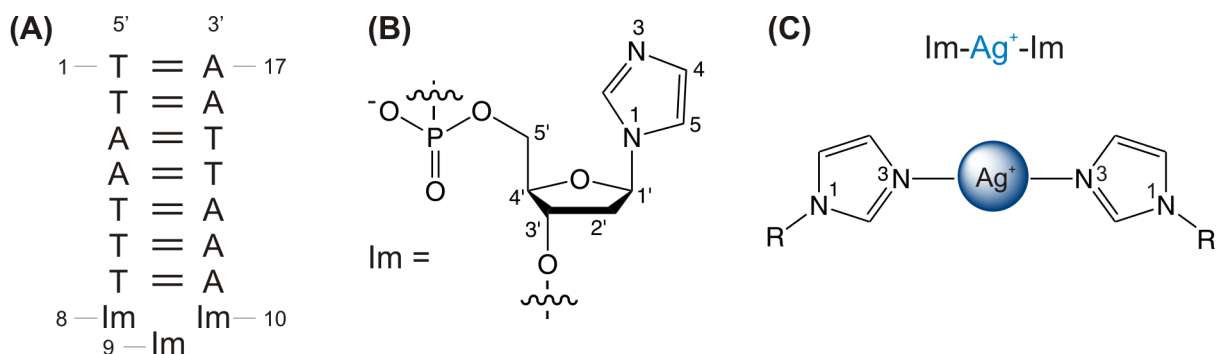


**Figure 3-1** Description of the oligonucleotide system under investigation. **(A)** Schematic representation of the hairpin with the numbering scheme used throughout this thesis (A = adenine, T = thymine, Im = imidazole). **(B)** Chemical structure of the artificial imidazole nucleoside including the atom numbering scheme. **(C)** Artificial imidazole-silver-imidazole base pair coordinating the  $\text{Ag}^+$  ion between the N3 nitrogens.

those previous experiments by imidazole nucleosides because of their superior  $\text{Ag}^+$ -binding properties. In particular, DFT calculations of two 1-methylimidazoles and one  $\text{Ag}^+$  ion as putative metal-mediated base pair show that the energy difference between the fully optimized geometry and the planar geometry with cisoid methyl groups necessary for a Watson-Crick base pair surrogate is small enough to allow a planar conformation that is required for implementation into artificial oligonucleotides. Moreover, the C(methyl)-C(methyl) distance of 10.8 Å as found in the calculation is in the range of the average distance between the C1' atoms of idealized B-DNA (10.85 Å).<sup>[195]</sup> Besides, the presence of three hydrogen atoms in imidazole as compared to two hydrogen atoms in triazole yields more  $^1\text{H}$ -NMR resonances, thereby increasing the number of possible constraints available for the structure refinement. All these conveniences make this oligonucleotide an ideal candidate to study structural changes upon addition of  $\text{Ag}^+$  ions as well as to characterize the metal binding properties of the metal-mediated bases pair by NMR. Furthermore, as the reaction with metal ions is always in competition with the reaction of protons, it is important to know also the acid-base properties. Therefore, the acid-base properties of each imidazole moiety in the oligonucleotide were investigated using NMR. To study the influence of the structure on these properties also the deoxynucleoside 5'-monophosphate  $\text{dImMP}^{2-}$  was synthesized by the collaborating group of Prof. Dr. Jens Müller. By combination of potentiometric pH titration and  $^1\text{H}$  and  $^{31}\text{P}$ -NMR chemical shift experiments its acid-base behaviour was determined and the micro acidity constants of  $\text{H}_2(\text{dImMP})^\pm$  could be obtained. These data was used for a direct comparison with the acid-base properties of the imidazole moieties embedded in the oligonucleotide.



## 3.2 Results and discussion

### 3.2.1 The 1-(2'-deoxy- $\beta$ -D-ribofuranosyl)imidazole 5'-monophosphate ( $\text{dImMP}^{2-}$ )

Despite the evident relationship to purine nucleotides, the unsubstituted imidazole ribonucleotide, upon removal of the annelated pyrimidine ring, has not been studied yet. This is also true for its 2'-deoxy derivative,  $\text{dImMP}^{2-}$  (Figure 3-2). The nucleotide analogue  $\text{dImMP}^{2-}$  can be incorporated into a short DNA strand which, upon addition of  $\text{Ag}^+$  gives rise to special structures like metalated duplexes (see chapter 3.2.3).<sup>[196]</sup> In the absence of  $\text{Ag}^+$ , the protonation state of the imidazole bases strongly affect local structures (see also chapter 3.2.2).<sup>[197,198]</sup> To be able to rationalize the following NMR solution structures and to interrelate them with the acid-base and metal ion-binding behaviour of the DNA analogue, the acid-base properties of  $\text{dImMP}^{2-}$  were studied. These studies allow a general prediction of the metal ion-binding properties of  $\text{dImMP}^{2-}$  and a comparison with those of the purine nucleotides.

#### 3.2.1.1 Potentiometric pH titrations of $\text{H}_2(\text{dImMP})^+$

$\text{dImMP}^{2-}$  (Figure 3-2) can accept three protons, two at the phosphate group and one at the imidazole moiety. The primary proton from the diprotonated phosphate group is certainly lost

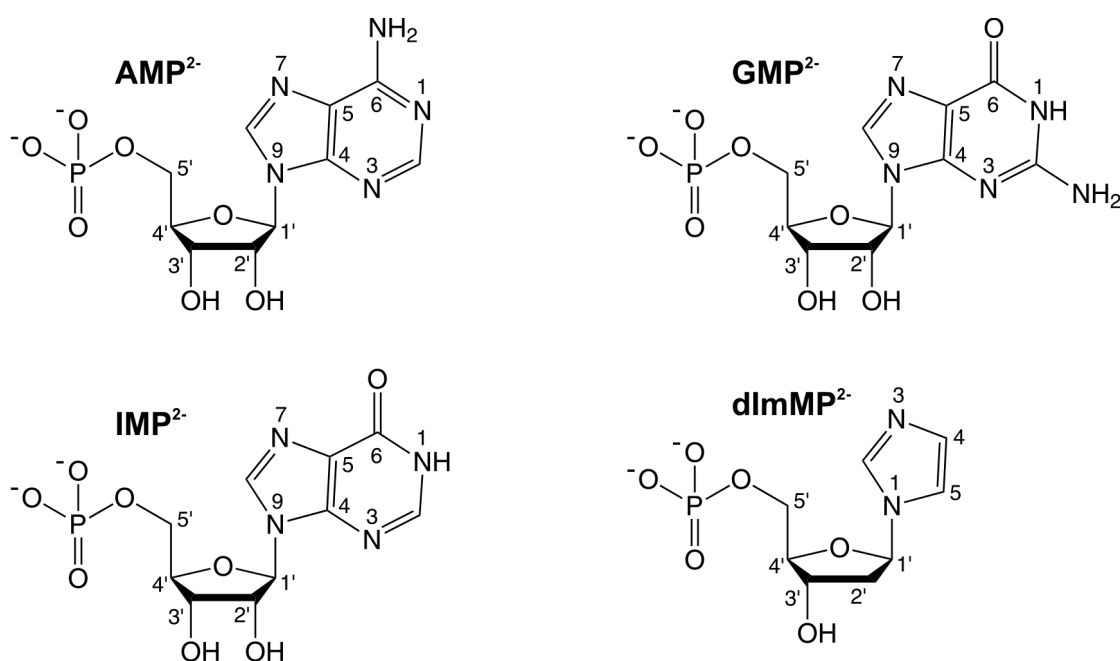
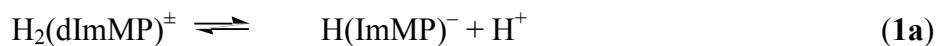
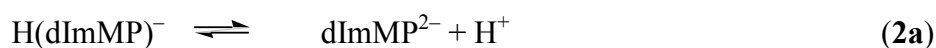


**Figure 3-2** Chemical structures of the purine nucleotides adenosine 5'-monophosphate ( $\text{AMP}^{2-}$ ), guanosine 5'-monophosphate ( $\text{GMP}^{2-}$ ), and inosine 5'-monophosphate ( $\text{IMP}^{2-}$ ) in comparison with the one of 1-(2'-deoxy- $\beta$ -D-ribofuranosyl)imidazole 5'-monophosphate ( $\text{dImMP}^{2-}$ ).

due to the  $pK_a < 1$ . Based on the structural similarity with  $H_3(dGMP)^+$  (Figure 3-2), which carries a proton at N7 facilitating the release of the primary proton, it can be assumed that  $pK_{H_3(dImMP)}^H \approx pK_{H_3(dGMP)}^H = 0.35 \pm 0.2$ .<sup>[199]</sup> Two further deprotonation reactions occur at the monoprotonated phosphate group and the also monoprotonated imidazole residue giving rise to the following two deprotonation equilibria:



$$K_{H_2(dImMP)}^H = [H(dImMP)^-][H^+]/[H_2(dImMP)^\pm] \quad (1b)$$



$$K_{H(dImMP)}^H = [dImMP^{2-}][H^+]/[H(dImMP)^-] \quad (2b)$$

No other equilibria are expected in the physiological pH range because (i)  $pK = 12.5$  for the *cis* arrangement of the 2'- and 3'-hydroxyl groups as present in a ribose residue.<sup>[200]</sup> For a 2-deoxyribose residue one may conclude that  $pK_a > 13$  because a 2',3'-hydroxy arrangement favors deprotonation of one of the two OH groups due to intramolecular hydrogen bond formation in the resulting anion.<sup>[200]</sup> Similarly, (ii) deprotonation of neutral imidazole<sup>[201]</sup> occurs with  $pK_a = 14.4$  and in the case of benzimidazole<sup>[201,202]</sup> with  $pK_a = 12.8$ . Consequently, for a N1-substituted imidazole derivative like  $dImMP^{2-}$ , which is twofold negatively charged, it is safe to conclude that also here the assumption  $pK_a > 13$  holds. Such deprotonations can only be achieved under very special conditions and in the presence of positive charges, e.g., metal ions.<sup>[118]</sup>

The acidity constants defined in equations 1b and 2b were determined by potentiometric pH titration and are given in Table 3-1 comparing the data for some related systems,<sup>[144,203-215]</sup> including 1-methylimidazole (MeIm; entry 5) and 2-deoxyribose 5-monophosphate ( $dRibMP^{2-}$ ; entry 2). The acidity constants of  $H(dRibMP)^-$  and  $H(MeIm)^+$  are not very far apart from each other ( $\Delta pK_a = 0.9$ ) but the imidazole residue is clearly somewhat more basic compared to the phosphate group.

Concluding from the above observations the first constant for the deprotonation of  $H_2(dImMP)^\pm$ , i.e.,  $pK_{H_2(dImMP)}^H = 5.85 \pm 0.03$ , is determined mainly by the release of the proton from the  $P(O)_2(OH)^-$  group, and the second,  $pK_{H(dImMP)}^H = 6.88 \pm 0.04$ , by the deprotonation of the monoprotonated imidazole residue. These two acidity constants differ by about one  $pK_a$  unit meaning that the buffer regions of the two acid-base residues of  $dImMP^{2-}$  overlap.

**Table 3-1** Negative logarithms of the acidity constants of  $H_2(dImMP)^\pm$  (equations 1 and 2), together with the corresponding data for some related compounds.<sup>a,b</sup>

entry	acid	pK <sub>a</sub> values for the sites		ref
		P(O) <sub>2</sub> (OH) <sup>−</sup>	(N3)H <sup>+</sup>	
1	CH <sub>3</sub> OPO <sub>2</sub> (OH) <sup>−</sup>	6.36±0.01		[204,212]
2 <sup>[c]</sup>	H(dRibMP) <sup>−</sup>	6.31±0.07		_ <sup>[c]</sup>
3 <sup>[d]</sup>	H <sub>2</sub> (dImMP) <sup>±</sup>	5.85±0.03	6.88±0.04	_ <sup>[d]</sup>
4 <sup>[e]</sup>	H(dRibIm) <sup>+</sup>		6.09±0.07	_ <sup>[e]</sup>
5 <sup>[f]</sup>	H(MeIm) <sup>+</sup>		7.20±0.02	[208]
6 <sup>[f]</sup>	H(MeBzIm) <sup>+</sup>		5.67±0.01	[209]
7	H <sub>2</sub> (dGMP) <sup>±</sup>	6.29±0.01	2.69±0.03 <sup>g</sup>	[214]
8	H(dGuo) <sup>+</sup>		2.30±0.04 <sup>g</sup>	[144,215]

<sup>a</sup> The constants were determined by potentiometric pH titrations (except entry 4) in aqueous solution (25 °C;  $I = 0.1$  M, NaNO<sub>3</sub>). So-called practical (or mixed) constants<sup>[213]</sup> are listed (see also Section 4.4.4). <sup>b</sup> The error limits given are *three times* the standard error of the mean value ( $3\sigma$ ) or the sum of the probable systematic errors, whichever is larger; error limits for any derived data, including  $\Delta pK_a$  values, were calculated according to the error propagation after Gauss. <sup>c</sup> The acidity constant of monoprotonated 5-ribose monophosphate (RibMP<sup>2−</sup>) ( $pK_{H(RibMP)}^H = 6.24 \pm 0.01$ )<sup>[210]</sup> can be transformed to the one of 2-deoxyribose 5-monophosphate (dRibMP<sup>2−</sup>) by adding  $0.07 \pm 0.07$  log unit. This correction term follows from results obtained for a series of nucleoside 5'-monophosphates and 2'-deoxynucleoside 5'-monophosphates<sup>[211]</sup> and reflects the effect due to the replacement of OH by H at C2' of the ribose residue (for details see ref.<sup>[211]</sup>). <sup>d</sup> This work. <sup>e</sup> At 25°C and physiological ionic strength (i.e.,  $I$  ca. 0.02 M) the value for monoprotonated 1-(2'-deoxy-β-D-ribofuranosyl)-imidazole (dRibIm),  $pK_{H(dRibIm)}^H = 6.01 \pm 0.05$ , was determined by [<sup>1</sup>H]-NMR shift measurements.<sup>[195]</sup> It is well known that for this type of compounds<sup>[205]</sup> the  $pK_a$  values increase slightly with increasing  $I$ : For example, for monoprotonated imidazole (Im)  $pK_{H(Im)}^H = 7.05 \pm 0.01$  at  $I = 0.1$  M<sup>[206]</sup> and  $7.13 \pm 0.01$  at  $I = 0.5$  M<sup>[208]</sup> hold and for monoprotonated pyridine (Py) the values are  $pK_{H(Py)}^H = 5.26 \pm 0.01$  ( $I = 0.1$  M)<sup>[203]</sup> and  $5.34 \pm 0.02$  ( $I = 0.5$  M).<sup>[207]</sup> We assume that the effect for H(dRibIm)<sup>+</sup> is similar and add 0.08 pK unit with the generous error limit of  $\pm 0.05$  to the mentioned value. The estimated result for  $I = 0.1$  M, i.e.,  $pK_{H(dRibIm)}^H = (6.01 \pm 0.05) + (0.08 \pm 0.05) = 6.09 \pm 0.07$ , is listed above. <sup>f</sup> MeIm = 1-methylimidazole; MeBzIm = 1-methylbenzimidazole. <sup>g</sup> This value refers to the (N7)H<sup>+</sup> unit of the guanine residue, i.e. the site corresponding to N3 of an imidazole residue (Figure 3-2). Deprotonation of the (N1)H unit in dGMP<sup>2−</sup> and in dGuo occurs with  $pK_{dGMP}^H = 9.56 \pm 0.02$  (cf.<sup>[214]</sup>) and  $pK_{dGuo}^H = 9.24 \pm 0.03$ ,<sup>[214,215]</sup> respectively.

Consequently, the acidity constants determined by potentiometric pH titrations as given in Table 3-1 are macro acidity constants which quantify the overall situation for the  $\text{H}_2(\text{dImMP})^\pm$  species, but they describe only approximately the individual proton-binding sites (see Section 3.2.1.2).

The distribution curves of the various species as derived from the macro acidity constants are shown in Figure 3-3. These curves confirm the overlapping buffer regions. A consequence

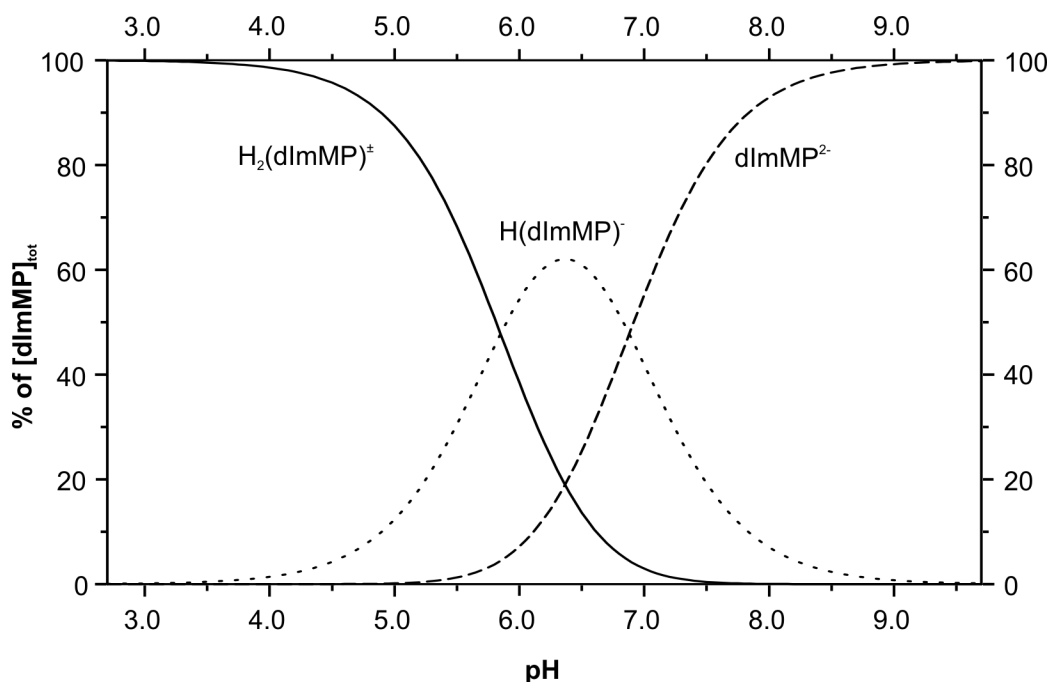


**Figure 3-3** Effect of pH on the concentration of the species present in an aqueous solution of dImMP (25 °C;  $I = 0.1 \text{ M}$ ,  $\text{NaNO}_3$ ). The calculations are based on the acidity constants listed in Table 3-1 and the results are plotted as the percentage of the total dImMP present.

of this observation is that the  $\text{H}(\text{dImMP})^-$  species reaches a formation degree of only about 62 %. However, despite this "shortcoming" (see Section 3.2.1.2) the various acidity constants listed in Table 3-1 will be discussed first.

Table 3-1 allows many comparisons, but a few need to be emphasized:

- (i) The  $\text{p}K_a$  values for monoprotonated methyl monophosphate (entry 1) and 2'-deoxyribose-5'-monophosphate (entry 2) are astonishingly similar. This indicates that the solvation of the phosphate group in both compounds is comparable.
- (ii) The above observation differs from the entries 4 and 5. Here replacement of a methyl group by the 2'-deoxyribose moiety at N1 of imidazole leads to a significant acidification of the  $(\text{N3})\text{H}^+$  unit. In this case the substituents seem to affect solvation probably because the 5'-OH group forms to some extent a hydrogen bond with N3 and thus facilitates deprotonation of

(N3)H<sup>+</sup>. Related hydrogen bonds have recently also been suggested for xanthosine-5'-monophosphate.<sup>[216]</sup>

(iii) It is expected that the monoprotonated phosphate group in H<sub>2</sub>(dImMP)<sup>±</sup> (entry 3) is more acidic than the one in H(dRibMP)<sup>−</sup> (entry 2) because the positively charged monoprotonated imidazole residue should facilitate deprotonation of the P(O)<sub>2</sub>(OH)<sup>−</sup> group.

(iv) Along the same line, the deprotonation of the (N3)H<sup>+</sup> unit in H(dImMP)<sup>−</sup> (entry 3, column 4) is hindered compared to the same deprotonation reaction in H(dRibIm)<sup>+</sup> (entry 4), due to the presence of the negatively charged PO<sub>3</sub><sup>2−</sup> residue (for a detailed analysis consult section 3.2.1.2 and Figure 3-4).

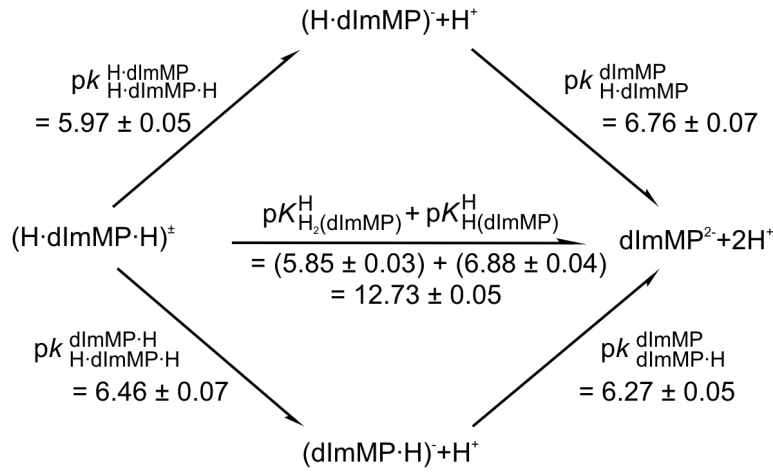
(v) Annulation of 1-methylimidazole (entry 5) to form 1-methylbenzimidazole (entry 6) leads to a drop in basicity of N3 by about 1.5 pK units. This contrasts sharply with the annulation of dImMP<sup>2−</sup> by a pyrimidine ring (entry 3) giving dGMP<sup>2−</sup> (entry 7). In the latter case the basicity of N7 drops by more than 4 pK units. Clearly, the electron-withdrawing effect of the substituted pyrimidine ring (Figure 3-2) is much larger than that of a benzene ring.

Some further related points need to be discussed in the next section in the context of the evaluation of the micro acidity constants (Figure 3-4).

### 3.2.1.2 Microconstant scheme for H<sub>2</sub>(dImMP)<sup>±</sup>

For a quantification of the individual acid-base sites in dImMP<sup>2−</sup> it is necessary to determine so-called micro acidity constants.<sup>[199,217]</sup> These micro acidity constants are connected with the macro acidity constants as shown in Figure 3-4. It is immediately evident that the scheme contains four micro acidity constants but that there are only three independent equations (lower part of the Figure 3-4), which interlink the macro with the micro acidity constants. Hence, one of these micro acidity constants needs to be determined or estimated to be able to complete the scheme.

In a recent study it has been shown for a series of 2'-deoxynucleoside 5'-monophosphates (dNMP<sup>2−</sup>) that they all have  $pK_{H(dNMP)}^H = 6.27 \pm 0.05$ .<sup>[211]</sup> Consequently, it is reasonable to assume that the micro acidity constant  $pK_{dImMP-H}^{dImMP}$  is well represented by the mentioned value because in the second deprotonation step (the lower pathway in the scheme) the imidazole residue is uncharged, as it is the case in the H(dNMP)<sup>−</sup> species. Insertion of the acidity constant in the lower pathway at the right side of the scheme allows now to calculate the other three micro acidity constants by applying the equations given in the lower part of Figure 3-4.



$$K_{H_2(dImMP)}^H = k_{H·dImMP / H·dImMP·H} + k_{dImMP·H / H·dImMP·H} \quad (a)$$

$$\frac{1}{K_{H(dImMP)}^H} = \frac{1}{k_{dImMP / H·dImMP}} + \frac{1}{k_{dImMP / dImMP·H}} \quad (b)$$

$$\begin{aligned} K_{H_2(dImMP)}^H \cdot K_{H(dImMP)}^H &= k_{H·dImMP / H·dImMP·H} \cdot k_{dImMP·H / H·dImMP·H} \\ &= k_{dImMP / H·dImMP} \cdot k_{dImMP / dImMP·H} \end{aligned} \quad (c)$$

**Figure 3-4** Scheme for the deprotonation equilibrium of  $(H·dImMP·H)^{\pm}$  defining the micro acidity constants ( $k$ ) and showing their interrelation with the measured macro acidity constants ( $K$ ) and the connection between the two tautomers  $(H·dImMP)^{-}$  and  $(dImMP·H)^{-}$  and the other species present. In  $(H·dImMP)^{-}$  the proton is at N3 of the imidazole residue and in  $(dImMP·H)^{-}$  it is bound at the phosphate residue (Figure 3-2; bottom). In  $(H·dImMP·H)^{\pm}$  both sites are protonated. The arrows indicate the direction for which the acidity constants are defined. The acidity constants measured for a series of 2'-deoxynucleoside 5'-monophosphates ( $dNMP^{2-}$ ), i.e., of  $pK_{dImMP·H}^{dImMP} = 6.27 \pm 0.05$ ,<sup>[211]</sup> for the deprotonation of  $P(O)_2(OH)^{-}$  in  $(dImMP·H)^{-}$ , i.e., for the micro acidity constant  $pK_{H(dNMP)}^H$  determined in the lower pathway of the scheme at the right. These values permit the calculation of the other micro acidity constants with equations a, b, and c given in the lower part of the above figure. The error limits are defined in footnote 'b' of Table 3-1.

These calculated constants are inserted at their corresponding positions in the scheme of Figure 3-4.

Using the values of these micro acidity constants permits to calculate the ratio between the tautomers<sup>[217]</sup> with either a protonated imidazole residue or a monoprotonated phosphate residue for the  $H(dIMP)^{-}$  species (equation 3):

$$R = \frac{[(H·dImMP)^{-}]}{[(dImMP·H)^{-}]} \quad (3a)$$

$$= \frac{k_{H·dImMP / H·dImMP·H}}{k_{dImMP·H / H·dImMP·H}} = \frac{10^{-(5.97 \pm 0.05)}}{10^{-(6.46 \pm 0.07)}} \quad (3b)$$

$$= 10^{(0.49 \pm 0.09)} = \frac{3.09 \pm 0.64}{1} \quad (3c)$$

$$= \frac{76}{24} \left( \frac{79}{21}, \frac{71}{29} \right) \quad (3d)$$

Indeed, this result (the upper and lower limits are given in parentheses) proves that both monoprotinated tautomeric species occur in appreciable amounts. Nevertheless, the imidazole residue is somewhat more basic than the phosphate group as already indicated in Section 3.2.1.1. Consequently, the imidazole-protonated species (at N3),  $(\text{H}\cdot\text{dImMP})^-$ , dominates with a formation degree of about 75 % whereas the phosphate-protonated species,  $(\text{dImMP}\cdot\text{H})^-$ , forms only to about 25 %. It should be noted that the above given ratio  $R$  is independent of the pH of the solution because it represents an intramolecular equilibrium. Thus, a given amount of  $\text{H}(\text{dImMP})^-$ , it may be large or small, will always be present in the ratio of about 75 to 25 %.

With the micro acidity constants of Figure 3-4 at hand, several additional, quite enlightening conclusions are possible:

(i) In  $\text{H}(\text{dRibIm})^+$  the proton from the  $(\text{N3})\text{H}^+$  site is released with  $\text{p}K_{\text{H}(\text{dRibIm})}^{\text{H}} = 6.09 \pm 0.07$  (Table 3-1, entry 4). In accordance with point iv in Section 3.2.1.1, the presence of a negatively charged  $\text{P}(\text{O})_2(\text{OH})^-$  group hampers the release of the  $(\text{N3})\text{H}^+$  proton in  $(\text{H}\cdot\text{ImMP}\cdot\text{H})^\pm$  by  $\Delta \text{p}K_{\text{a}} = \text{p}k_{\text{H}\cdot\text{dImMP}\cdot\text{H}}^{\text{dImMP}\cdot\text{H}} - \text{p}K_{\text{H}(\text{dRibIm})}^{\text{H}} = (6.46 \pm 0.07) - (6.09 \pm 0.07) = 0.37 \pm 0.10$ . This difference in acidity is within the error limits identical to the  $\text{H}_2(\text{dGMP})^\pm/\text{H}(\text{dGuo})^+$  pair (Table 3-1, entries 7, 8), i.e.,  $\Delta \text{p}K_{\text{a}} = \text{p}K_{\text{H}_2(\text{dGMP})}^{\text{H}} - \text{p}K_{\text{H}(\text{dGuo})}^{\text{H}} = 2.69 \pm 0.03) - (2.30 \pm 0.04) = 0.39 \pm 0.05$ . Note that the sterical conditions concur in both comparisons (Figure 3-1) and consequently the  $\Delta \text{p}K_{\text{a}}$  values are identical despite the large variations in the absolute size of the acidity constants considered.

(ii) Instead of taking into account the influence of the  $\text{P}(\text{O})_2(\text{OH})^-$  group on the release of a proton from the  $(\text{N3})\text{H}^+ / (\text{N7})\text{H}^+$  site, one may also look at the effect of  $(\text{N3})\text{H}^+$  on the release of a proton from the  $\text{P}(\text{O})_2(\text{OH})^-$  group by comparing  $\text{H}(\text{dRibMP})^-$  with  $\text{H}_2(\text{dImMP})^\pm$ , i.e.,  $\Delta \text{p}K = \text{p}k_{\text{H}\cdot\text{dImMP}}^{\text{H}\cdot\text{dImMP}} - \text{p}k_{\text{H}\cdot\text{dImMP}\cdot\text{H}}^{\text{H}\cdot\text{dImMP}} = (6.31 \pm 0.07) - (5.97 \pm 0.05) = 0.34 \pm 0.09$ . This difference is within the error limits identical to those discussed in (i). This is a prerequisite because the Coulomb effects are always reciprocal and in all cases considered here the effects of single charged sites are compared.

The outcome of the above quantitative comparisons is very comforting because it underlines the internal consistency of the acidity constants assembled in Table 3-1 and Figure 3-4. The retarding effect of a twofold negatively charged  $\text{PO}_3^{2-}$  group on the deprotonation of  $(\text{N3})\text{H}^+$  in  $(\text{H}\cdot\text{dImMP})^-$  is larger as the comparison with  $\text{H}(\text{dRibIm})^+$  shows:  $\text{p}k_{\text{H}\cdot(\text{dRibIm})}^{\text{H}\cdot\text{dImMP}} - \text{p}k_{\text{H}\cdot\text{dImMP}}^{\text{dImMP}} = (6.76 \pm 0.07) - (6.09 \pm 0.07) = 0.67 \pm 0.10$ . Evidently the effect is approximately doubled as one would expect.

### 3.2.1.3 $[^{31}\text{P}]$ -NMR shift studies of dImMP<sup>2-</sup>

Determination of the chemical shift of  $^{31}\text{P}$ ,  $\delta_{\text{P}}$ , in dependence on pD in D<sub>2</sub>O should reflect the acid-base properties of the phosphate group. Indeed, such a dependence is observed (Figure 3-5).

An evaluation of the experimental data given in Figure 3-5A shows that all data points fit on the dotted line. However, as described above (Section 3.2.1.2, Figure 3-3) the deprotonation reactions of  $\text{H}_2(\text{dImMP})^{\pm}$  and  $\text{H}(\text{dImMP})^{-}$  overlap. To minimize the influence of the deprotonation of the monoprotonated imidazole residue on the deprotonation of the monoprotonated phosphate residue, the seven data points at  $\text{pD} > 7.2$  were deleted in the evaluation. Indeed, the  $\text{pK}_{\text{a}}$  value dropped from  $6.58 \pm 0.06$  to  $6.49 \pm 0.06$  in D<sub>2</sub>O as solvent. To validate the situation further, the data points at  $\text{pD}$  7.19, 6.88, and 6.72 were also systematically deleted in the fitting process to give the  $\text{pK}_{\text{a/D}_2\text{O}}$  values of  $6.50 \pm 0.10$ ,  $6.51 \pm 0.15$ , and  $6.42 \pm 0.12$ , respectively. We consider as the best result  $\text{pK}_{\text{a/D}_2\text{O}} = 6.50 \pm 0.10$ , which is based on the seven data points up to  $\text{pD}$  6.88 (solid line in Figure 3-5A), because at this  $\text{pD}$

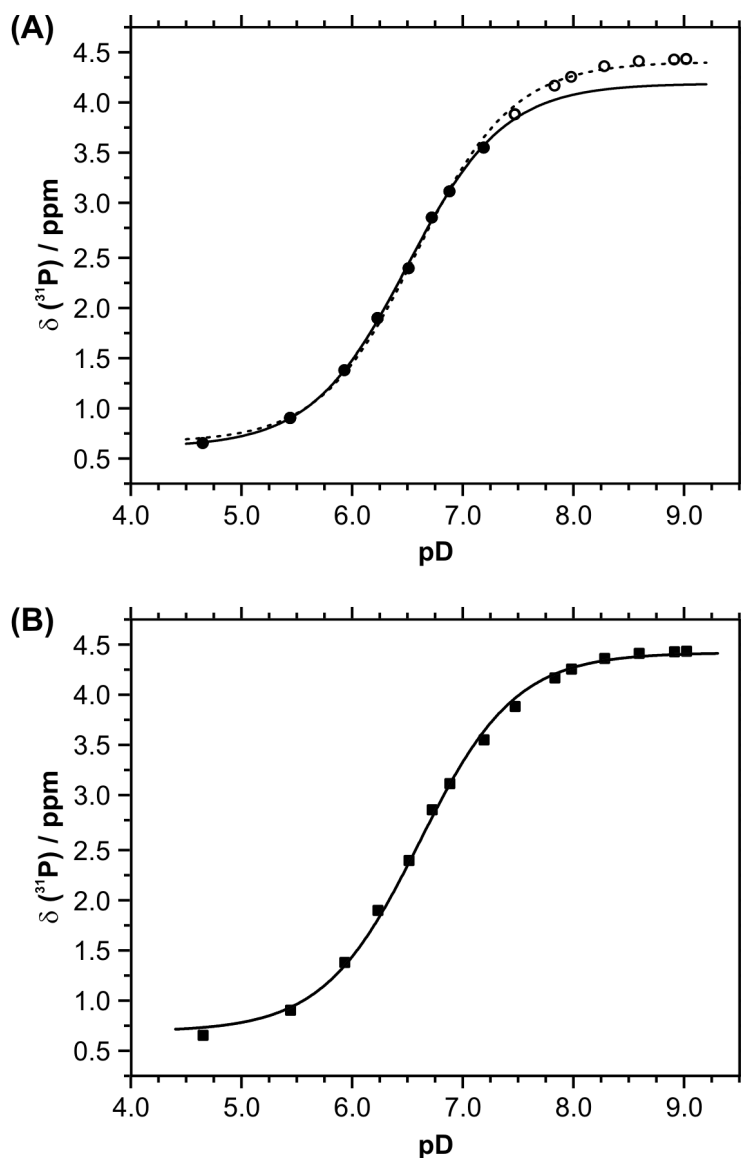


**Figure 3-5** Variation of the chemical shift  $\delta_{\text{P}}$  for  $^{31}\text{P}$  of the phosphate group of dImMP (1.8 mM) in dependence on pD (25 °C;  $I = 0.12 \text{ M}$ ,  $\text{NaClO}_4$ ; see also Section 4.4.2). **(A)** The dotted curve represents the calculated best fit through all experimental data, whereas in the calculation for the solid curve only the data points up to  $\text{pD}$  6.88 were used. **(B)** The solid curve is the calculated best fit of the experimental data using the micro acidity constants  $\text{pK}_{\text{D-dImMP}}^{\text{D-dImMP}} = 6.51 \pm 0.05$  and  $\text{pK}_{\text{D-ImMP}}^{\text{dImMP}} = 7.31 \pm 0.07$  (obtained from the upper pathway in Figure 3-4 with equation 4). The resulting chemical shifts are  $\delta_{\text{P/H-dImMP-H}} = 0.687 \pm 0.113$  (3 $\sigma$ ),  $\delta_{\text{P/H-dImMP}} = 3.687 \pm 0.183$  and  $\delta_{\text{P/dImMP}} = 4.422 \pm 0.084$ ; and the corresponding shift differences are  $\Delta \delta_2 = -3.000 \pm 0.215$  and  $\Delta \delta_1 = -0.735 \pm 0.201$  (see also foot-notes 'a' and 'b' of Table 3-2 in Section 3.2.1.4).



the protonated imidazole residue is still present to about 80 %.

Transformation<sup>[218]</sup> of the latter mentioned constant (valid in D<sub>2</sub>O) to H<sub>2</sub>O as solvent by applying equation 4 gives  $pK_{a/H_2O} = 5.96 \pm 0.10$  ( $3\sigma$ ).

$$pK_{a/H_2O} = (pK_{a/D_2O} - 0.45) / 1.015 \quad (4)$$

This value is within the error limits identical to the micro acidity constant given at the left in the upper pathway of Figure 3-4 verifying this method. From this observation two things can be concluded: (i) By deleting a number of data points (see the solid line in Figure 3-5A) it is indeed possible to determine the micro acidity constant for the deprotonation of the phosphate group under conditions where the imidazole group is protonated. (ii) The agreement between the micro acidity constant as measured by [<sup>31</sup>P]-NMR shift experiments ( $5.96 \pm 0.10$ ) and the one calculated ( $5.97 \pm 0.05$ ) for  $pK_{H \cdot dImMP \cdot H}^{H \cdot dImMP}$  in Figure 3-4 shows that our previous assumption, i.e.  $pK_{H(dNMP)}^H = 6.27 \pm 0.05 = pK_{dImMP \cdot H}^{dImMP}$ , as made in Section 3.2.1.2, is justified. Further verification of all data is provided by the excellent fit of all 15 [<sup>31</sup>P]-NMR data points (Figure 3-5B) by using the two micro acidity constants given in the upper pathway of Figure 3-4.

With the mentioned micro acidity constant experimentally confirmed, the effect of a protonated imidazole residue on the deprotonation of the monoprotonated phosphate group in dImMP can now be quantified. The corresponding acidification follows from equation 5:

$$\Delta pK_a = pK_{dImMP \cdot H}^{dImMP} - pK_{H \cdot dImMP \cdot H}^{H \cdot dImMP} \quad (5a)$$

$$= (6.27 \pm 0.05) - (5.97 \pm 0.05) \quad (5b)$$

$$= 0.30 \pm 0.07 \quad (5c)$$

This result is most reasonable and in agreement with the related observations discussed in points (i) and (ii) of Section 3.2.1.2.

To conclude, potentiometric pH titrations allow the determination of acidity constants in an exact manner, but this method does not provide any direct information at which sides the protons are released. Therefore, it is satisfying to see that the site attributions made earlier in Sections 3.2.1.1 and 3.2.1.2, which were solely based on the comparison of constants, are confirmed by the NMR shift experiments described above as well as by those to follow in the next Section.

### 3.2.1.4 $[^1\text{H}]$ -NMR shift studies of dImMP<sup>2-</sup>

One expects that the chemical shifts ( $\delta\text{H}$ ) of the imidazole H2, H4, and H5 protons (Figure 3-2) are affected by the protonation/deprotonation of N3. Indeed, with decreasing pD, downfield shifts are observed, as has been described in the literature (Figure 3-6).<sup>[142,150,211]</sup>

As expected, the chemical shift of H2, being closest to the imidazole-N3 site, is most affected by the protonation /deprotonation reaction. A curve-fitting of the experimental data for each of the three protons (Figure 3-6A) yields a single  $pK_a$  value only, the average of which is  $pK_a = 7.13 \pm 0.12$ . The corresponding acidity constant valid for H<sub>2</sub>O (equation 4) is  $pK_{a/\text{H}_2\text{O}} = 6.58 \pm 0.12$ . A comparison of this value with the macro acidity constants given on the horizontal arrow in Figure 3-4 shows that it is about 0.3  $pK_a$  units below  $pK_{\text{H}(\text{dImMP})}^{\text{H}} = 6.88$ . More important, this value from the  $[^1\text{H}]$ -NMR shift experiments is also below  $pK_{\text{H-dImMP}}^{\text{dImMP}} = 6.76 \pm 0.07$  but above  $pK_{\text{H-dImMP-H}}^{\text{dImMP-H}} = 6.46 \pm 0.07$ . Therefore, this value from the  $[^1\text{H}]$ -NMR shift experiments does not reflect any of the micro acidity constants, a situation that cannot be improved easily for the three protons considered.

The deletion of data points, as done with the  $[^{31}\text{P}]$ -NMR measurements (Figure 3-6), is of course also an option. Because

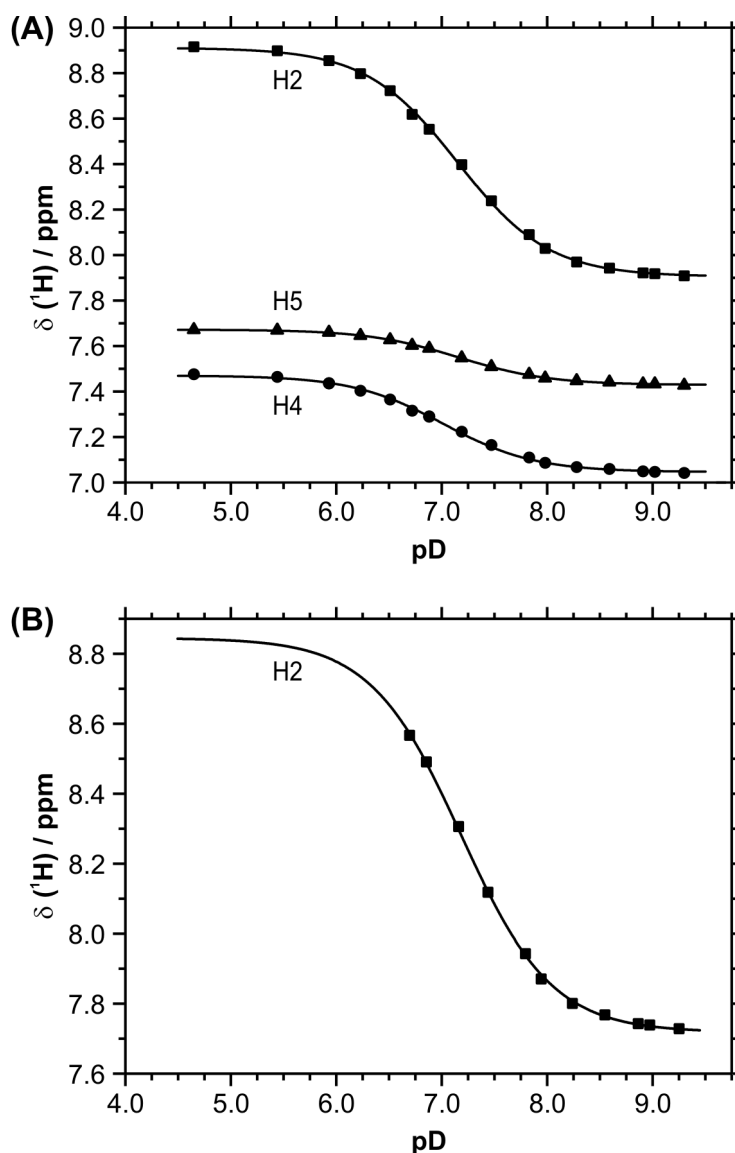


**Figure 3-6** Variation of the chemical shift  $\delta_{\text{H}}$  for the protons of the imidazole residue in dImMP (1.8 mM) in dependence on pD (25 °C;  $I = 0.12$  M, NaClO<sub>4</sub>; see also Section 4.4.2). **(A)** The solid curves are the calculated best fits of the experimental data using the micro acidity constants  $pK_{\text{D-dImMP}}^{\text{D-dImMP}} = 6.51 \pm 0.05$  and  $pK_{\text{D-dImMP}}^{\text{dImMP}} = 7.31 \pm 0.07$ . **(B)** The solid curve represents the calculated best fit of the experimental data in the pD range of 6.72 to 9.30 and gives the micro acidity constant  $pK_{\text{D-dImMP}}^{\text{dImMP}} = 7.22 \pm 0.05$  (3  $\sigma$ ); the corresponding chemical shifts are  $\delta_{\text{H-dImMP}} = 8.853 \pm 0.037$  and  $\delta_{\text{dImMP}} = 7.900 \pm 0.009$ , which gives a shift difference of  $\Delta \delta_1 = 0.953 \pm 0.038$  (see also footnotes 'a' and 'b' of Table 3-2).

the chemical shift differences for H4 and H5 are too small to allow a detailed evaluation, we concentrated on the chemical shifts of H2: If the four data points at  $\text{pH} < 6.4$  were deleted and then systematically also the points at  $\text{pD}$  6.51, 6.58, 6.72, and 7.19, the  $\text{p}K_a$  values  $7.19 \pm 0.05$ ,  $7.22 \pm 0.05$ ,  $7.20 \pm 0.06$ , and  $7.15 \pm 0.10$ , respectively, can be obtained. With regard to the micro acidity constant  $\text{p}K_{\text{D-dImMP}}^{\text{dImMP}}$  we consider the value  $7.22 \pm 0.05$  as the best result (Figure 3-6B). Transformation of this value to an aqueous solution ( $\text{H}_2\text{O}$ ) with equation 4 gives  $\text{p}K_{\text{H-dImMP}}^{\text{dImMP}} = 6.67 \pm 0.05$ . Comparison of this result with the corresponding value in Figure 3-4 (upper pathway at the right), i.e.,  $\text{p}K_{\text{H-dImMP}}^{\text{dImMP}} = 6.76 \pm 0.07$ , shows that the agreement is reasonable, though not completely satisfying. However, this can be explained as the deprotonation of the imidazole residue takes place under the influence of an increasing from one to two negative charges at the phosphate group. Hence, here we have the stronger 2+/1+ Coulomb interaction, whereas previously in Section 3.2.1.3 it was a 1+/1+ interaction only (see also the corresponding discussion in Section 3.2.1.2).

The validity of the chemical shift change data for all three protons was checked in the following way: We used the micro acidity constants given in the upper pathway of Figure 3-4 and transformed these with equation 4 to the  $\text{p}K_a$  values valid for  $\text{D}_2\text{O}$  as solvent,  $\text{p}K_{\text{D-dImMP-D}}^{\text{D-dImMP}} = 6.51 \pm 0.05$  and  $\text{p}K_{\text{D-dImMP}}^{\text{dImMP}} = 7.31 \pm 0.07$ . Indeed, using these two micro acidity constants the experimental data for all three protons can be fitted excellently as the solid curves in Figure 3-6A prove. Application of the macro acidity constants does not lead to such satisfactory fits as is obvious from the error limits which are about twice as large (Table 3-2 and Table 3-3).

**Table 3-2** Chemical shifts (in ppm) of the protons for the protonated, that is, deuterated, and the free forms of dImMP.<sup>a,b</sup>

H	$\delta_{\text{H-dImMP-H}}$	$\delta_{\text{H-dImMP}}$	$\delta_{\text{dImMP}}$	$\Delta\delta_2$	$\Delta\delta_1$
	ppm				
H-2	8.919±0.012	8.643±0.020	7.902±0.008	0.276±0.023	0.741±0.021
H-4	7.477±0.006	7.300±0.010	7.043±0.004	0.177±0.012	0.257±0.011
H-5	7.674±0.004	7.610±0.006	7.428±0.003	0.064±0.007	0.182±0.008

<sup>a</sup> The chemical shifts were calculated with the transformed micro acidity constants (Figure 3-4, upper pathway; application of equation 4) based on the experiments in  $\text{D}_2\text{O}$  that yield the data plotted in Figure 3-6 (25 °C;  $I = 0.12 \text{ M}$ ,  $\text{NaClO}_4$ ). The shift differences,  $\Delta\delta$ , resulting from increasing deprotonation of the species are also listed, that is,  $\Delta\delta_2 = \delta_{\text{H-dImMP-H}} - \delta_{\text{H-dImMP}}$  and  $\Delta\delta_1 = \delta_{\text{H-dImMP}} - \delta_{\text{dImMP}}$ . <sup>b</sup> The specified error ranges for the calculated chemical shifts ( $\delta$ ) and the shift differences ( $\Delta\delta$ ) are three times the standard deviations ( $3\sigma$ ) in each case.

**Table 3-3** Chemical shifts (in ppm) of the protons for the protonated, that is, deuterated, and the free forms of dImMP based on the macro acidity constants.<sup>a</sup>

H	$\delta_{\text{H}\cdot\text{dImMP}\cdot\text{H}}$	$\delta_{\text{H}\cdot\text{dImMP}}$	$\delta_{\text{dImMP}}$	$\Delta\delta_2$	$\Delta\delta_1$
	<b>ppm</b>				
H-2	8.938±0.030	8.614±0.039	7.887±0.020	0.324±0.049	0.727±0.044
H-4	7.486±0.011	7.294±0.015	7.037±0.008	0.192±0.019	0.257±0.017
H-5	7.678±0.008	7.602±0.011	7.425±0.006	0.076±0.014	0.177±0.013

<sup>a</sup> The macro acidity constants are  $\text{p}k_{\text{D}_2(\text{dImMP})}^{\text{D}} = 6.39 \pm 0.03$  and  $\text{p}k_{\text{D}(\text{dImMP})}^{\text{D}} = 7.43 \pm 0.04$  as calculated with equation 4 and the constants given on the horizontal arrow in Figure 3-4. For further details see footnotes 'a' and 'b' of Table 3-2.

The described fitting procedure, using the micro acidity constants, also provides the chemical shift data for the  $(\text{H}\cdot\text{dImMP}\cdot\text{H})^{\pm}$ ,  $(\text{H}\cdot\text{dImMP})^{-}$ , and  $\text{dImMP}^{2-}$  species (Table 3-2). From the  $\Delta\delta_1$  and  $\Delta\delta_2$  shift differences listed in columns 5 and 6 of Table 3-2 it becomes clear that the chemical shifts are largely governed by the deprotonation of  $(\text{N3})\text{H}^{+}$  in  $(\text{H}\cdot\text{dImMP})^{-}$  as the effect of the  $\text{P}(\text{O})_2(\text{OH})^{-}$  deprotonation in  $(\text{H}\cdot\text{dImMP}\cdot\text{H})^{\pm}$  is much smaller. This result is in accord with the larger distances of the phosphate group to the monitored protons.

To summarize, from the right hand part of Figure 3-4 it is evident that the imidazole residue in  $\text{dImMP}^{2-}$  is by about 0.5 pK units more basic than the phosphate residue in the same molecule. Consequently, about 75 % (equation 3) of the  $\text{H}(\text{dImMP})^{-}$  species carry the proton at the imidazole residue and exist as the  $(\text{H}\cdot\text{dImMP})^{-}$  tautomer. The second tautomer,  $(\text{dImMP}\cdot\text{H})^{-}$ , is a minority species, but with a formation degree of about 25 % it is not negligible. These acid-base properties allow the prediction, based on known metal ion affinities of imidazoles<sup>[208]</sup> and phosphates,<sup>[150]</sup> that the primary binding site in complex formations of metal ions like  $\text{Ca}^{2+}$ ,  $\text{Mg}^{2+}$  and even  $\text{Mn}^{2+}$  is the phosphate residue. In contrast, for metal ions like  $\text{Co}^{2+}$ ,  $\text{Ni}^{2+}$ ,  $\text{Cu}^{2+}$  or  $\text{Zn}^{2+}$  the primary binding site is most likely the imidazole residue and in accord with the results observed for  $\text{AMP}^{2-}$  also macrochelate formation can occur.<sup>[219]</sup> Apparently, the macrochelate formation in the case of the artificial nucleotide,  $\text{dImMP}^{2-}$ , is more pronounced due to the higher basicity of the N site compared to the  $\text{M}(\text{AMP})$  complexes.  $\text{Zn}(\text{dImMP})$  and  $\text{Cd}(\text{dImMP})$  promise to be especially interesting because the involved metal ions have a rather similar affinity towards the imidazole and phosphate groups. This should give rise to equilibria between three isomeric

complexes,<sup>[199,216]</sup> that is, macrochelates as well as monodentate-bound species coordinated either to the imidazole or the phosphate residue.

Considering that a nucleotide unit in a nucleic acid involves a singly charged phosphate-diester bridge, which is of no relevance regarding proton binding in the physiological pH range, the basicity of the imidazole residue becomes crucial and this basicity should be well represented by the (dImMP·H)<sup>−</sup> species, i.e., by the micro acidity constant  $pK_{\text{H} \cdot \text{dImMP} \cdot \text{H}}^{\text{dImMP} \cdot \text{H}} = 6.46 \pm 0.07$  (Figure 3-4, lower pathway at the left). Therefore, this value is a good basis for comparisons with the acid-base properties of the imidazole moieties within the hairpin (see the following sections).

### 3.2.2 The hairpin structure of an oligonucleotide containing artificial imidazole nucleobases is strongly influenced by pH

#### 3.2.2.1 The modified DNA adopts a hairpin in solution

For our structural investigations we started with  $[^1\text{H}]$ -NMR experiments of the oligonucleotide (Figure 3-1A) in the absence of transition metals at neutral pH.  $[^1\text{H}, ^1\text{H}]$ -NOESY spectra at different temperatures reveal a well resolved *sequential walk* region and thus the proton resonances could be mostly assigned following the *sequential walk* along the H1' and aromatic protons (Figure 3-7). Three additional regions (H2'/aromatic, H2''/aromatic and aromatic/aromatic) served to cross-validate the assignments. The seven H8 resonances appear between 8.0 – 8.3 ppm and are well separated from the seven thymine H6 resonances that are found between 7.0 -7.5 ppm (Figure 3-7). Only very weak and broad

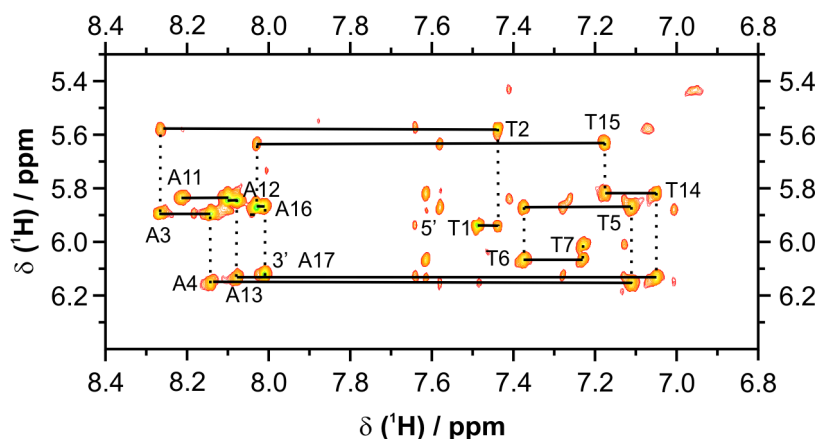


**Figure 3-7** 2D  $[^1\text{H}, ^1\text{H}]$ -NOESY spectrum of the *sequential walk* region of the hairpin at pD 7.2 (100 %  $\text{D}_2\text{O}$ , 120 mM  $\text{NaClO}_4$ , 298 K). The *sequential walk* is indicated by black dotted and solid lines. The labels represent the bases using the numbering scheme introduced in Figure 3-1 (A = adenine, T = thymine).

aromatic resonances were observed for the three imidazole moieties, and consequently the *sequential walk* could not be followed throughout the loop. Nevertheless, based on the sugar-sugar region in the NOESY spectrum as well as TOCSY and  $[^{13}\text{C}, ^1\text{H}]$ -HSQC spectra, the signals of the three artificial

nucleotides could be reliably identified and assigned. Typical resonances for a B-type helical conformation were observed for nucleotides T1-T7 and A11-T17. Moreover, the  $[^1\text{H}, ^1\text{H}]$ -TOCSY spectrum reveals strong H1'-H2' crosspeaks for all nucleotides, except for Im8, indicating a 2'-endo ("south-") conformation for these residues as usually found in B-DNA. The  $[^1\text{H}, ^1\text{H}]$ -NOESY spectrum acquired in  $\text{H}_2\text{O}$  shows a large overlap of the imino proton resonances. Nevertheless, 13 inter-strand correlations (mainly between adenine H2 and H1' on the opposite strand) prove the formation of a helical region with seven distinct adenine-thymine Watson-Crick base pairs. The  $[^{31}\text{P}]$ -NMR spectrum shows a set of signals between 0 and -0.5 ppm and a small broad peak at 0.45 ppm which is consistent with a

general hairpin structure.

However, it is difficult to distinguish unambiguously between a hairpin structure and a regular double helix by simple  $^1\text{H}$ -NMR experiments. We therefore determined the hydrodynamic radius  $r_{\text{H}}$  of the oligonucleotide by DOSY (diffusion-ordered spectroscopy) spectra as well as DLS (dynamic light scattering) measurements as already described in Section 2.2.1.3. These two independent methods gave identical values within the error limits of  $1.46 \pm 0.09$  and  $1.4 \pm 0.2$  nm, respectively. A theoretical calculation of  $r_{\text{H}}$  using well-established equations<sup>[193]</sup> and assuming a hairpin structure is in good agreement with the experimental values observed by DOSY and DLS (Table 3-9), providing evidence that indeed a hairpin structure is formed in the absence of  $\text{Ag}^+$  ions.

The structure calculation was performed starting from 200 initial structures calculated with DYANA,<sup>[113]</sup> which were then refined with XPLOR<sup>[114]</sup> (for details see Materials and

**Table 3-4** NMR restraints and structural statistics for the hairpin structure at pD 7.2.<sup>a</sup>

	pD 7.2
NOE-derived distance restraints	354
Natural base pairs	316
Imidazole nucleotides (Im8-Im10)	38
Intranucleotide	147
Internucleotide ( $ i - j  = 1$ )	185
Long-range ( $ i - n  \geq 2$ )	22
Repulsive	0
NOE restraint per residue	20.8
NOE violation $> 0.2$ Å	0
Dihedral restraints	148
Dihedral violations $> 5^\circ$	0
Hydrogen bond restraints	28
r.m.s.d. (for all heavy atoms to the best structure [Å])	
Overall	1.58±0.35
Helix	0.89±0.29
Loop (Im8-Im10)	2.66±0.82

<sup>a</sup>All statistics are given for the respective 20 lowest energy structures out of 200 calculated structures

methods Section 4.4.3). The structure determination is based on 354 conformationally restrictive NOE distance restraints, 148 dihedral restraints, and 28 hydrogen bond restraints (Table 3-4). The solution structure of the modified DNA hairpin is shown in Figure 3-8.

The DNA adopts a stable hairpin structure with a well-defined helical region closed by an unstructured loop composed of the three imidazole moieties. The overall r.m.s.d. (root-mean-square deviation) of all heavy atoms from the 20 lowest energy structures is  $1.6 \pm 0.4$  Å and the independent superposition of the helical region results in an r.m.s.d. of  $0.9 \pm 0.3$  Å

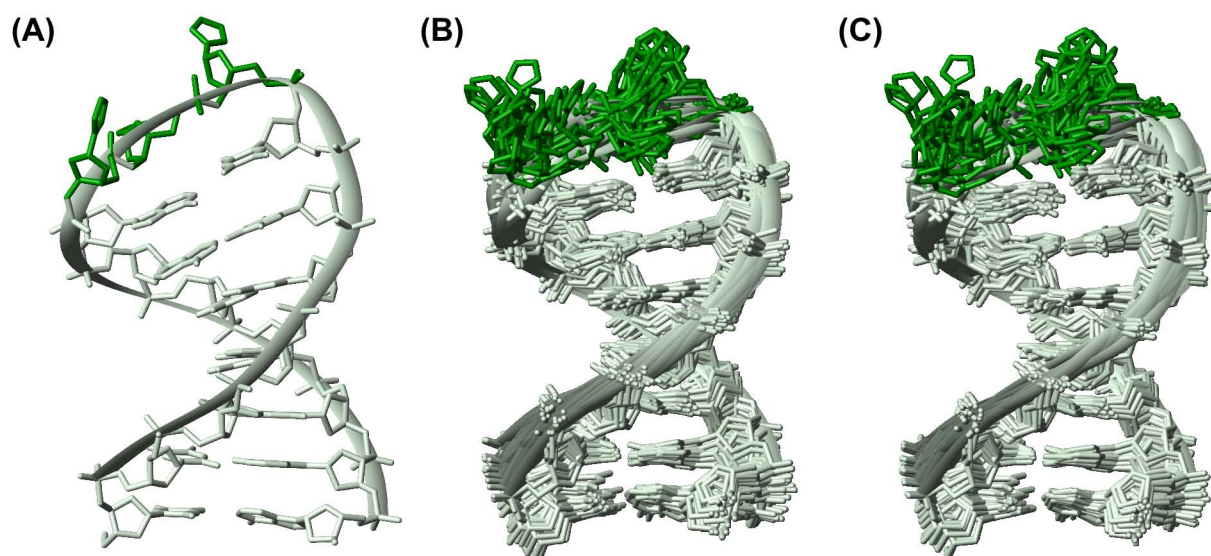


**Figure 3-8** NMR solution structure of the hairpin at neutral pH. The natural adenine-thymine base pairs are light and the imidazole nucleobases are bright coloured. **(A)** Lowest energy structure out of 200 calculated. **(B)** Overall superposition of all heavy atoms of the 20 lowest energy structures. **(C)** Superposition of all heavy atoms in the stem (nucleotides 1-7 and 11-17) of the 20 lowest energy structures.

(Table 3-4). The poor definition of the loop region is well in line with the small number of resonances observed and probably due to the semi-protonated state of the artificial nucleotides: The  $pK_a$  of the imidazole bases can be assumed to be around 6.4 (see sections 3.2.1 and 3.2.2.2) and consequently is close to the pH of 7.2 as used in the measurements. Obviously, no stable hydrogen bonding network is established between the imidazole moieties under these conditions.



### 3.2.2.2 $[^1\text{H}]$ -NMR shift experiments

In contrast to the natural occurring nucleobases which are all neutral in the physiological pH range  $5 < \text{pH} < 9$ , the artificial imidazole base is in a semi-protonated state at the N3 position around neutral pH (see Section 3.2.1). Thus, the deprotonation of the artificial nucleobases in the hairpin can be investigated in a pH range between about 4.8 and 10.4 without destroying the hydrogen bonds of the natural Watson-Crick base pairs of the neighbouring bases. For a detailed analysis of the acid-base properties of the oligonucleotide for each imidazole moiety  $[^1\text{H}]$ -NMR chemical shift experiments in  $\text{D}_2\text{O}$  were performed to determine the intrinsic  $\text{pK}_a$  values (Figure 3-9).

Starting in acidic solution at pD 4.8, all aromatic protons of the imidazole nucleobases show sharp and strong resonances; the H2 protons appear in the range of 8.6 - 9 ppm and the H4 and H5 protons at around 7.3 - 7.8 ppm. In general, the most downfield resonances are the

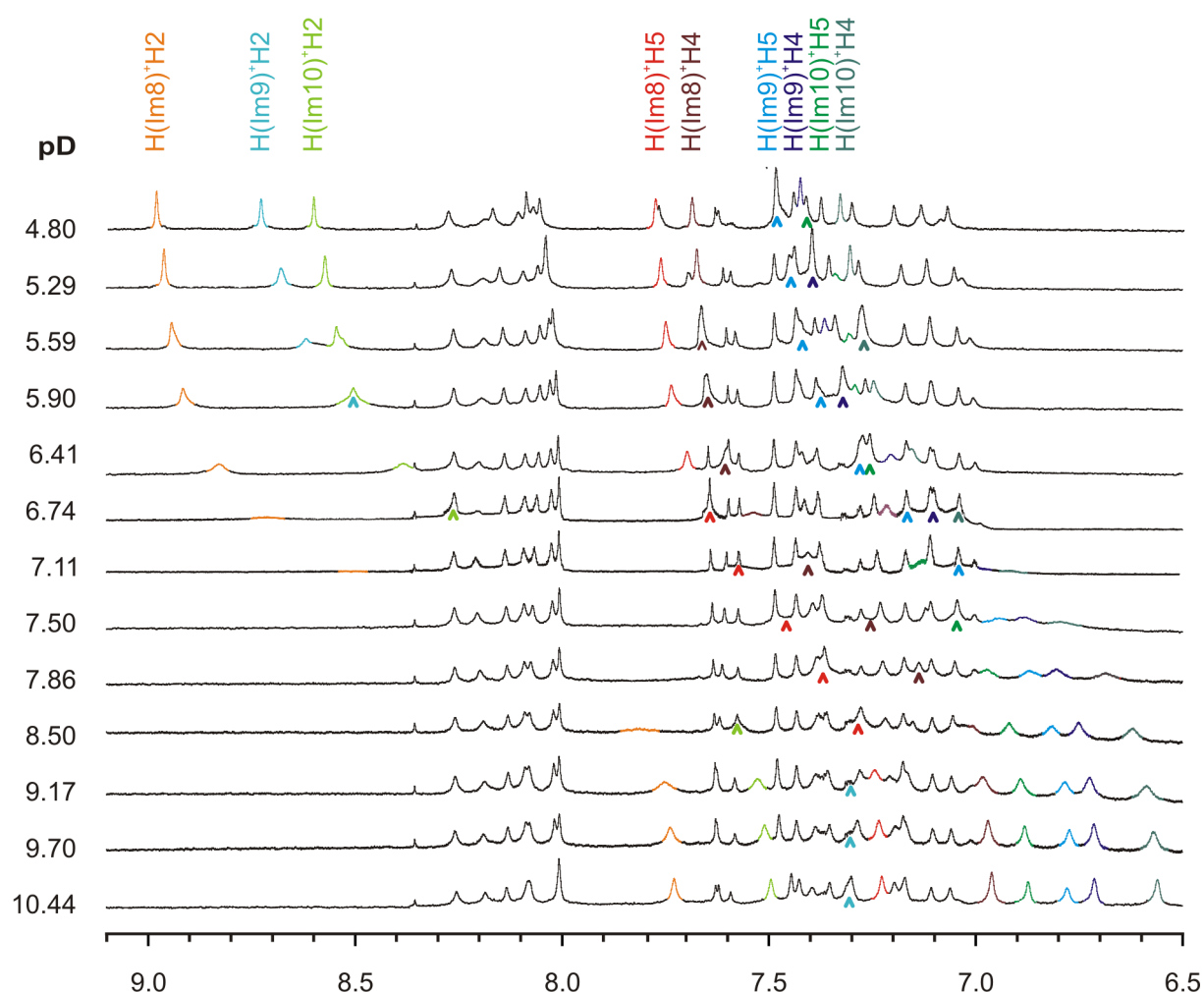


**Figure 3-9** Stack plot displaying the aromatic part of the  $[^1\text{H}]$ -NMR spectrum (6.5-9.1 ppm) of the oligonucleotide in  $\text{D}_2\text{O}$  in dependence on pD. The aromatic resonances of the imidazole moieties are coloured (H(Im8)<sup>+</sup>: H2 light red, H4 dark red, H5 red; H(Im9)<sup>+</sup>: H2 light blue, H4 dark blue; H5 blue; H(Im10)<sup>+</sup>: H2 light green, H4 dark green, H5 green).

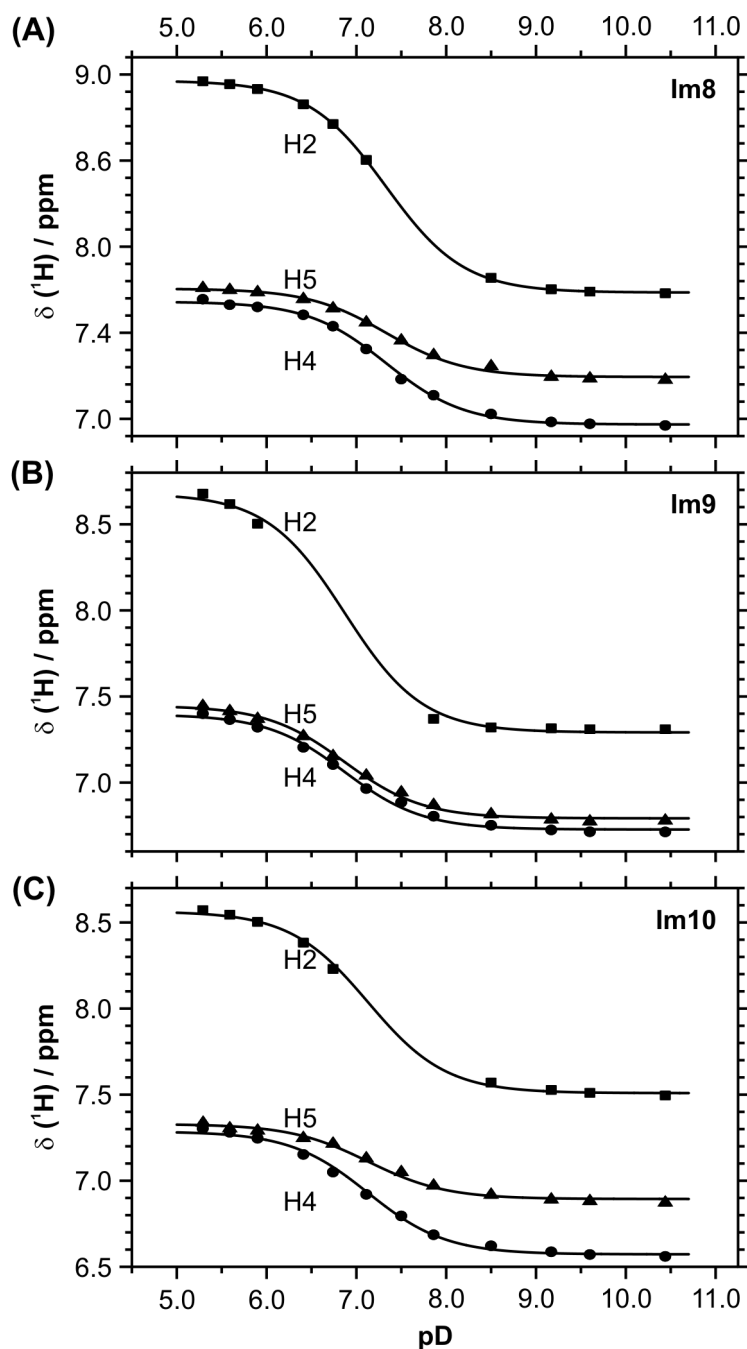


**Figure 3-10** pD dependence of the  $[^1\text{H}]$ -NMR chemical shifts of the H2 (■), H4 (●) and H5 (▲) protons of the three imidazole nucleobases a) Im8, b) Im9 and c) Im10 (25 °C,  $I = 0.12\text{ M}$ ,  $\text{NaClO}_4$ ). For the exact chemical shifts of the protonated and deprotonated forms, see also Table 3-5. The solid curves are the calculated best fits of the experimental data using the averaged  $\text{p}K_{\text{a,D}_2\text{O}}$  values given in Table 3-5.

Im8 protons followed by Im9 and then Im10 protons. However, with increasing pD all aromatic imidazole signals shift to higher field, broaden out and the H2 resonances even disappear around  $\text{pD} = 7$ . As the pH is raised above 9 all signals reappear continuously shifting upfield. Above  $\text{pD} = 9.7$  sharp resonances with similar intensity to the ones found at  $\text{pD} 4.8$  are observed without exhibiting further shifts. The pD dependence of the chemical shifts for each H2, H4 and H5 proton of the imidazole moieties is shown in Figure 3-10 as it was evaluated by a NEWTON-GAUSS non-linear least-square curve-fitting procedure as previously described.<sup>[143,150,220]</sup> All aromatic protons of the imidazole moieties display a strong pH dependent change in chemical shift; H2 being the most strongly affected proton due to the closer vicinity to the protonation site N3. The graphs

(Figure 3-10) further reveal that Im9 behaves differently compared to Im8 and Im10 with regard to the change of chemical shifts. While an increasing difference in change of the chemical shift between H4 and H5 is observed for Im8 and Im10, the difference in

**Table 3-5** Chemical shifts of H2, H4 and H5 for the three protonated (i.e., deuterated) imidazole residues ( $\text{H}(\text{dlm}8)^+$ ,  $\text{H}(\text{dlm}9)^+$  and  $\text{H}(\text{dlm}10)^+$ ) and their deprotonated form determined in  $\text{D}_2\text{O}$  (25 °C;  $I = 0.12 \text{ M}$ ,  $\text{NaClO}_4$ ) by  $[\text{H}]\text{-NMR}$  are given in columns 3 and 4. These chemical shifts were calculated by using the average value of the acidity constant (column 7); the range of error given once the standard deviation. In column 5 the shift differences  $\Delta\delta$ , resulting from deprotonation of the species, are listed:  $\Delta\delta = \delta_{\text{Him}} - \delta_{\text{Im}}$ . Values for  $\text{p}K_{\text{a,D}_2\text{O}}$  of the individual protons (column 6) are given with one standard deviation ( $1 \sigma$ ). The result for  $\text{p}K_{\text{a,D}_2\text{O}}$  (column 7) is the weighted mean with one standard deviation ( $1 \sigma$ ) of the individual values obtained from the various protons; this value is transformed to aqueous solution ( $\text{H}_2\text{O}$ ) by applying  $\text{p}K_{\text{a,H}_2\text{O}} = (\text{p}K_{\text{a,D}_2\text{O}} - 0.45)/1.015$  ref to give  $\text{p}K_{\text{a,H}_2\text{O}}$  (column 8). The error range given here is three times the standard error of the mean value.

H	$\delta_{\text{H-dlm}}$	$\delta_{\text{dlm}}$	$\Delta\delta$	$\text{p}K_{\text{a/D}_2\text{O,av.}}$	$\text{p}K_{\text{a/D}_2\text{O}}$	$\text{p}K_{\text{a/H}_2\text{O}}$	
ppm							
<b>H(Im8)<sup>+</sup></b>	H-2	8.964±0.002	7.734±0.003	1.230±0.004	7.331±0.008	7.329±0.012	6.78±0.03
	H-4	7.680±0.006	6.967±0.006	0.713±0.008	7.308±0.020		
	H-5	7.756±0.006	7.243±0.006	0.513±0.008	7.348±0.037		
<b>H(Im9)<sup>+</sup></b>	H-2	8.679±0.020	7.291±0.015	1.388±0.025	6.575±0.018		
	H-4	7.396±0.009	6.727±0.007	0.669±0.011	6.860±0.039	6.874±0.014 <sup>[a]</sup>	6.33±0.04 <sup>[a]</sup>
	H-5	7.447±0.008	6.792±0.007	0.655±0.011	6.888±0.037		
<b>H(Im10)<sup>+</sup></b>	H-2	8.564±0.009	7.513±0.006	1.051±0.011	7.052±0.026	7.134±0.075	6.58±0.23
	H-4	7.286±0.009	6.580±0.008	0.706±0.012	7.064±0.032		
	H-5	7.329±0.010	6.882±0.004	0.447±0.011	7.284±0.026		
<b>H(Im)<sup>+</sup></b>							6.01±0.05 <sup>[b]</sup>
<b>H(ImMP)<sup>-</sup></b>							6.46±0.07 <sup>[c]</sup>

<sup>[a]</sup> The  $\text{p}K_{\text{a,D}_2\text{O}}$  and the according  $\text{p}K_{\text{a,H}_2\text{O}}$  of the Im9 residue was determined using only the individual acidity constants of H4 and H5 due to complete disappearance of the H2 resonance between pD 6 and 8. <sup>[b]</sup> Taken from ref.<sup>[195]</sup> <sup>[c]</sup> Taken from section 3.2.1.

chemical shift stays identical within the error limits for Im9. The chemical shifts of the discussed protons as well as the individual  $pK_{a,D_2O}$  values obtained by the calculations are summarised in Table 3-5. From the latter, the weighted means were taken to give the final intrinsic acidity constants valid for  $D_2O$  which were then converted to  $pK_{a,H_2O}$  values according to equation 4.<sup>[218]</sup> The solid curves in Figure 3-10 are the calculated best fits of the experimental data applying the intrinsic  $pK_{a,D_2O}$  values of the imidazole moieties. For Im8 and Im10 the individual acidity constants of the three aromatic protons are in good agreement, while in the case of Im9 the  $pK_{a,D_2O}$  was calculated using only the H4 and H5 resonance. The H2 signal of Im9 could not be evaluated properly because it disappears above pD 6 and reappears only at pD 8 (Figure 3-9). Nevertheless, also this curve can be fitted nicely with the final intrinsic  $pK_{a,D_2O}$  value of Im9. These three acidity constants and for comparison reason also the  $pK_{a,H_2O}$  values of the imidazole base in the nucleoside and in the 5'-nucleotide are also assembled in Table 3-5.

The lowest acidity constant is observed for Im9 with  $pK_{a,H_2O} = 6.33 \pm 0.04$ , implying that this imidazole moiety is deprotonated first. The most obvious reason for this finding is the position between two additional positive charges at the neighbouring protonated imidazole moieties which probably facilitates the deprotonation of Im9. This would also explain the even lower value compared to the one observed for the single nucleotide  $H_2(dImMP)^{\pm}$ . Another reason might be that Im9 has the larger surface exposed to the solvent, compared to Im8 and Im10, as it is located in the centre of the loop. Therefore it is most likely that an electrostatic screening takes place by the solvent.<sup>[221]</sup>

The acidity constant of Im10 is  $6.58 \pm 0.23$  and unfortunately, the large error limits do not allow any accurate conclusions. On the one hand the value is identical to the value found for the mononucleotide  $H_2(dImMP)^{\pm}$  but it is also in the same range as the one of Im9 and even Im8 (Table 3-5). Nevertheless, it can be assumed that Im10 is deprotonated after Im9 but before Im8. The acidity constant of Im8 ( $pK_{a,H_2O} = 6.78 \pm 0.03$ ) is not only the largest of the three imidazole moieties but is also 0.3 log units larger than the one of  $H_2(dImMP)^{\pm}$ . It is known from literature that such a decrease in acidity can originate from an additional electrostatic energy input of the neighbouring nucleobases.<sup>[221]</sup> Such an input can be also assumed for Im8 due the previous deprotonation of Im9 and Im10. Compared to the situation in Im9 the deprotonation of Im8 takes place under the influence of an increasing negative charge from 0 to -2 at the neighbouring imidazole nucleotides explaining the distinct differences in acidity constants.

The results reveal that the acidity constants of the imidazole moieties Im8, Im9 and Im10 differ unambiguously not only from the mononucleotide  $\text{H}_2(\text{dImMP})^\pm$  but also from each other. This demonstrates how the presence of electrostatic interaction with neighbouring electronic groups such as nucleobases, phosphates, or the pentose-sugar units of nucleic acids in close vicinity causes perturbation of the intrinsic acidity constants.

### 3.2.2.3 Spectral features of the hairpin at different pH conditions

With the intrinsic acidity constants of the three imidazole moieties at hand, it will now be interesting to investigate the hairpin structure at low pH with fully protonated imidazole residues as well as the deprotonated form at high pH. Although the solution

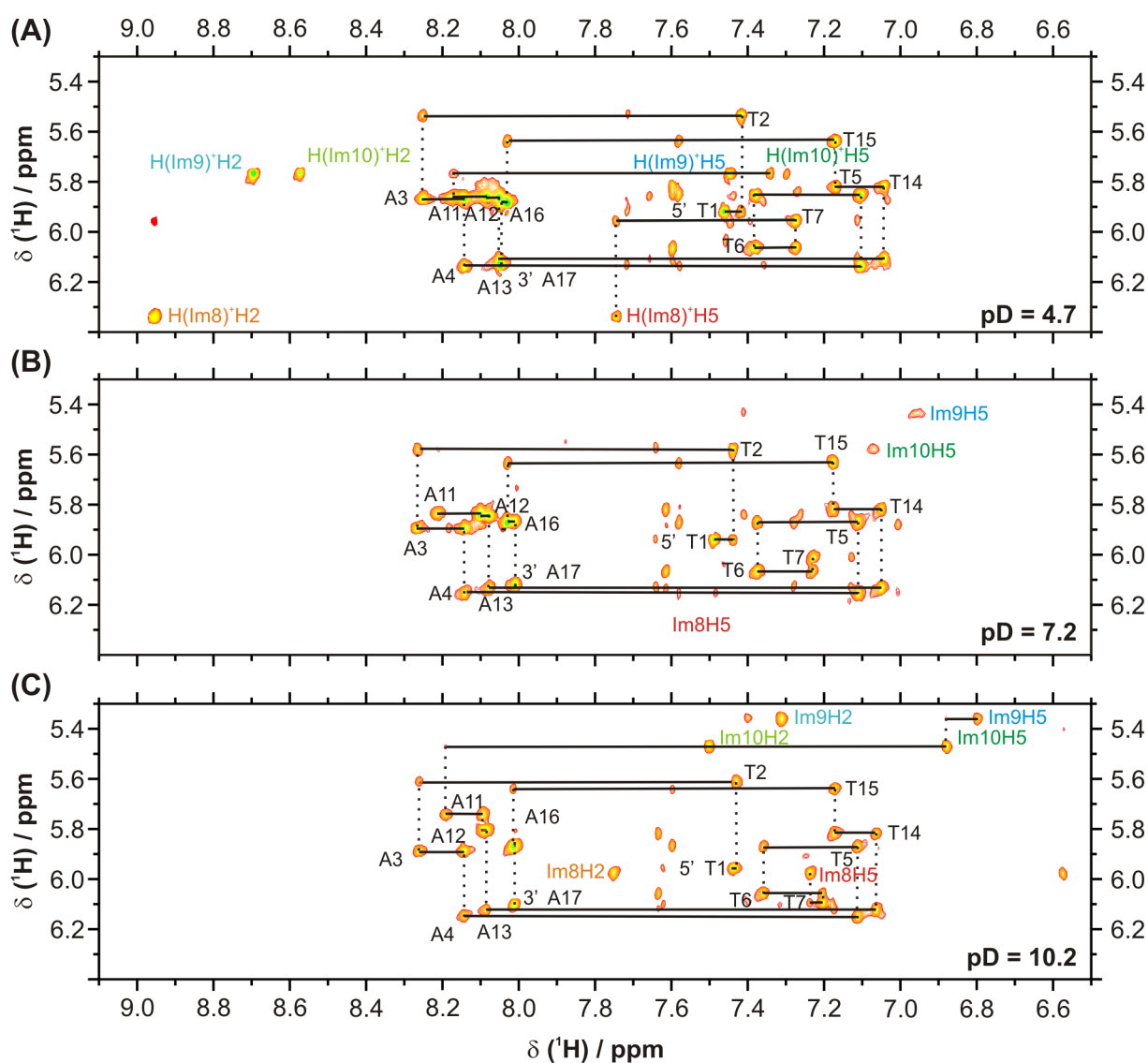


**Figure 3-11** Comparison of the 2D  $^1\text{H}$ ,  $^1\text{H}$ -NOESY spectra of the hairpin at acidic, neutral and basic pH. The corresponding *sequential walk* regions of the hairpin at (A) pD 4.7, (B) pD 7.2 and (C) pD 10.2 are shown (100 %  $\text{D}_2\text{O}$ , 120 mM  $\text{NaClO}_4$ , 298 K). The *sequential walk* is indicated by dotted and solid lines. The labels represent the bases using the numbering scheme introduced in Figure 3-1 (A = adenine, T = thymine, Im = imidazole). At acidic and basic pH more and sharper resonances were observed compared to neutral pH.

structure studies of the hairpin acquired by NMR at neutral pH show a pretty unstructured loop, the results of the  $[^1\text{H}]$ -NMR chemical shift experiments strongly suggest a well defined loop at acidic and basic pH. Based on this finding additional 2D NMR spectra were recorded at pD 4.7 and pD 10.2. Consistent with the sharp resonances of the aromatic protons in the artificial nucleobase at high and low pH, these NMR spectra reveal various new peaks that can be attributed to the imidazole nucleobases. In Figure 3-11 the *sequential walk* region, the section of crosspeaks between H1' and aromatic protons, of the  $[^1\text{H}, ^1\text{H}]$ -NOESY spectra at pD 4.7, and pD 10.2 is shown and for comparison reason also the one at pD 7.2. It is evident that in principle these regions look very similar, however at acidic and basic pH more signals appear. Nevertheless, it was not possible to follow the *sequential walk* throughout the entire sequence at anyone of the three pD values (see solid and dotted black lines in Figure 3-11),

**Table 3-6** The chemical shifts of the aromatic and the sugar protons H1', H2' and H2'' of the three imidazole residues and the adjacent residues T7 and A11 at pD 4.7, pD 7.2, and pD 10.2.

		H2	H4	H5	H6	H8	CH <sub>3</sub>	H1'	H2'	H2''
		ppm								
<b>pD 4.7</b>	T7				7.28		1.47	5.97	2.09	2.19
	H(Im8) <sup>+</sup>	8.96	7.67	7.75				6.35	2.59	2.74
	H(Im9) <sup>+</sup>	8.70	7.40	7.45				5.78	2.18	2.38
	H(Im10) <sup>+</sup>	8.58	7.31	7.35				5.77	2.13	2.41
	A11	7.45				8.18		5.87	2.79	2.93
<b>pD 7.2</b>	T7				7.23		1.53	6.01	2.09	2.23
	Im8	-	-	7.49				6.16	2.41	2.57
	Im9	-	6.91	6.96				5.43	1.96	2.10
	Im10	-	6.82	7.07				5.57	2.09	2.22
	A11	7.41				8.21		5.83	2.79	2.94
<b>pD 10.2</b>	T7				7.21		1.56	6.10	2.07	2.24
	Im8	7.75	6.98	7.24				5.98	2.37	2.40
	Im9	7.31	6.73	6.80				5.36	1.94	2.06
	Im10	7.50	6.58	6.88				5.47	2.03	2.11
	A11	7.40				8.19		5.74	2.77	2.88

because it is always interrupted by the artificial imidazole moieties. However, at acidic and basic pH also nearly all non-exchangeable proton resonances could be assigned (Table 3-6) by using also other sections of the [ $^1\text{H}$ ,  $^1\text{H}$ ]-NOESY spectra as well as additional TOCSY and [ $^{13}\text{C}$ ,  $^1\text{H}$ ]-HSQC spectra (for further details see Materials and methods Section 4.4.2). The pattern of the helical part at all pH conditions is almost identical, therefore the assignment was done in the same manner as already described for pD 7.2 (see Section 3.2.2.1).<sup>[196]</sup> By contrast, the loop regions vary significantly from each other, indicating that the structure of the loop is heavily dependent on the pH conditions. The chemical shifts of the aromatic and the sugar protons H1', H2' and H2'' of the three imidazole residues and the adjacent residues T7 and A11 at pD 4.7, pD 7.2, and pD 10.2 are summarized in Table 3-6. The small chemical shift changes of T7 and A11 reveal that also at the neighbouring nucleotides are slightly affected by the protonation / deprotonation reaction of the imidazole moieties. In contrast to the protons of the imidazole moieties which shift only upfield, the H1', H2'', and the CH<sub>3</sub> protons of T7 exhibit a downfield shift most likely due to a change of the loop structure.

#### 3.2.2.4 The structure of the hairpins at pD 4.7 and pD 10.2

The structure calculations of the hairpin at pD 4.7 and pD 10.2 were performed in the same manner as the one at pD 7.2 starting from 200 initial structures calculated with DYANA,<sup>[113]</sup> which were then refined with XPLOR<sup>[114]</sup> (for details see Materials and methods Section 4.4.3). The resulting 20 lowest energy structures out of 200 calculated are shown in Figure 3-12 and the structural statistics are assembled in Table 3-7. At pD 4.7 the structure determination is based on 417 conformationally restrictive NOE distance restraints,

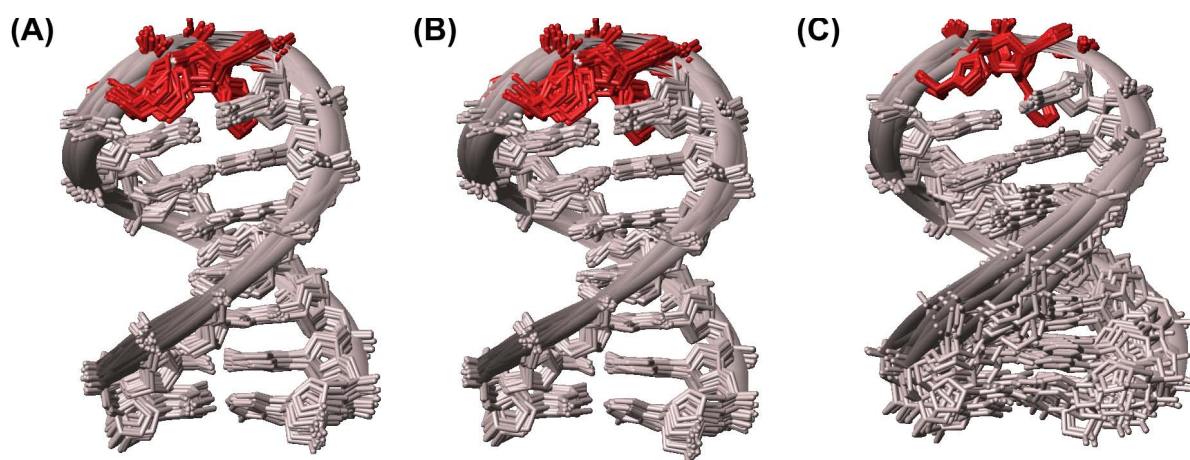


**Figure 3-12** NMR solution structure of the hairpin at acidic pH. The natural adenine-thymine base pairs are light and the imidazole nucleobases are bright coloured. (A) Superposition of all heavy atoms of the 20 lowest energy structures. (B) Superposition of all heavy atoms in the stem (nucleotides 1-7 and 11-17) of the 20 lowest energy structures. (C) Superposition of all heavy atoms in the loop (nucleotides 8-10) of the 20 lowest energy structures.



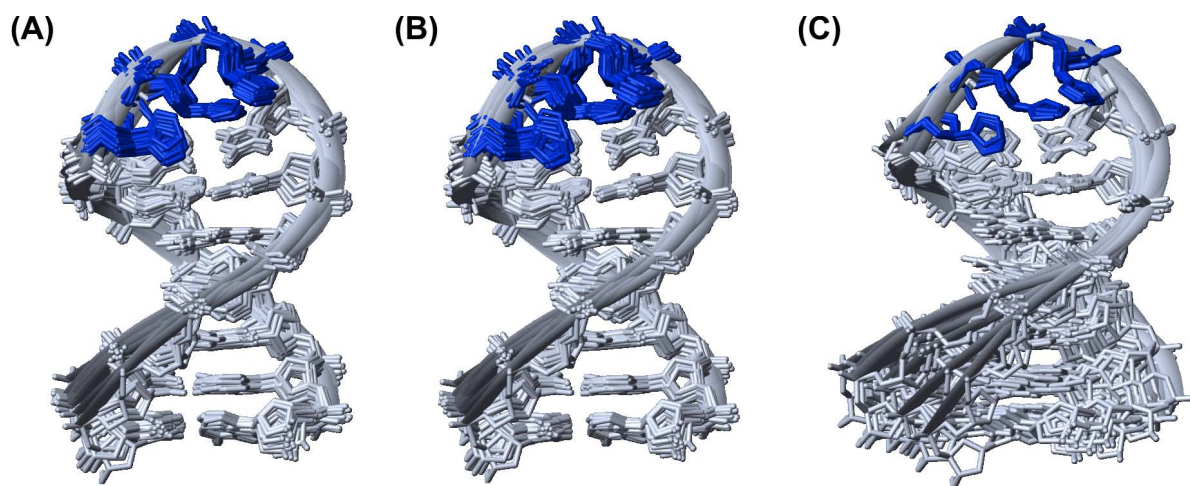


**Figure 3-13** NMR solution structure of the hairpin at basic pH. The natural adenine-thymine base pairs are light and the imidazole nucleobases are bright coloured. **(A)** Superposition of all heavy atoms of the 20 lowest energy structures. **(B)** Superposition of all heavy atoms in the stem (nucleotides 1-7 and 11-17) of the 20 lowest energy structures. **(C)** Superposition of all heavy atoms in the loop (nucleotides 8-10) of the 20 lowest energy structures.

**Table 3-7** NMR restraints and structural statistics for the hairpin at pD 4.7 and pD 10.2.<sup>a</sup>

	pD 4.7	pD 10.2
NOE-derived distance restraints	417	411
Natural base pairs	319	316
Imidazole nucleotides (Im8-Im10)	98	95
Intranucleotide	170	164
Internucleotide ( $ i - j  = 1$ )	216	208
Long-range ( $ i - n  \geq 2$ )	31	39
Repulsive	0	0
NOE restraint per residue	24.5	24.2
NOE violation $> 0.2$ Å	0	0
Dihedral restraints	153	153
Dihedral violations $> 5^\circ$	0	0
Hydrogen bond restraints	28	28
r.m.s.d. (for all heavy atoms to the best structure [Å])		
Overall	0.74±0.15	0.74±0.19
Helix	0.66±0.15	0.70±0.18
Loop (Im8-Im10)	0.48±0.18	0.49±0.34

<sup>a</sup>All statistics are given for the respective 20 lowest energy structures out of 200 calculated structures



153 dihedral torsion angles as well as 28 hydrogen bond restraints. The overall r.m.s.d. is  $0.74 \pm 0.15$  for all heavy atoms of the 20 lowest energy structures. Likewise, the structures of the hairpin at pD 10.2 were calculated from 411 NOE-derived distance restraints, 153 dihedral torsion angles, and 28 hydrogen bond restraints leading to a overall r.m.s.d. of  $0.74 \pm 0.15$ . At pD 7.2 only 38 NOE distance restraints (Table 3-4) define the loop while at acidic conditions 98 and at basic conditions 95 constraints (Table 3-7), respectively, offer a precise view of the respective structural features. Especially the large number of internucleotide and long-range distance restraints improves tremendously the overall picture of the loop region. Consequently, the loop is the least well-defined part at neutral pH, whereas at acidic and basic conditions the independent superposition of the loop region results in low r.m.s. deviations of  $0.48 \pm 0.18$  and  $0.49 \pm 0.34$ , respectively (Table 3-7, Figure 3-12, Figure 3-13). An overlay of the lowest-energy structure at pD 4.7 (red), pD 7.2 (green) and pD 10.2 (blue) is depicted in Figure 3-14A. It becomes immediately obvious that the structures of the helices do not differ significantly from each other while the loop conformation is evidently strongly influenced by

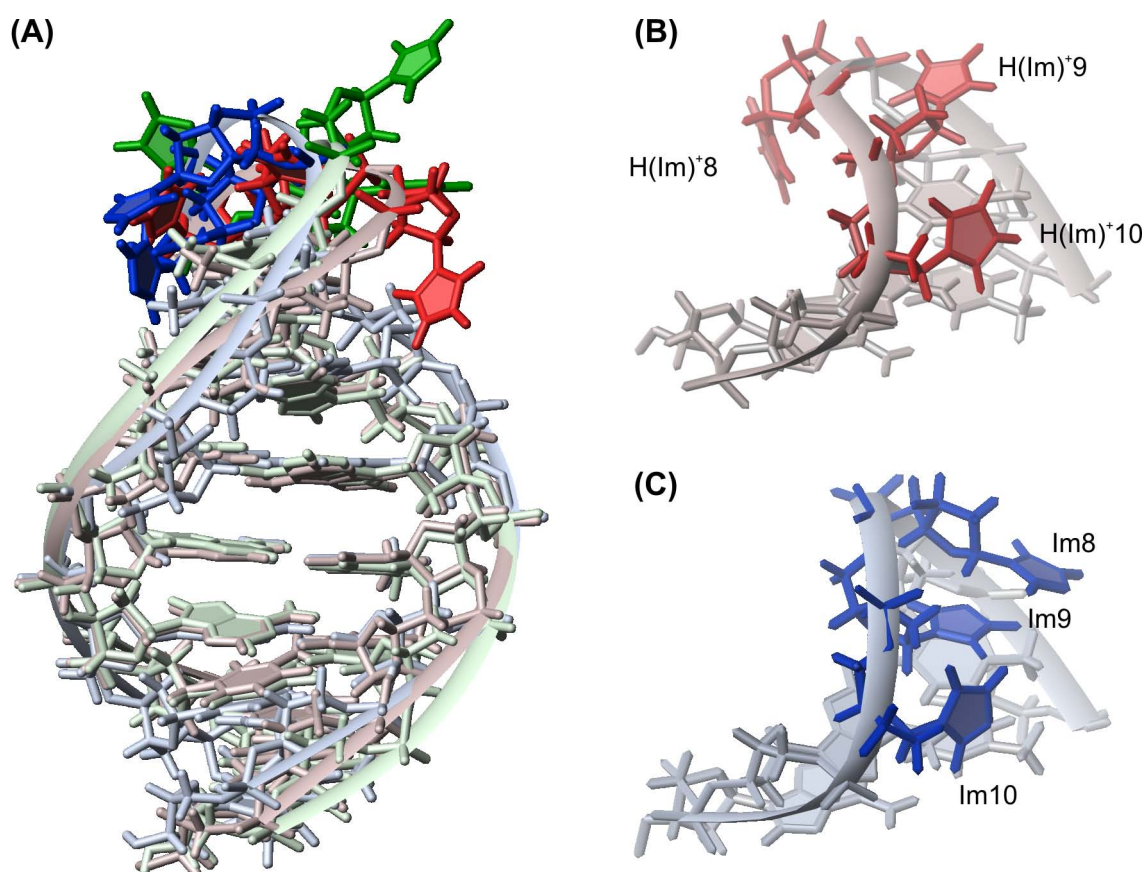


**Figure 3-14** Structural features of the loop region in dependence on the pD. **(A)** Overlay of the lowest energy structures of the hairpin at pD 4.7 (red), pD 7.2 (green) and pD 10.2 (blue). Magnification of the loop at **(B)** pD 4.7 and **(C)** pD 10.2 exhibits two different but well-defined loop conformations.

pH. By taking a closer look it turns out that the loop adopts two distinct conformation at acidic and at basic pH (Figure 3-12), respectively, while at neutral pH no well defined structure can be observed (Figure 3-8). At pD 4.7 the imidazole residues Im9 and Im10 point towards the major groove whereas Im8 is oriented in the opposite direction towards the core of the helix (Figure 3-14B). Apparently, the imidazole moieties try to avoid each other which most likely follows from a large repulsive force due to the positive charges of the protonated N3 atoms. Moreover, these positive charged groups of Im9 and Im10 are oriented towards the negatively charged phosphate-sugar backbone, thus allowing optimal charge compensation. By contrast, at high pH all imidazole residues are aligned towards the major groove (Figure 3-14C) and also the entire loop is stretched in this direction. On closer inspection it even seems that the three artificial residues actively push the loop into the major groove, leading to the kink in the backbone between Im10 and A11. In addition Im9 is nicely lying on top of T7 therefore extra stacking interactions can be assumed which is strongly supported by the numerous observed crosspeaks between the non-exchangeable protons of these two bases (T7H6-I9H4, T7H6-I9H5, T7CH<sub>3</sub>-I9H2, T7CH<sub>3</sub>-I9H4, and T7CH<sub>3</sub>-I9H5).

### 3.2.2.5 The loop conformation is dependent on pH

Upon increase of pH the loop adopts two distinct conformations with completely different structural characteristics most likely originating from changes of the overall charge. Considering three additional positive charges at low pH, the structure is arranged in a way that the electropositive locations are in rather close neighbourhood to the negatively charged phosphate backbone. In accordance with these results the electrostatic surface potential reveals no spots which are particular high electropositive (Figure 3-15). Apparently, the good charge compensation of the hairpin upon decrease of pH is mainly achieved by the rearrangement of the loop, even though additional hydrogen bonds could potentially also stabilize the positive charges. However, no additional hydrogen bonds at the extra N3 protons were found. At basic conditions the situation is certainly different. The spatial proximity of T7 and Im9 causes that the uncharged loop is more affected by stacking interactions rather than by electrostatic forces. This is also supported by the electrostatic surface potential which displays no distinctive features (Figure 3-15C). Still, at acidic and basic pH the shape of the hairpins are very similar as in both cases the artificial imidazole moieties are embedded within the structure (Figure 3-14 and Figure 3-15). Despite the poor definition of the loop at neutral pH, the 20 lowest energy structures at pD 7.2 (Figure 3-8) clearly reveal that in contrast to acidic and basic conditions the imidazole moieties are mostly loomed out of the

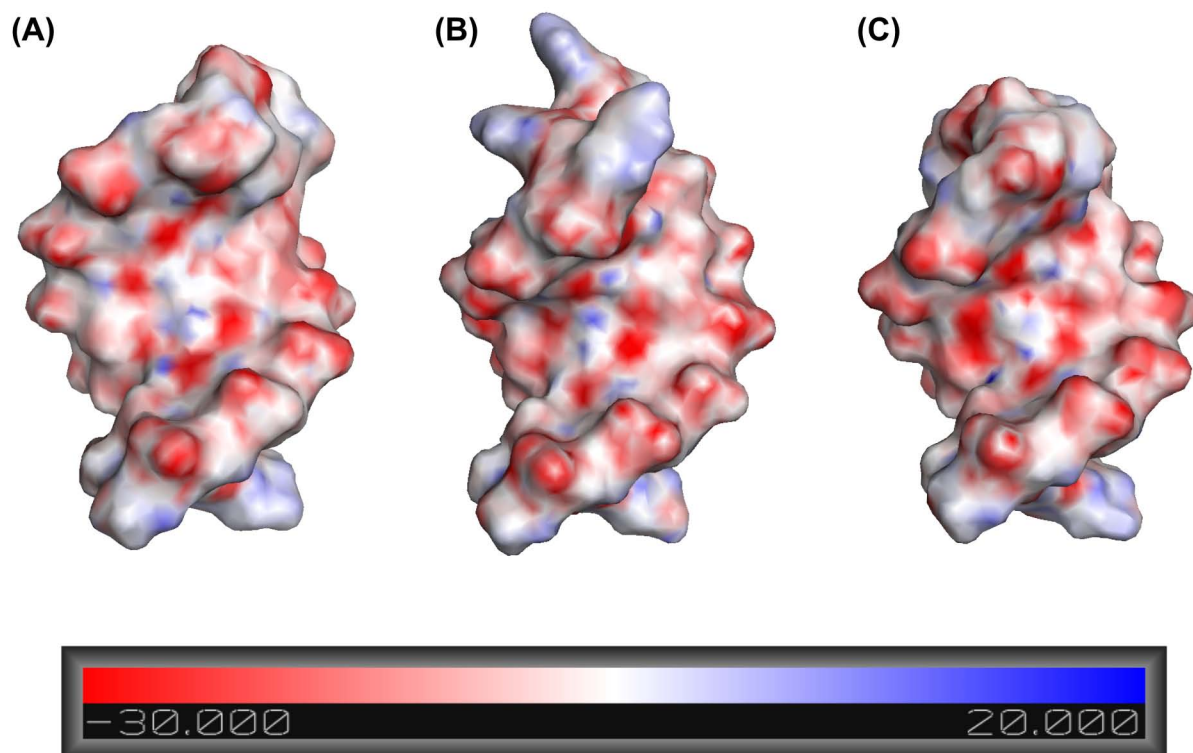


**Figure 3-15** Electrostatic surface potential of the hairpin at (A) pD 4.7, (B) pD 7.2, and (C) pD 10.2. The electrostatic surface potential of the three-dimensional DNA structures was calculated using QNIFT<sup>[222]</sup> and visualized with PYMOL (<http://www.pymol.org>). For further details see Materials and methods section 4.4.3.4. Red indicates negative ( $-30 \text{ kTe}^{-1}$ ), white neutral ( $5 \text{ kTe}^{-1}$ ), and blue positive ( $20 \text{ kTe}^{-1}$ ) charges. No spots which are particular high electropositive or electronegative were found for any of the pH conditions indicating a good charge compensation just by rearrangement of the hairpin.

structure. At this point it remains to be determined whether the undefined loop structure is the result of a structural intermediate between the two distinct loop conformations or whether the exchange rate of the N3 protons is too fast for the NMR time scale and therefore not resolved.

As already mentioned, natural nucleobases are neutral at physiological pH consistent with the requirements of the Watson-Crick base pairing pattern. However, it is also well known that  $pK_a$  values can be shifted into physiological range due to additional hydrogen bonds, direct metal ion interaction (in close vicinity), or favourable electrostatic influences.<sup>[223-226]</sup> Especially, in folded RNA perturbed  $pK_a$ s are the rule rather than the exception because nucleobases with shifted  $pK_a$ s are prerequisite for acid-base catalysis.<sup>[226]</sup>

As the  $pK_a$  values of the imidazole moieties are already in the range of physiological pH, our oligonucleotide constitutes a model system for reaction centres in catalytically active RNA exhibiting acid-base catalysis. Therefore it is a big advantage that the  $pK_a$  values of the imidazole moiety allow structural investigation of the fully protonated (all three imidazoles nucleobases are protonated at the N3 position) but also of the fully deprotonated form (all

three imidazoles nucleobases are deprotonated at the N3 position) of the oligonucleotide without destroying the natural Watson-Crick base pairs. The structure determination shows that the imidazoles moieties are not involved in additional hydrogen bonds and that additional metal ion interaction can be excluded also. Therefore, the difference in  $pK_a$  values can primarily be explained by the influence of the local environment, for example by arrangement of the functional groups in close proximity to negatively charged phosphoryl oxygens.

### 3.2.3 Structure conversion from hairpin to duplex upon addition of silver ions

#### 3.2.3.1 The oligonucleotide adopts a duplex structure in the presence of $\text{Ag}^+$ ions

After the exhaustive investigation of the oligonucleotide in the absence of transition metals, one equivalent of  $\text{Ag}^+$  ions was added i.e. the amount needed to form a duplex with three metal-mediated base pairs (for details see Materials and methods section 4.4.1). The NMR spectra change considerably with significant improvement of the quality. Especially in the *sequential walk* region many new intense and sharp resonances appear (Figure 3-18B) that can be attributed to the imidazole moieties. This indicates a

rigid structure around the imidazole nucleotides as is expected for the formation of imidazole-silver-imidazole base pairs with the N3 nitrogen atoms coordinating the  $\text{Ag}^+$  ions (Figure 3-1C). As a result of the palindromic sequence and the  $C_2$  symmetry of the double

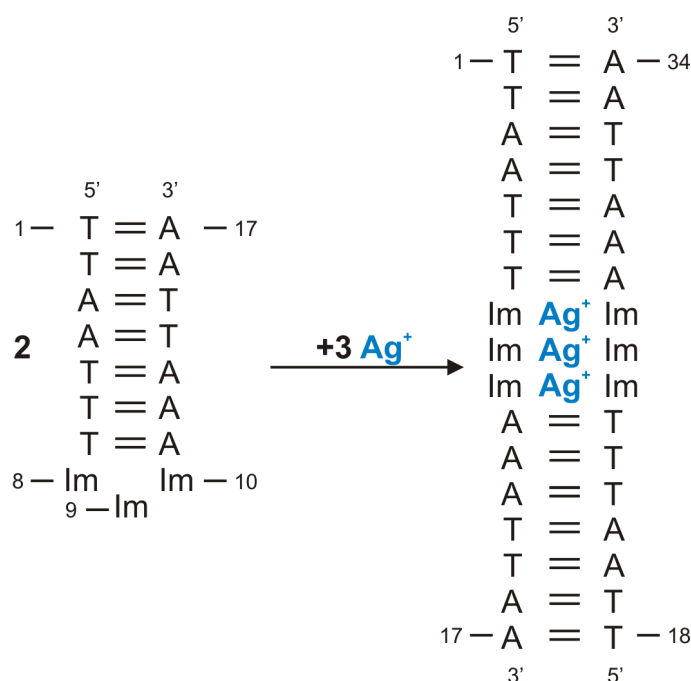


**Figure 3-16** Schematic depiction of the hairpin to duplex transition of the oligonucleotide.

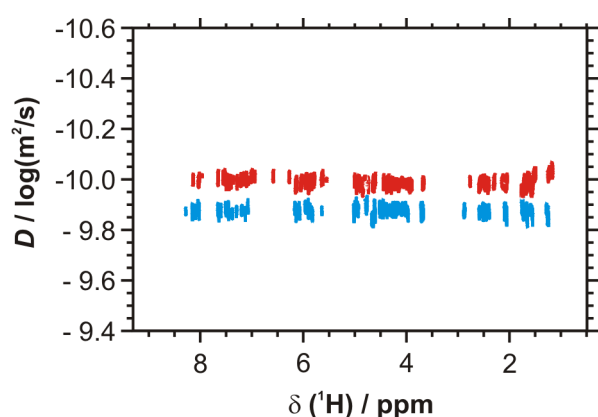


**Figure 3-17** Overlay of the DOSY spectra of the oligonucleotide in the absence of  $\text{Ag}^+$  (blue) and in the presence of 1 eq  $\text{Ag}^+$  (red) demonstrates a structure conversion from hairpin to duplex upon addition of  $\text{Ag}^+$  ions.

helix, resonances of 17 nucleotides, i.e. exactly half the total number, can be observed and assigned. Interestingly, all H2 and H4 proton resonances of the imidazole moieties display a remarkable upfield shift of 0.40 - 1.08 ppm upon metalation (Table 3-9) indicating increased stacking interactions. The resonances of the nucleotides neighbouring the imidazole moieties show slight changes in chemical shift compared to the hairpin, whereas the helical

nucleotides display a very similar pattern. The [ $^1\text{H}, ^1\text{H}$ ]-TOCSY spectrum exhibits strong H1'-H2' crosspeaks indicating a 2'-endo conformation for all nucleotides except for the artificial imidazole building blocks. However, all [ $^{31}\text{P}$ ]-NMR resonances were found to be in the region typical for a regular B-helical structure.<sup>[227]</sup>

As already described for the hairpin, the hydrodynamic radius  $r_{\text{H}}$  was determined by DOSY and DLS measurements. The values of the  $r_{\text{H}}$  amount to  $1.9 \pm 0.3$  nm and  $1.8 \pm 0.2$  nm, respectively and are significantly larger than the ones found for the hairpin in the absence of  $\text{Ag}^+$  ions (Figure 3-17 and Table 3-8). Moreover, the  $r_{\text{H}}$  matches perfectly the theoretical radius (1.81 nm) which was calculated based on the assumption of a double helical structure again confirming duplex structure formation.

**Table 3-8** Hydrodynamic radii  $r_{\text{H}}$  of the hairpin and the metal-modified duplex as determined by DOSY ( $r_{\text{H,DOSY}}$ ) and DLS ( $r_{\text{H,DLS}}$ ). Shown are also the theoretical length  $L$  of the respective DNA based on an average distance between base pairs of 0.34 nm along the helix axis, the ratio  $q = L/d$  (with  $d = 2.0$  nm being the diameter of B-DNA), and the theoretical hydrodynamic radius  $r_{\text{H}}$ . The latter was calculated according to a spherical model for  $q < 2$  or to a symmetrical cylinder model for  $q > 2$  (for further details see also section 2.2.1.3).

				Theoretical values		Experimental values	
				Spherical model	Cylinder model	DOSY	DLS
	bp	L	q	$r_{\text{H}}$	$r_{\text{H}}$	$r_{\text{H}}$	$r_{\text{H}}$
		nm					
<b>Hairpin</b>	8.5	2.55	1.28	1.28	1.36	$1.46 \pm 0.09$	$1.43 \pm 0.19$
<b>Duplex</b>	17	5.44	2.72	2.72	1.81	$1.90 \pm 0.25$	$1.75 \pm 0.19$

### 3.2.3.2 $\text{Ag}^+$ -mediated base pairs are formed in the DNA double helix

To provide final proof that imidazole-silver-imidazole base pairs are formed,  $^{15}\text{N}$ -labelled imidazole nucleosides were incorporated into the oligonucleotide. The [ $^{15}\text{N}, ^1\text{H}$ ]-HSQC (heteronuclear single quantum coherence) spectra of the oligonucleotide in the absence and in the presence of  $\text{Ag}^+$  are shown in panels (C) and (D) of Figure 3-18. Prior to the addition of the transition metal ions, only a few not very well-resolved cross-peaks are visible, indicating the presence of a rather unstructured hairpin loop. The [ $^{15}\text{N}$ ]-NMR chemical shifts cluster around 188 ppm for the N1 atoms (involved in the glycosidic bonds) and 221 ppm for the

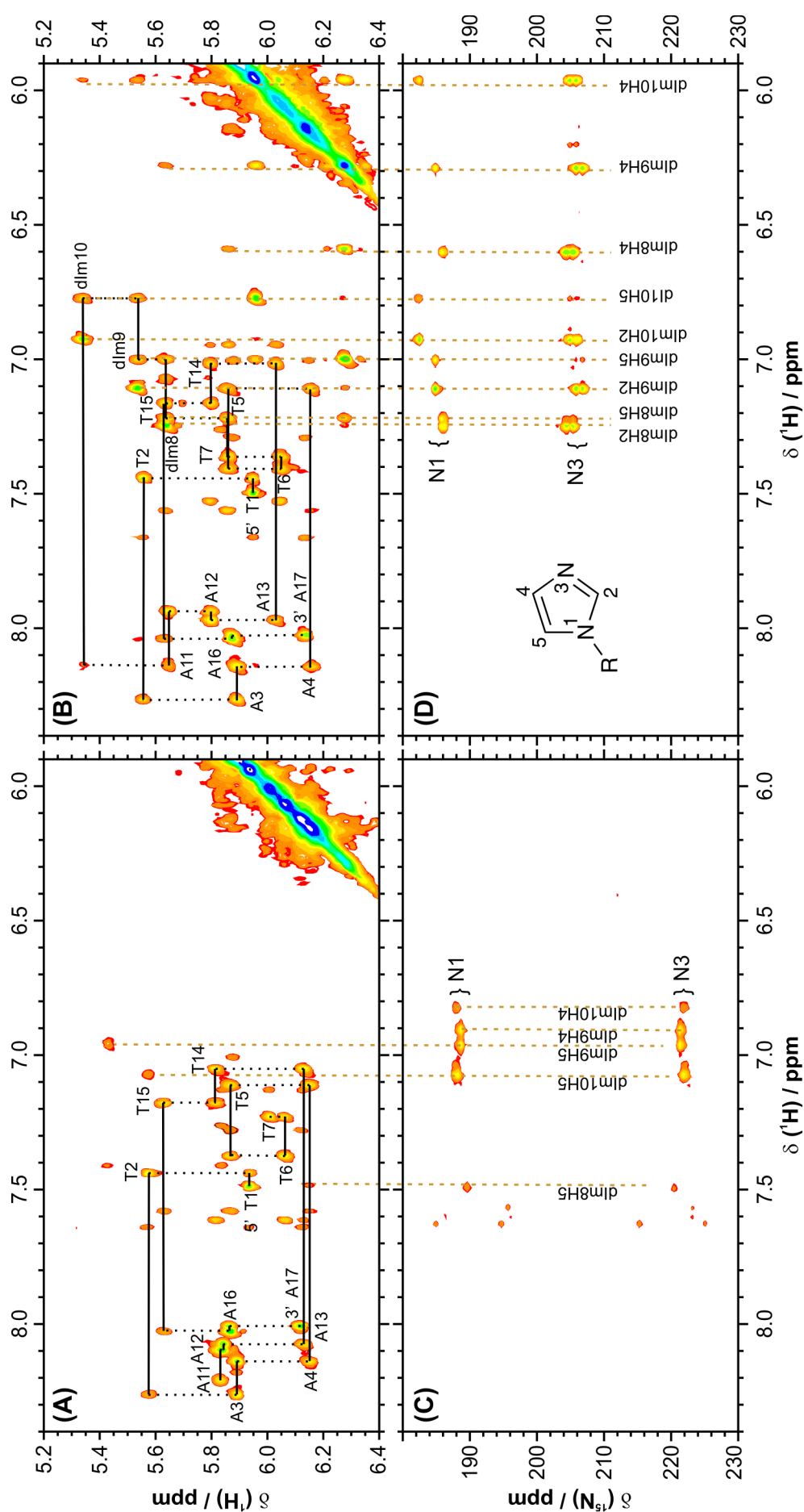


**Figure 3-18** Comparison of sections of the  $[\text{H}, ^{15}\text{N}]$ -HSQC spectra of hairpin (A, C) and metalated helix (B, D). As can be seen more and sharper resonances become visible for the metalated duplex compared to the hairpin. In panels (A) and (B), the *sequential walk* is indicated by solid and dotted lines. The labels represent the bases using the numbering scheme introduced in Figure 3-1 (A = adenine, T = thymine, Im = imidazole). A *sequential walk* can only be followed in regions adopting a helical structure. Thus, a comparison of panels (A) and (B) clearly shows that the imidazole nucleotides are included within the helical structure only upon formation of metal-mediated base pairs. In panels (C) and (D), sections of the  $[\text{H}, ^{15}\text{N}]$ -HSQC spectra show the upfield shift of the endocyclic imidazole nitrogen atoms N1 and N3 (for atom numbering scheme, see panel D) that indicates the formation of silver(I)-mediated base pairs. The black dotted vertical lines interconnect cross-peaks of identical protons within the different panels.



**Table 3-9** Chemical shift changes of the H2, H4, H5, N1, and N3 imidazole resonances upon metalation of the oligonucleotide at pD 7.2.

	Im8			Im9			Im10		
	$\delta_{\text{Hairpin}}$	$\delta_{\text{Duplex}}$	$\Delta\delta$	$\delta_{\text{Hairpin}}$	$\delta_{\text{Duplex}}$	$\Delta$	$\delta_{\text{Hairpin}}$	$\delta_{\text{Duplex}}$	$\Delta$
	ppm								
<b>H-2</b>	8.33	7.25	-1.08	7.51	7.11	-0.40	7.87	6.93	-0.94
<b>H-4</b>	7.31	6.59	-0.72	6.89	6.28	-0.61	6.82	5.96	-0.86
<b>H-5</b>	7.50	7.22	-0.28	6.96	7.00	+0.04	7.08	6.78	-0.30
<b>N-1</b>	189.5	186.3	-3.2	188.6	185.3	-3.3	188.1	183.0	-5.1
<b>N-3</b>	220.5	205.5	-15.0	221.4	206.9	-14.5	221.9	206.0	-15.9

N3 atoms (Table 3-9). In the presence of one equivalent of  $\text{Ag}^+$ , the resolution of the HSQC spectrum improves dramatically indicating a more rigid structure and thus being well in line with the formation of a double helix. All nitrogen resonances experience an upfield shift. The N1 resonances shift to about 185 ppm ( $\Delta\delta \approx -3$  ppm) while the N3 resonances appear at about 206 ppm ( $\Delta\delta \approx -15$  ppm). This significant upfield shift clearly argues for a metal coordination to the N3 positions<sup>[228]</sup> and is also indicative of increased stacking interactions as expected in a helix. Most importantly, the  $^{15}\text{N}$  resonances of the N3 atoms

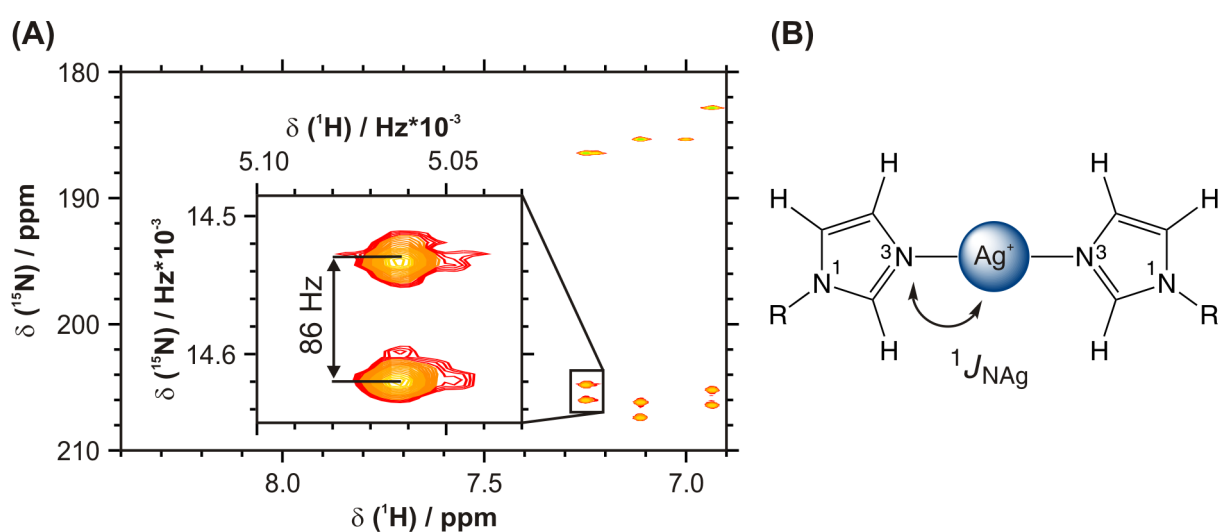


**Figure 3-19** Direct evidence for the formation of imidazole-silver-imidazole base pairs. **(A)** Section of the  $^{15}\text{N}$ ,  $^1\text{H}$ -HSQC (recorded at higher resolution than that displayed in Figure 3-18D with the magnification of the Im8 N3-H2 and N3-H5 cross-peaks as an example to illustrate the  $^1J(^{15}\text{N}, ^{107/109}\text{Ag})$  coupling of 86 Hz. **(B)** The chemical structure shows the connectivities within the metal-mediated base pair, highlighting the bond along which the  $^1J$  coupling is observed.



show a splitting of 86 Hz in the presence of  $\text{Ag}^+$  ions (Figure 3-19). This splitting is caused by a direct coupling between the nitrogen and the silver atoms, i.e. a  $^1J(^{15}\text{N}, ^{107/109}\text{Ag})$  coupling (Figure 3-19A). This provides the first direct proof for the formation of an azole-silver-azole base pair. To the best of our knowledge this is also the first time that such a coupling has been measured in aqueous solution at ambient temperature.  $^1J(^{15}\text{N}, ^{107/109}\text{Ag})$  coupling constants are observed rarely because  $\text{Ag}^+$  usually binds to nitrogen donors in a highly labile fashion.<sup>[229]</sup> Under such conditions, the rapid ligand exchange removes the coupling between silver and any other magnetic nucleus on the ligand. The observed  $^1J(^{15}\text{N}, ^{107/109}\text{Ag})$  coupling therefore proves that the  $\text{Ag}^+$  ions are tightly bound to the artificial nucleosides and exchange reactions are slow. As a result of the  $C_2$  symmetry of the double helix, only three distinguishable imidazole N3 atoms are observed per duplex, which all show the same coupling within the resolution limits. It was not possible to differentiate between the  $^1J(^{15}\text{N}, ^{107}\text{Ag})$  and  $^1J(^{15}\text{N}, ^{109}\text{Ag})$  couplings because of heavy overlap of the N3 signals in the  $^{15}\text{N}$ -INEPT (insensitive nuclei enhancement by polarisation transfer) spectrum (Figure 3-20) and because of relatively large line widths of the N3 signals of 17 Hz in the  $^{15}\text{N}, ^1\text{H}$ -HSQC spectrum, respectively. However, from the large line width it is obvious that both couplings must be present because the N1 signals display a width of only 7 Hz (Figure 3-19A). Thus, it is most likely that the 86 Hz correspond to an average value of  $^1J(^{15}\text{N}, ^{107}\text{Ag})$  and  $^1J(^{15}\text{N}, ^{109}\text{Ag})$

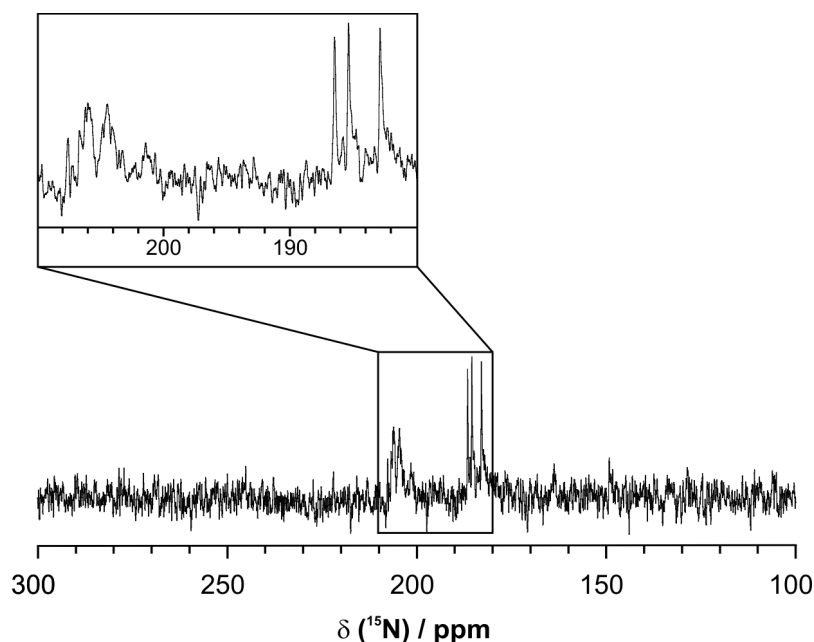


**Figure 3-20**  $^{15}\text{N}$ -INEPT spectrum of the  $\text{Ag}^+$ -containing DNA duplex. The lowfield signals of the imidazole N3 are split due to the  $^1J(^{15}\text{N}, ^{107/109}\text{Ag})$  coupling of 86 Hz, but also overlap heavily. This spectrum has been recorded on a Bruker AV 500 MHz machine, equipped with a BBO probe (298 K,  $\text{D}_2\text{O}$ , 40 k scans, SW = 213 ppm).

because of the almost identical natural abundance of  $^{107}\text{Ag}$  and  $^{109}\text{Ag}$  (51.8 % vs. 48.2 %). The individual coupling constants can be calculated based on the gyromagnetic ratios that differ by only 15 % ( $\gamma(^{109}\text{Ag})/\gamma(^{107}\text{Ag}) = 1.15$ ),<sup>[230]</sup> yielding  $^1J(^{15}\text{N}, ^{107}\text{Ag}) \approx 80 \text{ Hz}$  and  $^1J(^{15}\text{N}, ^{109}\text{Ag}) \approx 92 \text{ Hz}$ .<sup>[231]</sup> In general, the  $^1J(^{15}\text{N}, ^{107/109}\text{Ag})$  value of 86 Hz represents the largest coupling (by about 20 Hz) of this type reported as yet

either in solution or the solid state.<sup>[231-233]</sup>

To obtain further details of the  $\text{Ag}^+$ -binding, [ $^{109}\text{Ag}$ ,  $^1\text{H}$ ]-HMQC experiments were set up similar to the one used for silver-substituted yeast metallothionein.<sup>[234]</sup> To date, this example is the only one where such an experiment could be successfully applied to a large biomolecule. Unfortunately, in our case no signal could be obtained probably due to the following reasons:

- (i) To implement the experiment successfully, the magnitude of the  $^3J(^1\text{H}, ^{109}\text{Ag})$  coupling constant needs to be known, and it must be measurable.  $^3J(^1\text{H}, ^{109}\text{Ag})$  constants in the literature were found between 6.3 - 10.5 Hz.<sup>[232,235-239]</sup> Coupling constants this small require a long time for the preparation and refocusing intervals to achieve maximum sensitivity. Unfortunately the short  $T_2$  values owing to the large size of the molecule result in significant signal decay during these long intervals, and therefore in a reduction in the sensitivity of the HMQC experiment.
- (ii) As a result of the large  $^{109}\text{Ag}$  chemical shift range ( $> 1300$  ppm), the effective bandwidth of the transmitter pulse can present a limitation in the absence of a priori knowledge of the  $^{109}\text{Ag}$  resonance frequency.
- (iii) In the above mentioned experiment,<sup>[234]</sup> the  $\text{Ag}^+$  ions were bound to sulphur ligands, i.e. much stronger than when bound to nitrogen like in our case.

### 3.2.3.3 Solution structure of the DNA double helix

The solution structure of the resulting double helix is shown in Figure 3-21. The structure was determined based on 848 conformationally restrictive NOE distance restraints, 218 dihedral restraints, 56 hydrogen bond restraints, and 18 additional imidazole-imidazole restraints (Table 3-10). During structure refinement a non-crystallographic symmetry (NCS) term was applied to accomplish perfect  $C_2$  symmetry based on the NMR spectra (see above). The overall r.m.s.d. of all heavy atoms of the 20 lowest energy structures is  $1.26 \pm 0.37$  Å. The individual superposition of the artificial nucleotides results in an r.m.s.d. of  $0.49 \pm 0.16$  Å. A total of 198 NOE-derived distance constraints were obtained just for the artificial nucleotides, including 6 interstrand and 36 direct stacking NOEs of the imidazole rings. The large number of distance restraints obtained for these residues helped tremendously to define the precise orientation of the artificial bases. Overall, the metalated DNA retains its B-form helix upon formation of  $\text{Ag}^+$ -mediated base pairs in its centre. The solution structure provides the first structural insight into a nucleic acid with consecutive metal-mediated base pairs. It also proves that a DNA double helix can adopt the regular B-type conformation while at the same

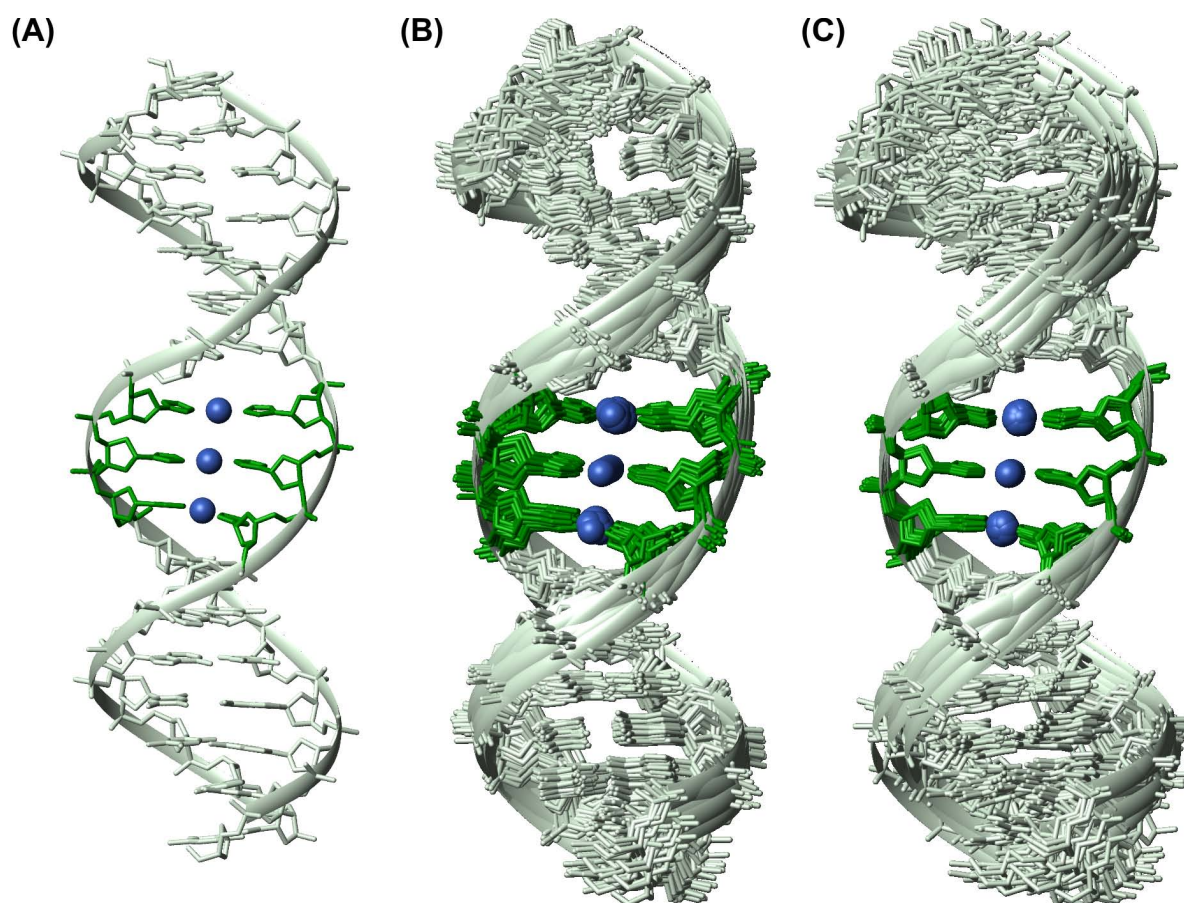


**Figure 3-21** NMR solution structure of the duplex containing the  $\text{Ag}^+$ -mediated imidazole base pairs in its centre. The natural adenine-thymine base pairs are lightly and the imidazole nucleobases are brightly coloured. **(A)** Lowest energy structure out of 200 calculated. **(B)** Overall superposition of all heavy atoms of the 20 lowest energy structures. **(C)** Superposition of all heavy atoms of the artificial imidazole residues (nucleotides 7-10 and 25-28) of the 20 lowest energy structures.

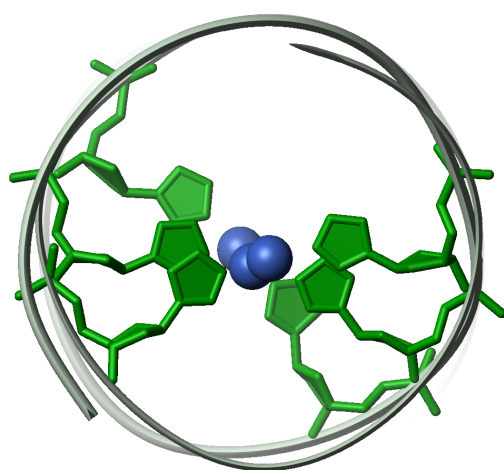


**Figure 3-22** Top view on the three consecutive metal-mediated base pairs along the helix axis. The backbone ribbon is displayed for the whole duplex. It can clearly be discerned that the metal ions align along the helical axis.

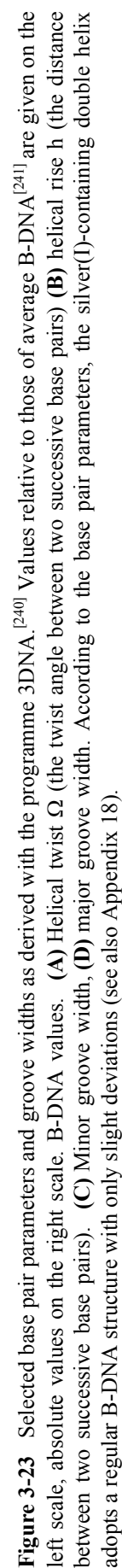
time arranging metal ions along its helical axis (Figure 3-22), as is evident from the base pair parameters shown in Figure 3-23 and Appendix 18, calculated with the programme 3DNA.<sup>[240]</sup> In general, the absolute values of the respective parameters are shown on the right whereas the values relative to those of average B-DNA<sup>[241]</sup> are given on the left. Tilt  $\tau$  (i.e. the dihedral angle for rotation of a base pair around its short axis, with respect to its neighbour), roll  $\rho$  (i.e. the dihedral angle for rotation of a base pair around its long axis, with respect to its neighbour), inclination  $\eta$  (i.e. the angle between

**Table 3-10** NMR restraints and structural statistics of the metal-containing DNA duplex structures.<sup>a</sup>

	Duplex
NOE-derived distance restraints	848
Natural base pairs	650
Imidazole nucleotides (Im8-Im10, Im25-Im27)	198
Intranucleotide	366
Internucleotide ( $ i - j  = 1$ )	442
Long-range ( $ i - n  \geq 2$ )	40
Repulsive	0
NOE restraint per residue	24.9
NOE violation $> 0.2$ Å	0
Dihedral restraints	218
Dihedral violations $> 5^\circ$	0
Hydrogen bond restraints	56
Imidazole-imidazole restraints	18
r.m.s.d. (for all heavy atoms to the best structure [Å])	
Overall	1.26±0.37
Helix	0.57±0.13
Im8-Im10 / Im25-Im27	0.49±0.16

<sup>a</sup>All statistics are given for the respective 20 lowest energy structures out of 200 calculated structures

the long axis of a base pair and a plane perpendicular to the helix axis) and global displacement (i.e. translation of a base pair within its mean plane with respect to the helix axis) of all nucleobases adopt values close to those of B-DNA (Appendix 18). Interestingly, small deviations from the B-type structure are observed for the helical twist  $\Omega$  (i.e. the twist angle between two successive base pairs) and the helical rise  $h$  (i.e. the distance between two successive base pairs) (Figure 3-23A, C). Both parameters are global parameters based on C1'-C1' vectors. The helical twist  $\Omega$  adopts values of about  $36^\circ$ , with the exception of the two central base pair steps between the three metal-mediated base pairs, The helical twist of these three metal-mediated base pairs amounts to only  $\sim 28^\circ$ , indicating a slight unwinding of the



three metal-mediated base pairs amounts to only  $\sim 28^\circ$ , indicating a slight unwinding of the double helix. This unwinding seems to be caused by an opening of the minor groove, while the major groove remains largely unchanged (Figure 3-23A, B, D). As this slight distortion of the B-type DNA conformation occurs only at the centre of the duplex, it appears as if intrinsic structural parameters of the artificial base pairs are the main contributors. Along the same line, the helical rise  $h$  is typically in the range of 3.4 Å, again with significant deviations from

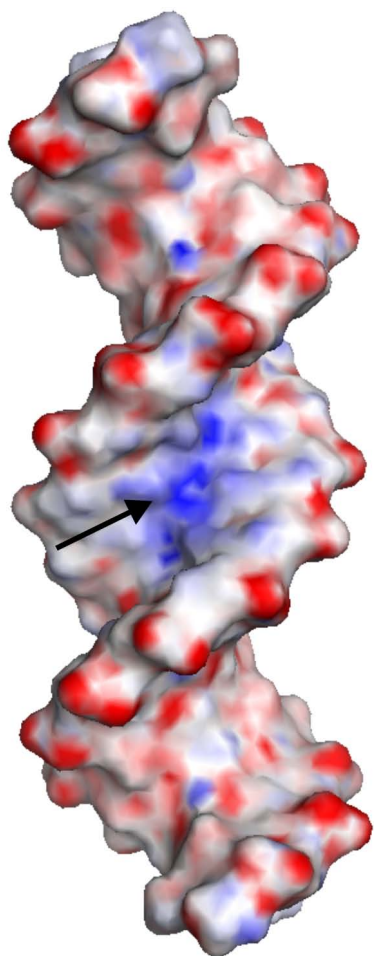


**Figure 3-24** Electrostatic surface potential of the duplex at pH 7.2. The electrostatic surface potential of the three-dimensional DNA structures was calculated using QNIFFT<sup>[222]</sup> and visualized with PYMOL (<http://www.pymol.org>) (for further details see Materials and methods section 4.4.3.4). Red indicates negative ( $-30 \text{ kTe}^{-1}$ ), white neutral ( $5 \text{ kTe}^{-1}$ ), and blue positive ( $20 \text{ kTe}^{-1}$ ) charges. An unusual high electropositivity is observed in the minor groove around the imidazole moieties (black arrow).

this value in the central region of the double helix (Figure 3-23C).  $h$  increases to 4.3(1) Å between adjacent adenine-thymine and imidazole-silver-imidazole base pairs and to 4.1(3) Å between consecutive metal-mediated base pairs. Interestingly, the rise between a natural and an artificial base pair is slightly larger than that in between two artificial base pairs. The increased rise therefore appears not to result from a potential interaction of adjacent metal ions along the helical axis but rather to be an intrinsic property of the imidazole-silver-imidazole base pair. In this context, the metal-metal distances between neighbouring  $\text{Ag}^+$  ions along the helical axis amount to 3.92 Å and 3.97 Å for the lowest-energy structure, and vary between 3.79 and 4.51 Å for the 20 best structures. The value of almost 4 Å for the lowest-energy structure appears to rule out direct metal-metal interactions. This distance is unexpectedly large, especially considering that attractive argentophilic interactions are frequently observed between closely spaced  $\text{Ag}^+$  ions.<sup>[242]</sup> On the other hand, the high variation – also manifested in the relatively large standard deviation of the helical rise  $h$  for the central two base pair steps – shows that the energy differences between conformations with differing metal-metal distances are small. As a result, only minor energetic changes can lead to structures with a significant metal-metal interaction. For example, a recent theoretical study on DNA containing  $\text{Cu}^{2+}$ -mediated base pairs proved that metal-metal distances down to 3.22 Å are possible within

the structural context of a DNA double helix.<sup>[243]</sup> At this point it remains unclear whether the observed metal-metal distances are merely the result of an overestimation of the electrostatic repulsion during the structure calculations or whether they might actually be a bit shorter.

The view on the electrostatic surface potential map reveals an unusual high electropositivity in the minor groove close to the imidazole moieties nicely showing the arrangement of the metal ions like pearls on a string (Figure 3-24). Even though the duplex is double the size of the hairpin the intense blue spots indicate a much higher electropositivity than observed for the hairpin at pD 4.7 (Figure 3-15) that also possess three positive charges. It seems that in contrast to the hairpin at pD 4.7 no charge compensation occurs in the direct surrounding.

### 3.3 Conclusion and outlook

Metal-mediated base pairs allow the incorporation of metal ions in a defined fashion along the axis of nucleic acid helices. Such precise control is necessary for potential applications as nanomagnets, as self-assembling molecular wires or as catalysts in chemical reactions. Here we have shown that artificial imidazole nucleobases are a powerful tool to insert and subsequently array  $\text{Ag}^+$  ions in a predictable manner into a DNA helix by forming very stable imidazole-silver-imidazole base pairs. A 17 nt long oligonucleotide containing three imidazole (Im) moieties as nucleobase surrogates was studied in detail by NMR in the absence and in the presence of  $\text{Ag}^+$  ions. Extensive structure analysis reveals that a structure conversion from hairpin to duplex takes place upon addition of  $\text{Ag}^+$  ions. This result was confirmed by determination of the hydrodynamic radii with DOSY and DLS measurements in the absence and in the presence of  $\text{Ag}^+$  ions.

In the absence of  $\text{Ag}^+$  ions the oligonucleotide adopts a stable hairpin with the three imidazole moieties located in the loop. At neutral pH no distinct loop conformation could be observed due to the semi-protonated artificial imidazole nucleobases. In contrast, for the fully protonated form at pD 4.7 as well as for the fully deprotonated form at pD 10.2 two well-defined loop structures were observed. In both cases the imidazole moieties are embedded within the helix and are arranged in such a way that good charge compensation is achieved. At pD 4.7 the positive charges have a maximum distance between each other and are directed towards the negatively charged phosphate backbone. Compared to the acidic ambience, at basic pH all imidazole moieties point into the major groove where an additional stacking between T7 and Im9 can be assumed. Thus, the conversion of the loop upon increase of pH is due to the change of the overall charge. Besides, investigations of the acid-base properties of the imidazole moieties reveal differences in the acidity constants compared to the mononucleotide  $\text{H}_2(\text{dImMP})^\pm$  but also to each other. This nicely shows that the acidity constant is strongly influenced by electrostatic interaction with the surrounding close by.

In the presence of  $\text{Ag}^+$  ions the oligonucleotides forms a stable duplex with three silver mediated imidazole base pairs in the middle. The determination of the three dimensional structure provides the first structure of a B-type DNA double helix containing consecutive metal-mediated base pairs. The solution structure of the self-complementary oligonucleotide shows that the metal ions are incorporated along the helical axis. In the sole previously determined structure of a DNA duplex with metal-mediated base pairs, the metal ions were located at the periphery of the helix due to the Z-type conformation of the helix.<sup>[44]</sup> NMR is a



powerful tool not only to determine three dimensional structures of nucleic acids but also to detect precisely metal ion binding sites and to elucidate specific metal ion coordination spheres in nucleic acids.<sup>[244]</sup> Thus, the observation of  $^1J(^{15}\text{N}, ^{107/109}\text{Ag})$  couplings in aqueous solution at room temperature provides a direct proof for the formation of the metal-mediated base pairs. Moreover, analysis of the base pair parameters shows that the incorporation of the artificial metal-containing base pairs takes place without major conformational distortions. A slight unwinding of the helix in the region of the imidazole-silver-imidazole base pairs provides the opportunity for the development of small molecules that selectively recognize this structural motif. Silver-silver distances between consecutive metal-mediated base pairs amount to 3.92 Å and 3.97 Å for the lowest-energy structure. Nevertheless, direct silver-silver interactions cannot be ruled out completely because the duplex structure seems to be rather dynamic, thereby allowing shorter metal-metal distances without large energy barriers.

Until metal-modified nucleic acids can be applied as electronic devices it is still a long way. On the one hand, cheap methods to synthesise large amounts of these metal modified oligonucleotides are required. *In vitro* transcription using *T7* RNA polymerase as mentioned in the previous chapter could be a good opportunity to overcome the drawback of synthesis. So far this method could not successfully be applied to modified nucleobases but the incorporation of artificial bases is well establish for several DNA polymerases.<sup>[245-251]</sup> Thus, mutation of the *T7* RNA polymerase, others than described in the previous chapter, could help to overcome this difficulty. On the other hand, also the electrical properties of the metal modified nucleic acids need to be investigated in detail. To date no comprehensive study of these electrical properties is known for such oligonucleotides. Nevertheless, it should be possible to set up experiments similar to that applied by Barton and co-workers to natural nucleic acids.<sup>[252]</sup> The results of such a characterisation together with our structural information at hand may even make it possible to tune the electrical properties of such metal-modified nucleic acids.



## 4 Materials and methods

### 4.1 Materials and chemicals

DNA oligonucleotides were purchased from MICROSYNTH, Balgach (Switzerland). Both, ribose as well as deoxyribose nucleotide 5'-triphosphates came from GE HEALTHCARE (formerly AMERSHAM BIOSCIENCES EUROPE GmbH), Otelfingen (Switzerland), except for UTP, which was from SIGMA-ALDRICH-FLUKA, Buchs (Switzerland).  $^{13}\text{C}$ ,  $^{15}\text{N}$ -labeled UTPs were obtained from SILANTES GmbH, München (Germany), now part of CAMBRIDGE ISOTOPE LABORATORIES, Andover (USA). Aqueous acrylamide solution (AccuGel 29:1) and TBE (Tris-borate-EDTA) buffer for the purification of RNA and DNA were purchased from NATIONAL DIAGNOSTICS, Hissle Hull (UK), and urea (UltraPure) from EUROBIO, Les Ulis (France). The wild type and the double mutant Y639F / S641A of the T7 RNA polymerase used for *in vitro* transcription was homemade by my colleague Susann Paulus.<sup>[116,253]</sup> The mutations were inserted by standard PCR mutagenesis procedure. Tyrosin was substituted by phenylalanin at position 639 (Y639F) and serin was substituted by alanin at position 641 (S641A). For desalting VIVASPIN 2 from VIVASCIENCE Hannover (Germany) with a molecular weight cut-off of 3 kDa or NAP 10 columns from GE HEALTHCARE were used.

Deuterated reagents, that are  $\text{D}_2\text{O}$  (100 %),  $\text{D}_2\text{O}$  (99.999 % D),  $\text{D}_2\text{O}$  (99.98 % D), NaOD (40 % in  $\text{D}_2\text{O}$ ; 99.9 % D), and  $\text{DNO}_3$  (65 % in  $\text{D}_2\text{O}$ ; 99.5 % D) were from ARMAR CHEMICALS, Doettlingen (Switzerland).

The buffer solutions of pH 4.00 and 7.00 were obtained from METROHM AG, Herisau (Switzerland) and the one at pH 9.21 was from METTLER-TOLEDO GmbH, Schwerzenbach (Switzerland); all buffer solutions based on standard reference materials (SRM) of the US NATIONAL INSTITUTE OF SCIENCE and TECHNOLOGY (NIST).

All chemicals were at least puriss p.a. and purchased from FLUKA-SIGMA-ALDRICH, Buchs (Switzerland) or BRUNSCHWIG CHEMIE, Amsterdam (The Netherlands).

## 4.2 Instrumentation

The electroelution apparatus BIOTRAP and the BT1 and the BT2 elutrap membranes were purchased from WHATMAN, London (UK). The used centrifuges were a 5415R, 5415D, and a 5804R with rotor F-45-24-11 and 5804R with rotor A-4-44 from EPPENDORF, Hamburg (Germany), as well as a RC5C PLUS from SORVALL, LANGENSELBOLD (Germany) with a SA-600, a SH-3000, and a SLA-3000 rotor. The purified RNA samples were vacuum-dried in a Concentrator 5301 from EPPENDORF.

NMR spectra were recorded on a BRUKER AV2-400 MHz spectrometer with a 5 mm QNP probehead, a BRUKER AV2-500 MHz spectrometer using either a 5 mm BBI or a 5 mm BBO probehead, a BRUKER DRX-500 MHz spectrometer with a 5 mm BBI probehead, a BRUKER AV-600 MHz spectrometer with a CP-TCI z-axis pulsed-field gradient CryoProbe<sup>®</sup>, or a BRUKER AV-700 MHz spectrometer with a CP-TXI z-axis pulsed-field gradient CryoProbe<sup>®</sup>, at the NMR facility of the Chemical Institutes at the University of Zurich.

Ultraviolet (UV) measurements were carried out on a CARY 500 SCAN UV-VIS-NIR and on a CARY 100 UV-VIS spectrophotometer from VARIAN INC., Palo Alto (USA) connected to a circulating temperature controller using a 10 mm QS cuvette from HELLMMA, Mühlheim (Germany).

Circular dichroism (CD) spectra were recorded on a J-810 spectropolarimeter from JASCO Inc., (Japan) using a 10 mm QS cuvette from HELLMMA. Data evaluation was done by using JASCO spectra manager-spectra analysis.

Dynamic light scattering (DLS) was performed on a DYNA PRO TITAN Instrument from WYATT TECHNOLOGY, Santa Barbara (USA).

The potentiometric pH titrations were carried out with an E536 potentiograph connected to an E665 dosimat and a 6.0253.100 AQUATRODE-PLUS combined macro glass electrode from METROHM. The instrument was calibrated using the buffer solutions pH 4.00, 7.00 and 9.21 mentioned above.

The pH values were measured with a HAMILTON Minitrode glass electrode from HAMILTON AG, Bonaduz, (Switzerland) connected to a METROHM 605 digital pH meter. The buffer solutions pH 4.00, 7.00 and 9.21 mentioned above were used to calibrate the instrument.

The H<sub>2</sub>O used in all experiments was treated with a TKA genepure water purification system from TKA WASSERAUFBEREITUNGSSYSTEME, Niederelbert, (Germany).

## 4.3 Methods chapter 2

### 4.3.1 Sample preparation

DNA sequences were purchased from MICROSYNTH while the RNA and the RNA-DNA sequences were synthesized by *in vitro* transcription with the *T7* RNA polymerase from the corresponding double stranded DNA template.<sup>[116]</sup> RNA-DNA constructs containing the chemically more stable dT instead of U were transcribed with the double mutant Y639F / S641A *T7* RNA polymerase, which does not discriminate deoxyribose against ribose sugars.<sup>[179,181-186]</sup> All RNA, RNA-DNA, and DNA sequences used in chapter 2 are listed below.

#### RNA sequences

<b>PM01</b>	<b>a</b>	5'-GGAGCGCGUUGUCCCUC-3'
	<b>b</b>	3'-CCUCGCGCUUCAGGGAG-5'
<b>PM02</b>	<b>a</b>	5'-GGAGCGCGUUUUUUGUCCCUC-3'
	<b>b</b>	3'-CCUCGCGCUUUUUUCAGGGAG-5'
<b>PM03</b>		5'-GGAGCGCGUUUUUUCGCGCUCC-3'
		3'-CCUCGCGCUUUUUUGCGCGAGG-5'
<b>PM04</b>		5'-GGAGUUUUUUUUUUCUCC-3'
		3'-CCUCUUUUUUUUUUGAGG-5'
<b>PM05</b>		5'-GGAGUUUUUUUUUUUUUUUUUUUCUCC-3'
		3'-CCUCUUUUUUUUUUUUUUUUUUUUGAGG-5'
<b>PM09</b>	<b>a</b>	5'-GGAGCGCGUUGUCCCUC-3'
	<b>b</b>	3'-CCUCGCGCUUCAGGGAG-5'

#### RNA sequences with dTTP instead of UTP

<b>PM01(T)</b>	<b>a</b>	5'-GGAGCGCGTTGTCCCTC-3'
	<b>b</b>	3'-CCTCGCGCTTCAGGGAG-5'
<b>PM03(T)</b>		5'-GGAGCGCGTTTTTTTCGCGCTCC-3'
		3'-CCTCGCGCTTTTTTTCGCGGAGG-5'

#### DNA sequences

<b>PM 10</b>	<b>a</b>	5'-GGAGCGCGTTTGTCCCTC-3'
	<b>b</b>	3'-CCTCGCGCTTTCAGGGAG-5'
<b>PM 11</b>	<b>a</b>	5'-GGAGCGCGTTGTCCCTC-3'
	<b>b</b>	3'-CCTCGCGCTTCAGGGAG-5'

Transcriptions were performed using 1.2  $\mu\text{M}$  double stranded DNA template, 5 mM ATP, CTP, and GTP in 1x transcription buffer (40 mM Tris-HCl, pH 7.5, 40 mM DTT, 2 mM spermidine, 0.01 % triton X-100). The concentrations of UTP and dTTP, respectively, as well as of  $\text{MgCl}_2$  were optimized for each sequence and are assembled in Table 4-1. In addition the amount of the *T7* RNA polymerase was tweaked individually for each polymerase batch. Natural isotope abundance samples were transcribed of all constructs, whereas a fully  $^{13}\text{C}$ ,  $^{15}\text{N}$ -enriched sample was only obtained of **PM03**. All transcripts as well as the purchased DNA sequences were purified by denaturing 18 % (w/v) polyacrylamide gel electrophoresis (PAGE), UV-shadowed and excised from the gel followed by electroelution and ethanol precipitation. Desalting was done with NAP-10 columns or Vivaspin 2 at 4 °C and 4'500 g. After lyophilization, the samples were dissolved in 200  $\mu\text{L}$   $\text{D}_2\text{O}$  and subsequently the oligonucleotide concentration was determined by UV-VIS spectrophotometry using the extinction coefficients at 260 nm ( $\epsilon_{260}$ ) listed below in Table 4-1. Formation of the linear array of  $\text{Hg}^{2+}$  ions was induced by the addition of one equivalent  $\text{Hg}(\text{ClO}_4)_2$  solution. One equivalent is defined as the amount of  $\text{Hg}^{2+}$  needed to form the complete set of U–Hg–U and accordingly T–Hg–T base pairs in a given duplex. However, the procedure varied slightly, thus the details are described separately for each experiment below.

**Table 4-1** The  $\epsilon_{260}$  and  $M_w$  of all RNA, RNA-DNA, and DNA constructs as well as the detailed transcription conditions of the RNA and RNA-DNA constructs. wt = wild type

	$\epsilon_{260}$ [ $\text{mM}^{-1}\text{cm}^{-1}$ ]	$M_w$ [ $\text{g mol}^{-1}$ ]	[UTP] [mM]	[dTTP] [mM]	[ $\text{MgCl}_2$ ] [mM]	RNAP
<b>PM01 a</b>	154.7	5394.3	5	-	20	wt
<b>PM01 b</b>	156.6	5417.3	5	-	45	wt
<b>PM01(T) a</b>	153.5	5386.4	-	5	45	Y639F/S641A
<b>PM01(T) b</b>	155.5	5411.4	-	5	45	Y639F/S641A
<b>PM02 a</b>	193.5	6618.9	5	-	45	wt
<b>PM02 b</b>	195.2	6642.0	7.5	-	45	wt
<b>PM03</b>	199.7	6963.2	5	-	45	wt
<b>PM03(T)</b>	192.0	6949.3	-	5	45	Y639F/S641A
<b>PM04</b>	172.5	5586.3	15	-	30	wt
<b>PM05</b>	269.5	8647.9	30	-	30	wt
<b>PM09 a</b>	164.4	5700.4	5	-	45	wt
<b>PM09 b</b>	166.3	5723.5	5	-	45	wt
<b>PM10 a</b>	159.0	5482.6	-	-	-	-
<b>PM10 b</b>	161.9	5491.6	-	-	-	-
<b>PM11 a</b>	150.9	5178.4	-	-	-	-
<b>PM11 b</b>	153.8	5187.4	-	-	-	-

### 4.3.2 NMR spectroscopy

All NMR measurements were performed in 5-mm SHIGEMI NMR tubes with 200  $\mu\text{L}$  sample volume at 25  $^{\circ}\text{C}$ . The samples were lyophilized and resuspended in either 90 %  $\text{H}_2\text{O}$  / 10 %  $\text{D}_2\text{O}$  or 100 %  $\text{D}_2\text{O}$  and the pH and accordingly the pD was adjusted to 6.8 and 7.2, respectively, prior to acquisition. Experiments were carried out either in the absence or in the presence of  $\text{Hg}(\text{ClO}_4)_2$ . After addition of  $\text{Hg}(\text{ClO}_4)_2$  the samples were heated up to 70  $^{\circ}\text{C}$  for 4 minutes and cooled down by 1  $^{\circ}\text{C}/30$  sec to 25  $^{\circ}\text{C}$  in a MASTERCYCLER PERSONAL (EPPENDORF) PCR instrument. Excess  $\text{Hg}^+$  was removed by treating the sample for 2 h or 24 h with the chelating resin CHELEX-100 from BIO-RAD, Hercules (USA).

$[^1\text{H}]$ -NMR spectra were measured in  $\text{D}_2\text{O}$  with presaturation water suppression.  $[^1\text{H}, ^1\text{H}]$ -NOESY spectra of **PM03** (0.6 mM) and **PM03(T)** (0.4 mM) were acquired in  $\text{D}_2\text{O}$  with a mixing time of 250 ms.  $[^{13}\text{C}, ^1\text{H}]$ -HSQC spectra of  $^{13}\text{C}, ^{15}\text{N}$ -labeled **PM03** in  $\text{H}_2\text{O}$  /  $\text{D}_2\text{O}$  were recorded separately for the aromatic (sw = 70 ppm,  $\text{O1} = 135$  ppm) and the aliphatic (sw = 120 ppm,  $\text{O1} = 50$  ppm) range of the  $^{13}\text{C}$  resonances.  $^1J_{\text{HN}}$ -HSQC and  $^3J_{\text{HN}}$ -HSQC spectra of **PM03** were carried out in  $\text{H}_2\text{O}$  /  $\text{D}_2\text{O}$  using  $^1J_{\text{HN}} = 90$  Hz and  $^3J_{\text{HN}} = 20$  Hz, respectively.

To calculate the hydrodynamic radii  $r_H$  of **PM01-PM05** DOSY spectra were measured in  $\text{D}_2\text{O}$  with the standard BRUKER pulsprogram stebpgp1s, which applies stimulated echoes using bipolar gradient pulses for diffusion. The diffusion time ( $\Delta$ ), the gradient length ( $\delta$ ) and the recovery delay after gradient pulses were set to 350 ms, 4 ms and 200  $\mu\text{s}$ , respectively, while the gradient strength was incremented from 11.8 to 32 G/cm in 64-80 steps. The hydrodynamic radii  $r_H$  of the molecules can be calculated from the measured diffusion coefficients by reformulating the STOKES-EINSTEIN equation (1):

$$D = \frac{kT}{6\pi r \eta} \quad (3) \qquad r = \frac{kT}{6\pi D \eta} \quad (4)$$

where  $D$  is the diffusion coefficient, which was obtained from the DOSY experiment in  $\text{m}^2\text{s}^{-1}$ ,  $k$  is the BOLTZMANN constant with  $1.381 \cdot 10^{-23} \text{ NmK}^{-1}$ ,  $T$  is the temperature in K (298 K) and  $\eta$  is the dynamic viscosity of the solvent ( $0.89 \cdot 10^{-3} \text{ Nsm}^{-2}$  for  $\text{H}_2\text{O}$  at 298 K).

All spectra were processed with TOPSPIN 1.2, 1.3, or 2.0 (BRUKER) and analysed with SPARKY (<http://www.cgl.uscf.edu/home/sparky/>), except the DOSY spectra which were processed using the standard DOSY protocol of TOPSPIN 2.0 with logarithmic scaling in the F1 (diffusion coefficients) dimension.

### 4.3.3 UV melting studies

Temperature dependent absorption spectra were measured of **PM01**, **PM02**, **PM03**, **PM04** and **PM05** using a concentration of 0.5  $\mu\text{M}$  duplex form. The experiments were recorded in the absence and in the presence of 1 equivalent  $\text{Hg}^{2+}$  adding the  $\text{Hg}(\text{ClO}_4)_2$  just prior to acquisition. Besides, additional melting studies of 2  $\mu\text{M}$  **PM01**, **PM01(T)**, and **PM09** without and with 1.0 equivalents of  $\text{Hg}^{2+}$  were performed. Thereby the respective amount of  $\text{Hg}(\text{ClO}_4)_2$  was added at least one week before acquisition in order to accomplish equilibrium. All experiments were performed in aqueous solution with 5 mM MOPS (pH = 6.8) and 100 mM  $\text{NaClO}_4$ . The  $\text{HgClO}_4$  was taken from a 5 mM stock solution. Prior to measurement, the samples were degassed for 30 s, transferred to a 10 mm cuvette with a total volume of 1 mL and carefully covered with paraffin oil to avoid evaporation. The cuvette was then heated from 20 to 95  $^\circ\text{C}$  in 0.5  $^\circ\text{C}/\text{min}$  steps and absorption spectra were recorded every 0.2  $^\circ\text{C}$  at 260 nm over a temperature range. The data from two repeated heating and cooling cycles were gathered to check for reproducibility and reversibility. Furthermore, the melting curves were fitted with equations all derived from a VAN'T HOFF analysis<sup>[254,255]</sup> describing one transition with either no baseline (equation 3), with linear increasing baseline in the folded state (equation 4), with linear increasing baseline in the unfolded state (equation 5), or linear increasing baseline in the folded and unfolded state (equation 6). In some cases the curves could not be properly fitted by these equations, if so, the inflexion point was determined to achieve the melting temperature. All data were analysed using ORIGIN<sup>®</sup> version 7.0 (ORIGINLAB TM CORPORATION)

$$y(x) = \frac{A_f + A_u \cdot e^a}{1 + e^a} \quad (6)$$

$$y(x) = \frac{(b_f + m_f \cdot x) + A_u \cdot e^a}{1 + e^a} \quad (5)$$

$$y(x) = \frac{A_f + (b_u + m_u \cdot x) \cdot e^a}{1 + e^a} \quad (8)$$

$$y(x) = \frac{(b_f + m_f \cdot x) + (b_u + m_u \cdot x) \cdot e^a}{1 + e^a} \quad (7)$$

$$\text{with } a = \Delta H_1 \cdot \frac{\frac{1}{T_{m1}} - \frac{1}{x}}{8.31451}.$$



#### 4.3.4 Circular dichroism

CD spectra were recorded in a 10 mm quartz cuvette with a total volume of 1 mL. Each measurement was repeated twice with a speed of 100 nm/min at 25 °C.  $\text{Hg}(\text{ClO}_4)_2$  was added stepwise (0.2, 0.4, 0.6, 0.8, 1.0, 1.5 and 2.0 eq.) from a 5 mM or 10 mM stock solution. 2  $\mu\text{M}$  duplex of **PM01-PM04** in 100 mM  $\text{NaClO}_4$  were measured over the spectral range of 195-320 nm. After addition of  $\text{Hg}^{2+}$  the samples were heated in a MASTERCYCLER PERSONAL PCR instrument as described in section 4.3.2 and the pH was adjusted to 6.8. Besides, experiments of 5  $\mu\text{M}$  duplex form of **PM01**, **PM01(T)**, and **PM09** in 5 mM MOPS (pH = 6.8) and 100 mM  $\text{NaClO}_4$  were carried out over the spectral range of 220-320 nm. After addition of  $\text{Hg}^{2+}$  the samples were heated up to 70 °C for 4 minutes and then left at room temperature for 5 minutes to cool down before acquisition.

#### 4.3.5 Dynamic light scattering

DLS of **PM01-PM05** was measured at 298 K in a 12  $\mu\text{L}$  cuvette using directly the NMR samples (100 %  $\text{D}_2\text{O}$ , 100 mM  $\text{NaClO}_4$ , pD 7.2). All Samples were centrifuged for 40 minutes at 4 °C and 13'500g prior to the experiment in order to precipitate any dust that might hamper DLS measurements. In addition, the samples that were treated with  $\text{Hg}^{2+}$  and/or Chelex, were filtered through 0.02  $\mu\text{m}$  pores after centrifugation. At least five measurements of each sample were recorded. The factor 0.8122 was applied to the obtained  $r_{H,DLS}$  values correcting the solvent viscosity coefficient to  $\text{D}_2\text{O}$ .<sup>[159]</sup>

#### 4.3.6 Perturbed angular correlation of gamma rays (PAC)

All PAC experiments were carried out at the ISOLDE facility in CERN using a setup with six detectors and a temperature of  $1 \pm 2$  °C, which was controlled by a Peltier element. The radioactive  $^{199\text{m}}\text{Hg}$  ( $t_{1/2} = 43$  min, half-life of intermediate nuclear state = 2.3 ns) was produced on the day of the experiment by irradiating a liquid lead target with 1 GeV protons, followed by ionization to  $1^+$  charge state, acceleration to 60 keV, and then selection using an on line mass separator. 200  $\mu\text{L}$  of water was placed in a small teflon cup sitting on a copper device, frozen in liquid nitrogen and mounted at the ISOLDE GLM beam line in a vacuum chamber to trap the  $^{199\text{m}}\text{Hg}$ . Radioactive  $^{199\text{m}}\text{Hg}$  was then implanted in the ice typically for 1 hour and subsequently the ice was thawed slowly ( $\approx 10$  min) in a fume hood to minimize the risk of contamination from mercury vapour. For a proper hybridisation the oligonucleotide solutions (**PM01**, **PM09**, **PM10**, and **PM11**) were heated up to 70 °C for 5 minutes and then the radioactive  $^{199\text{m}}\text{Hg}$  as well as the nonradioactive  $\text{Hg}(\text{ClO}_4)_2$  was added. The samples were

left to equilibrate for 10 min. Finally, sucrose was added to produce a 55 % w/w solution with a total volume of 350  $\mu\text{L}$ . The final samples contained 25  $\mu\text{M}$  oligonucleotide, 100 mM  $\text{NaClO}_4$ , 5 mM MOPS pH = 6.8 and 0.1, 0.9, or 1.1 equivalents of  $\text{Hg}^{2+}$ . All PAC measurements were performed immediately after preparation of the samples. The entire handling of the machines as well as fitting the PAC data was carried out by the group of Prof. Lars Hemmingsen, University of Copenhagen. In general, data acquisition and data fitting was performed as described by Hemmingsen et al.<sup>[189,256]</sup> The instrument time resolution and time calibration were determined to be 0.846 ns (full width at half maximum) and 0.0503 ns per channel, respectively. All fits were carried out with 300 data points, disregarding the 10 first points due to systematic errors in these.

## 4.4 Methods chapter 3

### 4.4.1 Sample preparation

The oligonucleotide with natural isotope abundance as well as the one with 98 % enriched  $^{15}\text{N}$  imidazole moieties was synthesised by group members of Prof. Jens Müller Westfälische Wilhelms-Universität Münster, Germany. The oligonucleotides were prepared using an EXPEDITE 8909 synthesizer in the DMT-off mode and purified by HPLC with a NUCLEOGEN 60-7 DEAE column following standard procedures.<sup>[244]</sup>

The duplex formation was initiated by the addition of 1.5 equivalent of  $\text{Ag}^+$  ions (0.2 M  $\text{AgNO}_3$ ). One equivalent is defined as the amount of  $\text{Ag}^+$  needed to form the three imidazole-silver-imidazole base pairs in the duplex. The solution was heated up to 70 °C, followed by slowly cooling to ambient temperature to ensure a homogeneous hybridization. The excess of  $\text{Ag}^+$  ions were removed by the addition of a chelating resin CHELEX-100 from BIO-RAD Hercules (USA).

### 4.4.2 NMR spectroscopy

All NMR measurements were performed in 5-mm SHIGEMI NMR tubes with 200  $\mu\text{L}$  sample volume. After desalting and lyophilisation the samples were dissolved in either  $\text{H}_2\text{O}$  /  $\text{D}_2\text{O}$  (9:1) or 100 %  $\text{D}_2\text{O}$  containing 120 mM  $\text{NaClO}_4$ . The DNA concentration was between 0.5 and 1.4 mM and the pH or pD, respectively, was adjusted prior to the acquisition of the NMR spectra.

Non-exchangeable resonances of the hairpin were assigned from 2D [ $^1\text{H}$ ,  $^1\text{H}$ ]-NOESY (250-ms mixing time, 293, 298 and 303 K) and [ $^1\text{H}$ ,  $^1\text{H}$ ]-TOCSY (50-ms mixing time, 298 K) spectra at pD 4.7, 7.2 and 10.2 in  $\text{D}_2\text{O}$  as well as from [ $^{13}\text{C}$ ,  $^1\text{H}$ ]-HSQC (298 K) spectra at pH 5.4 and 7.4 in  $\text{H}_2\text{O}$  and long-range [ $^{15}\text{N}$ ,  $^1\text{H}$ ]-HSQC ( $^3J_{\text{NH}} = 20$  Hz, 298 K) spectra at pD 7.2 in  $\text{D}_2\text{O}$ . 2D [ $^1\text{H}$ ,  $^1\text{H}$ ]-NOESY (250-ms mixing time, 298 K), [ $^1\text{H}$ ,  $^1\text{H}$ ]-TOCSY (50-ms mixing time, 298 K), [ $^{13}\text{C}$ ,  $^1\text{H}$ ]-HSQC (298 K), and long-range [ $^{15}\text{N}$ ,  $^1\text{H}$ ]-HSQC ( $^3J_{\text{NH}} = 20$  Hz, 298 K) spectra at pD 7.2 in  $\text{D}_2\text{O}$  were used to assign the non-exchangeable resonances of the duplex. In both cases only very few exchangeable proton resonances could be assigned due to the large overlap of the thymine N3H resonances. To differentiate unambiguously between a hairpin structure and a regular double helix, DOSY spectra of the hairpin and of the duplex were acquired and processed as described in section 4.3.2. All [ $^1\text{H}$ ,  $^1\text{H}$ ] and [ $^{13}\text{C}$ ,  $^1\text{H}$ ]-spectra were recorded at natural isotope abundance, whereas [ $^{15}\text{N}$ ,  $^1\text{H}$ ]-spectra were recorded with DNA containing 98 % enriched  $^{15}\text{N}$  imidazole moieties.

1D [ $^{31}\text{P}$ ] and [ $^1\text{H}$ ]-NMR spectra of the mononucleotide dImMP $^{2-}$  (1.8 mM) as well as 1D [ $^1\text{H}$ ]-NMR spectra of the hairpin (0.2 mM) in dependence on pD were recorded in  $\text{D}_2\text{O}$  at 298 K and  $I = 0.12\text{ M}$  ( $\text{NaClO}_4$ ). Chemical shifts for [ $^{31}\text{P}$ ]-NMR measurements were referenced to the external standard 85 %  $\text{H}_3\text{PO}_4$  ( $\text{H}_2\text{O}$ ,  $\delta = 0\text{ ppm}$ ) and [ $^1\text{H}$ ]-NMR measurements to the external standard 3-(trimethyl-silyl)propane-1-sulfonate ( $\text{D}_2\text{O}$ ,  $\delta = 0\text{ ppm}$ ), respectively. The pD of the solution was adjusted by dotting with a glass stick using relatively concentrated  $\text{DNO}_3$  and  $\text{NaOD}$  solutions. The actual pD values of the solutions were obtained by adding 0.4 to the pH meter reading.<sup>[257,258]</sup> The experimental data were analysed by means of the NEWTON-GAUSS nonlinear least-square method. Results were obtained with the aid of a computer-based curve-fitting program, which was based on the general equation published previously.<sup>[143,150,220]</sup> The  $\text{p}K_{\text{a,H}_2\text{O}}$  values for  $\text{H}_2\text{O}$  solutions were calculated from the  $\text{p}K_{\text{a,D}_2\text{O}}$  values valid in  $\text{D}_2\text{O}$  according to  $\text{p}K_{\text{a,D}_2\text{O}} = 1.015 \text{p}K_{\text{a,H}_2\text{O}} + 0.45$ .<sup>[218]</sup>

The NMR data were processed with TOPSPIN 1.2, 1.3, and 2.0 (BRUKER) and analyzed by using SPARKY (<http://www.cgl.uscf.edu/home/sparky/>). NOE peak volumes were integrated with the GAUSSIAN peak fitting function in SPARKY.

### 4.4.3 Structure calculation

The NOE distances were estimated from the integrated peak volumes obtained from the 2D [ $^1\text{H}$ ,  $^1\text{H}$ ]-NOESY spectra acquired at 298 K with a mixing time of 250 ms. Distances were calibrated by using the CALIBA macro in DYANA.<sup>[113]</sup> The NOEs were grouped into four categories, corresponding to strong (1.8-3.0 Å), medium (1.8-4.5 Å), weak (3.0-6.0 Å) and very weak (4.0-7.0 Å). The structure calculations were performed with DYANA 1.5<sup>[113]</sup> and XPLOR-NIH 2.15.0<sup>[114]</sup> using the standard implemented force field parameters. The structure coordinates are deposited at the Protein Data Bank (hairpin at pD 4.7: 2K67, at pD 7.2: 2K68, at pD 10.2: 2K69 and duplex: 2KE8), and the NMR chemical shift assignments at the BIOMAGRESBANK (hairpin: 15860, duplex: 16138).

#### 4.4.3.1 Insertion of new residues into parameter and topology files

The imidazole residue as well as the protonated imidazole residue was inserted as IMI and  $\text{IMI}^+$ , respectively, into the parameter and topology files. The new residues were then patched into the oligonucleotide like a standard nucleotide using the structural parameters from previous DFT calculations.<sup>[195]</sup> The partial charges of IMI and  $\text{IMI}^+$  were adapted from protonated and unprotonated 1-methylimidazole calculated with the VORONOI DEFORMATION

DENSITY method by Tushar van der Wijst, Group Prof. Lippert TU Dortmund.<sup>[259]</sup> The Ag<sup>+</sup> ions were defined with a single positive charge, a sigma = 2.8500, and eps = 0.1600. All other parameters changed or inserted in the parameter and topology files of XPLOR are summarized in Appendix 8 and Appendix 9. Finally, to generate the metal modified IMI-Ag-IMI base pairs the generatedna.inp file was modified as follow (bold entries):

generatedna.inp

```

topology
  @nucleic.top
end
                                autogenerate angles=true

                                { *topology.                * }

                                { *Generate the patch topology,* }
                                { *which will be used in the   * }
                                { *PATCH command.            * }

PREsidue PAGI                { *patch for changing partial charges in the presence* }
                                { *of Ag+ and addition of new bonds and angles      * }

                                ADD BOND 7AG 1N3                { *These are the covalent bonds* }
                                ADD BOND 7AG 6N3                { *between the IMIs and the      * }
                                ADD BOND 8AG 2N3                { *Ag-ions                      * }
                                ADD BOND 8AG 5N3
                                ADD BOND 9AG 3N3
                                ADD BOND 9AG 4N3

                                ADD ANGLE 1N3 7AG 6N3          ADD ANGLE 2N3 8AG 5N3
                                ADD ANGLE 3N3 9AG 4N3
                                ADD ANGLE 1C2 1N3 7AG          ADD ANGLE 1C4 1N3 7AG
                                ADD ANGLE 2C2 2N3 8AG          ADD ANGLE 2C4 2N3 8AG
                                ADD ANGLE 3C2 3N3 9AG          ADD ANGLE 3C4 3N3 9AG
                                ADD ANGLE 4C2 4N3 9AG          ADD ANGLE 4C4 4N3 9AG
                                ADD ANGLE 5C2 5N3 8AG          ADD ANGLE 5C4 5N3 8AG
                                ADD ANGLE 6C2 6N3 7AG          ADD ANGLE 6C4 6N3 7AG

END

end
parameter

  @nucleic.par                { *This file is in subdirectory TOPPAR.* }
                                { *Append parameters for metal cluster.* }

  nbonds                      { *This statement specifies the* }
    atom cdie shift eps=1.0 e14fac=0.4 { *nonbonded interaction energy* }
    cutnb=7.5 ctonnb=6.0 ctofnb=6.5    { *options. Note the reduced * }
    nbxmod=5 vswitch            { *nonbonding cutoff to save  * }
  end                            { *CPU time.                  * }
end

{-----}
                                { *We are generating one strand at a time.* }

segment
  name="A"                    { *This name has to match the      * }
                                { *four characters in columns 73-* }
                                { *76 in the coordinate          * }
                                { *file; in XPLOR this name is    * }
  chain                        { *referred to as SEGId.          * }

```

```

        LINK NUC  HEAD - *  TAIL + *  END
        FIRST 5TER  TAIL + *  END          {*5-terminus without phosphate.*}
        LAST 3TER  HEAD - *  END          {*3-terminus.                *}

        coordinates @strandA.pdb          {*Interpret coordinate file to *}
    end                                    {*obtain sequence.            *}
end

                                        {*It comes as RNA; now we have*}
                                        {*to apply deoxy patches for  *}
                                        {*each residue.                *}

for $1 in ( 1 2 3 4 5 6 7 8 9 10 11 12 13 14 15 16 17) loop main
    patch deox reference=nil=( resid $1 ) end
end loop main

coordinates @strandA.pdb                {*Here we actually read the*}
                                        {*coordinates.                *}

{-----}
segment                                {*Generate second strand.*}

    name="A"

    chain

        LINK NUC  HEAD - *  TAIL + *  END
        FIRST 5TER  TAIL + *  END
        LAST 3TER  HEAD - *  END

        coordinates @ strandB.pdb
    end
end

for $1 in ( 18 19 20 21 22 23 24 25 26 27 28 29 30 31 32 33 34 ) loop main
    patch deox reference=nil=( resid $1 ) end
end loop main

coordinates @strandB.pdb                {*Here we actually read the*}
                                        {*coordinates.                *}

{-----}
                                        {*Now generate metal cluster.*}
segment

    name="A"

    chain

        coordinates @silber.pdb
    end
end

coordinates @silber.pdb

{-----}
                                        {*Now generate the covalent links be-*}
                                        {*tween the cluster and the protein. *}

patch  PAGI
    reference=1=( resid 8 )
    reference=2=( resid 9 )
    reference=3=( resid 10 )
    reference=4=( resid 25 )
    reference=5=( resid 26 )
    reference=6=( resid 27 )

```

```

        reference=7=( resid 35 )
        reference=8=( resid 36 )
        reference=9=( resid 37 )
    end

{-----}
    flags exclude vdw elec end          { *Do hydrogen building w/o vdw* }
                                         { *and elec.                  * }

    hbuild                               { *This statement builds missing* }
        selection=( hydrogen )          { *hydrogens, which are needed * }
        phistep=45                      { *for the force field.        * }
    end

    constraints fix=( not hydrogen ) end { * Minimize hydrogen positions. * }
    flags include vdw elec end
    minimize powell
        nstep=40
    end
    constraints fix=( not all ) end

    write coordinates output=generatedna.pdb end { *Write out coordinates.* }
    write structure output=generatedna.psf end   { *Write the structure file.* }

    stop

```

#### 4.4.3.2 Structure calculation of the hairpin

All structure calculations of the DNA hairpin at different pD values were performed in the same manner. Based on [<sup>31</sup>P]-NMR spectra, the  $\alpha$ ,  $\zeta$  angles were set to exclude the *trans*-range,<sup>[227]</sup> except at the imidazole moieties, which were left unrestrained. Sugar pucker restraints were included based on TOCSY experiments with a 50 ms mixing time. All natural nucleotides showed strong H1'-H2' and H1'-H3' crosspeaks and were restrained to S-type. The imidazole moieties were set to S-type as well, except of Im8 at pD 7.2 which was left unconstrained due to the missing characteristic pattern. The other backbone torsion angles ( $\beta$ ,  $\gamma$ ,  $\epsilon$ ) were set to standard B-form values in the helical region of the structure (T1-T7, A11-A17). Based on the intranucleotide H1'-aromatic NOEs, the torsion angle  $\chi$  was restrained to  $-120 \pm 20^\circ$  (*anti*) for all residues, except the imidazole moieties, which were left unconstrained.

First, 200 initial structures were calculated with DYANA using distances restraints and dihedral restraints only. The 10 lowest energy structures were used to calculate 200 starting structures with XPLOR-NIH, which were subsequently refined. Weak planarity for all identified base pairs was enforced during refinement and hydrogen bonds of these base pairs were maintained by distance restraints.

#### 4.4.3.3 Structure calculation of the duplex

Torsion angles and sugar pucker restraints were set based on the NMR data as described for the hairpin. The backbone torsion angles were set to exclude the *trans*-range and cover the B-DNA range. The sugar pucker was restrained to *S*-type and the glycosidic torsion angle  $\chi$  was set to  $-120 \pm 20^\circ$  (*anti*) for all residues, apart from the imidazole moieties, which were left unrestrained. First, an extended structure was generated including the geometrical parameters of the imidazole-silver-imidazole base pair obtained from DFT calculations.<sup>[195]</sup> Starting from the extended strand a set of 2000 structures was calculated using NOE distances and dihedral restraints. Besides the planarity and hydrogen bond distance restraints of the natural base pairs, planarity and distance restraints for the imidazole-silver-imidazole base pairs were also included to maintain the coordinative bond properties. Based on the perfect  $C_2$  symmetry observed in the NMR spectra showing only one half of the duplex, a non-crystallographic symmetry (NCS) term was introduced. The 200 structures with lowest energies were used for further refinement using additional RAMA and ORIE database terms.

#### 4.4.3.4 Visualisation and analysis of the structures

After refinement, the structures were evaluated for convergence. Acceptance criteria were low overall energies and no significant NOE ( $> 0.2 \text{ \AA}$ ) or dihedral ( $> 5^\circ$ ) violations. The twenty lowest energy structures out of 200 calculated of the hairpins and the duplex were visualized and analyzed by using MOLMOL.<sup>[6]</sup>

The electrostatic surface potential of the three-dimensional DNA structures was calculated using QNIFFT<sup>[222]</sup> and visualized with PYMOL (<http://www.pymol.org>). Thereby the complete nonlinear POISSON-BOLTZMANN equation (NLPB) need to be solved due to the high charge density of nucleic acids, rather than the linearised equation (LPB), which is generally used for proteins.<sup>[222]</sup> Red indicates negative ( $-30 \text{ kTe}^{-1}$ ), white neutral ( $5 \text{ kTe}^{-1}$ ), and blue positive ( $20 \text{ kTe}^{-1}$ ) charges.

Base pair parameters were derived using the programme 3DNA.<sup>[240]</sup> In the 20 lowest energy duplex structures, the imidazole moieties were substituted by guanine to permit the use of the programme. As a result, the programme misleadingly assumed the presence of three central base pairs with *syn*-oriented nucleobases (see Appendix 19 for a compilation of the glycosidic torsion angles  $\chi$ ). Hence, the values obtained for tilt and rise for the base-pair steps involving imidazole nucleotides are meaningless.



#### 4.4.4 Determination of the acidity constants of $\text{H}_2(\text{ImMP})^\pm$ with potentiometric pH titrations

The acidity constants  $K_{\text{H}_2(\text{dImMP})}^{\text{H}}$  and  $K_{\text{H}(\text{dImMP})}^{\text{H}}$  of  $\text{H}_2(\text{dImMP})^\pm$  were determined by titrating 30 mL of aqueous 0.42 mM  $\text{HNO}_3$  (25 °C;  $I = 0.1$  M,  $\text{NaNO}_3$ ) in the presence and in the absence of 0.1 mM  $\text{dImMP}^{2-}$  under  $\text{N}_2$  with up to 1 mL of 0.02 M  $\text{NaOH}$ . In order to save the scarce nucleotide after each titration the pair of solutions was adjusted again to the initial pH of around 4.3 by adding a small volume (about 0.13 mL) of 0.1 M  $\text{HNO}_3$ , and then the titration was repeated.

The determined acidity constants ( $I = 0.1$  M ( $\text{NaNO}_3$ ) and 25 °C) are so-called practical mixed or BRØNSTED constants,<sup>[213]</sup> which may be converted into the corresponding concentration constants by subtracting 0.02 from the measured  $\text{pK}_a$  values.<sup>[213]</sup> It should be emphasized that the ionic product of water ( $K_w$ ) does not enter into the calculation because the differences in  $\text{NaOH}$  consumption between solution with and without nucleotides are evaluated.

The experimental data were evaluated by means of a curve-fitting procedure using a NEWTON-GAUSS nonlinear least-square program that utilised the difference in  $\text{NaOH}$  consumption between the aforementioned pairs of titrations, that is, with and without the nucleotide, at increments of 0.1 pH units. The acidity constants were calculated within the pH range of 4.3-7.5, which corresponds to a neutralisation degree of about 97 % for the equilibrium  $\text{H}_2(\text{dImMP})^\pm / \text{H}(\text{dImMP})^-$  and to one of 80 % for the equilibrium  $\text{H}(\text{dImMP})^- / (\text{dImMP})^{2-}$ . The final acidity constants are the averages of six measurements with three independent pairs of titration solutions. The error limits correspond to three times the standard error of the mean value ( $3\sigma$ ).

#### 4.4.5 Dynamic light scattering

DLS measurements were performed as described in Section 4.3.5 using directly the NMR samples (100 %  $\text{D}_2\text{O}$ , 120 mM  $\text{NaClO}_4$ ,  $\text{pD } 7.2$ ). Samples treated with  $\text{Ag}^+$  ions and CHELEX 100<sup>®</sup> were in addition filtered through 0.02  $\mu\text{m}$  pores after centrifugation.



## 5 Summary

Nucleic acids become increasingly popular as versatile building blocks in nanotechnology. The bottom-up approach for the generation of DNA-inspired nanostructures benefits from their superb, predictable self-assembly properties and their well-defined, repetitive structural features.<sup>[9,10]</sup> Despite their many advantages, nucleic acids lack sufficient conducting properties that are a prerequisite as candidate for electrical nanodevices. One promising way to overcome this deficit is the site-specific functionalization with metal ions. Just recently, a new method was established that uses metal-mediated base pairs to insert and subsequently array metal ions in a predictable manner into DNA.<sup>[36]</sup> Such precise control of defined metal incorporation is necessary for potential applications as nanomagnets, as self-assembling molecular wires or as catalysts in chemical reactions. Metal-mediated base pairs comprise natural or artificial nucleobases and rely on coordinative bonds to a central metal ion instead of (or in addition to) hydrogen bonds. Depending on the choice of nucleosides, metal ions, and the oligonucleotide sequence, a plethora of metal-modified double helices can be generated. To date, examples for DNA, GNA (glycol nucleic acids), and PNA (peptide nucleic acids) duplexes containing one or two metal-mediated base pairs interspersed between natural ones have been described. For DNA, double helices with stretches of up to 19 consecutive metalated base pair as well as duplexes with different metal-mediated base pairs at pre-defined positions could be assembled.<sup>[37,39,41]</sup>

Even though a rapid development in this research field is taking place, there are still a lot of drawbacks that require much more research efforts in order to apply such oligonucleotides as magnetic or electrical devices in nanotechnology. Besides the unanswered question, whether such metal-modified nucleic acids have indeed enhanced conductive properties, one major problem is the synthesis of these nucleic acids containing long continuous stretches of metal-mediated base pairs. The chemical coupling of the phosphoramidites to build up DNA strands is well established and also allows the incorporation of specially designed artificial nucleosides. Nevertheless, it is time-consuming and very expensive to obtain large amounts that are required for further analysis and for the application of nucleic acids as nanomaterial. Moreover, to further develop metal-modified nucleic acids and their range of application, structural information of these oligonucleotides are required. Up to now only one metal-containing DNA and GNA duplex, respectively, was structurally characterized. Neither of these contains successive metalated base pairs and neither of the helices adopts the canonical B-type structure.<sup>[44,194]</sup>

In the first part of the thesis, several palindromic as well as non-palindromic RNA sequences with 2, 3, 6, 10, and up to 20 consecutive uracil residues were transcribed and spectroscopically investigated. By *in vitro* trans-

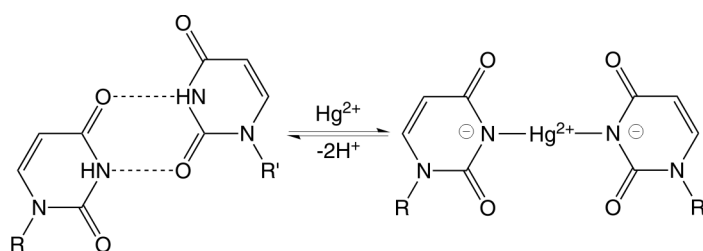


**Figure S1** Proposed formation of the  $\text{Hg}^{2+}$ -mediated uracil-mercury-uracil base pair from a *cis*-uracil-uracil-wobble pair.

cription using *T7* RNA polymerase it is possible to insert long stretches of the same nucleotide without much loss of processivity. Moreover, just by mutating two amino acids (Y639F / S641A) of the *T7* RNA polymerase the corresponding sequences could be transcribed with similar yields containing the thymine deoxynucleotide instead of the uracil nucleotide. However, for continuous stretches of more than ten identical residues the transcription yield decrease significantly and additional abortion products are observed. It seems that the *T7* RNA polymerase loses its precision partially, when too many nucleotides of the same kind are lined up in one row. Nevertheless, in all cases distinct transcription bands were obtained and the different transcription products could be well separated by denaturing 18 % PAGE.

From the literature it is known that  $\text{Hg}^{2+}$  ions can establish interstrand crosslink between mismatched thymines in DNA duplexes. Upon replacement of N3H protons,  $\text{Hg}^{2+}$  ions coordinate between the N3 nitrogens of the thymines and at the same time get lined up in the middle of the DNA helix.<sup>[57]</sup> To investigate whether  $\text{Hg}^{2+}$  ions bind mispaired uracil in a similar fashion, we studied these RNA construct in the absence and in the presence of  $\text{Hg}^{2+}$  ions by UV-VIS, CD (circular dichroism), and NMR (nuclear magnetic resonance) spectroscopy as well as DLS (dynamic light scattering) methods.

The UV melting studies revealed that upon addition of 1 equivalent  $\text{Hg}^{2+}$  (the amount of  $\text{Hg}^{2+}$  needed to form the complete set of U-Hg-U base pairs in a given duplex) all constructs exhibit a distinct increase in melting temperature. This indicates that  $\text{Hg}^{2+}$  is inserted into the UU pairs thereby stabilizing the duplex structures (Figure S1).

Also the CD measurements, which provide information on structural changes, show a similar trend for all RNA constructs. In general, a maximum at 260 nm and a minimum at 210 nm is observed indicating A-form helical regions in all constructs even in the absence of  $\text{Hg}^{2+}$ . Upon addition of  $\text{Hg}^{2+}$  the maximum decreases and experiences a slight red shift whereas the opposite effect is found for the minimum. However, the overall shape remains unchanged demonstrating that  $\text{Hg}^{2+}$  binds to the RNA strands in a way that does not disrupt the natural A-form helix.

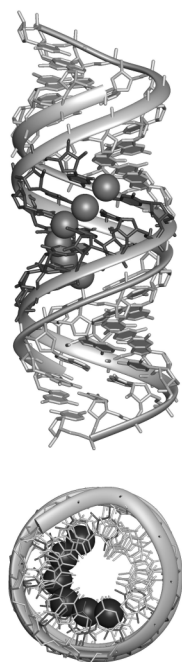


**Figure S2** Model of a metal-modified A-helical RNA.

DOSY (diffusion ordered spectroscopy) as well as DLS measurements are well-established methods to determine independently the hydrodynamic radii  $r_H$  of nucleic acids. In particular, a rearrangement from hairpin to duplex, which can be expected for all palindromic sequences upon addition of  $\text{Hg}^{2+}$  ions, should display a clear change of  $r_H$ . Indeed, for all palindromic sequences such an increase of  $r_H$  was found.

These results together with additional NMR measurements reveal that  $\text{Hg}^{2+}$  ions indeed replace the protons of the uracil nucleobases, inserting themselves in-between two such bases. However, the  $\text{Hg}^{2+}$ -binding was not as strong as recently observed for DNA. The RNA sequences containing thymine instead of uracil retain the A-helical form typical for RNA and behave like their corresponding natural RNA sequences upon addition of  $\text{Hg}^{2+}$  ions. Therefore the smaller binding affinity can be only attributed to differences of the A-helical and B-helical structure (Figure S2).

These first examples of metal-mediated RNA double helices demonstrate that RNA appears to be also a viable candidate for the generation of metal-modified nucleic acids. Moreover, it turned out that the application of polymerases is a powerful method to obtain such metal-modified oligonucleotides fast, efficiently, and in large amounts.

In the second and main part of the thesis the structure of a 17 nt long oligonucleotide with three artificial imidazole base pairs was extensively studied by NMR in the absence and in the presence of  $\text{Ag}^+$  ions (Figure S3). It was previously shown that upon addition of  $\text{Ag}^+$  such a type of sequence undergoes a structure conversion from hairpin to duplex forming consecutive metal-mediated base pairs.<sup>[45]</sup>

The synthesis of the oligonucleotides was performed by a collaborating group in Münster. Previous DFT calculations of two 1-methyl-imidazoles and one  $\text{Ag}^+$  ion as putative metal-

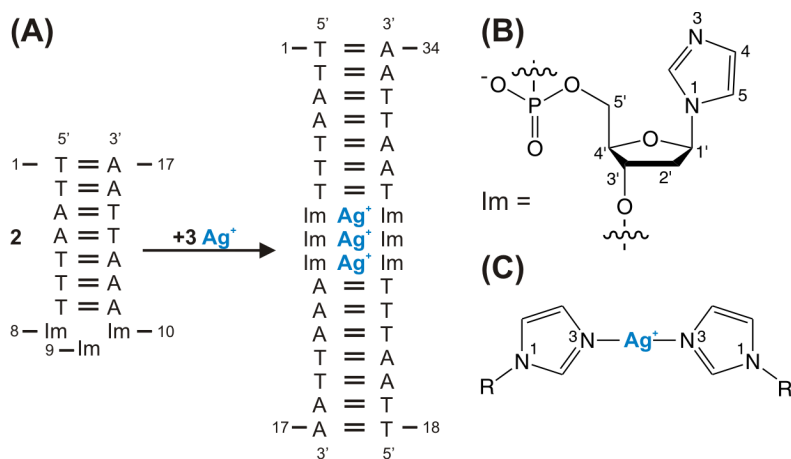
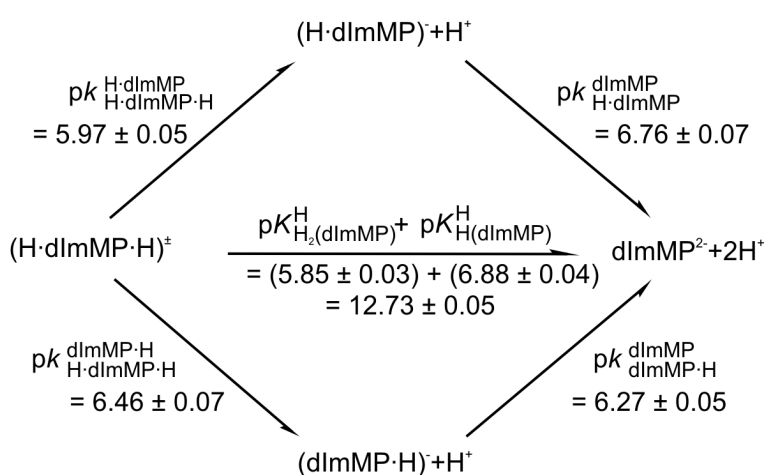


**Figure S3** Description of the oligonucleotide system containing artificial imidazole moieties.

mediated base pair indicate that the imidazole-silver-imidazole base pair perfectly matches the geometry that is required for implementation into B-helical DNA.

As the metalation of nucleic acids is often in competition with protonation, the acid-base properties of the imidazole nucleotide were investigated first. Within a range of  $1 < \text{pH} < 13$  two deprotonation reactions can be expected, one at the phosphate group and the second at the N3 nitrogen of the imidazole moiety. The two macro acidity constants  $\text{p}K_{\text{H}_2(\text{dImMP})}^{\text{H}} = 5.85 \pm 0.03$  and  $\text{p}K_{\text{H}(\text{dImMP})}^{\text{H}} = 6.88 \pm 0.04$  were determined by potentiometric titration. These constants differ only by about one  $\text{p}K_{\text{a}}$  unit implying that the buffer regions of the two protonations sites overlap. Even though the constants describe only approximately the individual deprotonation position it can be assumed that  $\text{p}K_{\text{H}_2(\text{dImMP})}^{\text{H}}$  is mainly determined by the proton release at the phosphate group and  $\text{p}K_{\text{H}(\text{dImMP})}^{\text{H}}$  by the deprotonation of the imidazole. To quantify the acid-base properties of the sites, micro acidity constants were calculated, and the ratio between the imidazole-protonated form  $(\text{H} \cdot \text{dImMP})^-$  and the phosphate-protonated  $(\text{dImMP} \cdot \text{H})^-$  form of the  $\text{H}(\text{dImMP})^-$  species was determined. The results reveal that  $(\text{H} \cdot \text{dImMP})^-$  is predominantly present (75 %), but also  $(\text{dImMP} \cdot \text{H})^-$  occurs in appreciable amounts (25 %). In addition  $[^{31}\text{P}]$ -NMR shift experiments that represent the



$$K_{\text{H}_2(\text{dImMP})}^{\text{H}} = k_{\text{H} \cdot \text{dImMP} / \text{H} \cdot \text{dImMP} \cdot \text{H}^+} \cdot k_{\text{dImMP} \cdot \text{H} / \text{H} \cdot \text{dImMP} \cdot \text{H}} \quad (\text{a})$$

$$\frac{1}{K_{\text{H}(\text{dImMP})}^{\text{H}}} = \frac{1}{k_{\text{dImMP} / \text{H} \cdot \text{dImMP}}} + \frac{1}{k_{\text{dImMP} / \text{dImMP} \cdot \text{H}}} \quad (\text{b})$$

$$\begin{aligned} K_{\text{H}_2(\text{dImMP})}^{\text{H}} \cdot K_{\text{H}(\text{dImMP})}^{\text{H}} &= k_{\text{H} \cdot \text{dImMP} / \text{H} \cdot \text{dImMP} \cdot \text{H}^+} \cdot k_{\text{dImMP} \cdot \text{H} / \text{H} \cdot \text{dImMP} \cdot \text{H}} \\ &= k_{\text{dImMP} / \text{H} \cdot \text{dImMP}} \cdot k_{\text{dImMP} / \text{dImMP} \cdot \text{H}} \end{aligned} \quad (\text{c})$$

**Figure S4** Scheme for the deprotonation equilibrium of  $(\text{H} \cdot \text{dImMP} \cdot \text{H})^\pm$ .

deprotonation at the phosphate group, and  $[^1\text{H}]$ -NMR shift experiments of the three aromatic imidazole protons that render the deprotonation at the imidazole moiety were performed. The experimental data nicely supports the developed deprotonation scheme (Figure S4). The determined micro acidity constant  $\text{p}k_{\text{H} \cdot \text{dImMP} \cdot \text{H}}^{\text{dImMP} \cdot \text{H}} = 6.46 \pm 0.07$  of the  $(\text{H} \cdot \text{dImMP} \cdot \text{H})^\pm$  species is a good basis for comparison on the acid-base properties of the imidazole residues in the oligonucleotides, because it also carries a single negative

charge like the phospho diester bridge.

For our structural investigations we started with  $[^1\text{H}]$ -NMR spectroscopy of the oligonucleotides in the absence of  $\text{Ag}^+$  ions at pD 7.2. As already mentioned above in the absence of transition metal ions such a type of sequence adopts a hairpin structure with the artificial nucleosides located in the loop. The resulting  $[^1\text{H}, ^1\text{H}]$ -NOESY spectrum reveals a nicely resolved *sequential walk* region but with only few and very broad crosspeaks for the imidazole residues. Therefore the *sequential walk* could not be followed through the entire sequence interrupted by the imidazole moieties. Nevertheless, the imidazole residues were reliably assigned by additional NMR experiments. As it is difficult to differentiate between a hairpin structure and a regular duplex just by the crosspeak pattern in the  $[^1\text{H}, ^1\text{H}]$ -NOESY, the hydrodynamic radius  $r_{\text{H}}$  of the oligonucleotide was determined by DOSY and DLS measurements. These two independent methods gave identical values within the error limits of  $1.5 \pm 0.1$  and  $1.4 \pm 0.2$  nm, respectively, and are in good agreement with the theoretical calculations assuming a hairpin structure. The structure determination revealed a stable hairpin with a well-defined helical region closed by an unstructured loop which is composed of the three imidazole moieties. The poor definition of the loop region is due to the semi-protonated state of the artificial nucleotides.

To determine the intrinsic acidity constants for each imidazole residue,  $[^1\text{H}]$ -NMR chemical shift experiments in  $\text{D}_2\text{O}$  were performed. With increasing pH all aromatic protons of the artificial nucleobases shift upfield, broaden out, or even disappear around neutral pH. In more basic conditions all resonances reappear with similar intensity to the ones observed at low pH. Analysis of the chemical shift changes yields the intrinsic acidity constants with  $\text{p}K_{\text{a,Im8}} = 6.78 \pm 0.03$ ,  $\text{p}K_{\text{a,Im9}} = 6.33 \pm 0.04$ , and  $\text{p}K_{\text{a,Im10}} = 6.58 \pm 0.23$ . The lowest acidity constant is observed for Im9, because it is situated between two additional positive charges of the neighbouring imidazole moieties that probably facilitate deprotonation. The acidity constant of Im8 is not only the largest of the three imidazole moieties but is also 0.3 log units larger than the one of  $\text{H(dImMP)}^-$ . This nicely shows that the intrinsic acidity constants are strongly influenced by electrostatic interaction with the neighbouring nucleobases and therefore the  $\text{p}K_{\text{a}}$  values can be perturbed. As the  $\text{p}K_{\text{a}}$  values of the imidazole moieties are in the physiological range, this oligonucleotide constitutes a model system for reaction centres in large RNAs and thus bears important implications for acid-base catalysis in such RNAs.

The previous results of the  $[^1\text{H}]$ -NMR chemical shift experiments strongly suggest a well defined loop at acidic and basic pH. Therefore additional  $[^1\text{H}, ^1\text{H}]$ -NOESY spectra of the fully protonated (pD 4.7) and the fully deprotonated (pD 10.2) form were recorded. In principle,

the spectra look very similar to the one recorded at pD 7.2, but at acidic and basic pH more signals appear that can be attributed to the imidazole residues. However, the *sequential walk* can still not be followed through the entire sequence. Structure calculations at acidic and basic pH suggest that the helical part is almost identical at all pH conditions, whereas the loop regions vary significantly from each other (Figure S5). Nevertheless, the shape of the hairpin at acidic and basic pH is very similar as in both cases

the artificial imidazole moieties are embedded within the helix. In contrast to the structure at neutral ambience, at pD 4.7 and pD 10.2 two distinct loop conformations were observed demonstrating that the loop structure is strongly dependent on pH. At pD 4.7 the structure is mainly affected by the three positive charges of the imidazole moieties, which try to avoid closeness in space. Moreover, they are oriented towards the negatively charged phosphate-sugar backbone thus allowing optimal charge compensation. At high pH all imidazole residues are aligned towards the major groove with Im9 lying on the top of T7. Therefore extra stacking interactions can be assumed which is also supported by various crosspeaks. In both cases, the calculation of the electrostatic surface potential at pD 4.7 and pD 10.2 reveals no areas that are particular high positively or negatively charged.

Upon addition of one equivalent  $\text{Ag}^+$  ions i.e. the amount needed to form a duplex with three metal-mediated base pairs, the quality of the  $[\text{H}, \text{H}]\text{-NOESY}$  spectrum at pD 7.2

improves significantly indicating that a fundamental reorientation of the hairpin takes place. Especially in the *sequential walk* region, many new intense and sharp resonances appear that can be attributed to the imidazole moieties and thus the *sequential walk* could be completely assigned. Moreover, all residues show the distinctive pattern for a regular B-form helix suggesting a rigid structure around the

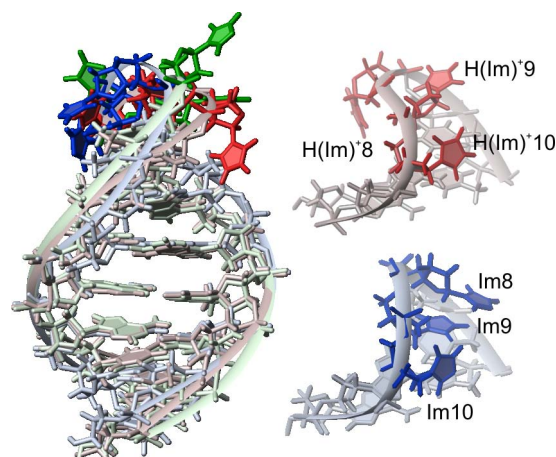


**Figure S5** Left: Lowest-energy structure of the hairpin at acidic (red), neutral (green), and basic (blue) pH. Right: The observed loop structure at acidic (top) and basic (bottom) pH.

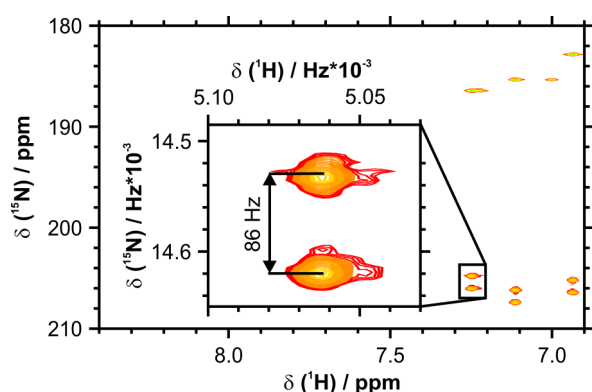


**Figure S6**  $^1J(^{15}\text{N}, ^{107/109}\text{Ag})$  coupling of 86 Hz as observed in the  $[\text{H}, \text{H}]\text{-NOESY}$  spectrum.



imidazole nucleotides as it is expected for the formation of imidazole-silver-imidazole base pairs. DOSY and DLS measurements clearly display an increase of  $r_H$  ( $1.9 \pm 0.3$  nm and  $1.8 \pm 0.2$  nm, respectively), which is also well in line with the theoretical value of a supposed double helical structure. To further prove the metal coordination,  $^{15}\text{N}$ -labelled imidazole nucleosides were incorporated into the oligonucleotide and  $[^{15}\text{N},^1\text{H}]$ -HSQC spectra in the absence and in the presence of  $\text{Ag}^+$  were recorded. Upon addition of  $\text{Ag}^+$  ions all nitrogen resonances experience an upfield shift. The N1 resonances shift about 3 ppm while the N3 resonances shift about 15 ppm. Direct coordination of silver to nitrogen causes a strong upfield shift as it is found for the N3 nitrogens indicating that the  $\text{Ag}^+$  ions indeed coordinate at the N3 positions. Even more important, in the presence of  $\text{Ag}^+$  ions the N3 resonances show a splitting of 86 Hz. This splitting is caused by a direct coupling between the N3 nitrogens and the silver atoms, i.e. a  $^1J(^{15}\text{N}, ^{107/109}\text{Ag})$  coupling (Figure S6), and provides the final evidence for the formation of the imidazole-silver-imidazole base pairs. Furthermore, such a coupling verifies that

the exchange reaction is very slow and therefore the  $\text{Ag}^+$  ions must be tightly bound to the artificial nucleosides and well embedded within the double helical structure. The structure calculations of the duplex show that the metalated DNA retains its B-form helix upon formation of  $\text{Ag}^+$ -mediated base pairs in its centre (Figure S7). Detailed analysis of the base pair parameters reveal only a slight unwinding and stretching of the helix in the region of the imidazole-silver-imidazole base pairs without disturbing the major conformation. Silver-silver distances were found between 3.79 and 4.51 Å for the 20 lowest energy-structures. This high variation shows that the energy differences between conformations with different metal-metal distances are very small. The solution structure provides the first structural insight into a nucleic acid with consecutive metal-mediated base pairs and it also proves that a DNA double helix can adopt the regular B-type conformation while at the same time stringing together metal ions along its helical axis.

This work describes a new method to generate metal-modified nucleic acid fast, efficiently, and in large amounts, and presents the first solution structure of an oligonucleotide

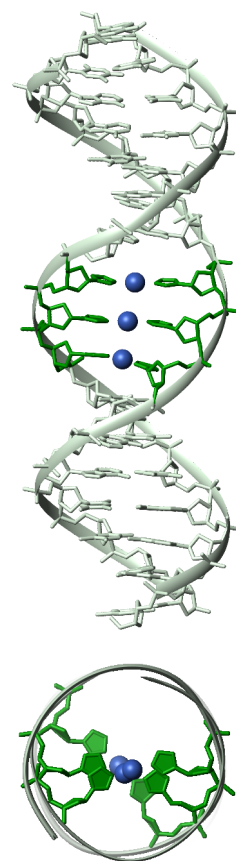


**Figure S7** Lowest energy structure of the duplex containing artificial imidazole nucleosides.

with consecutive metal-mediated base pairs. These results are two important steps towards the application of nucleic acids in nanoscience.

## 6 Zusammenfassung

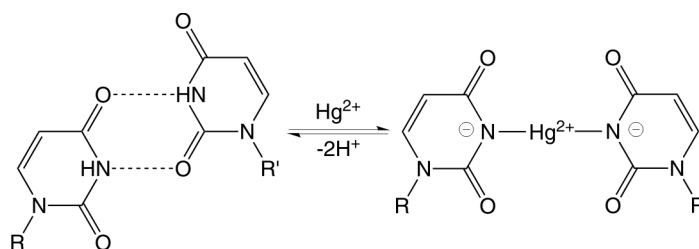
Nukleinsäuren rücken als vielseitig einsetzbarer Grundbaustein immer mehr in den Fokus der Nanotechnologie. Gerade in der bottom-up Strategie zum Aufbau geordneter Nanostrukturen überzeugen Nukleinsäuren durch ihre programmierbare Selbstorganisation und durch ihren diskreten Aufbau aus sich wiederholenden Untereinheiten.<sup>[9,10]</sup>

Eine Grundvoraussetzung für den Einsatz in elektronischen Bauelementen ist die elektrische Leitfähigkeit, die in Nukleinsäuren aber nur unzureichend vorhanden ist. Eine Möglichkeit dieses zu ändern, ist die spezifische Funktionalisierung der Nukleinsäuren mit Metallionen. In einer kürzlich entwickelten Methode werden Metall-Basenpaare benutzt, um die Metallionen an bestimmten Positionen im Inneren der DNS anzuordnen.<sup>[36]</sup> Solch eine präzise Anordnung ist unabdingbar für den potenziellen Einsatz als Nanomagnet, selbstorganisierter molekularer Leiter oder als Katalysator in chemischen Reaktionen. Metall-Basenpaare bestehen aus natürlichen oder künstlichen Nukleobasen die anstelle von (oder zusätzlich zu) Wasserstoffbrücken, koordinative Bindungen zu einem zentralen Metallion ausbilden. Je nach Wahl des Nukleotids, des Metallions und der Oligonukleotidsequenz kann eine Vielfalt von metall-modifizierten Duplexes erschaffen werden. Solche Metall-Basenpaare wurden bereits in DNS, GNS (Glykolnukleinsäuren), sowie in PNS (Peptidnukleinsäure) Duplexes eingefügt, wobei in DNS sogar der Einbau von bis zu 19 aufeinanderfolgenden Metall-Basenpaaren gelang. Mit Hilfe unterschiedlicher Metall-Basenpaare konnten außerdem zwei verschiedene Metalle in die gleiche Duplex integriert werden.<sup>[37,39,41]</sup>

Trotz der rasanten Entwicklung auf diesem Gebiet, ist es noch ein weiter Weg bis zur tatsächlichen Verwendung von Nukleinsäuren in der Nanotechnologie. Neben der unbeantworteten Frage, ob solche metall-modifizierten Nukleinsäuren tatsächlich eine höhere elektrische Leitfähigkeit besitzen, ist die Synthese von Oligonukleotiden, die viele aufeinander folgende Metall-Basenpaaren enthalten, ein weiteres Problem. Die automatische Festphasensynthese ist eine etablierte Methode um DNA Stränge herzustellen und ermöglicht auch den Einbau künstlicher Nukleotide. Auf der anderen Seite ist die Produktion großer Mengen solcher metall-modifizierter Nukleinsäuren mit dieser Methode sehr zeitaufwendig und teuer. Um metall-funktionalisierte Nukleinsäuren für den Einsatz in der Nanotechnologie weiter zu optimieren, sind außerdem Informationen über die Struktur der Helix und über die Geometrie der Metall-Basenpaare unentbehrlich. Bis heute konnte aber nur eine metall-modifizierte DNS und eine GNS Duplex strukturell charakterisiert werden. Jedoch enthielt

keine der Beiden aufeinanderfolgende Metall-Basenpaare und sie lagen auch nicht in der kanonischen B-helikalen Struktur vor.<sup>[44,194]</sup>

Im ersten Teil der Arbeit wurden verschiedene palindromische sowie nicht-palindromische RNS Sequenzen mit 2, 3, 6, 10 oder auch 20 aufeinanderfolgenden Uracil Nukleotiden transkribiert und spektroskopisch untersucht. *In vitro*



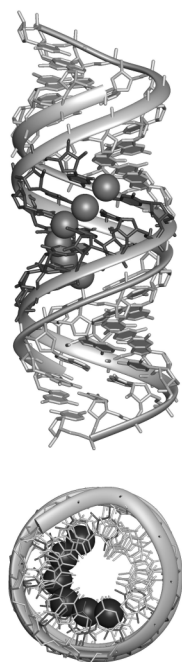
**Figur S1** Bildung eines Uracil-Quecksilber-Uracil Basenpaares aus einem *cis*-Uracil-Uracil Wobblepaar.

Transkription mit *T7* RNA Polymerase ist eine geeignete Methode um lange Stränge mit gleichen Nukleotiden herzustellen. Durch Mutation zweier Aminosäuren (Y639F / S641A) ist es außerdem möglich, die entsprechenden Sequenzen mit dem Deoxynukleotid Thymin, anstelle von Uracil, mit ähnlich guten Ausbeuten zu erhalten. Bei mehr als zehn identischen Nukleobasen hintereinander sinkt die Transkriptionsausbeute jedoch deutlich und es entstehen zusätzliche Abbruchprodukte. Es scheint, als ob die *T7* RNA Polymerase durch die große Anzahl gleicher aufeinander folgender Nukleotide nicht mehr so präzise arbeiten kann. Dennoch wurden für alle Sequenzen definierte Transkriptionsbanden erhalten, die anschliessend durch 18 % PAGE (Polyacrylamidgel-Elektrophorese) gut voneinander getrennt werden konnten.

In der Literatur ist schon seit längerem bekannt, dass  $\text{Hg}^{2+}$ -Ionen in DNS-helikalen Strukturen missgepaarte Thymine miteinander verbinden können. Dabei ersetzen die  $\text{Hg}^{2+}$ -Ionen die N3H Protonen und koordinieren an die N3 Stickstoffe der zwei Thymine, wodurch sich die Metallionen in der Mitte der DNA Helix anordnen.<sup>[57]</sup> Um zu ermitteln, ob die  $\text{Hg}^{2+}$ -Ionen die missgepaarten Uracile auf die selbe Art und Weise koordinieren, wurden die RNA Sequenzen mit und ohne  $\text{Hg}^{2+}$ -Ionen mit UV-VIS, CD (Circular Dichroismus) und NMR (Kernspinresonanz) Spektroskopie sowie mit DLS (Dynamische Lichtstreuung) untersucht.

Die UV-Schmelztemperaturanalysen zeigen, dass sich die Schmelztemperatur aller Konstrukte durch Zugabe eines Äquivalents  $\text{Hg}^{2+}$ -Ionen erhöht. Das ist ein Indiz dafür, dass die  $\text{Hg}^{2+}$ -Ionen in die Uracil-Uracil Basenpaare eingebaut werden und so die Duplex Struktur stabilisieren (Figur S1).

CD Spektroskopie ist eine geeignete Methode um strukturelle Änderungen festzustellen. Bei Zugabe von  $\text{Hg}^{2+}$ -Ionen zeigen alle RNA Konstrukte den gleichen Trend. Alle Sequenzen weisen einen A-Helix typischen Verlauf auf mit einem Maximum bei 260 nm und einem Minimum bei 220 nm. Durch Zugabe von  $\text{Hg}^{2+}$ -Ionen wird das Maximum kleiner und



**Figur S2** Modell einer metal-modifizierten A-RNA.

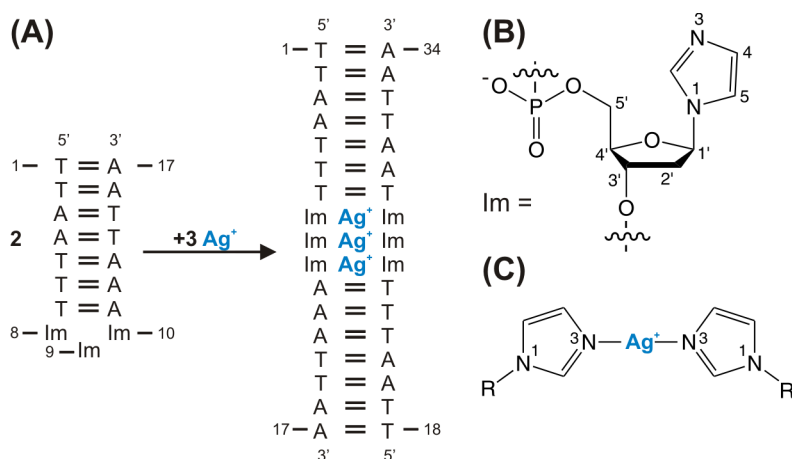
verschiebt sich zu größeren Wellenlängen, während man am Minimum den umgekehrten Effekt beobachten kann. Das Profil der Kurve bleibt aber gleich. Dies zeigt, dass durch die Koordination der  $\text{Hg}^{2+}$ -Ionen die A-helikale Struktur nicht zerstört wird. DOSY (Diffusions geordnete Spektroskopie) und DLS sind zwei Methoden um den hydrodynamischen Radius  $r_H$  von Nukleinsäuren zuverlässig und unabhängig voneinander zu bestimmen. Die Zugabe von  $\text{Hg}^{2+}$ -Ionen führt bei allen palindromischen Sequenzen zu einer Zunahme des Radiuses. So ein Anstieg kann nur auf die Umordnung einer Haarnadelstruktur zur Duplex unter Bildung von Metall-Basenpaaren zurückgeführt werden.

Diese Ergebnisse zusammen mit zusätzlichen NMR Messungen demonstrieren, dass die  $\text{Hg}^{2+}$ -Ionen tatsächlich die Protonen der Uracile ersetzen und linear zwischen den Basen koordinieren. Auf der anderen Seite wird jedoch deutlich, dass die Bindung von  $\text{Hg}^{2+}$ -Ionen zu RNS nicht so stark wie zu DNS ist. Die RNS Konstrukte, die Thymin anstelle

von Uracil enthalten, bilden ebenfalls A-helikale Strukturen und verhalten sich bei Zugabe von  $\text{Hg}^{2+}$ -Ionen genau wie ihre entsprechenden reinen RNA Sequenzen. Die geringere Bindungsstärke kann deshalb nur auf Unterschiede zwischen der A-Form und der B-Form Helix zurückgeführt werden (Figur S2).

Diese ersten metallfunktionalisierten RNS Sequenzen machen deutlich, dass auch RNS Stränge geeignet sind, um metall-modifizierte Nukleinsäuren zu generieren. Außerdem erwies sich die *in vitro* Transkription mit T7 RNA Polymerase als eine schnelle und effiziente Methode, um große Mengen solcher modifizierter Oligonukleotide herzustellen.

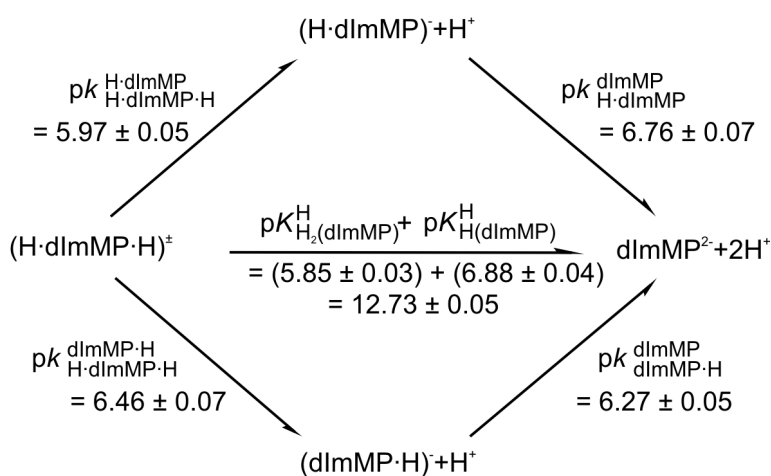
Im zweiten und umfangreichsten Teil der Arbeit wurde die Struktur eines 17 nt langen Oligonukleotids, das drei künstliche Imidazolbasen enthält, mittels NMR Spektroskopie in Gegenwart und in Abwesenheit von  $\text{Ag}^+$ -Ionen untersucht (Figure S3). Es ist



**Figur S3** Beschreibung des DNS Oligonukleotidsystems mit der künstlichen Imidazolbase.

bekannt, dass solch eine Sequenz bei Zugabe von  $\text{Ag}^+$ -Ionen sich von einer Haarnadelstruktur zu einer Duplex umlagert und dabei drei Metall-Basenpaare bildet.<sup>[45]</sup> Das verwendete Oligonukleotid wurde von einer Partnergruppe aus Münster synthetisiert. DFT Rechnungen von zwei 1-Methylimidazolen und einem  $\text{Ag}^+$ -Ion als vermeintliches Metall-Basenpaar offenbaren eine optimale Geometrie für die Integration in eine B-helikale Struktur.

Da die Koordination von Metallionen an Nukleinsäuren häufig mit Protonierungsreaktionen konkurriert, wurden zunächst die Säure-Basen Eigenschaften des einzelnen Imidazolnukleotiden untersucht. In einem pH Bereich von 1 - 13 sind zwei Deprotonierungsschritte zu erwarten, einer an der Phosphatgruppe und ein zweiter am Imidazol. Durch potentiometrische Titrations konnten die zwei Makrosäurekonstanten  $\text{p}K_{\text{H}(\text{dImMP})}^{\text{H}} = 5.85 \pm 0.03$  und  $\text{p}K_{\text{H}_2(\text{dImMP})}^{\text{H}} = 6.88 \pm 0.04$  bestimmt werden. Da sich diese Konstanten aber nur um eine  $\text{p}K_{\text{a}}$  Einheit unterscheiden, überlappen die Pufferbereiche der zwei Protonierungsstellen. Die Makrosäurekonstanten beschreiben also nur annäherungsweise die Orte der einzelnen Protonierungsreaktionen. Dennoch ist zu vermuten, dass  $\text{p}K_{\text{H}_2(\text{dImMP})}^{\text{H}}$  hauptsächlich durch die Deprotonierung an der Phosphatgruppe und  $\text{p}K_{\text{H}(\text{dImMP})}^{\text{H}}$  durch die Deprotonierung am Imidazol beeinflusst wird. Um die beiden Säure-



$$K_{\text{H}_2(\text{dImMP})}^{\text{H}} = k_{\text{H} \cdot \text{dImMP} \cdot \text{H}^+}^{\text{H} \cdot \text{dImMP}} \cdot k_{\text{H} \cdot \text{dImMP} \cdot \text{H}}^{\text{dImMP} \cdot \text{H}} \quad (\text{a})$$

$$\frac{1}{K_{\text{H}(\text{dImMP})}^{\text{H}}} = \frac{1}{k_{\text{H} \cdot \text{dImMP}}^{\text{dImMP}}} + \frac{1}{k_{\text{dImMP}}^{\text{dImMP} \cdot \text{H}}} \quad (\text{b})$$

$$\begin{aligned} K_{\text{H}_2(\text{dImMP})}^{\text{H}} \cdot K_{\text{H}(\text{dImMP})}^{\text{H}} &= k_{\text{H} \cdot \text{dImMP} \cdot \text{H}^+}^{\text{H} \cdot \text{dImMP}} \cdot k_{\text{H} \cdot \text{dImMP} \cdot \text{H}}^{\text{dImMP} \cdot \text{H}} \\ &= k_{\text{H} \cdot \text{dImMP}}^{\text{dImMP}} \cdot k_{\text{dImMP} \cdot \text{H}}^{\text{dImMP}} \end{aligned} \quad (\text{c})$$

**Figur S4** Deprotonierungsschema von  $(\text{H} \cdot \text{dImMP} \cdot \text{H})^+$ .

Basen Konstanten genau zu bestimmen wurden die Mikrosäurekonstanten berechnet und das Verhältnis zwischen der imidazolprotonierten  $(\text{H} \cdot \text{dImMP})^-$  und der phosphatprotonierten  $(\text{dImMP} \cdot \text{H})^-$  Form von  $\text{H}(\text{dImMP})^-$  ermittelt. Die Ergebnisse belegen, dass  $(\text{H} \cdot \text{dImMP})^-$  die vorherrschende Spezies ist (75 %), aber auch nennenswerte Mengen an  $(\text{dImMP} \cdot \text{H})^-$  (25 %) vorliegen. Zusätzlich wurden Änderungen der  $^{31}\text{P}$ -NMR und der  $^1\text{H}$ -NMR chemischen Ver-

schiebung der Phosphatgruppe beziehungsweise der drei aromatischen Imidazolprotonen, in Abhängigkeit des pH-Wertes bestimmt. Mit diesen experimentellen Daten konnte die Richtigkeit des entwickelten Deprotonierungsschemas (Figur S4) bestätigt werden. Die berechnete Mikrosäurekonstante  $pK_{H \cdot dImMP \cdot H}^{dImMP \cdot H} = 6.46 \pm 0.07$  von  $(dImMP \cdot H)^-$  dient außerdem als Grundlage für den Vergleich der Säure-Basen-Eigenschaften der in der DNS eingebauten Imidazolnukleotide, da es ebenfalls wie diese eine negative Ladung enthält.

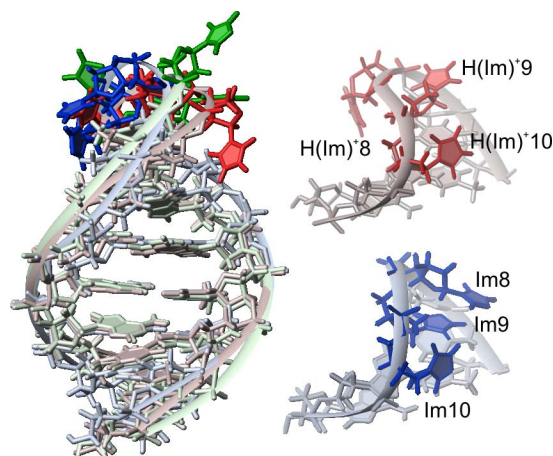
Um die dreidimensionale Struktur des Oligonukleotiden in Abwesenheit von  $Ag^+$ -Ionen mittels NMR zu lösen, wurden zahlreiche  $[^1H]$ -NMR Spektren bei pD 7.2 aufgenommen. Wie bereits erwähnt, bilden derartige Sequenzen in Abwesenheit von Übergangsmetallen Haarnadelstrukturen, wobei sich die künstlichen Nukleotide im Loop anordnen. Das  $[^1H, ^1H]$ -NOESY Spektrum zeigt eine gut aufgelöste *sequential walk* Region. Für die künstlichen Imidazol-Bausteine wurden aber nur wenige und sehr breite NOE-Signale gefunden, so dass der *sequential walk* nicht durch die gesamte Sequenz verfolgt werden konnte. Dennoch war es möglich alle Imidazolnukleotide mit Hilfe anderer NMR Spektren zuverlässig zu bestimmen. Weiterhin wurde der hydrodynamische Radius  $r_H$  mit DOSY und DLS Experimenten gemessen, da mittels  $[^1H, ^1H]$ -NOESY Spektren nicht eindeutig zwischen einer Haarnadelstruktur und einer Doppelhelix unterschieden werden kann. Aus beiden Methoden resultierte ein fast gleicher  $r_H$  mit  $1.5 \pm 0.1$  beziehungsweise  $1.4 \pm 0.2$  nm. Diese Ergebnisse stimmen hervorragend mit dem theoretisch berechneten  $r_H$  der Haarnadelstruktur überein. Die anschließenden Strukturrechnungen präsentieren eine stabile Haarnadelstruktur mit einer wohldefinierten helikalen Region und einem unstrukturierten Loop, was auf die Semi-Protonierung der Imidazolbasen zurückzuführen ist.

Um die intrinsischen Säurekonstanten der eingebauten Imidazolnukleotide zu bestimmen, wurden Änderungen der  $[^1H]$ -NMR chemischen Verschiebung in Abhängigkeit vom pH-Wert gemessen. Mit zunehmendem pH-Wert verschieben sich alle aromatischen Protonenresonanzen der künstlichen Nukleobasen ins höhere Feld und verbreitern sich. Bei pH = 7 sind diese so stark verbreitert, dass einige sogar gänzlich verschwinden. In basischer Umgebung sind alle Resonanzen mit der gleichen Intensität wie im sauren Bereich wieder sichtbar. Die Auswertung der Änderung der  $[^1H]$ -NMR chemischen Verschiebung ergab die spezifischen Säurekonstanten  $pK_{a, Im8} = 6.78 \pm 0.03$ ,  $pK_{a, Im9} = 6.33 \pm 0.04$  und  $pK_{a, Im10} = 6.58 \pm 0.23$ . Das Nukleotid Im9 hat die kleinste Säurekonstante, da wahrscheinlich die zwei positiven Ladungen der benachbarten Imidazolnukleobasen die Deprotonierung erleichtern. Im8 hat nicht nur die größte Säurekonstante von den Imidazolnukleotiden, sondern ist auch 0.3 log Einheiten basischer als  $H(dImMP)^-$ . Das macht deutlich, dass die

Säurekonstanten stark durch die elektrostatische Wechselwirkungen der direkten Umgebung beeinflusst werden. Die  $pK_a$  Werte der Imidazolbasen liegen alle im physiologischen pH-Bereich, so dass der Oligonukleotid als Modell für säure-basen katalytische Zentren in großen RNS Strukturen verwendet werden kann.

Die Resultate aus den Experimenten zur chemischen Verschiebung lassen eine definierte Loopstruktur im sauren als auch im basischen pH-Bereich vermuten. Um dies zu belegen wurden weitere  $[^1\text{H}, ^1\text{H}]$ -NOESY Spektren bei pD 4.7 and pD 10.2 aufgenommen. Diese Spektren sehen denen bei pD 7.2 sehr ähnlich, weisen jedoch deutlich mehr Signale für die künstlichen Imidazolbasen auf. Allerdings konnte auch hier der *sequential walk* nicht durch die komplette Sequenz verfolgt werden. Anschließende Strukturrechnungen der DNS bei pD 4.7 und pD 10.2 zeigen eine fast identische Helix, während der Loop signifikante Unterschiede aufweist (Figur S5). Die allgemeine Gestalt ist jedoch sehr ähnlich, da in beiden Fällen die Imidazolnukleotide in die Helix eingebettet sind. Im Gegensatz zu der Haarnadelstruktur im neutralen pH-Bereich, bildet sich im sauren als auch im basischen pH ein wohlstrukturierter Loop. Bei pD 4.7 sind die Imidazolbasen komplett protoniert und versuchen aufgrund der positiven Ladung einander auszuweichen. Die protonierten Gruppen sind zum negativ geladenen Phosphatrückgrat gerichtet und ermöglichen so einen optimalen Ladungsausgleich. Im basischen pH orientieren sich alle Imidazolnukleotide in Richtung der *Großen Furche*. Im9 liegt direkt über T7 und die zahlreichen NOE Signale zwischen diesen beiden Nukleotiden lassen eine zusätzliche Stapel-Wechselwirkung vermuten. Berechnungen des elektrostatischen Oberflächenpotenzials der protonierten und der unprotonierten Form weisen keine ungewöhnlich stark positiv oder stark negativ geladene Gebiete auf.

Die Zugabe von einem Äquivalent  $\text{Ag}^+$ -Ionen bewirkt eine offensichtliche Änderung des  $[^1\text{H}, ^1\text{H}]$ -NOESY Spektrums, was auf eine grundlegende Strukturänderung von Haarnadel zu Duplex zurückzuführen ist. Gerade in der *sequential walk* Region erscheinen viele starke neue



**Figur S5** Rechts: NMR Struktur der Haarnadel-form im sauren (rot), neutralen (grün), and basischen (blau) pH-Bereich. Links: Vergrößerung der Loop Struktur im basischen (rot) und im sauren (blau) pH Bereich.



Resonanzen der Imidazolbasen, so dass nun der *sequential walk* durch die gesamte Sequenz verfolgt werden kann. Das typische B-helikale Muster, das auch für alle Imidazolnukleotide gefunden wurde, ist ein Indiz, dass sich stabile Imidazol-Silber-Imidazol Basenpaare gebildet haben. DOSY und DLS Messungen der DNS in Gegenwart von  $\text{Ag}^+$ -Ionen belegen einen eindeutigen Anstieg des  $r_H$  zu  $1.9 \pm 0.3$  nm und  $1.8 \pm 0.2$  nm. Diese Radien stimmen gut mit

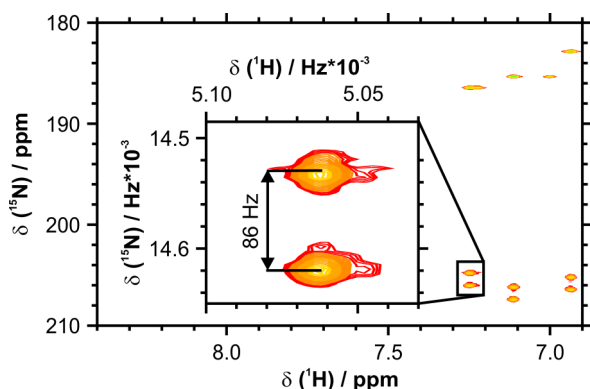


**Figure S6**  $^1J(^{15}\text{N}, ^{107/109}\text{Ag})$  Kopplung von 86 Hz im  $[\text{}^{15}\text{N}, \text{}^1\text{H}]$ -HSQC Spektrum.

den theoretisch berechneten Werten einer Duplexstruktur überein. Um die Koordination der  $\text{Ag}^+$ -Ionen an die künstlichen Basenpaare zusätzlich zu belegen, wurden  $^{15}\text{N}$ -markierte Imidazole in das Oligonukleotid eingebaut und  $[\text{}^{15}\text{N}, \text{}^1\text{H}]$ -HSQC Spektren in Ab- und Anwesenheit von  $\text{Ag}^+$ -Ionen aufgenommen.

Durch Zugabe der  $\text{Ag}^+$ -Ionen verschieben sich alle Stickstoffresonanzen ins höhere

Feld, d.h. die N1 Resonanzen um ca. 3 ppm und die N3 Resonanzen um ca. 15 ppm. Es ist bekannt, dass eine direkte Koordination von Silber an Stickstoff zu einer starken Hochfeldverschiebung, wie es für N3 beobachtet wurde, führt. Diese Hochfeldverschiebung ist somit ein direkter Beweis für die Koordination der  $\text{Ag}^+$ -Ionen an die N3 Position der Imidazolbasen. Interessanterweise zeigen die N3 Resonanzen zusätzlich eine Aufspaltung von 86 Hz. So eine Aufspaltung ist nur auf eine direkte Kopplung zwischen den N3 Stickstoffen und den  $\text{Ag}^+$ -Ionen zurückzuführen, d.h. eine  $^1J(^{15}\text{N}, ^{107/109}\text{Ag})$  Kopplung (Figure S6) und liefert einen weiteren Beleg für die Bildung eines Imidazol-Silber-Imidazol Basenpaares. Die große Kopplung macht außerdem deutlich, dass die  $\text{Ag}^+$ -Ionen fest an die künstlichen Basen gebunden und gut in die helikale Struktur eingebettet sind. Die Strukturrechnungen zeigen, dass die metall-modifizierte DNS in der B-helikalen Struktur vorliegt. Eine umfangreiche Analyse der Basenpaarparameter ergab eine leichtes Aufwinden und Dehnen der Helix im Bereich der Imidazol-Silber-Imidazol Basenpaare, ohne jedoch die

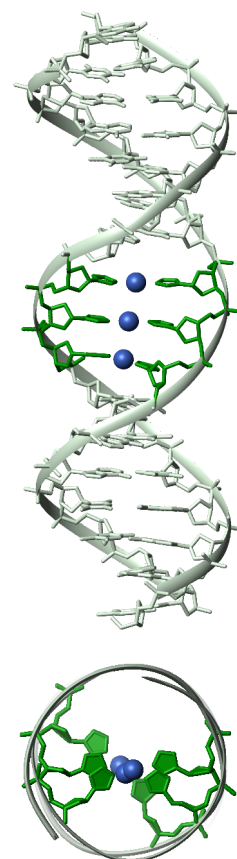


**Figure S7** NMR Struktur der silber-modifizierten Duplex.

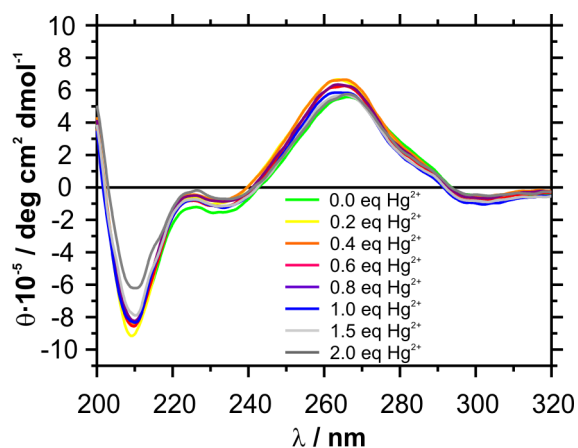
B-helikale Konformation zu zerstören. Die Silber-Silber Abstände in den 20 energieniedrigsten Strukturen variieren zwischen 3.79 und 4.51 Å. Diese großen Schwankungen machen deutlich, dass die Energiedifferenz zwischen verschiedenen Konformationen mit unterschiedlichen Metall-Metall Abständen nur sehr gering ist. Durch diese NMR Struktur ist es zum ersten Mal möglich einen detaillierten Blick auf den Aufbau von Nukleinsäuren mit aneinandergereihten Metall-Basenpaaren zu bekommen. Außerdem beweist sie, dass eine DNS Duplex die B-Konformation beibehalten kann auch wenn gleichzeitig Metallionen entlang der helikalen Achse angeordnet sind.

Die Arbeit beschreibt eine neue Methode um schnell und effizient große Mengen metall-modifizierter Nukleinsäuren herzustellen und präsentiert die erste dreidimensionale Nukleinsäure-Struktur mit aufeinanderfolgenden Metall-Basenpaaren. Diese Ergebnisse sind außerordentlich bedeutsam für die Weiterentwicklung metall-funktionalisierter Nukleinsäuren und deren Verwendung in der Nanotechnologie.

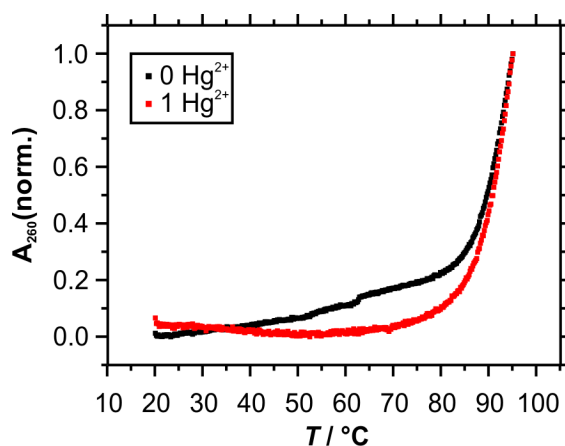
## 7 Appendices

- Appendix 1** CD spectra of **PM01** upon stepwise addition of  $\text{Hg}^{2+}$  ions.
- Appendix 2** UV melting curves of 1  $\mu\text{M}$  **PM03** in the absence and in the presence of 1 eq  $\text{Hg}^{2+}$  ions.
- Appendix 3** UV melting curves of 1  $\mu\text{M}$  **PM04** in the absence and in the presence of 1 eq  $\text{Hg}^{2+}$  ions.
- Appendix 4** CD spectra of 1  $\mu\text{M}$  **PM04** upon stepwise addition of  $\text{Hg}^{2+}$  ions.
- Appendix 5** UV melting curves of 1  $\mu\text{M}$  **PM05** in the absence and in the presence of 1 eq  $\text{Hg}^{2+}$  ions.
- Appendix 6** UV melting curves of 2  $\mu\text{M}$  **PM01** in the absence and in the presence of 1 eq  $\text{Hg}^{2+}$  ions.
- Appendix 7** UV melting curves of 1  $\mu\text{M}$  **PM03(T)** in the absence and in the presence of 1 eq  $\text{Hg}^{2+}$  ions.
- Appendix 8** Integration of the imidazole residue in the library of DYANA 1.5.
- Appendix 9** Integration of the imidazole residue and the imidazole-silver-imidazole base pair in the parameter and topology files of XPLOR NIH 2.15.0.
- Appendix 10** [ $^1\text{H}$ ]-NMR chemical shift assignments of the oligonucleotide DNA\_IMI in the absence of  $\text{Ag}^+$  ions at pD 7.2.
- Appendix 11** All distance and dihedral angle restraints for the structure calculation of DNA\_IMI in the absence of silver(I) ions at pD 7.2.
- Appendix 12** [ $^1\text{H}$ ]-NMR chemical shift assignments of the oligonucleotide DNA\_IMI in the absence of  $\text{Ag}^+$  ions at pD 4.7.
- Appendix 13** All distance and dihedral angle restraints for the structure calculation of DNA\_IMI in the absence of  $\text{Ag}^+$  ions at pD 4.7.
- Appendix 14** [ $^1\text{H}$ ]-NMR chemical shift assignments of the oligonucleotide DNA\_IMI in the absence of  $\text{Ag}^+$  ions at pD 10.2.
- Appendix 15** All distance and dihedral angle restraints for the structure calculation of DNA\_IMI in the absence of  $\text{Ag}^+$  ions at pD 10.2.
- Appendix 16** [ $^1\text{H}$ ]-NMR chemical shift assignments of the oligonucleotide DNA\_IMI in the presence of  $\text{Ag}^+$  ions at pD 7.2.
- Appendix 17** All distance and dihedral angle restraints for the structure calculation of DNA\_IMI in the presence of  $\text{Ag}^+$  ions at pD 7.2.
- Appendix 18** The base pair parameter of the DNA duplex structure as derived with the programme 3DNA.
- Appendix 19** Glycosidic angle  $\chi / ^\circ$  of the DNA duplex structure as derived with the programme 3DNA.

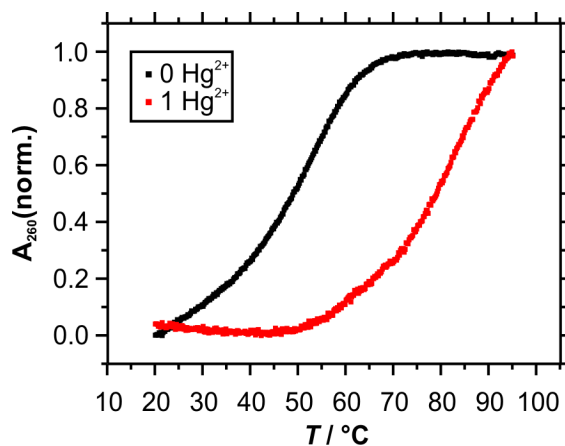
**Appendix 1** CD spectra of 2  $\mu\text{M}$  **PM01** in 100 mM  $\text{NaClO}_4$  at pH 6.8 and 298 K upon stepwise addition of  $\text{Hg}^{2+}$  ions.



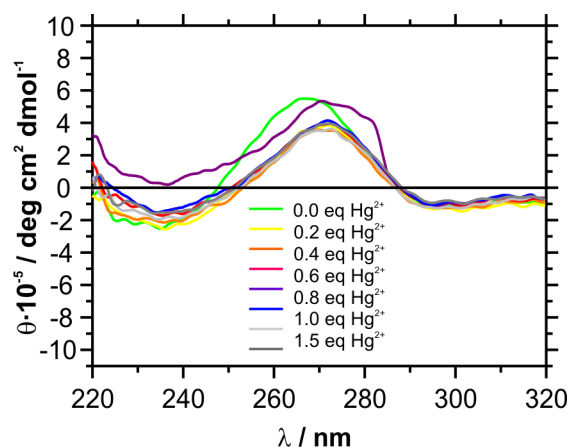
**Appendix 2** UV melting curve of 1  $\mu\text{M}$  **PM03** in 100 mM  $\text{NaClO}_4$  and 5 mM MOPS pH 6.8 in the absence and in the presence of 1 eq  $\text{Hg}^{2+}$  ions.



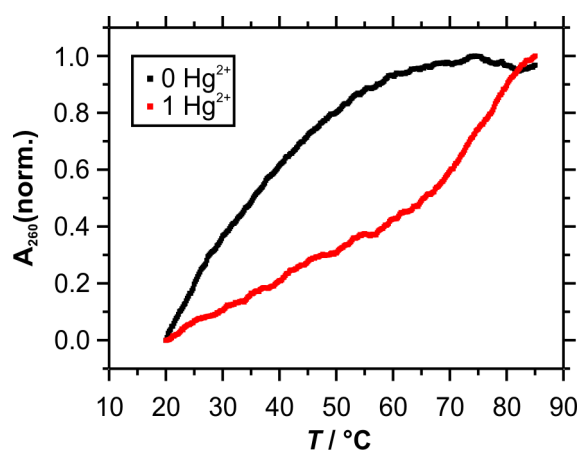
**Appendix 3** UV melting curve of 1  $\mu\text{M}$  **PM04** in 100 mM  $\text{NaClO}_4$  and 5 mM MOPS pH 6.8 in the absence and in the presence of 1 eq  $\text{Hg}^{2+}$  ions.



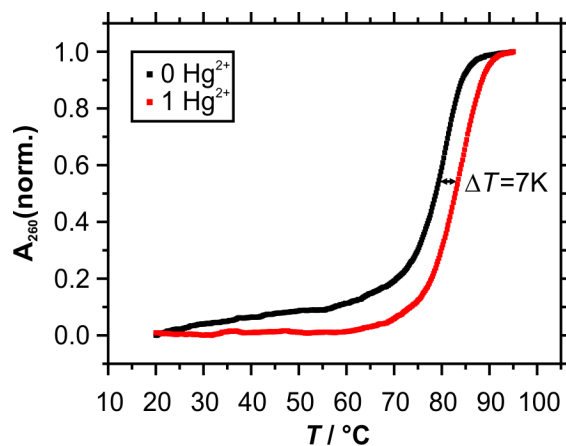
**Appendix 4** CD spectra of 4  $\mu\text{M}$  **PM04** in 100 mM  $\text{NaClO}_4$  at pH 6.8 and 298 K upon stepwise addition of  $\text{Hg}^{2+}$  ions.



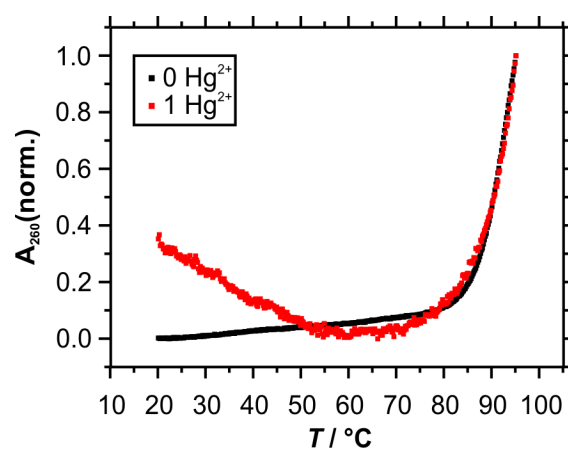
**Appendix 5** UV melting curve of 1  $\mu\text{M}$  **PM05** in 100 mM  $\text{NaClO}_4$  and 5 mM MOPS pH 6.8 in the absence and in the presence of 1 eq  $\text{Hg}^{2+}$  ions.



**Appendix 6** UV melting curve of 2  $\mu\text{M}$  **PM01** in 100 mM  $\text{NaClO}_4$  and 5 mM MOPS pH 6.8 in the absence and in the presence of 1 eq  $\text{Hg}^{2+}$  ions.



**Appendix 7** UV melting curve of 1  $\mu\text{M}$  **PM03(T)** in 100 mM  $\text{NaClO}_4$  and 5 mM MOPS pH 6.8 in the absence and in the presence of 1 eq  $\text{Hg}^{2+}$  ions.



**Appendix 8** Inclusion of the imidazole residue in the library of DYANA 1.5.Additions in *dyana.lib*

RESIDUE	IMI	9	31	3	30						
1 ZETA	0	0	0.0000	1	2	3	6	0			
2 ALPHA	0	0	0.0000	2	3	6	7	0			
3 BETA	0	0	0.0000	3	6	7	11	0			
4 GAMMA	0	0	0.0000	6	7	11	13	0			
5 DELTA	0	0	0.0000	7	11	13	30	0			
6 NU2	0	0	0.0000	11	13	15	19	29			
7 NU1	0	0	0.0000	13	15	19	21	29			
8 CHI	0	0	0.0000	21	19	22	23	29			
9 EPSI	0	0	0.0000	11	13	31	30	0			
1 C3'	C_ALI	0	0.2330	-0.9681	-5.8551	2.5577	2	0	0	0	0
2 O3'	O_EST	0	-0.5090	-0.6348	-4.7127	1.7719	1	3	0	0	0
3 P	P_ALI	0	1.3850	0.4817	-3.6875	2.2842	2	4	5	6	0
4 OP1	O_BYL	0	0.8470	1.7976	-4.3635	2.3259	3	0	0	0	0
5 OP2	O_BYL	0	-0.8470	0.0167	-3.0215	3.5214	3	0	0	0	0
6 O5'	O_EST	0	-0.5090	0.5255	-2.5916	1.1193	3	7	0	0	0
7 C5'	C_ALI	0	0.1180	1.4216	-1.4863	1.2135	6	8	9	11	0
8 H5'	H_ALI	0	0.0210	2.4568	-1.8260	1.2707	7	0	0	0	10
9 H5"	H_ALI	0	0.0210	1.2157	-0.8907	2.1041	7	0	0	0	10
10 Q5'	PSEUD	0	0.0000	1.8362	-1.3584	1.6874	0	0	0	0	0
11 C4'	C_ALI	0	0.0360	1.2779	-0.5959	0.0000	7	12	21	13	0
12 H4'	H_ALI	0	0.0560	1.5099	-1.1747	-0.8952	11	0	0	0	0
13 C3'	C_ALI	0	0.2330	2.1963	0.6228	0.0000	11	15	14	30	0
14 H3'	H_ALI	0	0.0250	3.1027	0.4293	0.5756	13	0	0	0	0
15 C2'	C_ALI	0	-0.3070	1.3731	1.7403	0.5780	19	16	17	13	0
16 H2'	H_ALI	0	0.0810	1.4019	1.6718	1.6635	15	0	0	0	18
17 H2"	H_ALI	0	0.0810	1.7912	2.6897	0.2499	15	0	0	0	18
18 Q2'	PSEUD	0	0.0000	1.5965	2.1808	0.9567	0	0	0	0	0
19 C1'	C_ALI	0	0.3760	0.0000	1.4100	0.0000	21	20	22	15	0
20 H1'	H_ALI	0	0.0090	-0.0659	1.7932	-1.0183	19	0	0	0	0
21 O4'	O_EST	0	-0.3680	0.0000	0.0000	0.0000	11	19	0	0	0
22 N1	N_AMI	0	-0.0420	-1.1209	1.9441	0.8017	19	23	28	0	0
23 C5	C_ARO	0	0.3910	-2.3784	2.2371	0.3436	22	24	25	0	0
24 H5	H_ARO	0		-2.8975	2.1875	-0.6022	23	0	0	0	0
25 C4	C_ARO	0	-0.0600	-3.0716	2.6978	1.4177	23	26	27	0	0
26 H4	H_ARO	0		-4.0315	2.4284	1.5651	25	0	0	0	0
27 N3	N_AMI	0	-0.5430	-2.2897	2.7047	2.5414	25	28	0	0	0
28 C2	C_ARO	0	0.2660	-1.1186	2.2402	2.1184	22	27	29	0	0
29 H2	H_ARO	0	0.0460	-0.2357	2.0985	2.7240	28	0	0	0	0
30 O3'	O_EST	0	-0.5090	2.6047	0.9094	-1.3466	13	31	0	0	0
31 P	P_ALI	0	1.3850	3.5778	2.1447	-1.6417	30	0	0	0	0

## Appendix 9 Inclusion of the imidazole residue and the imidazole-silver-imidazole base pair in the parameter and topology files of XPLOR NIH 2.15.0.

### Additions in *nucleic.top*

```

MASS  XCD1    12.01100  !SJ 22/02/08 IMI
MASS  XCD1+   12.01100  !SJ 22/02/08 IMI+
MASS  XCD2    12.01100  !SJ 22/02/08 IMI
MASS  XCD2+   12.01100  !SJ 22/02/08 IMI+
MASS  XCL     12.01100  !SJ 22/02/08 IMI
MASS  XCL+    12.01100  !SJ 22/02/08 IMI+
MASS  XNB+    14.00670  !SJ 22/02/08 IMI+
MASS  XNS+    14.00670  !SJ 22/02/08 IMI+
MASS  AG      107.86820  !SJ 26/02/08 PAGI

RESIDUE IMI !SJ 21/02/08 IMI
GROUP
  ATOM P      TYPE=XP      CHARGE= 1.20      END
  ATOM O1P    TYPE=XO2     CHARGE=-0.40     END
  ATOM O2P    TYPE=XO2     CHARGE=-0.40     END
  ATOM O5'    TYPE=XOS     CHARGE=-0.36     END
GROUP
  ATOM C5'    TYPE=XC2     CHARGE=-0.07     END
  ATOM H5'    TYPE=XH      CHARGE= 0.035     END
  ATOM H5''   TYPE=XH      CHARGE= 0.035     END
GROUP
  ATOM C4'    TYPE=XCH     CHARGE=0.065     END
  ATOM H4'    TYPE=XH      CHARGE=0.035     END
  ATOM O4'    TYPE=XOS     CHARGE=-0.30     END
  ATOM C1'    TYPE=XCH     CHARGE=0.165     END
  ATOM H1'    TYPE=XH      CHARGE=0.035     END
GROUP
  ATOM N1     TYPE=XNS     CHARGE=-0.024     END
  ATOM C5     TYPE=XCD2    CHARGE=-0.054     END
  ATOM H5     TYPE=XH      CHARGE= 0.052     END
  ATOM C2     TYPE=XCL     CHARGE= 0.029     END
  ATOM H2     TYPE=XH      CHARGE= 0.067     END
  ATOM N3     TYPE=XNB     CHARGE=-0.232     END
  ATOM C4     TYPE=XCD1    CHARGE=-0.044     END
  ATOM H4     TYPE=XH      CHARGE= 0.055     END
GROUP
  ATOM C2'    TYPE=XCH     CHARGE= 0.115     END
  ATOM H2'    TYPE=XH      CHARGE= 0.035     END
  ATOM O2'    TYPE=XOH     CHARGE=-0.40     END
  ATOM H2''   TYPE=XHO     CHARGE= 0.25      END
GROUP
  ATOM C3'    TYPE=XCH     CHARGE=-0.035     END
  ATOM H3'    TYPE=XH      CHARGE= 0.035     END
GROUP
  ATOM O3'    TYPE=XOS     CHARGE=-0.36     END

  BOND P O1P    BOND P O2P    BOND P O5'
  BOND O5' C5'  BOND C5' C4'  BOND C4' O4'  BOND C4' C3'  BOND O4' C1'
  BOND C1' N1   BOND C1' C2'  BOND N1 C5   BOND N1 C2   BOND C5 C4
  BOND C4 N3    BOND N3 C2   BOND C2' C3'  BOND C3' O3'  {*BOND O3' +P*}
  BOND C2' O2'  BOND O2' H2'
  BOND C1' H1'  BOND C2' H2''  BOND C3' H3'  BOND C4' H4'  BOND C5' H5'
  BOND C5' H5'' BOND C2 H2   BOND C4 H4   BOND C5 H5

  DIHE P O5' C5' C4'  DIHE O5' C5' C4' O4'  DIHE O5' C5' C4' C3'
  DIHE O4' C1' N1 C5

```



```

! N O T E:  SUGAR RING TERMS SET UP AS W. OLSON DOES IT
DIHE O4'  C1'  C2'  C3' ! O-C-C-C, twofold term
DIHE O4'  C1'  C2'  C3'
DIHE C1'  C2'  C3'  C4'
DIHE C2'  C3'  C4'  O4' ! O-C-C-C, twofold term
DIHE C2'  C3'  C4'  O4'
DIHE C3'  C4'  O4'  C1'
DIHE C4'  O4'  C1'  C2'

! AND THE SPECIAL GAUCHE TERMS
DIHE C5'  C4'  C3'  O3'
DIHE O4'  C4'  C3'  O3'
DIHE O4'  C1'  C2'  O2'
DIHE C1'  C2'  C3'  O3'
DIHE C4'  C3'  C2'  O2'
DIHE O3'  C3'  C2'  O2'
DIHE C3'  C2'  O2'  H2''

! SO THE ALLHYDROGEN TERMS
DIHE O4'  C4'  C3'  H3'
DIHE O4'  C1'  C2'  H2'
DIHE C4'  O4'  C1'  H1'
DIHE C1'  O4'  C4'  H4'
DIHE C3'  C4'  C5'  H5'
DIHE C3'  C4'  C5'  H5''

improper H1'  C2'  O4'  N1
improper H2'  C3'  C1'  O2'
improper H3'  C4'  C2'  O3'
improper H4'  C5'  C3'  O4'
improper H5'  O5'  H5''  C4'

IMPR C1'  C5  C2  N1      ! THIS IS AN SP2 IMPROPER ABOUT N1
IMPR N1  C5  C4  N3      IMPR C5  C4  N3  C2      IMPR C4  N3  C2  N1
IMPR N3  C2  N1  C5      IMPR C2  N3  C4  C5
IMPR H2  N3  N1  C2      IMPR H5  N1  C4  C5      IMPR H4  C5  N3  C4

DONO H2'  O2'

ACCE N3      "  "
ACCE O1P  P
ACCE O2P  P
ACCE O2'  "  "
ACCE O3'  "  "
ACCE O4'  "  "
ACCE O5'  "  "

IC  P   O5'  C5'  C4'      1.5996  119.00 -151.39  110.04  1.5160
IC O5'  C5'  C4'  C3'      1.4401  108.83 -179.85  116.10  1.5284
IC C5'  C4'  C3'  O3'      1.5160  116.10   76.70  115.12  1.4212
IC O4'  C3'  *C4'  C5'      1.4572  104.06 -120.04  116.10  1.5160
IC C2'  C4'  *C3'  O3'      1.5284  100.16 -124.08  115.12  1.4212
IC C4'  C3'  C2'  C1'      1.5284  100.16   39.58  102.04  1.5251
IC C3'  C2'  C1'  N1      1.5284  101.97  144.39  113.71  1.4896
IC C3'  C2'  C1'  N1      1.5284  101.97  144.39  113.71  1.4896
IC C1'  C3'  *C2'  O2'      1.5284  102.04 -114.67  110.81  1.4212
IC H2'  O2'  C2'  C3'      0.9600  114.97  148.63  111.92  1.5284

! the all hydrogen part (NOT TOO CAREFULLY DONE /LN)
IC O4'  C2'  *C1'  H1'      0.0      0.0      -115.0  0.0      0.0
IC C1'  C3'  *C2'  H2''      0.0      0.0      115.0  0.0      0.0
IC C2'  C4'  *C3'  H3'      0.0      0.0      115.0  0.0      0.0
IC C3'  O4'  *C4'  H4'      0.0      0.0      -115.0  0.0      0.0

```

```

IC C4' O5' *C5' H5' 0.0 0.0 -115.0 0.0 0.0
IC C4' O5' *C5' H5'' 0.0 0.0 115.0 0.0 0.0

! THE BASE:
IC N1 N3 *C2 H2 0.0 0.0 180.0 0.0 0.0
IC N3 C5 *C4 H4 0.0 0.0 180.0 0.0 0.0
IC C4 C1 *C5 H5 0.0 0.0 180.0 0.0 0.0

END { * IMI *}

RESidue IMI+ !SJ 21/02/08 IMI+
GROUP
ATOM P TYPE=XP CHARGE= 1.20 END
ATOM O1P TYPE=XO2 CHARGE=-0.40 END
ATOM O2P TYPE=XO2 CHARGE=-0.40 END
ATOM O5' TYPE=XOS CHARGE=-0.36 END
GROUP
ATOM C5' TYPE=XC2 CHARGE=-0.07 END
ATOM H5' TYPE=XH CHARGE= 0.035 END
ATOM H5'' TYPE=XH CHARGE= 0.035 END
GROUP
ATOM C4' TYPE=XCH CHARGE= 0.065 END
ATOM H4' TYPE=XH CHARGE= 0.035 END
ATOM O4' TYPE=XOS CHARGE=-0.30 END
ATOM C1' TYPE=XCH CHARGE= 0.165 END
ATOM H1' TYPE=XH CHARGE= 0.035 END
GROUP
ATOM N1 TYPE=XNS+ CHARGE= 0.032 END
ATOM C5 TYPE=XCD2+ CHARGE=-0.003 END
ATOM H5 TYPE=XH CHARGE= 0.127 END
ATOM C2 TYPE=XCL+ CHARGE= 0.079 END
ATOM H2 TYPE=XH CHARGE= 0.145 END
ATOM N3 TYPE=XNB+ CHARGE=-0.028 END
ATOM H3 TYPE=XHN CHARGE= 0.254 END
ATOM C4 TYPE=XCD1+ CHARGE=-0.002 END
ATOM H4 TYPE=XH CHARGE= 0.133 END
GROUP
ATOM C2' TYPE=XCH CHARGE= 0.115 END
ATOM H2' TYPE=XH CHARGE= 0.035 END
ATOM O2' TYPE=XOH CHARGE=-0.40 END
ATOM H2'' TYPE=XHO CHARGE= 0.25 END
GROUP
ATOM C3' TYPE=XCH CHARGE=-0.035 END
ATOM H3' TYPE=XH CHARGE= 0.035 END
GROUP
ATOM O3' TYPE=XOS CHARGE=-0.36 END

BOND P O1P BOND P O2P BOND P O5'
BOND O5' C5' BOND C5' C4' BOND C4' O4' BOND C4' C3' BOND O4' C1'
BOND C1' N1 BOND C1' C2' BOND N1 C5 BOND N1 C2 BOND C5 C4
BOND C4 N3 BOND N3 C2 BOND C2' C3' BOND C3' O3' { *BOND O3' +P* }
BOND C2' O2' BOND O2' H2'
BOND C1' H1' BOND C2' H2'' BOND C3' H3' BOND C4' H4' BOND C5' H5'
BOND C5' H5'' BOND C2 H2 BOND C4 H4 BOND C5 H5 BOND N3 H3

DIHE P O5' C5' C4' DIHE O5' C5' C4' O4' DIHE O5' C5' C4' C3'
DIHE O4' C1' N1 C5

! N O T E: SUGAR RING TERMS SET UP AS W. OLSON DOES IT
DIHE O4' C1' C2' C3' ! O-C-C-C, twofold term
DIHE O4' C1' C2' C3'
DIHE C1' C2' C3' C4'
DIHE C2' C3' C4' O4' ! O-C-C-C, twofold term

```

DIHE C2' C3' C4' O4'  
 DIHE C3' C4' O4' C1'  
 DIHE C4' O4' C1' C2'

! AND THE SPECIAL GAUCHE TERMS

DIHE C5' C4' C3' O3'  
 DIHE O4' C4' C3' O3'  
 DIHE O4' C1' C2' O2'  
 DIHE C1' C2' C3' O3'  
 DIHE C4' C3' C2' O2'  
 DIHE O3' C3' C2' O2'  
 DIHE C3' C2' O2' H2''

! SO THE ALLHYDROGEN TERMS

DIHE O4' C4' C3' H3'  
 DIHE O4' C1' C2' H2'  
 DIHE C4' O4' C1' H1'  
 DIHE C1' O4' C4' H4'  
 DIHE C3' C4' C5' H5'  
 DIHE C3' C4' C5' H5''

improper H1' C2' O4' N1  
 improper H2' C3' C1' O2'  
 improper H3' C4' C2' O3'  
 improper H4' C5' C3' O4'  
 improper H5' O5' H5'' C4'

IMPR C1' C5 C2 N1 ! THIS IS AN SP2 IMPROPER ABOUT N1  
 IMPR N1 C5 C4 N3 IMPR C5 C4 N3 C2 IMPR C4 N3 C2 N1  
 IMPR N3 C2 N1 C5 IMPR C2 N3 C4 C5 IMPR H3 C4 C2 N3  
 IMPR H2 N3 N1 C2 IMPR H5 N1 C4 C5 IMPR H4 C5 N3 C4

DONO H2' O2'

ACCE N3 " "  
 ACCE O1P P  
 ACCE O2P P  
 ACCE O2' " "  
 ACCE O3' " "  
 ACCE O4' " "  
 ACCE O5' " "

IC P	O5'	C5'	C4'	1.5996	119.00	-151.39	110.04	1.5160
IC O5'	C5'	C4'	C3'	1.4401	108.83	-179.85	116.10	1.5284
IC C5'	C4'	C3'	O3'	1.5160	116.10	76.70	115.12	1.4212
IC O4'	C3'	*C4'	C5'	1.4572	104.06	-120.04	116.10	1.5160
IC C2'	C4'	*C3'	O3'	1.5284	100.16	-124.08	115.12	1.4212
IC C4'	C3'	C2'	C1'	1.5284	100.16	39.58	102.04	1.5251
IC C3'	C2'	C1'	N1	1.5284	101.97	144.39	113.71	1.4896
IC C3'	C2'	C1'	N1	1.5284	101.97	144.39	113.71	1.4896
IC C1'	C3'	*C2'	O2'	1.5284	102.04	-114.67	110.81	1.4212
IC H2'	O2'	C2'	C3'	0.9600	114.97	148.63	111.92	1.5284

! the all hydrogen part (NOT TOO CAREFULLY DONE /LN)

IC O4'	C2'	*C1'	H1'	0.0	0.0	-115.0	0.0	0.0
IC C1'	C3'	*C2'	H2''	0.0	0.0	115.0	0.0	0.0
IC C2'	C4'	*C3'	H3'	0.0	0.0	115.0	0.0	0.0
IC C3'	O4'	*C4'	H4'	0.0	0.0	-115.0	0.0	0.0
IC C4'	O5'	*C5'	H5'	0.0	0.0	-115.0	0.0	0.0
IC C4'	O5'	*C5'	H5''	0.0	0.0	115.0	0.0	0.0

! THE BASE:

IC N1	N3	*C2	H2	0.0	0.0	180.0	0.0	0.0
-------	----	-----	----	-----	-----	-------	-----	-----

```

IC N3   C5   *C4   H4       0.0    0.0    180.0  0.0    0.0
IC C4   C1   *C5   H5       0.0    0.0    180.0  0.0    0.0

END { * IMI+ * }!

RESidue AG  !SJ 21/02/08 PAGI
GROUp
  ATOM AG  TYPE=AG      CHARGE=1.0    END

END { * AG * }
```

### Additions in *nucleic.par*

```

bond XNS+  XCH      $kbon    1.475    !SJ 22/02/08 IMI+
bond XNS   XCL      $kbon    1.370    !SJ 22/02/08 IMI
bond XNS+  XCL+     $kbon    1.339    !SJ 22/02/08 IMI+
bond XCL   XNB      $kbon    1.321    !SJ 22/02/08 IMI
bond XCL+  XNB+     $kbon    1.341    !SJ 22/02/08 IMI+
bond XNB   XCD1     $kbon    1.378    !SJ 22/02/08 IMI
bond XNB+  XCD1+    $kbon    1.379    !SJ 22/02/08 IMI+
bond XCD1  XCD2     $kbon    1.377    !SJ 22/02/08 IMI
bond XCD1+ XCD2+    $kbon    1.365    !SJ 22/02/08 IMI+
bond XCD2  XNS      $kbon    1.382    !SJ 22/02/08 IMI
bond XCD2+ XNS+     $kbon    1.385    !SJ 22/02/08 IMI+
bond XCL   XH       $kbon    1.09     !SJ 22/02/08 IMI
bond XCL+  XH       $kbon    1.09     !SJ 22/02/08 IMI+
bond XCD1  XH       $kbon    1.09     !SJ 22/02/08 IMI
bond XCD1+ XH       $kbon    1.09     !SJ 22/02/08 IMI+
bond XCD2  XH       $kbon    1.09     !SJ 22/02/08 IMI
bond XCD2+ XH       $kbon    1.09     !SJ 22/02/08 IMI+
bond XNB+  XHN      $kbon    1.016    !SJ 22/02/08 IMI+
bond XNB   AG       $kbon    2.13     !SJ 26/03/08 PAGI

angle XH    XCD2  XNS      $kang    126.16 !SJ 22/02/08 IMI
angle XH    XCD2+ XNS+     $kang    122.00 !SJ 22/02/08 IMI+
angle XH    XCD2  XCD1     $kang    126.04 !SJ 22/02/08 IMI
angle XH    XCD2+ XCD1+    $kang    130.60 !SJ 22/02/08 IMI+
angle XH    XCD1  XCD2     $kang    127.93 !SJ 22/02/08 IMI
angle XH    XCD1+ XCD2+    $kang    131.12 !SJ 22/02/08 IMI+
angle XH    XCD1  XNB      $kang    121.59 !SJ 22/02/08 IMI
angle XH    XCD1+ XNB+     $kang    122.60 !SJ 22/02/08 IMI+
angle XH    XCL   XNB      $kang    125.80 !SJ 22/02/08 IMI
angle XH    XCL+  XNB+     $kang    126.04 !SJ 22/02/08 IMI+
angle XH    XCL   XNS      $kang    121.95 !SJ 22/02/08 IMI
angle XH    XCL+  XNS+     $kang    126.19 !SJ 22/02/08 IMI+
angle XCH   XNS   XCD2     $kang    126.70 !SJ 22/02/08 IMI
angle XCH   XNS+  XCD2+    $kang    125.33 !SJ 22/02/08 IMI+
angle XCH   XNS   XCL      $kang    126.84 !SJ 22/02/08 IMI
angle XCH   XNS+  XCL+     $kang    125.88 !SJ 22/02/08 IMI+
angle XCD2  XNS   XCL      $kang    106.46 !SJ 22/02/08 IMI
angle XCD2+ XNS+  XCL+     $kang    108.79 !SJ 22/02/08 IMI+
angle XNS   XCD2  XCD1     $kang    105.72 !SJ 22/02/08 IMI
angle XNS+  XCD2+ XCD1+    $kang    107.40 !SJ 22/02/08 IMI+
angle XNS   XCL   XNB      $kang    112.25 !SJ 22/02/08 IMI
angle XNS+  XCL+  XNB+     $kang    107.76 !SJ 22/02/08 IMI+
angle XCD2  XCD1  XNB      $kang    110.48 !SJ 22/02/08 IMI
angle XCD2+ XCD1+ XNB+     $kang    106.27 !SJ 22/02/08 IMI+
angle XCD1  XCD1  XNB      $kang    105.09 !SJ 22/02/08 IMI
angle XCD1+ XNB+  XCL+     $kang    109.78 !SJ 22/02/08 IMI+
angle XHN   XNB+  XCL+     $kang    124.45 !SJ 22/02/08 IMI+
angle XHN   XNB+  XCD1+    $kang    125.77 !SJ 22/02/08 IMI+
```

angle XH	XCH	XNS+	\$kang	109.47	!SJ	22/02/08	IMI+
angle XOS	XCH	XNS+	\$kang	111.00	!SJ	22/02/08	IMI+
angle XC2	XCH	XNS+	\$kang	111.00	!SJ	22/02/08	IMI+
angle XNB	AG	XNB	\$kang	180.00	!SJ	26/03/08	PAGI
angle XCL	XNB	AG	\$kang	127.28	!SJ	26/03/08	PAGI
angle XCD1	XNB	AG	\$kang	126.43	!SJ	26/03/08	PAGI
improper XCD2	XCD1	XNB	XCL	\$kimproper	0	0.0000	!SJ 22/02/08 IMI
improper XCD2+	XCD1+	XNB+	XCL+	\$kimproper	0	0.0000	!SJ 22/02/08 IMI+
improper XCD1	XNB	XCL	XNS	\$kimproper	0	0.0000	!SJ 22/02/08 IMI
improper XCD1+	XNB+	XCL+	XNS+	\$kimproper	0	0.0000	!SJ 22/02/08 IMI+
improper XNB	XCL	XNS	XCD2	\$kimproper	0	0.0000	!SJ 22/02/08 IMI
improper XNB+	XCL+	XNS+	XCD2+	\$kimproper	0	0.0000	!SJ 22/02/08 IMI+
improper XCL	XNB	XCD1	XCD2	\$kimproper	0	0.0000	!SJ 22/02/08 IMI
improper XCL+	XNB+	XCD1+	XCD2+	\$kimproper	0	0.0000	!SJ 22/02/08 IMI+
improper XH	XNB	XNS	XCL	\$kimproper	0	0.0000	!SJ 22/02/08 IMI
improper XH	XNB+	XNS+	XCL+	\$kimproper	0	0.0000	!SJ 22/02/08 IMI+
improper XH	XNS	XCD1	XCD2	\$kimproper	0	0.0000	!SJ 22/02/08 IMI
improper XH	XNS+	XCD1+	XCD2+	\$kimproper	0	0.0000	!SJ 22/02/08 IMI+
improper XH	XCD2	XNB	XCD1	\$kimproper	0	0.0000	!SJ 22/02/08 IMI
improper XH	XCD2+	XNB+	XCD1+	\$kimproper	0	0.0000	!SJ 22/02/08 IMI+
improper XHN	XCD1+	XCL+	XNB+	\$kimproper	0	0.0000	!SJ 20/02/08 IMI+
improper XH	XC2	XOS	XNS+	\$kimproper	0	-65.0000	!SJ 22/02/08 IMI+
improper XCH	X	X	XNS+	\$kimproper	0	0.0000	!SJ 22/02/08 IMI+
improper XNB+	X	X	XNS+	\$kimproper	0	0.0000	!SJ 22/02/08 IMI+
!		eps	sigma	eps(1:4)	sigma(1:4)		
NONBonded XCD1		0.0900	3.2970	0.0900	3.2970	!SJ 22/02/08	IMI
NONBonded XCD1+		0.0900	3.2970	0.0900	3.2970	!SJ 22/02/08	IMI+
NONBonded XCD2		0.0900	3.2970	0.0900	3.2970	!SJ 22/02/08	IMI
NONBonded XCD2+		0.0900	3.2970	0.0900	3.2970	!SJ 22/02/08	IMI+
NONBonded XCL		0.0900	3.2970	0.0900	3.2970	!SJ 22/02/08	IMI
NONBonded XCL+		0.0900	3.2970	0.0900	3.2970	!SJ 22/02/08	IMI+
NONBonded XHN		0.0045	2.6160	0.0900	3.2970	!SJ 22/02/08	IMI+
NONBonded XNB+		0.1600	2.8591	0.1600	2.8591	!SJ 22/02/08	IMI+
NONBonded XNS+		0.1600	2.8591	0.1600	2.8591	!SJ 22/02/08	IMI+
NONBonded AG		0.1600	2.8500	0.1600	2.8500	!SJ 26/03/08	PAGI

**Appendix 10**  $^1\text{H}$ -NMR chemical shift assignments of the oligonucleotide DNA\_IMI in the absence of silver(I) ions at pD 7.2.

	H1'	H2	H2'	H2''	H3'	H4	H4'	H5	H5'	H5''	H6	H7	H8
ppm													
T1	5.94		2.05	2.44	4.64		4.03		3.67	3.67	7.49	1.65	
T2	5.58		2.06	2.37	4.80		4.09		4.02	3.97	7.44	1.72	
A3	5.89	7.01	2.76	2.87	5.00		4.37		4.03	4.09			8.27
A4	6.15	7.58	2.56	2.86	4.95		4.44		4.21	4.23			8.14
T5	5.87		1.96	2.49	4.77		4.14		4.10	4.26	7.11	1.26	
T6	6.07		2.04	2.48	4.82		4.12		4.16	4.04	7.38	1.54	
T7	6.01		2.09	2.23	4.83		4.18		4.12	4.03	7.23	1.53	
Im8	6.16	-	2.41	2.57	4.69	7.36	4.33	7.49	-	4.03			
Im9	5.43	-	1.96	2.10	4.51	6.91	3.69	6.96	3.78	3.69			
Im10	5.57	-	2.09	2.22	4.51	6.82	3.22	7.07	2.89	3.40			
A11	5.83	7.41	2.79	2.94	4.83		4.30		3.94	3.84			8.21
A12	5.84	7.13	2.65	2.82	4.98		4.38		4.14	4.13			8.10
A13	6.13	7.62	2.52	2.84	4.93		4.24		4.08	4.12			8.08
T14	5.82		1.85	2.41	4.76		4.13		4.11	4.27	7.05	1.23	
T15	5.63		1.78	2.20	4.76		4.02		3.99	4.04	7.18	1.55	
A16	5.87	7.28	2.57	2.68	4.93		4.28		4.04	3.98			8.03
A17	6.12	7.64	2.49	2.28	4.60		4.13		4.18	4.06			8.01

**Appendix 11** All distance and dihedral angle restraints for the structure calculation of DNA\_IMI in the absence of Ag<sup>+</sup> ions at pD 7.2.

Distance restraints of non-exchangeable protons based on a 2D [<sup>1</sup>H,<sup>1</sup>H]-NOESY spectrum acquired at 700 MHz frequency at 298 K (100 % D<sub>2</sub>O, 120 mM NaClO<sub>4</sub>). Specified are the estimated distances in Å (left) , as well as the lower (middle) and the upper (right) boundaries.

assi (resi 1 and name H1')	(resi 1 and name H6)	3.80	2.00	0.70
assi (resi 1 and name H1')	(resi 1 and name H51)	6.00	2.00	1.00
assi (resi 1 and name H1')	(resi 2 and name H5")	6.00	2.00	1.00
assi (resi 1 and name H1')	(resi 2 and name H5")	3.80	2.00	0.70
assi (resi 1 and name H1')	(resi 2 and name H6)	3.80	2.00	0.70
assi (resi 1 and name H1')	(resi 2 and name H51)	5.00	2.00	1.00
assi (resi 1 and name H1')	(resi 17 and name H2)	6.00	2.00	1.00
assi (resi 1 and name H2')	(resi 1 and name H2)	6.00	2.00	1.00
assi (resi 1 and name H2')	(resi 1 and name H6)	2.50	0.70	0.50
assi (resi 1 and name H2')	(resi 1 and name H51)	5.00	2.00	1.00
assi (resi 1 and name H2')	(resi 2 and name H5")	6.00	2.00	1.00
assi (resi 1 and name H2')	(resi 2 and name H6)	3.80	2.00	0.70
assi (resi 1 and name H2')	(resi 2 and name H51)	3.80	2.00	0.70
assi (resi 1 and name H2')	(resi 17 and name H2)	6.00	2.00	1.00
assi (resi 1 and name H2")	(resi 1 and name H6)	3.80	2.00	0.70
assi (resi 1 and name H2")	(resi 2 and name H5")	5.00	2.00	1.00
assi (resi 1 and name H2")	(resi 2 and name H6)	3.80	2.00	0.70
assi (resi 1 and name H2")	(resi 2 and name H51)	3.80	2.00	0.70
assi (resi 1 and name H2")	(resi 17 and name H2)	6.00	2.00	1.00
assi (resi 1 and name H3')	(resi 1 and name H6)	5.00	2.00	1.00
assi (resi 1 and name H3')	(resi 2 and name H51)	6.00	2.00	1.00
assi (resi 1 and name H4')	(resi 1 and name H6)	5.00	2.00	1.00
assi (resi 1 and name H4')	(resi 2 and name H1')	6.00	2.00	1.00
assi (resi 1 and name H4')	(resi 2 and name H51)	6.00	2.00	1.00
assi (resi 1 and name H5')	(resi 1 and name H6)	3.80	2.00	0.70
assi (resi 1 and name H5')	(resi 1 and name H51)	6.00	2.00	1.00
assi (resi 1 and name H5')	(resi 2 and name H51)	6.00	2.00	1.00
assi (resi 1 and name H5")	(resi 1 and name H6)	3.80	2.00	0.70
assi (resi 1 and name H5")	(resi 1 and name H51)	6.00	2.00	1.00
assi (resi 1 and name H5")	(resi 2 and name H51)	6.00	2.00	1.00
assi (resi 1 and name H6)	(resi 2 and name H5")	6.00	2.00	1.00
assi (resi 1 and name H6)	(resi 2 and name H51)	3.80	2.00	0.70
assi (resi 1 and name H51)	(resi 2 and name H51)	3.80	2.00	0.70
assi (resi 2 and name H1')	(resi 2 and name H6)	3.80	2.00	0.70
assi (resi 2 and name H1')	(resi 2 and name H51)	6.00	2.00	1.00
assi (resi 2 and name H1')	(resi 3 and name H1')	6.00	2.00	1.00
assi (resi 2 and name H1')	(resi 3 and name H4')	6.00	2.00	1.00
assi (resi 2 and name H1')	(resi 3 and name H5")	5.00	2.00	1.00
assi (resi 2 and name H1')	(resi 3 and name H8)	5.00	2.00	1.00
assi (resi 2 and name H1')	(resi 17 and name H2)	6.00	2.00	1.00
assi (resi 2 and name H2')	(resi 2 and name H6)	2.50	0.70	0.50
assi (resi 2 and name H2')	(resi 2 and name H51)	5.00	2.00	1.00
assi (resi 2 and name H2')	(resi 3 and name H8)	3.80	2.00	0.70

---

assi (resi 2 and name H2')	(resi 17 and name H2)	6.00	2.00	1.00
assi (resi 2 and name H2'')	(resi 2 and name H6)	3.80	2.00	0.70
assi (resi 2 and name H2'')	(resi 2 and name H51)	5.00	2.00	1.00
assi (resi 2 and name H2'')	(resi 3 and name H2')	6.00	2.00	1.00
assi (resi 2 and name H2'')	(resi 3 and name H4')	6.00	2.00	1.00
assi (resi 2 and name H2'')	(resi 3 and name H5'')	5.00	2.00	1.00
assi (resi 2 and name H2'')	(resi 3 and name H8)	3.80	2.00	0.70
assi (resi 2 and name H3')	(resi 2 and name H6)	5.00	2.00	1.00
assi (resi 2 and name H4')	(resi 2 and name H6)	5.00	2.00	1.00
assi (resi 2 and name H5')	(resi 2 and name H6)	5.00	2.00	1.00
assi (resi 2 and name H5'')	(resi 2 and name H6)	3.80	2.00	0.70
assi (resi 2 and name H5'')	(resi 2 and name H51)	6.00	2.00	1.00
assi (resi 2 and name H6)	(resi 3 and name H8)	5.00	2.00	1.00
assi (resi 2 and name H51)	(resi 17 and name H2)	6.00	2.00	1.00
assi (resi 3 and name H1')	(resi 3 and name H2)	5.00	2.00	1.00
assi (resi 3 and name H1')	(resi 3 and name H8)	3.80	2.00	0.70
assi (resi 3 and name H1')	(resi 4 and name H1')	6.00	2.00	1.00
assi (resi 3 and name H1')	(resi 4 and name H4')	6.00	2.00	1.00
assi (resi 3 and name H1')	(resi 4 and name H5'')	5.00	2.00	1.00
assi (resi 3 and name H1')	(resi 4 and name H8)	3.80	2.00	0.70
assi (resi 3 and name H1')	(resi 16 and name H2)	6.00	2.00	1.00
assi (resi 3 and name H2')	(resi 3 and name H8)	2.50	0.70	0.50
assi (resi 3 and name H2')	(resi 4 and name H5'')	6.00	2.00	1.00
assi (resi 3 and name H2')	(resi 4 and name H8)	3.80	2.00	0.70
assi (resi 3 and name H2'')	(resi 3 and name H8)	3.80	2.00	0.70
assi (resi 3 and name H2'')	(resi 4 and name H5'')	5.00	2.00	1.00
assi (resi 3 and name H2'')	(resi 4 and name H8)	3.80	2.00	0.70
assi (resi 3 and name H3')	(resi 3 and name H8)	3.80	2.00	0.70
assi (resi 3 and name H3')	(resi 4 and name H8)	5.00	2.00	1.00
assi (resi 3 and name H4')	(resi 3 and name H8)	5.00	2.00	1.00
assi (resi 3 and name H4')	(resi 4 and name H8)	6.00	2.00	1.00
assi (resi 3 and name H5')	(resi 3 and name H8)	5.00	2.00	1.00
assi (resi 3 and name H5'')	(resi 3 and name H8)	5.00	2.00	1.00
assi (resi 3 and name H5'')	(resi 4 and name H8)	6.00	2.00	1.00
assi (resi 3 and name H2)	(resi 4 and name H1')	6.00	2.00	1.00
assi (resi 3 and name H2)	(resi 4 and name H2)	3.80	2.00	0.70
assi (resi 3 and name H2)	(resi 16 and name H1')	6.00	2.00	1.00
assi (resi 3 and name H2)	(resi 16 and name H2)	3.80	2.00	0.70
assi (resi 3 and name H2)	(resi 16 and name H8)	5.00	2.00	1.00
assi (resi 3 and name H8)	(resi 4 and name H8)	3.80	2.00	0.70
assi (resi 4 and name H1')	(resi 4 and name H2)	5.00	2.00	1.00
assi (resi 4 and name H1')	(resi 4 and name H8)	3.80	2.00	0.70
assi (resi 4 and name H1')	(resi 5 and name H1')	5.00	2.00	1.00
assi (resi 4 and name H1')	(resi 5 and name H4')	6.00	2.00	1.00
assi (resi 4 and name H1')	(resi 5 and name H5'')	5.00	2.00	1.00
assi (resi 4 and name H1')	(resi 5 and name H6)	3.80	2.00	0.70
assi (resi 4 and name H1')	(resi 5 and name H51)	5.00	2.00	1.00
assi (resi 4 and name H2')	(resi 4 and name H8)	2.50	0.70	0.50
assi (resi 4 and name H2')	(resi 5 and name H6)	3.80	2.00	0.70



assi (resi 4 and name H2')	(resi 5 and name H51)	3.80	2.00	0.70
assi (resi 4 and name H2'')	(resi 4 and name H8)	3.80	2.00	0.70
assi (resi 4 and name H2'')	(resi 5 and name H2')	6.00	2.00	1.00
assi (resi 4 and name H2'')	(resi 5 and name H5'')	5.00	2.00	1.00
assi (resi 4 and name H2'')	(resi 5 and name H6)	2.50	0.70	0.50
assi (resi 4 and name H2'')	(resi 5 and name H51)	3.80	2.00	0.70
assi (resi 4 and name H2'')	(resi 6 and name H51)	6.00	2.00	1.00
assi (resi 4 and name H3')	(resi 4 and name H8)	3.80	2.00	0.70
assi (resi 4 and name H3')	(resi 5 and name H6)	3.80	2.00	0.70
assi (resi 4 and name H3')	(resi 5 and name H51)	3.80	2.00	0.70
assi (resi 4 and name H4')	(resi 4 and name H8)	6.00	2.00	1.00
assi (resi 4 and name H5')	(resi 4 and name H8)	5.00	2.00	1.00
assi (resi 4 and name H5'')	(resi 4 and name H8)	5.00	2.00	1.00
assi (resi 4 and name H2)	(resi 5 and name H1')	5.00	2.00	1.00
assi (resi 4 and name H2)	(resi 15 and name H1')	5.00	2.00	1.00
assi (resi 4 and name H8)	(resi 5 and name H6)	5.00	2.00	1.00
assi (resi 4 and name H8)	(resi 5 and name H51)	3.80	2.00	0.70
assi (resi 5 and name H1')	(resi 5 and name H6)	3.80	2.00	0.70
assi (resi 5 and name H1')	(resi 5 and name H51)	6.00	2.00	1.00
assi (resi 5 and name H1')	(resi 6 and name H1')	6.00	2.00	1.00
assi (resi 5 and name H1')	(resi 6 and name H5'')	5.00	2.00	1.00
assi (resi 5 and name H1')	(resi 6 and name H6)	3.80	2.00	0.70
assi (resi 5 and name H1')	(resi 6 and name H51)	5.00	2.00	1.00
assi (resi 5 and name H2')	(resi 5 and name H6)	2.50	0.70	0.50
assi (resi 5 and name H2')	(resi 5 and name H51)	5.00	2.00	1.00
assi (resi 5 and name H2')	(resi 6 and name H6)	3.80	2.00	0.70
assi (resi 5 and name H2')	(resi 6 and name H51)	3.80	2.00	0.70
assi (resi 5 and name H2'')	(resi 5 and name H6)	3.80	2.00	0.70
assi (resi 5 and name H2'')	(resi 5 and name H6)	6.00	2.00	1.00
assi (resi 5 and name H2'')	(resi 6 and name H5'')	5.00	2.00	1.00
assi (resi 5 and name H2'')	(resi 6 and name H6)	3.80	2.00	0.70
assi (resi 5 and name H2'')	(resi 6 and name H51)	3.80	2.00	0.70
assi (resi 5 and name H3')	(resi 5 and name H6)	5.00	2.00	1.00
assi (resi 5 and name H3')	(resi 6 and name H51)	6.00	2.00	1.00
assi (resi 5 and name H4')	(resi 5 and name H6)	5.00	2.00	1.00
assi (resi 5 and name H4')	(resi 6 and name H51)	6.00	2.00	1.00
assi (resi 5 and name H5')	(resi 5 and name H6)	5.00	2.00	1.00
assi (resi 5 and name H5'')	(resi 5 and name H6)	5.00	2.00	1.00
assi (resi 5 and name H6)	(resi 6 and name H6)	5.00	2.00	1.00
assi (resi 5 and name H6)	(resi 6 and name H51)	3.80	2.00	0.70
assi (resi 5 and name H51)	(resi 6 and name H51)	3.80	2.00	0.70
assi (resi 5 and name H51)	(resi 6 and name H6)	6.00	2.00	1.00
assi (resi 6 and name H1')	(resi 6 and name H6)	3.80	2.00	0.70
assi (resi 6 and name H1')	(resi 6 and name H51)	5.00	2.00	1.00
assi (resi 6 and name H1')	(resi 7 and name H4')	6.00	2.00	1.00
assi (resi 6 and name H1')	(resi 7 and name H5'')	5.00	2.00	1.00
assi (resi 6 and name H1')	(resi 7 and name H6)	3.80	2.00	0.70
assi (resi 6 and name H1')	(resi 7 and name H51)	5.00	2.00	1.00
assi (resi 6 and name H1')	(resi 13 and name H2)	5.00	2.00	1.00

assi (resi 6 and name H2')	(resi 6 and name H6)	2.50	0.70	0.50
assi (resi 6 and name H2')	(resi 6 and name H51)	5.00	2.00	1.00
assi (resi 6 and name H1')	(resi 7 and name H5")	5.00	2.00	1.00
assi (resi 6 and name H2')	(resi 7 and name H6)	3.80	2.00	0.70
assi (resi 6 and name H2')	(resi 7 and name H51)	3.80	2.00	0.70
assi (resi 6 and name H2")	(resi 6 and name H6)	3.80	2.00	0.70
assi (resi 6 and name H2")	(resi 6 and name H51)	5.00	2.00	1.00
assi (resi 6 and name H2")	(resi 7 and name H5")	5.00	2.00	1.00
assi (resi 6 and name H2")	(resi 7 and name H6)	3.80	2.00	0.70
assi (resi 6 and name H2")	(resi 7 and name H51)	3.80	2.00	0.70
assi (resi 6 and name H3')	(resi 6 and name H6)	3.80	2.00	0.70
assi (resi 6 and name H3')	(resi 7 and name H51)	5.00	2.00	1.00
assi (resi 6 and name H4')	(resi 6 and name H6)	5.00	2.00	1.00
assi (resi 6 and name H4')	(resi 6 and name H51)	6.00	2.00	1.00
assi (resi 6 and name H4')	(resi 7 and name H51)	6.00	2.00	1.00
assi (resi 6 and name H5')	(resi 6 and name H6)	5.00	2.00	1.00
assi (resi 6 and name H5')	(resi 6 and name H51)	6.00	2.00	1.00
assi (resi 6 and name H5")	(resi 6 and name H6)	5.00	2.00	1.00
assi (resi 6 and name H5")	(resi 6 and name H51)	6.00	2.00	1.00
assi (resi 6 and name H6)	(resi 7 and name H6)	5.00	2.00	1.00
assi (resi 6 and name H6)	(resi 7 and name H51)	3.80	2.00	0.70
assi (resi 7 and name H1')	(resi 7 and name H6)	3.80	2.00	0.70
assi (resi 7 and name H1')	(resi 7 and name H51)	6.00	2.00	1.00
assi (resi 7 and name H1')	(resi 8 and name H2')	5.00	2.00	1.00
assi (resi 7 and name H1')	(resi 8 and name H2")	5.00	2.00	1.00
assi (resi 7 and name H1')	(resi 9 and name H4')	6.00	2.00	1.00
assi (resi 7 and name H1')	(resi 9 and name H5")	6.00	2.00	1.00
assi (resi 7 and name H1')	(resi 12 and name H2)	5.00	2.00	1.00
assi (resi 7 and name H2')	(resi 7 and name H6)	2.50	0.70	0.50
assi (resi 7 and name H2')	(resi 7 and name H51)	5.00	2.00	1.00
assi (resi 7 and name H2")	(resi 7 and name H6)	3.80	2.00	0.70
assi (resi 7 and name H2")	(resi 7 and name H51)	5.00	2.00	1.00
assi (resi 7 and name H3')	(resi 7 and name H6)	3.80	2.00	0.70
assi (resi 7 and name H4')	(resi 7 and name H6)	5.00	2.00	1.00
assi (resi 7 and name H5')	(resi 7 and name H6)	5.00	2.00	1.00
assi (resi 7 and name H5')	(resi 7 and name H51)	6.00	2.00	1.00
assi (resi 7 and name H5")	(resi 7 and name H6)	5.00	2.00	1.00
assi (resi 7 and name H5")	(resi 7 and name H51)	6.00	2.00	1.00
assi (resi 8 and name H1')	(resi 8 and name H2)	5.00	2.00	1.00
assi (resi 8 and name H1')	(resi 8 and name H5)	3.80	2.00	1.00
assi (resi 8 and name H1')	(resi 9 and name H4')	6.00	2.00	1.00
assi (resi 8 and name H1')	(resi 9 and name H5')	6.00	2.00	1.00
assi (resi 8 and name H1')	(resi 9 and name H5")	5.00	2.00	1.00
assi (resi 8 and name H2')	(resi 8 and name H5)	5.00	2.00	1.00
assi (resi 8 and name H2')	(resi 9 and name H5")	5.00	2.00	1.00
assi (resi 8 and name H2")	(resi 8 and name H5)	5.00	2.00	1.00
assi (resi 8 and name H2")	(resi 9 and name H4')	6.00	2.00	1.00
assi (resi 8 and name H2")	(resi 9 and name H5')	6.00	2.00	1.00
assi (resi 8 and name H2")	(resi 9 and name H5")	5.00	2.00	1.00

assi (resi 9 and name H1')	(resi 9 and name H2)	5.00	2.00	1.00
assi (resi 9 and name H1')	(resi 9 and name H5)	3.80	2.00	1.00
assi (resi 9 and name H1')	(resi 10 and name H5')	6.00	2.00	1.00
assi (resi 9 and name H1')	(resi 11 and name H2)	6.00	2.00	1.00
assi (resi 9 and name H2')	(resi 9 and name H5)	5.00	2.00	1.00
assi (resi 9 and name H2'')	(resi 9 and name H5)	5.00	2.00	1.00
assi (resi 9 and name H2'')	(resi 10 and name H5')	6.00	2.00	1.00
assi (resi 9 and name H2'')	(resi 10 and name H5'')	6.00	2.00	1.00
assi (resi 9 and name H4')	(resi 10 and name H5')	6.00	2.00	1.00
assi (resi 9 and name H4')	(resi 10 and name H5'')	6.00	2.00	1.00
assi (resi 9 and name H4')	(resi 11 and name H2)	5.00	2.00	1.00
assi (resi 9 and name H4')	(resi 11 and name H8)	6.00	2.00	1.00
assi (resi 9 and name H5')	(resi 11 and name H2)	5.00	2.00	1.00
assi (resi 9 and name H5'')	(resi 11 and name H2)	3.80	2.00	0.70
assi (resi 10 and name H1')	(resi 10 and name H2)	5.00	2.00	1.00
assi (resi 10 and name H1')	(resi 10 and name H5)	3.80	2.00	1.00
assi (resi 10 and name H1')	(resi 11 and name H8)	6.00	2.00	1.00
assi (resi 10 and name H2')	(resi 10 and name H5)	5.00	2.00	1.00
assi (resi 10 and name H2'')	(resi 10 and name H5)	5.00	2.00	1.00
assi (resi 10 and name H4')	(resi 11 and name H4')	6.00	2.00	1.00
assi (resi 10 and name H4')	(resi 11 and name H5')	6.00	2.00	1.00
assi (resi 10 and name H4')	(resi 11 and name H5'')	5.00	2.00	1.00
assi (resi 10 and name H4')	(resi 11 and name H8)	5.00	2.00	1.00
assi (resi 11 and name H1')	(resi 11 and name H2)	5.00	2.00	1.00
assi (resi 11 and name H1')	(resi 11 and name H8)	3.80	2.00	0.70
assi (resi 11 and name H1')	(resi 12 and name H5'')	5.00	2.00	1.00
assi (resi 11 and name H1')	(resi 12 and name H8)	3.80	2.00	0.70
assi (resi 11 and name H2')	(resi 11 and name H8)	3.80	2.00	0.70
assi (resi 11 and name H2')	(resi 12 and name H5'')	5.00	2.00	1.00
assi (resi 11 and name H2')	(resi 12 and name H8)	3.80	2.00	0.70
assi (resi 11 and name H2'')	(resi 11 and name H8)	3.80	2.00	0.70
assi (resi 11 and name H2'')	(resi 12 and name H2')	6.00	2.00	1.00
assi (resi 11 and name H2'')	(resi 12 and name H5'')	5.00	2.00	1.00
assi (resi 11 and name H2'')	(resi 12 and name H8)	3.80	2.00	0.70
assi (resi 11 and name H3')	(resi 11 and name H8)	5.00	2.00	1.00
assi (resi 11 and name H3')	(resi 12 and name H8)	6.00	2.00	1.00
assi (resi 11 and name H4')	(resi 11 and name H8)	5.00	2.00	1.00
assi (resi 11 and name H5')	(resi 11 and name H8)	5.00	2.00	1.00
assi (resi 11 and name H5'')	(resi 11 and name H8)	3.80	2.00	0.70
assi (resi 11 and name H2)	(resi 12 and name H2)	3.80	2.00	0.70
assi (resi 11 and name H8)	(resi 12 and name H8)	5.00	2.00	1.00
assi (resi 12 and name H1')	(resi 12 and name H2)	5.00	2.00	1.00
assi (resi 12 and name H1')	(resi 12 and name H8)	3.80	2.00	0.70
assi (resi 12 and name H1')	(resi 13 and name H1')	6.00	2.00	1.00
assi (resi 12 and name H1')	(resi 13 and name H5'')	5.00	2.00	1.00
assi (resi 12 and name H1')	(resi 13 and name H8)	3.80	2.00	0.70
assi (resi 12 and name H2')	(resi 12 and name H8)	2.50	0.70	0.50

assi (resi 12 and name H2')	(resi 13 and name H5")	5.00	2.00	1.00
assi (resi 12 and name H2')	(resi 13 and name H8)	3.80	2.00	0.70
assi (resi 12 and name H2")	(resi 12 and name H8)	3.80	2.00	0.70
assi (resi 12 and name H2")	(resi 13 and name H5")	5.00	2.00	1.00
assi (resi 12 and name H2")	(resi 13 and name H8)	3.80	2.00	0.70
assi (resi 12 and name H3')	(resi 12 and name H8)	3.80	2.00	0.70
assi (resi 12 and name H3')	(resi 13 and name H8)	5.00	2.00	1.00
assi (resi 12 and name H4')	(resi 12 and name H8)	5.00	2.00	1.00
assi (resi 12 and name H4')	(resi 13 and name H8)	6.00	2.00	1.00
assi (resi 12 and name H5')	(resi 12 and name H8)	5.00	2.00	1.00
assi (resi 12 and name H5")	(resi 12 and name H8)	5.00	2.00	1.00
assi (resi 12 and name H2)	(resi 13 and name H1')	5.00	2.00	1.00
assi (resi 12 and name H2)	(resi 13 and name H2)	3.80	2.00	0.70
assi (resi 13 and name H1')	(resi 13 and name H2)	5.00	2.00	1.00
assi (resi 13 and name H1')	(resi 13 and name H8)	3.80	2.00	0.70
assi (resi 13 and name H1')	(resi 14 and name H5")	5.00	2.00	1.00
assi (resi 13 and name H1')	(resi 14 and name H6)	3.80	2.00	0.70
assi (resi 13 and name H1')	(resi 14 and name H51)	5.00	2.00	1.00
assi (resi 13 and name H2')	(resi 13 and name H8)	2.50	0.70	0.50
assi (resi 13 and name H2')	(resi 14 and name H5")	5.00	2.00	1.00
assi (resi 13 and name H2')	(resi 14 and name H6)	3.80	2.00	0.70
assi (resi 13 and name H2')	(resi 14 and name H51)	3.80	2.00	0.70
assi (resi 13 and name H2")	(resi 13 and name H8)	3.80	2.00	0.70
assi (resi 13 and name H2")	(resi 14 and name H2')	6.00	2.00	1.00
assi (resi 13 and name H2")	(resi 14 and name H5")	5.00	2.00	1.00
assi (resi 13 and name H2")	(resi 14 and name H6)	2.50	0.70	0.50
assi (resi 13 and name H2")	(resi 14 and name H51)	3.80	2.00	0.70
assi (resi 13 and name H2")	(resi 15 and name H51)	6.00	2.00	1.00
assi (resi 13 and name H3')	(resi 13 and name H8)	3.80	2.00	0.70
assi (resi 13 and name H3')	(resi 14 and name H6)	5.00	2.00	1.00
assi (resi 13 and name H3')	(resi 14 and name H51)	5.00	2.00	1.00
assi (resi 13 and name H4')	(resi 13 and name H8)	5.00	2.00	1.00
assi (resi 13 and name H5')	(resi 13 and name H8)	5.00	2.00	1.00
assi (resi 13 and name H5")	(resi 13 and name H8)	5.00	2.00	1.00
assi (resi 13 and name H2)	(resi 14 and name H1')	5.00	2.00	1.00
assi (resi 13 and name H8)	(resi 14 and name H6)	5.00	2.00	1.00
assi (resi 13 and name H8)	(resi 14 and name H51)	3.80	2.00	0.70
assi (resi 14 and name H1')	(resi 14 and name H6)	3.80	2.00	0.70
assi (resi 14 and name H1')	(resi 14 and name H51)	6.00	2.00	1.00
assi (resi 14 and name H1')	(resi 15 and name H1')	6.00	2.00	1.00
assi (resi 14 and name H1')	(resi 15 and name H5')	5.00	2.00	1.00
assi (resi 14 and name H1')	(resi 15 and name H5")	5.00	2.00	1.00
assi (resi 14 and name H1')	(resi 15 and name H6)	3.80	2.00	0.70
assi (resi 14 and name H1')	(resi 15 and name H51)	5.00	2.00	1.00
assi (resi 14 and name H2')	(resi 14 and name H6)	2.50	0.70	0.50
assi (resi 14 and name H2')	(resi 14 and name H51)	5.00	2.00	1.00
assi (resi 14 and name H2')	(resi 15 and name H5")	5.00	2.00	1.00
assi (resi 14 and name H2')	(resi 15 and name H6)	3.80	2.00	0.70
assi (resi 14 and name H2')	(resi 15 and name H51)	3.80	2.00	0.70

assi (resi 14 and name H2")	(resi 14 and name H6)	3.80	2.00	0.70
assi (resi 14 and name H2")	(resi 14 and name H51)	6.00	2.00	1.00
assi (resi 14 and name H2")	(resi 15 and name H2')	6.00	2.00	1.00
assi (resi 14 and name H2")	(resi 15 and name H5")	5.00	2.00	1.00
assi (resi 14 and name H2")	(resi 15 and name H6)	3.80	2.00	0.70
assi (resi 14 and name H2")	(resi 15 and name H51)	3.80	2.00	0.70
assi (resi 14 and name H3')	(resi 14 and name H6)	5.00	2.00	1.00
assi (resi 14 and name H3')	(resi 15 and name H51)	6.00	2.00	1.00
assi (resi 14 and name H4')	(resi 14 and name H6)	5.00	2.00	1.00
assi (resi 14 and name H5')	(resi 14 and name H6)	5.00	2.00	1.00
assi (resi 14 and name H5")	(resi 14 and name H6)	5.00	2.00	1.00
assi (resi 14 and name H6)	(resi 15 and name H6)	5.00	2.00	1.00
assi (resi 14 and name H6)	(resi 15 and name H51)	3.80	2.00	0.70
assi (resi 14 and name H51)	(resi 15 and name H6)	6.00	2.00	1.00
assi (resi 14 and name H51)	(resi 15 and name H51)	3.80	2.00	0.70
assi (resi 15 and name H1')	(resi 15 and name H6)	3.80	2.00	0.70
assi (resi 15 and name H1')	(resi 15 and name H51)	6.00	2.00	1.00
assi (resi 15 and name H1')	(resi 16 and name H1')	6.00	2.00	1.00
assi (resi 15 and name H1')	(resi 16 and name H4')	6.00	2.00	1.00
assi (resi 15 and name H1')	(resi 16 and name H5")	5.00	2.00	1.00
assi (resi 15 and name H1')	(resi 16 and name H8)	5.00	2.00	1.00
assi (resi 15 and name H2')	(resi 15 and name H6)	2.50	0.70	0.50
assi (resi 15 and name H2')	(resi 15 and name H51)	3.80	2.00	0.70
assi (resi 15 and name H2')	(resi 16 and name H5")	5.00	2.00	1.00
assi (resi 15 and name H2')	(resi 16 and name H8)	3.80	2.00	0.70
assi (resi 15 and name H2")	(resi 15 and name H6)	3.80	2.00	0.70
assi (resi 15 and name H2")	(resi 15 and name H51)	6.00	2.00	1.00
assi (resi 15 and name H2")	(resi 16 and name H4')	6.00	2.00	1.00
assi (resi 15 and name H2")	(resi 16 and name H5")	5.00	2.00	1.00
assi (resi 15 and name H2")	(resi 16 and name H8)	3.80	2.00	0.70
assi (resi 15 and name H3')	(resi 15 and name H6)	5.00	2.00	1.00
assi (resi 15 and name H3')	(resi 15 and name H51)	6.00	2.00	1.00
assi (resi 15 and name H4')	(resi 15 and name H6)	5.00	2.00	1.00
assi (resi 15 and name H4')	(resi 15 and name H51)	6.00	2.00	1.00
assi (resi 15 and name H5')	(resi 15 and name H6)	5.00	2.00	1.00
assi (resi 15 and name H5")	(resi 15 and name H6)	5.00	2.00	1.00
assi (resi 15 and name H6)	(resi 16 and name H8)	5.00	2.00	1.00
assi (resi 16 and name H1')	(resi 16 and name H2)	5.00	2.00	1.00
assi (resi 16 and name H1')	(resi 16 and name H8)	3.80	2.00	0.70
assi (resi 16 and name H1')	(resi 17 and name H1')	6.00	2.00	1.00
assi (resi 16 and name H1')	(resi 17 and name H4')	6.00	2.00	1.00
assi (resi 16 and name H1')	(resi 17 and name H5')	6.00	2.00	1.00
assi (resi 16 and name H1')	(resi 17 and name H5")	5.00	2.00	1.00
assi (resi 16 and name H1')	(resi 17 and name H8)	3.80	2.00	0.70
assi (resi 16 and name H2')	(resi 16 and name H8)	2.50	0.70	0.50
assi (resi 16 and name H2')	(resi 17 and name H5')	6.00	2.00	1.00
assi (resi 16 and name H2')	(resi 17 and name H5")	5.00	2.00	1.00
assi (resi 16 and name H2')	(resi 17 and name H2)	6.00	2.00	1.00
assi (resi 16 and name H2')	(resi 17 and name H8)	3.80	2.00	0.70

assi (resi 16 and name H2")	(resi 16 and name H8)	3.80	2.00	0.70
assi (resi 16 and name H2")	(resi 17 and name H5')	5.00	2.00	1.00
assi (resi 16 and name H2")	(resi 17 and name H5")	5.00	2.00	1.00
assi (resi 16 and name H2')	(resi 17 and name H2)	6.00	2.00	1.00
assi (resi 16 and name H2")	(resi 17 and name H8)	3.80	2.00	0.70
assi (resi 16 and name H3')	(resi 16 and name H8)	3.80	2.00	0.70
assi (resi 16 and name H3')	(resi 17 and name H8)	5.00	2.00	1.00
assi (resi 16 and name H4')	(resi 16 and name H8)	5.00	2.00	1.00
assi (resi 16 and name H5')	(resi 16 and name H8)	5.00	2.00	1.00
assi (resi 16 and name H5")	(resi 16 and name H8)	5.00	2.00	1.00
assi (resi 16 and name H2)	(resi 17 and name H1')	5.00	2.00	1.00
assi (resi 16 and name H2)	(resi 17 and name H2)	3.80	2.00	0.70
assi (resi 17 and name H1')	(resi 17 and name H2)	5.00	2.00	1.00
assi (resi 17 and name H1')	(resi 17 and name H8)	3.80	2.00	0.70
assi (resi 17 and name H2')	(resi 17 and name H8)	2.50	0.70	0.50
assi (resi 17 and name H2")	(resi 17 and name H8)	3.80	2.00	0.70
assi (resi 17 and name H3')	(resi 17 and name H8)	5.00	2.00	1.00
assi (resi 17 and name H4')	(resi 17 and name H8)	5.00	2.00	1.00
assi (resi 17 and name H5')	(resi 17 and name H8)	5.00	2.00	1.00
assi (resi 17 and name H5")	(resi 17 and name H8)	5.00	2.00	1.00

H-bond restraints verified by 13 interstrand correlations (mainly between adenine-H2 and H1' on the opposite strand).

assi (resi 1 and name H3)	(resi 17 and name N1)	1.90	0.30	0.30
assi (resi 1 and name N3)	(resi 17 and name N1)	2.90	0.30	0.30
assi (resi 1 and name O4)	(resi 17 and name H61)	1.90	0.30	0.30
assi (resi 1 and name O4)	(resi 17 and name N6)	2.90	0.30	0.30
assi (resi 2 and name H3)	(resi 16 and name N1)	1.90	0.10	0.10
assi (resi 2 and name N3)	(resi 16 and name N1)	2.90	0.10	0.10
assi (resi 2 and name O4)	(resi 16 and name H61)	1.90	0.10	0.10
assi (resi 2 and name O4)	(resi 16 and name N6)	2.90	0.10	0.10
assi (resi 3 and name N1)	(resi 15 and name H3)	1.90	0.10	0.10
assi (resi 3 and name N1)	(resi 15 and name N3)	2.90	0.10	0.10
assi (resi 3 and name H61)	(resi 15 and name O4)	1.90	0.10	0.10
assi (resi 3 and name N6)	(resi 15 and name O4)	2.90	0.10	0.10
assi (resi 4 and name N1)	(resi 14 and name H3)	1.90	0.10	0.10
assi (resi 4 and name N1)	(resi 14 and name N3)	2.90	0.10	0.10
assi (resi 4 and name H61)	(resi 14 and name O4)	1.90	0.10	0.10
assi (resi 4 and name N6)	(resi 14 and name O4)	2.90	0.10	0.10
assi (resi 5 and name H3)	(resi 13 and name N1)	1.90	0.10	0.10
assi (resi 5 and name N3)	(resi 13 and name N1)	2.90	0.10	0.10
assi (resi 5 and name O4)	(resi 13 and name H61)	1.90	0.10	0.10
assi (resi 5 and name O4)	(resi 13 and name N6)	2.90	0.10	0.10

assi (resi 6 and name H3)	(resi 12 and name N1)	1.90	0.10	0.10
assi (resi 6 and name N3)	(resi 12 and name N1)	2.90	0.10	0.10
assi (resi 6 and name O4)	(resi 12 and name H61)	1.90	0.10	0.10
assi (resi 6 and name O4)	(resi 12 and name N6)	2.90	0.10	0.10
assi (resi 7 and name H3)	(resi 11 and name N1)	1.90	0.30	0.30
assi (resi 7 and name N3)	(resi 11 and name N1)	2.90	0.30	0.30
assi (resi 7 and name O4)	(resi 11 and name H61)	1.90	0.30	0.30
assi (resi 7 and name O4)	(resi 11 and name N6)	2.90	0.30	0.30

Phosphate-sugar-backbone dihedral restraints based on a 1D [ $^{31}\text{P}$ ]-NMR spectrum acquired at 400 MHz frequency at 298 K (100 %  $\text{D}_2\text{O}$ , 120 mM  $\text{NaClO}_4$ ) and cover the B-DNA range. Exact values were taken from the dihedral angle restraint files of the pdb entries 1RVI and 1RVH, which represent a B-DNA duplex.<sup>[260]</sup> Error boundaries of  $\pm 30^\circ$  were used for residues T1, T7, A11, A17 and  $\pm 20^\circ$  for residues T2, A3, A4, T5, T6, A12, A13, T14, T15, A16, respectively. Im8, Im9 and Im10 were left unrestrained.

assign	( resid n-1 and name O3')	( resid n and name P)	( resid n and name O5')	( resid n and name C5')	-60	{* $\alpha$ *}
assign	( resid n and name P)	( resid n and name O5')	( resid n and name C5')	( resid n and name C4')	180	{* $\beta$ *}
assign	( resid n and name O5')	( resid n and name C5')	( resid n and name C4')	( resid n and name C3')	60	{* $\gamma$ *}
assign	( resid n and name C3')	( resid n and name O3')	( resid n+1 and name P)	( resid n+1 and name O5')	-90	{* $\zeta$ *}

Sugar pucker restraints based on a [ $^1\text{H}$ ,  $^1\text{H}$ ]-TOCSY spectrum acquired at 700 MHz frequency at 298 K (100 %  $\text{D}_2\text{O}$ , 120 mM  $\text{NaClO}_4$ ). Helical B-type DNA is usually 2'-endo and gives strong H1'-H2' and H1'-H3' crosspeak in TOCSY experiment. Exact values were taken from the dihedral angle restraint file of the pdb entries 1RVI und 1RVH, which represent a B-DNA duplex.<sup>[260]</sup> Error boundaries of  $\pm 30^\circ$  were used for residues T1, T7, Im9, Im10 A11, A17 and  $\pm 20^\circ$  for residues T2, A3, A4, T5, T6, A12, A13, T14, T15, A16, respectively. Im8 was left unrestrained.

assign	( resid n and name C4')	( resid n and name O4')	( resid n and name C1')	( resid n and name C2')	-20	{* $\nu_0$ *}
--------	-------------------------	-------------------------	-------------------------	-------------------------	-----	---------------

assign	( resid n	and name O4')		
	( resid n	and name C1')		
	( resid n	and name C2')		
	( resid n	and name C3')	33	{* v <sub>1</sub> *}
assign	( resid n	and name C1')		
	( resid n	and name C2')		
	( resid n	and name C3')		
	( resid n	and name C4')	-22	{* v <sub>2</sub> *}
assign	( resid n	and name C2')		
	( resid n	and name C3')		
	( resid n	and name C4')		
	( resid n	and name O4')	4	{* v <sub>3</sub> *}
assign	( resid n	and name C3')		
	( resid n	and name C4')		
	( resid n	and name O4')		
	( resid n	and name C1')	16	{* v <sub>4</sub> *}

The torsion angle  $\chi$  defines the orientation of the base to the sugar around the glycosidic bond.  $\chi$  was restrained to *anti* orientation for all residues, with error boundaries of  $\pm 30^\circ$  for residues T1, T7, A11, A17 and  $\pm 20^\circ$  for residues T2, A3, A4, T5, T6, A12, A13, T14, T15, A16, respectively. Im8, Im9 and Im10 were left unrestrained.

assign	( resid n	and name O4')		
	( resid n	and name C1')		
	( resid n	and name N9)		
	( resid n	and name C4)	-120	{* $\chi$ of purines*}
assign	( resid n	and name O4')		
	( resid n	and name C1')		
	( resid n	and name N1)		
	( resid n	and name C4)	-120	{* $\chi$ of pyrimidines*}



**Appendix 12** [<sup>1</sup>H]-NMR chemical shift assignments of the oligonucleotide DNA\_IM1 in the absence of silver(I) ions at pD 4.7.

	H1'	H2	H2'	H2''	H3'	H4	H4'	H5	H5'	H5''	H6	H7	H8
	ppm												
T1	5.93		2.04	2.42	4.63		4.02		3.66	3.66	7.47	1.63	
T2	5.54		2.03	2.33	4.78		4.08		4.01	3.95	7.43	1.71	
A3	5.88	7.04	2.76	2.88	5.00		4.36		4.02	4.08			8.26
A4	6.15	7.59	2.57	2.86	4.95		4.43		4.20	4.22			8.15
T5	5.86		1.98	2.49	4.76		4.13		4.09	4.25	7.11	1.26	
T6	6.07		2.08	2.50	4.81		4.14		4.15	4.04	7.39	1.52	
T7	5.97		2.09	2.19	4.84		4.20		4.14	4.04	7.28	1.47	
Im8	6.35	8.96	2.59	2.74	-	7.67	4.43	7.75	4.11	4.13			
Im9	5.78	8.70	2.18	2.38	4.63	7.40	3.65	7.45	3.88	3.76			
Im10	5.77	8.58	2.13	2.41	4.55	7.31	3.56	7.35	2.84	3.35			
A11	5.87	7.45	2.79	2.93	4.82		4.29		3.96	3.83			8.18
A12	5.87	7.12	2.65	2.82	4.98		4.38		4.14	4.13			8.09
A13	6.12	7.60	2.51	2.84	4.92		4.25		4.06	4.13			8.06
T14	5.83		1.86	2.41	4.76		4.14		4.11	4.27	7.05	1.21	
T15	5.65		1.80	2.20	4.77		4.02		3.99	4.00	7.18	1.80	
A16	5.89	7.37	2.58	2.65	4.92		4.24		4.02	3.96			8.04
A17	6.14	7.72	2.52	2.31	4.61		4.13		4.17	4.07			8.06

**Appendix 13** All distance and dihedral angle restraints for the structure calculation of DNA\_IMI in the absence of Ag<sup>+</sup> ions at pD 4.7.

Distance restraints of non-exchangeable protons based on a 2D [<sup>1</sup>H,<sup>1</sup>H]-NOESY spectrum acquired at 700 MHz frequency at 298 K (100 % D<sub>2</sub>O, 120 mM NaClO<sub>4</sub>). Specified are the estimated distances in Å (left) , as well as the lower (middle) and the upper (right) boundaries.

assi (resi 1 and name H1')	(resi 1 and name H6)	3.80	2.00	0.70
assi (resi 1 and name H1')	(resi 1 and name H51)	6.00	2.00	1.00
assi (resi 1 and name H1')	(resi 2 and name H4')	6.00	2.00	1.00
assi (resi 1 and name H1')	(resi 2 and name H5'')	3.80	2.00	0.70
assi (resi 1 and name H1')	(resi 2 and name H6)	3.80	2.00	0.70
assi (resi 1 and name H1')	(resi 2 and name H51)	5.00	2.00	1.00
assi (resi 1 and name H1')	(resi 17 and name H2)	6.00	2.00	1.00
assi (resi 1 and name H2')	(resi 1 and name H6)	2.50	0.70	0.50
assi (resi 1 and name H2')	(resi 1 and name H51)	5.00	2.00	1.00
assi (resi 1 and name H2')	(resi 2 and name H5'')	6.00	2.00	1.00
assi (resi 1 and name H2')	(resi 2 and name H6)	3.80	2.00	0.70
assi (resi 1 and name H2')	(resi 2 and name H51)	3.80	2.00	0.70
assi (resi 1 and name H2')	(resi 17 and name H2)	6.00	2.00	1.00
assi (resi 1 and name H2'')	(resi 1 and name H6)	3.80	2.00	0.70
assi (resi 1 and name H2'')	(resi 2 and name H5'')	5.00	2.00	1.00
assi (resi 1 and name H2'')	(resi 2 and name H6)	3.80	2.00	0.70
assi (resi 1 and name H2'')	(resi 2 and name H51)	3.80	2.00	0.70
assi (resi 1 and name H2'')	(resi 17 and name H2)	6.00	2.00	1.00
assi (resi 1 and name H3')	(resi 1 and name H6)	5.00	2.00	1.00
assi (resi 1 and name H3')	(resi 2 and name H51)	6.00	2.00	1.00
assi (resi 1 and name H4')	(resi 1 and name H6)	5.00	2.00	1.00
assi (resi 1 and name H4')	(resi 2 and name H1')	6.00	2.00	1.00
assi (resi 1 and name H4')	(resi 2 and name H51)	6.00	2.00	1.00
assi (resi 1 and name H5')	(resi 1 and name H6)	3.80	2.00	0.70
assi (resi 1 and name H5')	(resi 1 and name H51)	6.00	2.00	1.00
assi (resi 1 and name H5')	(resi 2 and name H51)	6.00	2.00	1.00
assi (resi 1 and name H5'')	(resi 1 and name H6)	3.80	2.00	0.70
assi (resi 1 and name H5'')	(resi 1 and name H51)	6.00	2.00	1.00
assi (resi 1 and name H5'')	(resi 2 and name H51)	6.00	2.00	1.00
assi (resi 1 and name H6)	(resi 2 and name H5'')	6.00	2.00	1.00
assi (resi 1 and name H6)	(resi 2 and name H51)	3.80	2.00	0.70
assi (resi 1 and name H51)	(resi 2 and name H51)	3.80	2.00	0.70
assi (resi 2 and name H1')	(resi 2 and name H6)	3.80	2.00	0.70
assi (resi 2 and name H1')	(resi 2 and name H51)	6.00	2.00	1.00
assi (resi 2 and name H1')	(resi 3 and name H1')	6.00	2.00	1.00
assi (resi 2 and name H1')	(resi 3 and name H4')	6.00	2.00	1.00
assi (resi 2 and name H1')	(resi 3 and name H5'')	5.00	2.00	1.00
assi (resi 2 and name H1')	(resi 3 and name H8)	5.00	2.00	1.00
assi (resi 2 and name H1')	(resi 17 and name H2)	6.00	2.00	1.00
assi (resi 2 and name H2')	(resi 2 and name H6)	2.50	0.70	0.50
assi (resi 2 and name H2')	(resi 2 and name H51)	5.00	2.00	1.00
assi (resi 2 and name H2')	(resi 3 and name H8)	3.80	2.00	0.70
assi (resi 2 and name H2'')	(resi 2 and name H6)	3.80	2.00	0.70

assi (resi 2 and name H2")	(resi 2 and name H51)	5.00	2.00	1.00
assi (resi 2 and name H2")	(resi 3 and name H2')	6.00	2.00	1.00
assi (resi 2 and name H2")	(resi 3 and name H4')	6.00	2.00	1.00
assi (resi 2 and name H2")	(resi 3 and name H5")	5.00	2.00	1.00
assi (resi 2 and name H2")	(resi 3 and name H8)	3.80	2.00	0.70
assi (resi 2 and name H3')	(resi 2 and name H6)	5.00	2.00	1.00
assi (resi 2 and name H4')	(resi 2 and name H6)	5.00	2.00	1.00
assi (resi 2 and name H5')	(resi 2 and name H6)	5.00	2.00	1.00
assi (resi 2 and name H5")	(resi 2 and name H6)	3.80	2.00	0.70
assi (resi 2 and name H5")	(resi 2 and name H51)	6.00	2.00	1.00
assi (resi 2 and name H5")	(resi 3 and name H8)	6.00	2.00	1.00
assi (resi 2 and name H6)	(resi 3 and name H8)	5.00	2.00	1.00
assi (resi 2 and name H51)	(resi 17 and name H2)	6.00	2.00	1.00
assi (resi 3 and name H1')	(resi 3 and name H2)	5.00	2.00	1.00
assi (resi 3 and name H1')	(resi 3 and name H8)	3.80	2.00	0.70
assi (resi 3 and name H1')	(resi 4 and name H1')	6.00	2.00	1.00
assi (resi 3 and name H1')	(resi 4 and name H4')	6.00	2.00	1.00
assi (resi 3 and name H1')	(resi 4 and name H5")	5.00	2.00	1.00
assi (resi 3 and name H1')	(resi 4 and name H8)	3.80	2.00	0.70
assi (resi 3 and name H1')	(resi 16 and name H2)	6.00	2.00	1.00
assi (resi 3 and name H2')	(resi 3 and name H8)	2.50	0.70	0.50
assi (resi 3 and name H2')	(resi 4 and name H5")	6.00	2.00	1.00
assi (resi 3 and name H2')	(resi 4 and name H8)	3.80	2.00	0.70
assi (resi 3 and name H2")	(resi 3 and name H8)	3.80	2.00	0.70
assi (resi 3 and name H2")	(resi 4 and name H5")	5.00	1.00	0.70
assi (resi 3 and name H2")	(resi 4 and name H8)	3.80	2.00	0.70
assi (resi 3 and name H3')	(resi 3 and name H8)	3.80	2.00	0.70
assi (resi 3 and name H3')	(resi 4 and name H8)	5.00	2.00	1.00
assi (resi 3 and name H4')	(resi 3 and name H8)	5.00	2.00	1.00
assi (resi 3 and name H4')	(resi 4 and name H8)	6.00	2.00	1.00
assi (resi 3 and name H5')	(resi 3 and name H8)	5.00	2.00	1.00
assi (resi 3 and name H5")	(resi 3 and name H8)	5.00	2.00	1.00
assi (resi 3 and name H5")	(resi 4 and name H8)	6.00	2.00	1.00
assi (resi 3 and name H2)	(resi 4 and name H1')	6.00	2.00	1.00
assi (resi 3 and name H2)	(resi 4 and name H2)	3.80	2.00	0.70
assi (resi 3 and name H2)	(resi 16 and name H1')	6.00	2.00	1.00
assi (resi 3 and name H2)	(resi 16 and name H2)	3.80	2.00	0.70
assi (resi 3 and name H2)	(resi 16 and name H8)	5.00	2.00	1.00
assi (resi 3 and name H8)	(resi 4 and name H8)	3.80	2.00	0.70
assi (resi 4 and name H1')	(resi 4 and name H2)	5.00	2.00	1.00
assi (resi 4 and name H1')	(resi 4 and name H8)	3.80	2.00	0.70
assi (resi 4 and name H1')	(resi 5 and name H1')	5.00	2.00	1.00
assi (resi 4 and name H1')	(resi 5 and name H4')	6.00	2.00	1.00
assi (resi 4 and name H1')	(resi 5 and name H5")	5.00	2.00	1.00
assi (resi 4 and name H1')	(resi 5 and name H6)	3.80	2.00	0.70
assi (resi 4 and name H1')	(resi 5 and name H51)	5.00	2.00	1.00
assi (resi 4 and name H2')	(resi 4 and name H8)	2.50	0.70	0.50
assi (resi 4 and name H2')	(resi 5 and name H6)	3.80	2.00	0.70
assi (resi 4 and name H2')	(resi 5 and name H51)	3.80	2.00	0.70

assi (resi 4 and name H2")	(resi 4 and name H8)	3.80	2.00	0.70
assi (resi 4 and name H2")	(resi 5 and name H2')	6.00	2.00	1.00
assi (resi 4 and name H2")	(resi 5 and name H5")	5.00	2.00	1.00
assi (resi 4 and name H2")	(resi 5 and name H6)	2.50	0.70	0.50
assi (resi 4 and name H2")	(resi 5 and name H51)	3.80	2.00	0.70
assi (resi 4 and name H2")	(resi 6 and name H51)	6.00	2.00	1.00
assi (resi 4 and name H3')	(resi 4 and name H8)	3.80	2.00	0.70
assi (resi 4 and name H3')	(resi 5 and name H6)	3.80	2.00	0.70
assi (resi 4 and name H3')	(resi 5 and name H51)	3.80	2.00	0.70
assi (resi 4 and name H4')	(resi 4 and name H8)	5.00	2.00	1.00
assi (resi 4 and name H4')	(resi 5 and name H6)	6.00	2.00	1.00
assi (resi 4 and name H4')	(resi 5 and name H51)	6.00	2.00	1.00
assi (resi 4 and name H5')	(resi 4 and name H8)	5.00	2.00	1.00
assi (resi 4 and name H5")	(resi 4 and name H8)	5.00	2.00	1.00
assi (resi 4 and name H2)	(resi 5 and name H1')	5.00	2.00	1.00
assi (resi 4 and name H2)	(resi 15 and name H1')	5.00	2.00	1.00
assi (resi 4 and name H8)	(resi 5 and name H6)	5.00	2.00	1.00
assi (resi 4 and name H8)	(resi 5 and name H51)	3.80	2.00	0.70
assi (resi 5 and name H1')	(resi 5 and name H6)	3.80	2.00	0.70
assi (resi 5 and name H1')	(resi 5 and name H51)	6.00	2.00	1.00
assi (resi 5 and name H1')	(resi 6 and name H1')	6.00	2.00	1.00
assi (resi 5 and name H1')	(resi 6 and name H5")	5.00	2.00	1.00
assi (resi 5 and name H1')	(resi 6 and name H6)	3.80	2.00	0.70
assi (resi 5 and name H1')	(resi 6 and name H51)	5.00	2.00	1.00
assi (resi 5 and name H2')	(resi 5 and name H6)	2.50	0.70	0.50
assi (resi 5 and name H2')	(resi 5 and name H51)	5.00	2.00	1.00
assi (resi 5 and name H2')	(resi 6 and name H6)	3.80	2.00	0.70
assi (resi 5 and name H2')	(resi 6 and name H51)	3.80	2.00	0.70
assi (resi 5 and name H2")	(resi 5 and name H6)	3.80	2.00	0.70
assi (resi 5 and name H2")	(resi 5 and name H51)	6.00	2.00	1.00
assi (resi 5 and name H2")	(resi 6 and name H5")	5.00	2.00	1.00
assi (resi 5 and name H2")	(resi 6 and name H6)	3.80	2.00	0.70
assi (resi 5 and name H2")	(resi 6 and name H51)	3.80	2.00	0.70
assi (resi 5 and name H3')	(resi 5 and name H6)	5.00	2.00	1.00
assi (resi 5 and name H3')	(resi 6 and name H51)	6.00	2.00	1.00
assi (resi 5 and name H4')	(resi 5 and name H6)	5.00	2.00	1.00
assi (resi 5 and name H4')	(resi 6 and name H51)	6.00	2.00	1.00
assi (resi 5 and name H5')	(resi 5 and name H6)	5.00	2.00	1.00
assi (resi 5 and name H5")	(resi 5 and name H6)	5.00	2.00	1.00
assi (resi 5 and name H6)	(resi 6 and name H6)	5.00	2.00	1.00
assi (resi 5 and name H6)	(resi 6 and name H51)	3.80	2.00	0.70
assi (resi 5 and name H51)	(resi 6 and name H51)	3.80	2.00	0.70
assi (resi 5 and name H51)	(resi 6 and name H6)	6.00	2.00	1.00
assi (resi 6 and name H1')	(resi 6 and name H6)	3.80	2.00	0.70
assi (resi 6 and name H1')	(resi 6 and name H51)	5.00	2.00	1.00
assi (resi 6 and name H1')	(resi 7 and name H4')	6.00	2.00	1.00
assi (resi 6 and name H1')	(resi 7 and name H5")	5.00	2.00	1.00
assi (resi 6 and name H1')	(resi 7 and name H6)	3.80	2.00	0.70
assi (resi 6 and name H1')	(resi 7 and name H51)	5.00	2.00	1.00

assi (resi 6 and name H1')	(resi 13 and name H2)	5.00	2.00	1.00
assi (resi 6 and name H2')	(resi 6 and name H6)	2.50	0.70	0.50
assi (resi 6 and name H2')	(resi 6 and name H51)	5.00	2.00	1.00
assi (resi 6 and name H2')	(resi 7 and name H5'')	5.00	2.00	1.00
assi (resi 6 and name H2')	(resi 7 and name H6)	3.80	2.00	0.70
assi (resi 6 and name H2')	(resi 7 and name H51)	3.80	2.00	0.70
assi (resi 6 and name H2'')	(resi 6 and name H6)	3.80	2.00	0.70
assi (resi 6 and name H2'')	(resi 6 and name H51)	5.00	2.00	1.00
assi (resi 6 and name H2'')	(resi 7 and name H5'')	5.00	2.00	1.00
assi (resi 6 and name H2'')	(resi 7 and name H6)	3.80	2.00	0.70
assi (resi 6 and name H2'')	(resi 7 and name H51)	3.80	2.00	0.70
assi (resi 6 and name H3')	(resi 6 and name H6)	3.80	2.00	0.70
assi (resi 6 and name H3')	(resi 7 and name H51)	5.00	2.00	1.00
assi (resi 6 and name H4')	(resi 6 and name H6)	5.00	2.00	1.00
assi (resi 6 and name H4')	(resi 6 and name H51)	6.00	2.00	1.00
assi (resi 6 and name H4')	(resi 7 and name H51)	6.00	2.00	1.00
assi (resi 6 and name H5')	(resi 6 and name H6)	5.00	2.00	1.00
assi (resi 6 and name H5')	(resi 6 and name H51)	6.00	2.00	1.00
assi (resi 6 and name H5'')	(resi 6 and name H6)	5.00	2.00	1.00
assi (resi 6 and name H5'')	(resi 6 and name H51)	6.00	2.00	1.00
assi (resi 6 and name H6)	(resi 7 and name H6)	5.00	2.00	1.00
assi (resi 6 and name H6)	(resi 7 and name H51)	3.80	2.00	0.70
assi (resi 7 and name H1')	(resi 7 and name H6)	3.80	2.00	0.70
assi (resi 7 and name H1')	(resi 7 and name H51)	6.00	2.00	1.00
assi (resi 7 and name H1')	(resi 8 and name H2')	5.00	2.00	1.00
assi (resi 7 and name H1')	(resi 8 and name H2'')	5.00	2.00	1.00
assi (resi 7 and name H1')	(resi 8 and name H2)	5.00	2.00	1.00
assi (resi 7 and name H1')	(resi 8 and name H4)	5.00	2.00	1.00
assi (resi 7 and name H1')	(resi 8 and name H5)	5.00	2.00	1.00
assi (resi 7 and name H1')	(resi 9 and name H4')	6.00	2.00	1.00
assi (resi 7 and name H1')	(resi 9 and name H5')	5.00	2.00	1.00
assi (resi 7 and name H1')	(resi 9 and name H5'')	5.00	2.00	1.00
assi (resi 7 and name H1')	(resi 9 and name H4)	5.00	2.00	1.00
assi (resi 7 and name H1')	(resi 9 and name H5)	5.00	2.00	1.00
assi (resi 7 and name H1')	(resi 11 and name H2)	6.00	2.00	1.00
assi (resi 7 and name H1')	(resi 12 and name H2)	5.00	2.00	1.00
assi (resi 7 and name H2')	(resi 7 and name H6)	2.50	0.70	0.50
assi (resi 7 and name H2')	(resi 7 and name H51)	5.00	2.00	1.00
assi (resi 7 and name H2')	(resi 8 and name H2')	6.00	2.00	1.00
assi (resi 7 and name H2')	(resi 8 and name H5'')	5.00	2.00	1.00
assi (resi 7 and name H2'')	(resi 7 and name H6)	3.80	2.00	0.70
assi (resi 7 and name H2'')	(resi 7 and name H51)	5.00	2.00	1.00
assi (resi 7 and name H2'')	(resi 8 and name H2')	5.00	2.00	1.00
assi (resi 7 and name H2'')	(resi 8 and name H5'')	5.00	2.00	1.00
assi (resi 7 and name H2'')	(resi 8 and name H5)	6.00	2.00	1.00
assi (resi 7 and name H3')	(resi 7 and name H6)	3.80	2.00	0.70
assi (resi 7 and name H4')	(resi 7 and name H6)	5.00	2.00	1.00
assi (resi 7 and name H4')	(resi 8 and name H4)	5.00	2.00	1.00
assi (resi 7 and name H4')	(resi 8 and name H5)	5.00	2.00	1.00
assi (resi 7 and name H5')	(resi 7 and name H6)	5.00	2.00	1.00

---

assi (resi 7 and name H5')	(resi 7 and name H51)	6.00	2.00	1.00
assi (resi 7 and name H5')	(resi 8 and name H4)	6.00	2.00	1.00
assi (resi 7 and name H5')	(resi 8 and name H5)	6.00	2.00	1.00
assi (resi 7 and name H5'')	(resi 7 and name H6)	5.00	2.00	1.00
assi (resi 7 and name H5'')	(resi 7 and name H51)	6.00	2.00	1.00
assi (resi 7 and name H5'')	(resi 8 and name H4)	6.00	2.00	1.00
assi (resi 7 and name H51)	(resi 9 and name H1')	3.80	2.00	0.70
assi (resi 7 and name H51)	(resi 9 and name H2)	3.80	2.00	0.70
assi (resi 7 and name H51)	(resi 9 and name H5)	5.00	2.00	1.00
assi (resi 8 and name H1')	(resi 8 and name H2)	3.80	2.00	0.70
assi (resi 8 and name H1')	(resi 8 and name H4)	6.00	2.00	1.00
assi (resi 8 and name H1')	(resi 8 and name H5)	3.80	2.00	0.70
assi (resi 8 and name H1')	(resi 9 and name H5'')	6.00	2.00	1.00
assi (resi 8 and name H1')	(resi 9 and name H5)	6.00	2.00	1.00
assi (resi 8 and name H2')	(resi 8 and name H2)	5.00	2.00	1.00
assi (resi 8 and name H2')	(resi 8 and name H5)	2.50	0.70	0.50
assi (resi 8 and name H2')	(resi 9 and name H4')	6.00	2.00	1.00
assi (resi 8 and name H2')	(resi 9 and name H5')	5.00	2.00	1.00
assi (resi 8 and name H2')	(resi 9 and name H5'')	5.00	2.00	1.00
assi (resi 8 and name H2')	(resi 9 and name H5)	5.00	2.00	1.00
assi (resi 8 and name H2'')	(resi 8 and name H2)	6.00	2.00	1.00
assi (resi 8 and name H2'')	(resi 8 and name H5)	3.80	2.00	0.70
assi (resi 8 and name H2'')	(resi 9 and name H2')	6.00	2.00	1.00
assi (resi 8 and name H2'')	(resi 9 and name H4')	6.00	2.00	1.00
assi (resi 8 and name H2'')	(resi 9 and name H5')	5.00	2.00	1.00
assi (resi 8 and name H2'')	(resi 9 and name H5'')	3.80	2.00	0.70
assi (resi 8 and name H2'')	(resi 9 and name H5)	5.00	2.00	1.00
assi (resi 8 and name H4')	(resi 8 and name H2)	6.00	2.00	1.00
assi (resi 8 and name H5')	(resi 8 and name H4)	6.00	2.00	1.00
assi (resi 8 and name H5')	(resi 8 and name H5)	5.00	2.00	1.00
assi (resi 8 and name H5'')	(resi 8 and name H2)	5.00	2.00	1.00
assi (resi 8 and name H5')	(resi 8 and name H4)	5.00	2.00	1.00
assi (resi 8 and name H5')	(resi 8 and name H5)	6.00	2.00	1.00
assi (resi 8 and name H2)	(resi 9 and name H5)	6.00	2.00	1.00
assi (resi 8 and name H4)	(resi 12 and name H1')	5.00	2.00	1.00
assi (resi 8 and name H4)	(resi 12 and name H2)	5.00	2.00	1.00
assi (resi 8 and name H5)	(resi 9 and name H5)	5.00	2.00	1.00
assi (resi 8 and name H5)	(resi 12 and name H2)	6.00	2.00	1.00
assi (resi 9 and name H1')	(resi 9 and name H2)	3.80	2.00	0.70
assi (resi 9 and name H1')	(resi 9 and name H4)	6.00	2.00	1.00
assi (resi 9 and name H1')	(resi 9 and name H5)	3.80	2.00	0.70
assi (resi 9 and name H2')	(resi 9 and name H2)	3.80	2.00	0.70
assi (resi 9 and name H2')	(resi 9 and name H4)	5.00	2.00	1.00
assi (resi 9 and name H2')	(resi 9 and name H5)	3.80	2.00	0.70
assi (resi 9 and name H2'')	(resi 9 and name H2)	5.00	2.00	1.00
assi (resi 9 and name H2'')	(resi 9 and name H5)	3.80	2.00	0.70
assi (resi 9 and name H4')	(resi 9 and name H2)	6.00	2.00	1.00
assi (resi 9 and name H4')	(resi 10 and name H5')	5.00	2.00	1.00
assi (resi 9 and name H4')	(resi 10 and name H5'')	5.00	2.00	1.00

---

assi (resi 9 and name H4')	(resi 10 and name H2)	6.00 2.00 1.00
assi (resi 9 and name H4')	(resi 10 and name H5)	6.00 2.00 1.00
assi (resi 9 and name H4')	(resi 11 and name H1')	6.00 2.00 1.00
assi (resi 9 and name H4')	(resi 11 and name H2)	3.80 2.00 0.70
assi (resi 9 and name H4')	(resi 11 and name H8)	6.00 2.00 1.00
assi (resi 9 and name H5')	(resi 9 and name H2)	6.00 2.00 1.00
assi (resi 9 and name H5')	(resi 10 and name H5")	6.00 2.00 1.00
assi (resi 9 and name H5')	(resi 11 and name H2)	3.80 2.00 0.70
assi (resi 9 and name H5")	(resi 9 and name H2)	6.00 2.00 1.00
assi (resi 9 and name H5")	(resi 10 and name H5")	6.00 2.00 1.00
assi (resi 9 and name H5")	(resi 11 and name H2)	3.80 2.00 0.70
assi (resi 9 and name H2)	(resi 10 and name H4)	5.00 2.00 1.00
assi (resi 10 and name H1')	(resi 10 and name H2)	3.80 2.00 0.70
assi (resi 10 and name H1')	(resi 10 and name H4)	5.00 2.00 1.00
assi (resi 10 and name H1')	(resi 10 and name H5)	3.80 2.00 0.70
assi (resi 10 and name H1')	(resi 11 and name H8)	5.00 2.00 1.00
assi (resi 10 and name H2')	(resi 10 and name H2)	5.00 2.00 1.00
assi (resi 10 and name H2')	(resi 10 and name H5)	3.80 2.00 0.70
assi (resi 10 and name H2")	(resi 10 and name H2)	5.00 2.00 1.00
assi (resi 10 and name H2")	(resi 10 and name H5)	3.80 2.00 0.70
assi (resi 10 and name H4')	(resi 11 and name H1')	5.00 2.00 1.00
assi (resi 10 and name H4')	(resi 11 and name H4')	5.00 2.00 1.00
assi (resi 10 and name H4')	(resi 11 and name H5')	5.00 2.00 1.00
assi (resi 10 and name H4')	(resi 11 and name H5")	5.00 2.00 1.00
assi (resi 10 and name H4')	(resi 11 and name H8)	5.00 2.00 1.00
assi (resi 10 and name H5')	(resi 10 and name H2)	6.00 2.00 1.00
assi (resi 10 and name H5')	(resi 10 and name H5)	5.00 2.00 1.00
assi (resi 10 and name H5')	(resi 11 and name H2)	5.00 2.00 1.00
assi (resi 10 and name H5")	(resi 10 and name H2)	6.00 2.00 1.00
assi (resi 10 and name H5")	(resi 10 and name H5)	6.00 2.00 1.00
assi (resi 10 and name H5")	(resi 11 and name H1')	6.00 2.00 1.00
assi (resi 10 and name H5")	(resi 11 and name H4')	6.00 2.00 1.00
assi (resi 10 and name H5")	(resi 11 and name H5')	6.00 2.00 1.00
assi (resi 10 and name H5")	(resi 11 and name H5")	6.00 2.00 1.00
assi (resi 10 and name H5")	(resi 11 and name H8)	6.00 2.00 1.00
assi (resi 11 and name H1')	(resi 11 and name H2)	5.00 2.00 1.00
assi (resi 11 and name H1')	(resi 11 and name H8)	3.80 2.00 0.70
assi (resi 11 and name H1')	(resi 12 and name H5")	5.00 2.00 1.00
assi (resi 11 and name H1')	(resi 12 and name H8)	3.80 2.00 0.70
assi (resi 11 and name H2')	(resi 11 and name H8)	3.80 2.00 0.40
assi (resi 11 and name H2')	(resi 12 and name H5")	5.00 2.00 1.00
assi (resi 11 and name H2')	(resi 12 and name H8)	3.80 2.00 0.70
assi (resi 11 and name H2")	(resi 11 and name H8)	3.80 2.00 0.70
assi (resi 11 and name H2")	(resi 12 and name H2')	6.00 2.00 1.00
assi (resi 11 and name H2")	(resi 12 and name H5")	5.00 2.00 1.00
assi (resi 11 and name H2")	(resi 12 and name H8)	3.80 2.00 0.70
assi (resi 11 and name H3')	(resi 11 and name H8)	5.00 2.00 1.00
assi (resi 11 and name H3')	(resi 12 and name H8)	6.00 2.00 1.00
assi (resi 11 and name H4')	(resi 11 and name H8)	5.00 2.00 1.00

---

assi (resi 11 and name H5')	(resi 11 and name H8)	5.00	2.00	1.00
assi (resi 11 and name H5'')	(resi 11 and name H8)	3.80	2.00	0.70
assi (resi 11 and name H2)	(resi 12 and name H2)	3.80	2.00	0.70
assi (resi 11 and name H8)	(resi 12 and name H8)	5.00	2.00	1.00
assi (resi 12 and name H1')	(resi 12 and name H2)	5.00	2.00	1.00
assi (resi 12 and name H1')	(resi 12 and name H8)	3.80	2.00	0.70
assi (resi 12 and name H1')	(resi 13 and name H1')	6.00	2.00	1.00
assi (resi 12 and name H1')	(resi 13 and name H5'')	5.00	2.00	1.00
assi (resi 12 and name H1')	(resi 13 and name H8)	3.80	2.00	0.70
assi (resi 12 and name H2')	(resi 12 and name H8)	2.50	0.70	0.50
assi (resi 12 and name H2')	(resi 13 and name H5'')	5.00	2.00	1.00
assi (resi 12 and name H2')	(resi 13 and name H8)	3.80	2.00	0.70
assi (resi 12 and name H2'')	(resi 12 and name H8)	3.80	2.00	0.70
assi (resi 12 and name H2'')	(resi 13 and name H5'')	5.00	2.00	1.00
assi (resi 12 and name H2'')	(resi 13 and name H8)	3.80	2.00	0.70
assi (resi 12 and name H3')	(resi 12 and name H8)	3.80	2.00	0.70
assi (resi 12 and name H3')	(resi 13 and name H8)	5.00	2.00	1.00
assi (resi 12 and name H4')	(resi 12 and name H8)	5.00	2.00	1.00
assi (resi 12 and name H4')	(resi 13 and name H8)	6.00	2.00	1.00
assi (resi 12 and name H5')	(resi 12 and name H8)	5.00	2.00	1.00
assi (resi 12 and name H5'')	(resi 12 and name H8)	5.00	2.00	1.00
assi (resi 12 and name H2)	(resi 13 and name H1')	5.00	2.00	1.00
assi (resi 12 and name H2)	(resi 13 and name H2)	3.80	2.00	0.70
assi (resi 13 and name H1')	(resi 13 and name H2)	5.00	2.00	1.00
assi (resi 13 and name H1')	(resi 13 and name H8)	3.80	2.00	0.70
assi (resi 13 and name H1')	(resi 14 and name H5'')	5.00	2.00	1.00
assi (resi 13 and name H1')	(resi 14 and name H6)	3.80	2.00	0.70
assi (resi 13 and name H1')	(resi 14 and name H51)	5.00	2.00	1.00
assi (resi 13 and name H2')	(resi 13 and name H8)	2.50	0.70	0.50
assi (resi 13 and name H2')	(resi 14 and name H5'')	5.00	2.00	1.00
assi (resi 13 and name H2')	(resi 14 and name H6)	3.80	2.00	0.70
assi (resi 13 and name H2')	(resi 14 and name H51)	3.80	2.00	0.70
assi (resi 13 and name H2'')	(resi 13 and name H8)	3.80	2.00	0.70
assi (resi 13 and name H2'')	(resi 14 and name H2')	6.00	2.00	1.00
assi (resi 13 and name H2'')	(resi 14 and name H5'')	5.00	2.00	1.00
assi (resi 13 and name H2'')	(resi 14 and name H6)	2.50	0.70	0.50
assi (resi 13 and name H2'')	(resi 14 and name H51)	3.80	2.00	0.70
assi (resi 13 and name H2'')	(resi 15 and name H51)	6.00	2.00	1.00
assi (resi 13 and name H3')	(resi 13 and name H8)	3.80	2.00	0.70
assi (resi 13 and name H3')	(resi 14 and name H6)	5.00	2.00	1.00
assi (resi 13 and name H3')	(resi 14 and name H51)	5.00	2.00	1.00
assi (resi 13 and name H4')	(resi 13 and name H8)	5.00	2.00	1.00
assi (resi 13 and name H5')	(resi 13 and name H8)	5.00	2.00	1.00
assi (resi 13 and name H5'')	(resi 13 and name H8)	5.00	2.00	1.00
assi (resi 13 and name H2)	(resi 14 and name H1')	5.00	2.00	1.00
assi (resi 13 and name H8)	(resi 14 and name H6)	5.00	2.00	1.00
assi (resi 13 and name H8)	(resi 14 and name H51)	3.80	2.00	0.70
assi (resi 14 and name H1')	(resi 14 and name H6)	3.80	2.00	0.70



---

assi (resi 14 and name H1')	(resi 14 and name H51)	6.00	2.00	1.00
assi (resi 14 and name H1')	(resi 15 and name H1')	6.00	2.00	1.00
assi (resi 14 and name H1')	(resi 15 and name H5')	5.00	2.00	1.00
assi (resi 14 and name H1')	(resi 15 and name H5'')	5.00	2.00	1.00
assi (resi 14 and name H1')	(resi 15 and name H6)	3.80	2.00	0.70
assi (resi 14 and name H1')	(resi 15 and name H51)	5.00	2.00	1.00
assi (resi 14 and name H2')	(resi 14 and name H6)	2.50	0.70	0.50
assi (resi 14 and name H2')	(resi 14 and name H51)	5.00	2.00	1.00
assi (resi 14 and name H2')	(resi 15 and name H5'')	5.00	2.00	1.00
assi (resi 14 and name H2')	(resi 15 and name H6)	3.80	2.00	0.70
assi (resi 14 and name H2')	(resi 15 and name H51)	3.80	2.00	0.70
assi (resi 14 and name H2'')	(resi 14 and name H6)	3.80	2.00	0.70
assi (resi 14 and name H2'')	(resi 14 and name H51)	6.00	2.00	1.00
assi (resi 14 and name H2'')	(resi 15 and name H2')	6.00	2.00	1.00
assi (resi 14 and name H2'')	(resi 15 and name H5'')	5.00	2.00	1.00
assi (resi 14 and name H2'')	(resi 15 and name H6)	3.80	2.00	0.70
assi (resi 14 and name H2'')	(resi 15 and name H51)	3.80	2.00	0.70
assi (resi 14 and name H3')	(resi 14 and name H6)	5.00	2.00	1.00
assi (resi 14 and name H3')	(resi 15 and name H51)	6.00	2.00	1.00
assi (resi 14 and name H4')	(resi 14 and name H6)	5.00	2.00	1.00
assi (resi 14 and name H4')	(resi 15 and name H6)	6.00	2.00	1.00
assi (resi 14 and name H5')	(resi 14 and name H6)	5.00	2.00	1.00
assi (resi 14 and name H5'')	(resi 14 and name H6)	5.00	2.00	1.00
assi (resi 14 and name H6)	(resi 15 and name H6)	5.00	2.00	1.00
assi (resi 14 and name H6)	(resi 15 and name H51)	3.80	2.00	0.70
assi (resi 14 and name H51)	(resi 15 and name H6)	6.00	2.00	1.00
assi (resi 14 and name H51)	(resi 15 and name H51)	3.80	2.00	0.70
assi (resi 15 and name H1')	(resi 15 and name H6)	3.80	2.00	0.70
assi (resi 15 and name H1')	(resi 15 and name H51)	6.00	2.00	1.00
assi (resi 15 and name H1')	(resi 16 and name H1')	6.00	2.00	1.00
assi (resi 15 and name H1')	(resi 16 and name H4')	6.00	2.00	1.00
assi (resi 15 and name H1')	(resi 16 and name H5'')	5.00	2.00	1.00
assi (resi 15 and name H1')	(resi 16 and name H8)	5.00	2.00	1.00
assi (resi 15 and name H2')	(resi 15 and name H6)	2.50	0.70	0.50
assi (resi 15 and name H2')	(resi 15 and name H51)	3.80	2.00	0.70
assi (resi 15 and name H2')	(resi 16 and name H5'')	5.00	2.00	1.00
assi (resi 15 and name H2')	(resi 16 and name H8)	3.80	2.00	0.70
assi (resi 15 and name H2'')	(resi 15 and name H6)	3.80	2.00	0.70
assi (resi 15 and name H2'')	(resi 15 and name H51)	6.00	2.00	1.00
assi (resi 15 and name H2'')	(resi 16 and name H4')	6.00	2.00	1.00
assi (resi 15 and name H2'')	(resi 16 and name H5'')	3.80	2.00	0.70
assi (resi 15 and name H2'')	(resi 16 and name H8)	2.50	0.70	0.50
assi (resi 15 and name H3')	(resi 15 and name H6)	5.00	2.00	1.00
assi (resi 15 and name H3')	(resi 15 and name H51)	5.00	2.00	1.00
assi (resi 15 and name H4')	(resi 15 and name H6)	5.00	2.00	1.00
assi (resi 15 and name H4')	(resi 15 and name H51)	6.00	2.00	1.00
assi (resi 15 and name H5')	(resi 15 and name H6)	5.00	2.00	1.00
assi (resi 15 and name H5'')	(resi 15 and name H6)	5.00	2.00	1.00
assi (resi 15 and name H6)	(resi 16 and name H8)	5.00	2.00	1.00

assi (resi 16 and name H1')	(resi 16 and name H2)	5.00 2.00 1.00
assi (resi 16 and name H1')	(resi 16 and name H8)	3.80 2.00 0.70
assi (resi 16 and name H1')	(resi 17 and name H1')	6.00 2.00 1.00
assi (resi 16 and name H1')	(resi 17 and name H4')	6.00 2.00 1.00
assi (resi 16 and name H1')	(resi 17 and name H5')	6.00 2.00 1.00
assi (resi 16 and name H1')	(resi 17 and name H5'')	5.00 2.00 1.00
assi (resi 16 and name H1')	(resi 17 and name H8)	3.80 2.00 0.70
assi (resi 16 and name H2')	(resi 16 and name H8)	2.50 0.70 0.50
assi (resi 16 and name H2')	(resi 17 and name H5')	6.00 2.00 1.00
assi (resi 16 and name H2')	(resi 17 and name H5'')	5.00 2.00 1.00
assi (resi 16 and name H2')	(resi 17 and name H8)	3.80 2.00 0.70
assi (resi 16 and name H2'')	(resi 16 and name H8)	3.80 2.00 0.70
assi (resi 16 and name H2'')	(resi 17 and name H5')	6.00 2.00 1.00
assi (resi 16 and name H2'')	(resi 17 and name H5'')	5.00 2.00 1.00
assi (resi 16 and name H2'')	(resi 17 and name H2)	6.00 2.00 1.00
assi (resi 16 and name H2'')	(resi 17 and name H8)	3.80 2.00 0.70
assi (resi 16 and name H3')	(resi 16 and name H8)	3.80 2.00 0.70
assi (resi 16 and name H3')	(resi 17 and name H8)	5.00 2.00 1.00
assi (resi 16 and name H4')	(resi 16 and name H8)	5.00 2.00 1.00
assi (resi 16 and name H5')	(resi 16 and name H8)	5.00 2.00 1.00
assi (resi 16 and name H5'')	(resi 16 and name H8)	5.00 2.00 1.00
assi (resi 16 and name H2)	(resi 17 and name H1')	5.00 2.00 1.00
assi (resi 16 and name H2)	(resi 17 and name H2)	3.80 2.00 0.70
assi (resi 17 and name H1')	(resi 17 and name H2)	5.00 2.00 1.00
assi (resi 17 and name H1')	(resi 17 and name H8)	3.80 2.00 0.70
assi (resi 17 and name H2')	(resi 17 and name H8)	2.50 0.70 0.50
assi (resi 17 and name H2'')	(resi 17 and name H8)	3.80 2.00 0.70
assi (resi 17 and name H3')	(resi 17 and name H8)	5.00 2.00 1.00
assi (resi 17 and name H4')	(resi 17 and name H8)	5.00 2.00 1.00
assi (resi 17 and name H5')	(resi 17 and name H8)	5.00 2.00 1.00
assi (resi 17 and name H5'')	(resi 17 and name H8)	5.00 2.00 1.00

H-bond restraints verified by 13 interstrand correlations (mainly between adenine-H2 and H1' on the opposite strand).

assi (resi 1 and name H3)	(resi 17 and name N1)	1.90 0.30 0.30
assi (resi 1 and name N3)	(resi 17 and name N1)	2.90 0.30 0.30
assi (resi 1 and name O4)	(resi 17 and name H61)	1.90 0.30 0.30
assi (resi 1 and name O4)	(resi 17 and name N6)	2.90 0.30 0.30
assi (resi 2 and name H3)	(resi 16 and name N1)	1.90 0.10 0.10
assi (resi 2 and name N3)	(resi 16 and name N1)	2.90 0.10 0.10
assi (resi 2 and name O4)	(resi 16 and name H61)	1.90 0.10 0.10
assi (resi 2 and name O4)	(resi 16 and name N6)	2.90 0.10 0.10
assi (resi 3 and name N1)	(resi 15 and name H3)	1.90 0.10 0.10
assi (resi 3 and name N1)	(resi 15 and name N3)	2.90 0.10 0.10
assi (resi 3 and name H61)	(resi 15 and name O4)	1.90 0.10 0.10
assi (resi 3 and name N6)	(resi 15 and name O4)	2.90 0.10 0.10

assi (resi 4 and name N1)	(resi 14 and name H3)	1.90 0.10 0.10
assi (resi 4 and name N1)	(resi 14 and name N3)	2.90 0.10 0.10
assi (resi 4 and name H61)	(resi 14 and name O4)	1.90 0.10 0.10
assi (resi 4 and name N6)	(resi 14 and name O4)	2.90 0.10 0.10
assi (resi 5 and name H3)	(resi 13 and name N1)	1.90 0.10 0.10
assi (resi 5 and name N3)	(resi 13 and name N1)	2.90 0.10 0.10
assi (resi 5 and name O4)	(resi 13 and name H61)	1.90 0.10 0.10
assi (resi 5 and name O4)	(resi 13 and name N6)	2.90 0.10 0.10
assi (resi 6 and name H3)	(resi 12 and name N1)	1.90 0.10 0.10
assi (resi 6 and name N3)	(resi 12 and name N1)	2.90 0.10 0.10
assi (resi 6 and name O4)	(resi 12 and name H61)	1.90 0.10 0.10
assi (resi 6 and name O4)	(resi 12 and name N6)	2.90 0.10 0.10
assi (resi 7 and name H3)	(resi 11 and name N1)	1.90 0.30 0.30
assi (resi 7 and name N3)	(resi 11 and name N1)	2.90 0.30 0.30
assi (resi 7 and name O4)	(resi 11 and name H61)	1.90 0.30 0.30
assi (resi 7 and name O4)	(resi 11 and name N6)	2.90 0.30 0.30

Phosphate-sugar-backbone dihedral restraints based on a 1D [ $^{31}\text{P}$ ]-NMR spectrum acquired at 400 MHz frequency at 298 K (100 %  $\text{D}_2\text{O}$ , 120 mM  $\text{NaClO}_4$ ) and cover the B-DNA range. Exact values were taken from the dihedral angle restraint files of the pdb entries 1RVI and 1RVH, which represent a DNA duplex.<sup>[260]</sup> Error boundaries of  $\pm 30^\circ$  were used for residues T1, T7, A11, A17 and  $\pm 20^\circ$  for residues T2, A3, A4, T5, T6, A12, A13, T14, T15, A16, respectively. Im8, Im9 and Im10 were left unrestrained.

assign	( resid n-1 and name O3')		
	( resid n and name P)		
	( resid n and name O5')		
	( resid n and name C5')	-60	{* $\alpha$ *}
assign	( resid n and name P)		
	( resid n and name O5')		
	( resid n and name C5')		
	( resid n and name C4')	-180	{* $\beta$ *}
assign	( resid n and name O5')		
	( resid n and name C5')		
	( resid n and name C4')		
	( resid n and name C3')	60	{* $\gamma$ *}
assign	( resid n and name C3')		
	( resid n and name O3')		
	( resid n+1 and name P)		
	( resid n+1 and name O5')	-90	{* $\zeta$ *}

Sugar pucker restraints based on a [ $^1\text{H}$ ,  $^1\text{H}$ ]-TOCSY spectrum acquired at 700 MHz frequency at 298 K (100 %  $\text{D}_2\text{O}$ , 120 mM  $\text{NaClO}_4$ ). Helical B-type DNA is usually 2'-endo and gives strong H1'-H2' and H1'-H3' crosspeak in TOCSY experiment. Exact values were taken from the dihedral angle restraint file of the pdb entries 1RVI und 1RVH, which represent a DNA duplex.<sup>[260]</sup> Error boundaries of  $\pm 30^\circ$  were used for residues T1, T7, Im8, Im9, Im10 A11, A17 and  $\pm 20^\circ$  for residues T2, A3, A4, T5, T6, A12, A13, T14, T15, A16, respectively.

assign	( resid n	and name C4')		
	( resid n	and name O4')		
	( resid n	and name C1')		
	( resid n	and name C2')	-20	{* v <sub>0</sub> *}
assign	( resid n	and name O4')		
	( resid n	and name C1')		
	( resid n	and name C2')		
	( resid n	and name C3')	33	{* v <sub>1</sub> *}
assign	( resid n	and name C1')		
	( resid n	and name C2')		
	( resid n	and name C3')		
	( resid n	and name C4')	-22	{* v <sub>2</sub> *}
assign	( resid n	and name C2')		
	( resid n	and name C3')		
	( resid n	and name C4')		
	( resid n	and name O4')	4	{* v <sub>3</sub> *}
assign	( resid n	and name C3')		
	( resid n	and name C4')		
	( resid n	and name O4')		
	( resid n	and name C1')	16	{* v <sub>4</sub> *}

The torsion angle  $\chi$  defines the orientation of the base to the sugar around the glycosidic bond.  $\chi$  was restrained to *anti* orientation for all residues, with error boundaries of  $\pm 30^\circ$  for residues T1, T7, A11, A17 and  $\pm 20^\circ$  for residues T2, A3, A4, T5, T6, A12, A13, T14, T15, A16, respectively. Im8, Im9 and Im10 were left unrestrained.

assign	( resid n	and name O4' )		
	( resid n	and name C1' )		
	( resid n	and name N9 )		
	( resid n	and name C4 )	-120	{* $\chi$ of purines*}
assign	( resid n	and name O4' )		
	( resid n	and name C1' )		
	( resid n	and name N1 )		
	( resid n	and name C4 )	-120	{* $\chi$ of pyrimidines*}

**Appendix 14**  $^1\text{H}$ -NMR chemical shift assignments of the oligonucleotide DNA\_IM1 in the absence of silver(I) ions at pD 10.2.

	H1'	H2	H2'	H2''	H3'	H4	H4'	H5	H5'	H5''	H6	H7	H8
	ppm												
<b>T1</b>	5.96		2.06	2.41	4.63		4.02		3.67	3.66	7.44	1.62	
<b>T2</b>	5.61		2.05	2.35	4.79		4.09		4.02	3.96	7.43	1.72	
<b>A3</b>	5.89	7.05	2.75	2.86	5.00		4.36		4.02	4.09			8.26
<b>A4</b>	6.15	7.60	2.56	2.85	4.95		4.43		4.20	4.22			8.15
<b>T5</b>	5.87		1.94	2.47	4.77		4.12		4.10	4.25	7.12	1.26	
<b>T6</b>	6.06		2.01	2.44	4.82		4.10		4.12	4.03	7.36	1.56	
<b>T7</b>	6.10		2.07	2.24	4.82		4.17		4.10	4.02	7.21	1.56	
<b>Im8</b>	5.98	7.75	2.37	2.40	-	6.98	4.24	7.24	4.30	3.95			
<b>Im9</b>	5.36	7.31	1.94	2.06	4.51	6.73	3.71	6.8	3.76	3.61			
<b>Im10</b>	5.47	7.50	2.03	2.11	4.50	6.58	3.14	6.88	3.03	3.44			
<b>A11</b>	5.74	7.40	2.77	2.88	4.84		4.27		3.90	3.84			8.19
<b>A12</b>	5.81	7.18	2.63	2.79	4.98		4.37		4.14	4.11			8.09
<b>A13</b>	6.13	7.64	2.52	2.83	4.93		4.31		4.15	4.14			8.09
<b>T14</b>	5.82		1.86	2.39	4.75		4.11		4.09	4.26	7.07	1.25	
<b>T15</b>	5.64		1.77	2.18	4.75		4.01		3.97	4.12	7.17	1.56	
<b>A16</b>	5.87	7.31	2.56	2.65	4.92		4.27		4.02	3.97			8.02
<b>A17</b>	6.11	7.62	2.48	2.29	4.60		4.12		4.17	4.06			8.01

**Appendix 15** All distance and dihedral angle restraints for the structure calculation of DNA\_IMI in absence of Ag<sup>+</sup> ions at pD 10.2.

Distance constraints of non-exchangeable protons based on a 2D [<sup>1</sup>H,<sup>1</sup>H]-NOESY spectrum acquired at 700 MHz frequency at 298 K (100 % D<sub>2</sub>O, 120 mM NaClO<sub>4</sub>). Specified are the estimated distances in Å (left) , as well as the lower (middle) and the upper (right) boundaries.

assi (resi 1 and name H1')	(resi 1 and name H6)	3.80	2.00	0.70
assi (resi 1 and name H1')	(resi 1 and name H51)	6.00	2.00	1.00
assi (resi 1 and name H1')	(resi 2 and name H4')	6.00	2.00	1.00
assi (resi 1 and name H1')	(resi 2 and name H5'')	3.80	2.00	0.70
assi (resi 1 and name H1')	(resi 2 and name H6)	3.80	2.00	0.70
assi (resi 1 and name H1')	(resi 2 and name H51)	5.00	2.00	1.00
assi (resi 1 and name H1')	(resi 17 and name H2)	6.00	2.00	1.00
assi (resi 1 and name H2')	(resi 1 and name H6)	2.50	0.70	0.50
assi (resi 1 and name H2')	(resi 1 and name H51)	5.00	2.00	1.00
assi (resi 1 and name H2')	(resi 2 and name H5'')	6.00	2.00	1.00
assi (resi 1 and name H2')	(resi 2 and name H6)	3.80	2.00	0.70
assi (resi 1 and name H2')	(resi 2 and name H51)	3.80	2.00	0.70
assi (resi 1 and name H2')	(resi 17 and name H2)	6.00	2.00	1.00
assi (resi 1 and name H2'')	(resi 1 and name H6)	3.80	2.00	0.70
assi (resi 1 and name H2'')	(resi 2 and name H5'')	5.00	2.00	1.00
assi (resi 1 and name H2'')	(resi 2 and name H6)	3.80	2.00	0.70
assi (resi 1 and name H2'')	(resi 2 and name H51)	3.80	2.00	0.70
assi (resi 1 and name H2'')	(resi 17 and name H2)	6.00	2.00	1.00
assi (resi 1 and name H3')	(resi 1 and name H6)	5.00	2.00	1.00
assi (resi 1 and name H3')	(resi 2 and name H51)	6.00	2.00	1.00
assi (resi 1 and name H4')	(resi 1 and name H6)	5.00	2.00	1.00
assi (resi 1 and name H4')	(resi 2 and name H1')	6.00	2.00	1.00
assi (resi 1 and name H4')	(resi 2 and name H51)	6.00	2.00	1.00
assi (resi 1 and name H5')	(resi 1 and name H6)	3.80	2.00	0.70
assi (resi 1 and name H5')	(resi 1 and name H51)	6.00	2.00	1.00
assi (resi 1 and name H5')	(resi 2 and name H51)	6.00	2.00	1.00
assi (resi 1 and name H5'')	(resi 1 and name H6)	3.80	2.00	0.70
assi (resi 1 and name H5'')	(resi 1 and name H51)	6.00	2.00	1.00
assi (resi 1 and name H5'')	(resi 2 and name H51)	6.00	2.00	1.00
assi (resi 1 and name H6)	(resi 2 and name H5'')	6.00	2.00	1.00
assi (resi 1 and name H6)	(resi 2 and name H51)	3.80	2.00	0.70
assi (resi 1 and name H51)	(resi 2 and name H51)	3.80	2.00	0.70
assi (resi 2 and name H1')	(resi 2 and name H6)	3.80	2.00	0.70
assi (resi 2 and name H1')	(resi 2 and name H51)	6.00	2.00	1.00
assi (resi 2 and name H1')	(resi 3 and name H1')	6.00	2.00	1.00
assi (resi 2 and name H1')	(resi 3 and name H4')	6.00	2.00	1.00
assi (resi 2 and name H1')	(resi 3 and name H5'')	5.00	2.00	1.00
assi (resi 2 and name H1')	(resi 3 and name H8)	5.00	2.00	1.00
assi (resi 2 and name H1')	(resi 17 and name H2)	6.00	2.00	1.00
assi (resi 2 and name H2')	(resi 2 and name H6)	2.50	0.70	0.50
assi (resi 2 and name H2')	(resi 2 and name H51)	5.00	2.00	1.00
assi (resi 2 and name H2')	(resi 3 and name H8)	3.80	2.00	0.70
assi (resi 2 and name H2'')	(resi 2 and name H6)	3.80	2.00	0.70

assi (resi 2 and name H2")	(resi 2 and name H51)	5.00	2.00	1.00
assi (resi 2 and name H2")	(resi 3 and name H2')	6.00	2.00	1.00
assi (resi 2 and name H2")	(resi 3 and name H4')	6.00	2.00	1.00
assi (resi 2 and name H2")	(resi 3 and name H5")	5.00	2.00	1.00
assi (resi 2 and name H2")	(resi 3 and name H8)	3.80	2.00	0.70
assi (resi 2 and name H3')	(resi 2 and name H6)	5.00	2.00	1.00
assi (resi 2 and name H4')	(resi 2 and name H6)	5.00	2.00	1.00
assi (resi 2 and name H5')	(resi 2 and name H6)	5.00	2.00	1.00
assi (resi 2 and name H5")	(resi 2 and name H6)	3.80	2.00	0.70
assi (resi 2 and name H5")	(resi 2 and name H51)	6.00	2.00	1.00
assi (resi 2 and name H5")	(resi 3 and name H8)	6.00	2.00	1.00
assi (resi 2 and name H6)	(resi 3 and name H8)	5.00	2.00	1.00
assi (resi 2 and name H51)	(resi 17 and name H2)	6.00	2.00	1.00
assi (resi 3 and name H1')	(resi 3 and name H2)	5.00	2.00	1.00
assi (resi 3 and name H1')	(resi 3 and name H8)	3.80	2.00	0.70
assi (resi 3 and name H1')	(resi 4 and name H1')	6.00	2.00	1.00
assi (resi 3 and name H1')	(resi 4 and name H4')	6.00	2.00	1.00
assi (resi 3 and name H1')	(resi 4 and name H5")	5.00	2.00	1.00
assi (resi 3 and name H1')	(resi 4 and name H8)	3.80	2.00	0.70
assi (resi 3 and name H1')	(resi 16 and name H2)	6.00	2.00	1.00
assi (resi 3 and name H2')	(resi 3 and name H8)	2.50	0.70	0.50
assi (resi 3 and name H2')	(resi 4 and name H5")	6.00	2.00	1.00
assi (resi 3 and name H2')	(resi 4 and name H8)	3.80	2.00	0.70
assi (resi 3 and name H2")	(resi 3 and name H8)	3.80	2.00	0.70
assi (resi 3 and name H2")	(resi 4 and name H5")	5.00	2.00	1.00
assi (resi 3 and name H2")	(resi 4 and name H8)	3.80	2.00	0.70
assi (resi 3 and name H3')	(resi 3 and name H8)	3.80	2.00	0.70
assi (resi 3 and name H3')	(resi 4 and name H8)	5.00	2.00	1.00
assi (resi 3 and name H4')	(resi 3 and name H8)	5.00	2.00	1.00
assi (resi 3 and name H4')	(resi 4 and name H8)	6.00	2.00	1.00
assi (resi 3 and name H5')	(resi 3 and name H8)	5.00	2.00	1.00
assi (resi 3 and name H5")	(resi 3 and name H8)	5.00	2.00	1.00
assi (resi 3 and name H5")	(resi 4 and name H8)	6.00	2.00	1.00
assi (resi 3 and name H2)	(resi 4 and name H1')	6.00	2.00	1.00
assi (resi 3 and name H2)	(resi 4 and name H2)	3.80	2.00	0.70
assi (resi 3 and name H2)	(resi 16 and name H1')	6.00	2.00	1.00
assi (resi 3 and name H2)	(resi 16 and name H2)	3.80	2.00	0.70
assi (resi 3 and name H2)	(resi 16 and name H8)	5.00	2.00	1.00
assi (resi 3 and name H8)	(resi 4 and name H8)	5.00	2.00	1.00
assi (resi 4 and name H1')	(resi 4 and name H2)	5.00	2.00	1.00
assi (resi 4 and name H1')	(resi 4 and name H8)	3.80	2.00	0.70
assi (resi 4 and name H1')	(resi 5 and name H1')	5.00	2.00	1.00
assi (resi 4 and name H1')	(resi 5 and name H4')	6.00	2.00	1.00
assi (resi 4 and name H1')	(resi 5 and name H5")	5.00	2.00	1.00
assi (resi 4 and name H1')	(resi 5 and name H6)	3.80	2.00	0.70
assi (resi 4 and name H1')	(resi 5 and name H51)	5.00	2.00	1.00
assi (resi 4 and name H2')	(resi 4 and name H8)	2.50	0.70	0.50
assi (resi 4 and name H2')	(resi 5 and name H6)	3.80	2.00	0.70
assi (resi 4 and name H2')	(resi 5 and name H51)	3.80	2.00	0.70

assi (resi 4 and name H2")	(resi 4 and name H8)	3.80	2.00	0.70
assi (resi 4 and name H2")	(resi 5 and name H2')	5.00	2.00	1.00
assi (resi 4 and name H2")	(resi 5 and name H5")	3.80	2.00	0.70
assi (resi 4 and name H2")	(resi 5 and name H6)	2.50	0.70	0.50
assi (resi 4 and name H2")	(resi 5 and name H51)	3.80	2.00	0.70
assi (resi 4 and name H2")	(resi 6 and name H51)	6.00	2.00	1.00
assi (resi 4 and name H3')	(resi 4 and name H8)	3.80	2.00	0.70
assi (resi 4 and name H3')	(resi 5 and name H6)	3.80	2.00	0.70
assi (resi 4 and name H3')	(resi 5 and name H51)	3.80	2.00	0.70
assi (resi 4 and name H4')	(resi 4 and name H8)	6.00	2.00	1.00
assi (resi 4 and name H5')	(resi 4 and name H8)	5.00	2.00	1.00
assi (resi 4 and name H5")	(resi 4 and name H8)	5.00	2.00	1.00
assi (resi 4 and name H2)	(resi 5 and name H1')	5.00	2.00	1.00
assi (resi 4 and name H2)	(resi 15 and name H1')	5.00	2.00	1.00
assi (resi 4 and name H8)	(resi 5 and name H6)	5.00	2.00	1.00
assi (resi 4 and name H8)	(resi 5 and name H51)	3.80	2.00	0.70
assi (resi 5 and name H1')	(resi 5 and name H6)	3.80	2.00	0.70
assi (resi 5 and name H1')	(resi 5 and name H51)	6.00	2.00	1.00
assi (resi 5 and name H1')	(resi 6 and name H1')	6.00	2.00	1.00
assi (resi 5 and name H1')	(resi 6 and name H5")	5.00	2.00	1.00
assi (resi 5 and name H1')	(resi 6 and name H6)	3.80	2.00	0.70
assi (resi 5 and name H1')	(resi 6 and name H51)	5.00	2.00	1.00
assi (resi 5 and name H2')	(resi 5 and name H6)	2.50	0.70	0.50
assi (resi 5 and name H2')	(resi 5 and name H51)	5.00	2.00	1.00
assi (resi 5 and name H2')	(resi 6 and name H6)	3.80	2.00	0.70
assi (resi 5 and name H2')	(resi 6 and name H51)	3.80	2.00	0.70
assi (resi 5 and name H2")	(resi 5 and name H6)	3.80	2.00	0.70
assi (resi 5 and name H2")	(resi 5 and name H51)	6.00	2.00	1.00
assi (resi 5 and name H2")	(resi 6 and name H5")	5.00	2.00	1.00
assi (resi 5 and name H2")	(resi 6 and name H6)	3.80	2.00	0.70
assi (resi 5 and name H2")	(resi 6 and name H51)	3.80	2.00	0.70
assi (resi 5 and name H3')	(resi 5 and name H6)	5.00	2.00	1.00
assi (resi 5 and name H3')	(resi 6 and name H51)	6.00	2.00	1.00
assi (resi 5 and name H4')	(resi 5 and name H6)	5.00	2.00	1.00
assi (resi 5 and name H4')	(resi 6 and name H51)	6.00	2.00	1.00
assi (resi 5 and name H5')	(resi 5 and name H6)	5.00	2.00	1.00
assi (resi 5 and name H5")	(resi 5 and name H6)	5.00	2.00	1.00
assi (resi 5 and name H6)	(resi 6 and name H6)	5.00	2.00	1.00
assi (resi 5 and name H6)	(resi 6 and name H51)	3.80	2.00	0.70
assi (resi 5 and name H51)	(resi 6 and name H51)	3.80	2.00	0.70
assi (resi 5 and name H51)	(resi 6 and name H6)	6.00	2.00	1.00
assi (resi 6 and name H1')	(resi 6 and name H6)	3.80	2.00	0.70
assi (resi 6 and name H1')	(resi 6 and name H51)	5.00	2.00	1.00
assi (resi 6 and name H1')	(resi 7 and name H4')	6.00	2.00	1.00
assi (resi 6 and name H1')	(resi 7 and name H5")	5.00	2.00	1.00
assi (resi 6 and name H1')	(resi 7 and name H6)	3.80	2.00	0.70
assi (resi 6 and name H1')	(resi 7 and name H51)	5.00	2.00	1.00
assi (resi 6 and name H1')	(resi 13 and name H2)	5.00	2.00	1.00
assi (resi 6 and name H2')	(resi 6 and name H6)	2.50	0.70	0.50
assi (resi 6 and name H2')	(resi 6 and name H51)	5.00	2.00	1.00



---

assi (resi 6 and name H2')	(resi 7 and name H5")	5.00	2.00	1.00
assi (resi 6 and name H2')	(resi 7 and name H6)	3.80	2.00	0.70
assi (resi 6 and name H2')	(resi 7 and name H51)	3.80	2.00	0.70
assi (resi 6 and name H2")	(resi 6 and name H6)	3.80	2.00	0.70
assi (resi 6 and name H2")	(resi 6 and name H51)	5.00	2.00	1.00
assi (resi 6 and name H2")	(resi 7 and name H5")	5.00	2.00	1.00
assi (resi 6 and name H2")	(resi 7 and name H6)	3.80	2.00	0.70
assi (resi 6 and name H2")	(resi 7 and name H51)	3.80	2.00	0.70
assi (resi 6 and name H3')	(resi 6 and name H6)	3.80	2.00	0.70
assi (resi 6 and name H3')	(resi 7 and name H51)	5.00	2.00	1.00
assi (resi 6 and name H4')	(resi 6 and name H6)	5.00	2.00	1.00
assi (resi 6 and name H4')	(resi 6 and name H51)	6.00	2.00	1.00
assi (resi 6 and name H4')	(resi 7 and name H51)	6.00	2.00	1.00
assi (resi 6 and name H5')	(resi 6 and name H6)	5.00	2.00	1.00
assi (resi 6 and name H5')	(resi 6 and name H51)	6.00	2.00	1.00
assi (resi 6 and name H5")	(resi 6 and name H6)	5.00	2.00	1.00
assi (resi 6 and name H5")	(resi 6 and name H51)	6.00	2.00	1.00
assi (resi 6 and name H6)	(resi 7 and name H6)	5.00	2.00	1.00
assi (resi 6 and name H6)	(resi 7 and name H51)	3.80	2.00	0.70
assi (resi 6 and name H51)	(resi 8 and name H2)	6.00	2.00	1.00
assi (resi 6 and name H51)	(resi 8 and name H4)	5.00	2.00	1.00
assi (resi 6 and name H51)	(resi 9 and name H1')	6.00	2.00	1.00
assi (resi 6 and name H51)	(resi 9 and name H2)	6.00	2.00	1.00
assi (resi 6 and name H51)	(resi 9 and name H5)	6.00	2.00	1.00
assi (resi 6 and name H51)	(resi 10 and name H4)	6.00	2.00	1.00
assi (resi 7 and name H1')	(resi 7 and name H6)	3.80	2.00	0.70
assi (resi 7 and name H1')	(resi 7 and name H51)	6.00	2.00	1.00
assi (resi 7 and name H1')	(resi 8 and name H5)	5.00	2.00	1.00
assi (resi 7 and name H1')	(resi 8 and name H5")	3.80	2.00	0.70
assi (resi 7 and name H1')	(resi 9 and name H5")	5.00	2.00	1.00
assi (resi 7 and name H1')	(resi 11 and name H2)	6.00	2.00	1.00
assi (resi 7 and name H1')	(resi 12 and name H2)	5.00	2.00	1.00
assi (resi 7 and name H2')	(resi 7 and name H6)	2.50	0.70	0.50
assi (resi 7 and name H2')	(resi 7 and name H51)	5.00	2.00	1.00
assi (resi 7 and name H2')	(resi 8 and name H4')	6.00	2.00	1.00
assi (resi 7 and name H2')	(resi 8 and name H5")	5.00	2.00	1.00
assi (resi 7 and name H2")	(resi 8 and name H5)	5.00	2.00	1.00
assi (resi 7 and name H2")	(resi 7 and name H6)	3.80	2.00	0.70
assi (resi 7 and name H2")	(resi 8 and name H4')	5.00	2.00	1.00
assi (resi 7 and name H2")	(resi 8 and name H5")	3.80	2.00	0.70
assi (resi 7 and name H2")	(resi 8 and name H5)	5.00	2.00	1.00
assi (resi 7 and name H2")	(resi 9 and name H4)	6.00	2.00	1.00
assi (resi 7 and name H2")	(resi 9 and name H5)	5.00	2.00	1.00
assi (resi 7 and name H3')	(resi 7 and name H6)	5.00	2.00	1.00
assi (resi 7 and name H4')	(resi 7 and name H6)	5.00	2.00	1.00
assi (resi 7 and name H5')	(resi 7 and name H6)	5.00	2.00	1.00
assi (resi 7 and name H5')	(resi 7 and name H51)	6.00	2.00	1.00
assi (resi 7 and name H5")	(resi 7 and name H6)	5.00	2.00	1.00
assi (resi 7 and name H5")	(resi 7 and name H51)	6.00	2.00	1.00
assi (resi 7 and name H6)	(resi 8 and name H5")	5.00	2.00	1.00

---

assi (resi 7 and name H6)	(resi 9 and name H4)	6.00	2.00	1.00
assi (resi 7 and name H6)	(resi 9 and name H5)	6.00	2.00	1.00
assi (resi 7 and name H51)	(resi 8 and name H2)	6.00	2.00	1.00
assi (resi 7 and name H51)	(resi 9 and name H1')	6.00	2.00	1.00
assi (resi 7 and name H51)	(resi 9 and name H2)	5.00	2.00	1.00
assi (resi 7 and name H51)	(resi 9 and name H4)	5.00	2.00	1.00
assi (resi 7 and name H51)	(resi 9 and name H5)	5.00	2.00	1.00
assi (resi 7 and name H51)	(resi 10 and name H4)	6.00	2.00	1.00
assi (resi 8 and name H1')	(resi 8 and name H2)	3.80	2.00	0.70
assi (resi 8 and name H1')	(resi 8 and name H4)	6.00	2.00	1.00
assi (resi 8 and name H1')	(resi 8 and name H5)	3.80	2.00	0.70
assi (resi 8 and name H1')	(resi 9 and name H4')	6.00	2.00	1.00
assi (resi 8 and name H1')	(resi 9 and name H5')	6.00	2.00	1.00
assi (resi 8 and name H1')	(resi 9 and name H5'')	5.00	2.00	1.00
assi (resi 8 and name H1')	(resi 10 and name H4)	5.00	2.00	1.00
assi (resi 8 and name H2')	(resi 8 and name H2)	5.00	2.00	1.00
assi (resi 8 and name H2')	(resi 8 and name H5)	3.80	2.00	0.70
assi (resi 8 and name H2'')	(resi 8 and name H2)	5.00	2.00	1.00
assi (resi 8 and name H2'')	(resi 8 and name H5)	3.80	2.00	0.70
assi (resi 8 and name H2'')	(resi 9 and name H5')	6.00	2.00	1.00
assi (resi 8 and name H2'')	(resi 9 and name H5'')	5.00	2.00	1.00
assi (resi 8 and name H2'')	(resi 9 and name H5)	5.00	2.00	1.00
assi (resi 8 and name H4')	(resi 8 and name H5)	6.00	2.00	1.00
assi (resi 8 and name H4')	(resi 9 and name H5)	6.00	2.00	1.00
assi (resi 8 and name H4')	(resi 10 and name H4)	6.00	2.00	1.00
assi (resi 8 and name H5')	(resi 8 and name H5)	6.00	2.00	1.00
assi (resi 8 and name H5'')	(resi 8 and name H5)	5.00	2.00	1.00
assi (resi 8 and name H5'')	(resi 9 and name H5)	6.00	2.00	1.00
assi (resi 8 and name H5'')	(resi 11 and name H2)	6.00	2.00	1.00
assi (resi 8 and name H5)	(resi 10 and name H4)	6.00	2.00	1.00
assi (resi 9 and name H1')	(resi 9 and name H2)	3.80	2.00	0.70
assi (resi 9 and name H1')	(resi 9 and name H5)	3.80	2.00	0.70
assi (resi 9 and name H1')	(resi 10 and name H5'')	6.00	2.00	1.00
assi (resi 9 and name H1')	(resi 10 and name H5')	6.00	2.00	1.00
assi (resi 9 and name H1')	(resi 10 and name H4)	6.00	2.00	1.00
assi (resi 9 and name H1')	(resi 10 and name H5)	6.00	2.00	1.00
assi (resi 9 and name H1')	(resi 11 and name H2)	5.00	2.00	1.00
assi (resi 9 and name H2')	(resi 9 and name H2)	5.00	2.00	1.00
assi (resi 9 and name H2')	(resi 9 and name H4)	6.00	2.00	1.00
assi (resi 9 and name H2')	(resi 9 and name H5)	3.80	2.00	0.70
assi (resi 9 and name H2')	(resi 10 and name H5)	5.00	2.00	1.00
assi (resi 9 and name H2'')	(resi 9 and name H2)	5.00	2.00	1.00
assi (resi 9 and name H2'')	(resi 9 and name H4)	5.00	2.00	1.00
assi (resi 9 and name H2'')	(resi 9 and name H5)	3.80	2.00	0.70
assi (resi 9 and name H2'')	(resi 10 and name H5')	6.00	2.00	1.00
assi (resi 9 and name H2'')	(resi 10 and name H5'')	6.00	2.00	1.00
assi (resi 9 and name H3')	(resi 9 and name H5)	6.00	2.00	1.00
assi (resi 9 and name H3')	(resi 10 and name H5)	6.00	2.00	1.00
assi (resi 9 and name H4')	(resi 10 and name H5')	5.00	2.00	1.00

---

assi (resi 9 and name H4')	(resi 10 and name H5)	6.00	2.00	1.00
assi (resi 9 and name H4')	(resi 11 and name H2)	3.80	2.00	0.70
assi (resi 9 and name H5')	(resi 9 and name H5)	6.00	2.00	1.00
assi (resi 9 and name H5')	(resi 11 and name H2)	5.00	2.00	1.00
assi (resi 9 and name H5'')	(resi 9 and name H5)	6.00	2.00	1.00
assi (resi 9 and name H5'')	(resi 10 and name H5)	6.00	2.00	1.00
assi (resi 9 and name H5'')	(resi 11 and name H2)	3.80	2.00	0.70
assi (resi 9 and name H2)	(resi 10 and name H4)	6.00	2.00	1.00
assi (resi 10 and name H1')	(resi 10 and name H2)	3.80	2.00	0.70
assi (resi 10 and name H1')	(resi 10 and name H4)	6.00	2.00	1.00
assi (resi 10 and name H1')	(resi 10 and name H5)	3.80	2.00	0.70
assi (resi 10 and name H1')	(resi 11 and name H5')	5.00	2.00	1.00
assi (resi 10 and name H1')	(resi 11 and name H5'')	6.00	2.00	1.00
assi (resi 10 and name H1')	(resi 11 and name H8)	5.00	2.00	1.00
assi (resi 10 and name H2')	(resi 10 and name H2)	5.00	2.00	1.00
assi (resi 10 and name H2')	(resi 10 and name H5)	3.80	2.00	0.70
assi (resi 10 and name H2')	(resi 11 and name H8)	5.00	2.00	1.00
assi (resi 10 and name H2'')	(resi 10 and name H2)	5.00	2.00	1.00
assi (resi 10 and name H2'')	(resi 10 and name H5)	3.80	2.00	0.70
assi (resi 10 and name H2'')	(resi 11 and name H8)	5.00	2.00	1.00
assi (resi 10 and name H3')	(resi 10 and name H5)	6.00	2.00	1.00
assi (resi 10 and name H4')	(resi 11 and name H1')	6.00	2.00	1.00
assi (resi 10 and name H4')	(resi 11 and name H4')	6.00	2.00	1.00
assi (resi 10 and name H4')	(resi 11 and name H8)	5.00	2.00	1.00
assi (resi 10 and name H5')	(resi 10 and name H5)	6.00	2.00	1.00
assi (resi 10 and name H5'')	(resi 10 and name H5)	6.00	2.00	1.00
assi (resi 10 and name H5'')	(resi 11 and name H1')	6.00	2.00	1.00
assi (resi 10 and name H4)	(resi 11 and name H2)	6.00	2.00	1.00
assi (resi 11 and name H1')	(resi 11 and name H2)	6.00	2.00	1.00
assi (resi 11 and name H1')	(resi 11 and name H8)	3.80	2.00	0.70
assi (resi 11 and name H1')	(resi 12 and name H1')	6.00	2.00	1.00
assi (resi 11 and name H1')	(resi 12 and name H4')	6.00	2.00	1.00
assi (resi 11 and name H1')	(resi 12 and name H5'')	5.00	2.00	1.00
assi (resi 11 and name H1')	(resi 12 and name H8)	3.80	2.00	0.70
assi (resi 11 and name H2')	(resi 11 and name H8)	3.80	2.00	0.70
assi (resi 11 and name H2')	(resi 12 and name H5'')	5.00	2.00	1.00
assi (resi 11 and name H2')	(resi 12 and name H8)	3.80	2.00	0.70
assi (resi 11 and name H2'')	(resi 11 and name H8)	3.80	2.00	0.70
assi (resi 11 and name H2'')	(resi 12 and name H2')	6.00	2.00	1.00
assi (resi 11 and name H2'')	(resi 12 and name H5'')	5.00	2.00	1.00
assi (resi 11 and name H2'')	(resi 12 and name H8)	3.80	2.00	0.70
assi (resi 11 and name H3')	(resi 11 and name H8)	5.00	2.00	1.00
assi (resi 11 and name H3')	(resi 12 and name H8)	6.00	2.00	1.00
assi (resi 11 and name H4')	(resi 11 and name H8)	5.00	2.00	1.00
assi (resi 11 and name H5')	(resi 11 and name H8)	5.00	2.00	1.00
assi (resi 11 and name H5'')	(resi 11 and name H8)	3.80	2.00	0.70
assi (resi 11 and name H2)	(resi 12 and name H2)	3.80	2.00	0.70
assi (resi 11 and name H8)	(resi 12 and name H8)	5.00	2.00	1.00

---

assi (resi 12 and name H1')	(resi 12 and name H2)	5.00	2.00	1.00
assi (resi 12 and name H1')	(resi 12 and name H8)	3.80	2.00	0.70
assi (resi 12 and name H1')	(resi 13 and name H1')	6.00	2.00	1.00
assi (resi 12 and name H1')	(resi 13 and name H5")	5.00	2.00	1.00
assi (resi 12 and name H1')	(resi 13 and name H8)	3.80	2.00	0.70
assi (resi 12 and name H2')	(resi 12 and name H8)	2.50	0.70	0.50
assi (resi 12 and name H2')	(resi 13 and name H5")	5.00	2.00	1.00
assi (resi 12 and name H2')	(resi 13 and name H8)	3.80	2.00	0.70
assi (resi 12 and name H2")	(resi 12 and name H8)	3.80	2.00	0.70
assi (resi 12 and name H2")	(resi 13 and name H5")	5.00	2.00	1.00
assi (resi 12 and name H2")	(resi 13 and name H8)	3.80	2.00	0.70
assi (resi 12 and name H3')	(resi 12 and name H8)	3.80	2.00	0.70
assi (resi 12 and name H3')	(resi 13 and name H8)	5.00	2.00	1.00
assi (resi 12 and name H4')	(resi 12 and name H8)	5.00	2.00	1.00
assi (resi 12 and name H4')	(resi 13 and name H8)	6.00	2.00	1.00
assi (resi 12 and name H5')	(resi 12 and name H8)	5.00	2.00	1.00
assi (resi 12 and name H5")	(resi 12 and name H8)	5.00	2.00	1.00
assi (resi 12 and name H2)	(resi 13 and name H1')	5.00	2.00	1.00
assi (resi 12 and name H2)	(resi 13 and name H2)	3.80	2.00	0.70
assi (resi 13 and name H1')	(resi 13 and name H2)	5.00	2.00	1.00
assi (resi 13 and name H1')	(resi 13 and name H8)	3.80	2.00	0.70
assi (resi 13 and name H1')	(resi 14 and name H5")	5.00	2.00	1.00
assi (resi 13 and name H1')	(resi 14 and name H6)	3.80	2.00	0.70
assi (resi 13 and name H1')	(resi 14 and name H51)	5.00	2.00	1.00
assi (resi 13 and name H2')	(resi 13 and name H8)	2.50	0.70	0.50
assi (resi 13 and name H2')	(resi 14 and name H5")	5.00	2.00	1.00
assi (resi 13 and name H2')	(resi 14 and name H6)	3.80	2.00	0.70
assi (resi 13 and name H2')	(resi 14 and name H51)	3.80	2.00	0.70
assi (resi 13 and name H2")	(resi 13 and name H8)	3.80	2.00	0.70
assi (resi 13 and name H2")	(resi 14 and name H2')	6.00	2.00	1.00
assi (resi 13 and name H2")	(resi 14 and name H5")	5.00	2.00	1.00
assi (resi 13 and name H2")	(resi 14 and name H6)	2.50	0.70	0.50
assi (resi 13 and name H2")	(resi 14 and name H51)	3.80	2.00	0.70
assi (resi 13 and name H2")	(resi 15 and name H51)	6.00	2.00	1.00
assi (resi 13 and name H3')	(resi 13 and name H8)	3.80	2.00	0.70
assi (resi 13 and name H3')	(resi 14 and name H6)	5.00	2.00	1.00
assi (resi 13 and name H3')	(resi 14 and name H51)	5.00	2.00	1.00
assi (resi 13 and name H4')	(resi 13 and name H8)	5.00	2.00	1.00
assi (resi 13 and name H5')	(resi 13 and name H8)	5.00	2.00	1.00
assi (resi 13 and name H5")	(resi 13 and name H8)	5.00	2.00	1.00
assi (resi 13 and name H2)	(resi 14 and name H1')	5.00	2.00	1.00
assi (resi 13 and name H8)	(resi 14 and name H6)	5.00	2.00	1.00
assi (resi 13 and name H8)	(resi 14 and name H51)	3.80	2.00	0.70
assi (resi 14 and name H1')	(resi 14 and name H6)	3.80	2.00	0.70
assi (resi 14 and name H1')	(resi 14 and name H51)	6.00	2.00	1.00
assi (resi 14 and name H1')	(resi 15 and name H1')	6.00	2.00	1.00
assi (resi 14 and name H1')	(resi 15 and name H5')	5.00	2.00	1.00
assi (resi 14 and name H1')	(resi 15 and name H5")	5.00	2.00	1.00
assi (resi 14 and name H1')	(resi 15 and name H6)	3.80	2.00	0.70

assi (resi 14 and name H1')	(resi 15 and name H51)	5.00	2.00	1.00
assi (resi 14 and name H2')	(resi 14 and name H6)	2.50	0.70	0.50
assi (resi 14 and name H2')	(resi 14 and name H51)	5.00	2.00	1.00
assi (resi 14 and name H2')	(resi 15 and name H5'')	5.00	2.00	1.00
assi (resi 14 and name H2')	(resi 15 and name H6)	3.80	2.00	0.70
assi (resi 14 and name H2')	(resi 15 and name H51)	3.80	2.00	0.70
assi (resi 14 and name H2'')	(resi 14 and name H6)	3.80	2.00	0.70
assi (resi 14 and name H2'')	(resi 14 and name H51)	6.00	2.00	1.00
assi (resi 14 and name H2'')	(resi 15 and name H2')	6.00	2.00	1.00
assi (resi 14 and name H2'')	(resi 15 and name H5'')	5.00	2.00	1.00
assi (resi 14 and name H2'')	(resi 15 and name H6)	3.80	2.00	0.70
assi (resi 14 and name H2'')	(resi 15 and name H51)	3.80	2.00	0.70
assi (resi 14 and name H3')	(resi 14 and name H6)	5.00	2.00	1.00
assi (resi 14 and name H3')	(resi 15 and name H51)	6.00	2.00	1.00
assi (resi 14 and name H4')	(resi 14 and name H6)	5.00	2.00	1.00
assi (resi 14 and name H5')	(resi 14 and name H6)	5.00	2.00	1.00
assi (resi 14 and name H5'')	(resi 14 and name H6)	5.00	2.00	1.00
assi (resi 14 and name H6)	(resi 15 and name H6)	5.00	2.00	1.00
assi (resi 14 and name H6)	(resi 15 and name H51)	3.80	2.00	0.70
assi (resi 14 and name H51)	(resi 15 and name H6)	6.00	2.00	1.00
assi (resi 14 and name H51)	(resi 15 and name H51)	3.80	2.00	0.70
assi (resi 15 and name H1')	(resi 15 and name H6)	3.80	2.00	0.70
assi (resi 15 and name H1')	(resi 15 and name H51)	6.00	2.00	1.00
assi (resi 15 and name H1')	(resi 16 and name H1')	6.00	2.00	1.00
assi (resi 15 and name H1')	(resi 16 and name H4')	6.00	2.00	1.00
assi (resi 15 and name H1')	(resi 16 and name H5'')	5.00	2.00	1.00
assi (resi 15 and name H1')	(resi 16 and name H8)	5.00	2.00	1.00
assi (resi 15 and name H2')	(resi 15 and name H6)	2.50	0.70	0.50
assi (resi 15 and name H2')	(resi 15 and name H51)	3.80	2.00	0.70
assi (resi 15 and name H2')	(resi 16 and name H5'')	5.00	2.00	1.00
assi (resi 15 and name H2')	(resi 16 and name H8)	3.80	2.00	0.70
assi (resi 15 and name H2'')	(resi 15 and name H6)	3.80	2.00	0.70
assi (resi 15 and name H2'')	(resi 16 and name H4')	6.00	2.00	1.00
assi (resi 15 and name H2'')	(resi 16 and name H5'')	3.80	2.00	0.70
assi (resi 15 and name H2'')	(resi 16 and name H8)	3.80	2.00	0.70
assi (resi 15 and name H3')	(resi 15 and name H6)	5.00	2.00	1.00
assi (resi 15 and name H3')	(resi 15 and name H51)	6.00	2.00	1.00
assi (resi 15 and name H4')	(resi 15 and name H6)	5.00	2.00	1.00
assi (resi 15 and name H4')	(resi 15 and name H51)	6.00	2.00	1.00
assi (resi 15 and name H5')	(resi 15 and name H6)	5.00	2.00	1.00
assi (resi 15 and name H5'')	(resi 15 and name H6)	5.00	2.00	1.00
assi (resi 15 and name H6)	(resi 16 and name H8)	5.00	2.00	1.00
assi (resi 16 and name H1')	(resi 16 and name H2)	5.00	2.00	1.00
assi (resi 16 and name H1')	(resi 16 and name H8)	3.80	2.00	0.70
assi (resi 16 and name H1')	(resi 17 and name H1')	6.00	2.00	1.00
assi (resi 16 and name H1')	(resi 17 and name H4')	6.00	2.00	1.00
assi (resi 16 and name H1')	(resi 17 and name H5')	6.00	2.00	1.00
assi (resi 16 and name H1')	(resi 17 and name H5'')	5.00	2.00	1.00
assi (resi 16 and name H1')	(resi 17 and name H8)	3.80	2.00	0.70

assi (resi 16 and name H2')	(resi 16 and name H8)	2.50	0.70	0.50
assi (resi 16 and name H2')	(resi 17 and name H5')	6.00	2.00	1.00
assi (resi 16 and name H2')	(resi 17 and name H5'')	5.00	2.00	1.00
assi (resi 16 and name H2')	(resi 17 and name H8)	3.80	2.00	0.70
assi (resi 16 and name H2'')	(resi 16 and name H8)	3.80	2.00	0.70
assi (resi 16 and name H2'')	(resi 17 and name H5')	6.00	2.00	1.00
assi (resi 16 and name H2'')	(resi 17 and name H5'')	5.00	2.00	1.00
assi (resi 16 and name H2'')	(resi 17 and name H2)	6.00	2.00	1.00
assi (resi 16 and name H2'')	(resi 17 and name H8)	3.80	2.00	0.70
assi (resi 16 and name H3')	(resi 16 and name H8)	3.80	2.00	0.70
assi (resi 16 and name H3')	(resi 17 and name H8)	5.00	2.00	1.00
assi (resi 16 and name H4')	(resi 16 and name H8)	5.00	2.00	1.00
assi (resi 16 and name H5')	(resi 16 and name H8)	5.00	2.00	1.00
assi (resi 16 and name H5'')	(resi 16 and name H8)	5.00	2.00	1.00
assi (resi 16 and name H2)	(resi 17 and name H1')	5.00	2.00	1.00
assi (resi 16 and name H2)	(resi 17 and name H2)	3.80	2.00	0.70
assi (resi 17 and name H1')	(resi 17 and name H2)	5.00	2.00	1.00
assi (resi 17 and name H1')	(resi 17 and name H8)	3.80	2.00	0.70
assi (resi 17 and name H2')	(resi 17 and name H8)	2.50	0.70	0.50
assi (resi 17 and name H2'')	(resi 17 and name H8)	3.80	2.00	0.70
assi (resi 17 and name H3')	(resi 17 and name H8)	5.00	2.00	1.00
assi (resi 17 and name H4')	(resi 17 and name H8)	5.00	2.00	1.00
assi (resi 17 and name H5')	(resi 17 and name H8)	5.00	2.00	1.00
assi (resi 17 and name H5'')	(resi 17 and name H8)	5.00	2.00	1.00

H-bond restraints verified by 13 interstrand correlations (mainly between adenine-H2 and H1' on the opposite strand).

assi (resi 1 and name H3)	(resi 17 and name N1)	1.90	0.30	0.30
assi (resi 1 and name N3)	(resi 17 and name N1)	2.90	0.30	0.30
assi (resi 1 and name O4)	(resi 17 and name H61)	1.90	0.30	0.30
assi (resi 1 and name O4)	(resi 17 and name N6)	2.90	0.30	0.30
assi (resi 2 and name H3)	(resi 16 and name N1)	1.90	0.10	0.10
assi (resi 2 and name N3)	(resi 16 and name N1)	2.90	0.10	0.10
assi (resi 2 and name O4)	(resi 16 and name H61)	1.90	0.10	0.10
assi (resi 2 and name O4)	(resi 16 and name N6)	2.90	0.10	0.10
assi (resi 3 and name N1)	(resi 15 and name H3)	1.90	0.10	0.10
assi (resi 3 and name N1)	(resi 15 and name N3)	2.90	0.10	0.10
assi (resi 3 and name H61)	(resi 15 and name O4)	1.90	0.10	0.10
assi (resi 3 and name N6)	(resi 15 and name O4)	2.90	0.10	0.10
assi (resi 4 and name N1)	(resi 14 and name H3)	1.90	0.10	0.10
assi (resi 4 and name N1)	(resi 14 and name N3)	2.90	0.10	0.10
assi (resi 4 and name H61)	(resi 14 and name O4)	1.90	0.10	0.10
assi (resi 4 and name N6)	(resi 14 and name O4)	2.90	0.10	0.10

assi (resi 5 and name H3)	(resi 13 and name N1)	1.90 0.10 0.10
assi (resi 5 and name N3)	(resi 13 and name N1)	2.90 0.10 0.10
assi (resi 5 and name O4)	(resi 13 and name H61)	1.90 0.10 0.10
assi (resi 5 and name O4)	(resi 13 and name N6)	2.90 0.10 0.10
assi (resi 6 and name H3)	(resi 12 and name N1)	1.90 0.10 0.10
assi (resi 6 and name N3)	(resi 12 and name N1)	2.90 0.10 0.10
assi (resi 6 and name O4)	(resi 12 and name H61)	1.90 0.10 0.10
assi (resi 6 and name O4)	(resi 12 and name N6)	2.90 0.10 0.10
assi (resi 7 and name H3)	(resi 11 and name N1)	1.90 0.30 0.30
assi (resi 7 and name N3)	(resi 11 and name N1)	2.90 0.30 0.30
assi (resi 7 and name O4)	(resi 11 and name H61)	1.90 0.30 0.30
assi (resi 7 and name O4)	(resi 11 and name N6)	2.90 0.30 0.30

Phosphate-sugar-backbone dihedral restraints based on a 1D [ $^{31}\text{P}$ ]-spectrum acquired at 400 MHz frequency at 298 K (100 %  $\text{D}_2\text{O}$ , 120 mM  $\text{NaClO}_4$ ) and cover the B-DNA range. Exact values were taken from the dihedral angle restraint files of the pdb entries 1RVI und 1RVH, which represent a DNA duplex.<sup>[260]</sup> Error boundaries of  $\pm 30^\circ$  were used for residues T1, T7, A11, A17 and  $\pm 20^\circ$  for residues T2, A3, A4, T5, T6, A12, A13, T14, T15, A16, respectively. Im8, Im9 and Im10 were left unrestrained.

assign	( resid n-1 and name O3')	( resid n and name P)	( resid n and name O5')	( resid n and name C5')	-60	{* $\alpha$ *}
assign	( resid n and name P)	( resid n and name O5')	( resid n and name C5')	( resid n and name C4')	-180	{* $\beta$ *}
assign	( resid n and name O5')	( resid n and name C5')	( resid n and name C4')	( resid n and name C3')	60	{* $\gamma$ *}
assign	( resid n and name C3')	( resid n and name O3')	( resid n+1 and name P)	( resid n+1 and name O5')	-90	{* $\zeta$ *}

Sugar pucker restraints based on a [ $^1\text{H}$ ,  $^1\text{H}$ ]-TOCSY spectrum acquired at 700 MHz frequency at 298 K (100 %  $\text{D}_2\text{O}$ , 120 mM  $\text{NaClO}_4$ ). Helical B-type DNA is usually 2'-endo and gives strong H1'-H2' and H1'-H3' crosspeak in TOCSY experiment. Exact values were taken from the dihedral angle restraint file of the pdb entries 1RVI und 1RVH, which represent a DNA duplex.<sup>[260]</sup> Error boundaries of  $\pm 30^\circ$  were used for residues T1, T7, Im8, Im9, Im10 A11, A17 and  $\pm 20^\circ$  for residues T2, A3, A4, T5, T6, A12, A13, T14, T15, A16, respectively.

assign	( resid n	and name C4')		
	( resid n	and name O4')		
	( resid n	and name C1')		
	( resid n	and name C2')	-20	{* v <sub>0</sub> *}
assign	( resid n	and name O4')		
	( resid n	and name C1')		
	( resid n	and name C2')		
	( resid n	and name C3')	33	{* v <sub>1</sub> *}
assign	( resid n	and name C1')		
	( resid n	and name C2')		
	( resid n	and name C3')		
	( resid n	and name C4')	-22	{* v <sub>2</sub> *}
assign	( resid n	and name C2')		
	( resid n	and name C3')		
	( resid n	and name C4')		
	( resid n	and name O4')	4	{* v <sub>3</sub> *}
assign	( resid n	and name C3')		
	( resid n	and name C4')		
	( resid n	and name O4')		
	( resid n	and name C1')	16	{* v <sub>4</sub> *}

The torsion angle  $\chi$  defines the orientation of the base to the sugar around the glycosidic bond.  $\chi$  was restrained to *anti* orientation for all residues, with error boundaries of  $\pm 30^\circ$  for residues T1, T7, A11, A17 and  $\pm 20^\circ$  for residues T2, A3, A4, T5, T6, A12, A13, T14, T15, A16, respectively. Im8, Im9 and Im10 were left unrestrained.

assign	( resid n	and name O4' )		
	( resid n	and name C1' )		
	( resid n	and name N9 )		
	( resid n	and name C4 )	-120	{* $\chi$ of purines*}
assign	( resid n	and name O4' )		
	( resid n	and name C1' )		
	( resid n	and name N1 )		
	( resid n	and name C4 )	-120	{* $\chi$ of pyrimidines*}



**Appendix 16** [<sup>1</sup>H]-NMR chemical shift assignments of the oligonucleotide DNA\_IMI in the presence of 1 eq silver(I) ions at pD 7.2.

	H1'	H2	H2'	H2''	H3'	H4	H4'	H5	H5'	H5''	H6	H7	H8
ppm													
<b>T1/T18</b>	5.93		2.03	2.42	4.62		4.02		3.65	3.65	7.48	1.63	
<b>T2/T19</b>	5.53		2.04	2.34	4.78		4.07		4.01	3.95	7.42	1.69	
<b>A3/A20</b>	5.87	6.98	2.74	2.85	4.99		4.35		4.01	4.08			8.24
<b>A4/A21</b>	6.14	7.54	2.53	2.85	4.94		4.42		4.19	4.22			8.12
<b>T5/T22</b>	5.84		1.94	2.47	4.76		4.12		4.07	4.24	7.09	1.22	
<b>T6/T23</b>	6.03		2.10	2.52	4.81		4.12		-	4.03	7.39	1.48	
<b>T7/T24</b>	5.84		2.08	2.49	4.8		4.05		4.19	4.03	7.34	1.61	
<b>Im8/Im25</b>	5.61	7.22	2.13	2.52	4.79	6.57	4.17	7.20	4.05	4.01			
<b>Im9/Im26</b>	5.50	7.08	2.09	2.49	4.76	6.26	4.16	6.98	-	4.00			
<b>Im10/Im27</b>	5.31	6.90	1.90	2.29	4.74	5.94	4.07	6.75	-	3.94			
<b>A11/A28</b>	5.62	7.05	2.63	2.74	4.91		4.24		3.99	3.88			8.12
<b>A12/A29</b>	5.77	6.92	2.49	2.77	4.92		4.32		-	4.10			7.92
<b>A13/A30</b>	6.01	7.50	2.42	2.8	4.88		4.35		4.13	4.15			7.95
<b>T14/T31</b>	5.77		1.81	2.38	4.73		4.08		4.01	4.22	6.99	1.15	
<b>T15/T32</b>	5.61		1.75	2.18	4.75		4.00		3.98	4.04	7.14	1.51	
<b>A16/A33</b>	5.85	7.27	2.56	2.66	4.91		4.26		4.02	3.97			8.02
<b>A17/A34</b>	6.12	7.64	2.48	2.27	4.59		4.12		4.17	4.05			8.01

**Appendix 17** All distance and dihedral angle restraints for the structure calculation of DNA\_IMI in the presence of 1 eq Ag<sup>+</sup> ions at pD 7.2.

Distance restraints of non-exchangeable protons based on a 2D [<sup>1</sup>H,<sup>1</sup>H]-NOESY spectrum acquired at 700 MHz frequency at 298 K (100 % D<sub>2</sub>O, 120 mM NaClO<sub>4</sub>). Based on the perfect C2 symmetry observed in the NMR spectra showing only one half of the duplex, the restraints of T1-A17 were set identical with the ones of T18-A34. Specified are the estimated distances in Å (left), as well as the lower (middle) and the upper (right) boundaries.

assi (resi 1 and name H1')	(resi 1 and name H6)	3.80	2.00	0.70
assi (resi 1 and name H1')	(resi 1 and name H51)	5.00	2.00	1.00
assi (resi 1 and name H1')	(resi 2 and name H4')	6.00	2.00	1.00
assi (resi 1 and name H1')	(resi 2 and name H5'')	3.80	2.00	0.70
assi (resi 1 and name H1')	(resi 2 and name H6)	3.80	2.00	0.70
assi (resi 1 and name H1')	(resi 2 and name H51)	5.00	2.00	1.00
assi (resi 1 and name H1')	(resi 34 and name H2)	6.00	2.00	1.00
assi (resi 1 and name H2')	(resi 1 and name H6)	2.50	0.70	0.50
assi (resi 1 and name H2')	(resi 1 and name H51)	5.00	2.00	1.00
assi (resi 1 and name H2')	(resi 2 and name H5'')	5.00	2.00	1.00
assi (resi 1 and name H2')	(resi 2 and name H6)	3.80	2.00	0.70
assi (resi 1 and name H2')	(resi 2 and name H51)	3.80	2.00	0.70
assi (resi 1 and name H2')	(resi 34 and name H2)	6.00	2.00	1.00
assi (resi 1 and name H2'')	(resi 1 and name H6)	3.80	2.00	0.70
assi (resi 1 and name H2'')	(resi 1 and name H51)	6.00	2.00	1.00
assi (resi 1 and name H2'')	(resi 2 and name H4')	6.00	2.00	1.00
assi (resi 1 and name H2'')	(resi 2 and name H5'')	3.80	2.00	0.70
assi (resi 1 and name H2'')	(resi 2 and name H6)	3.80	2.00	0.70
assi (resi 1 and name H2'')	(resi 2 and name H51)	3.80	2.00	0.70
assi (resi 1 and name H2'')	(resi 34 and name H2)	6.00	2.00	1.00
assi (resi 1 and name H3')	(resi 1 and name H6)	5.00	2.00	1.00
assi (resi 1 and name H3')	(resi 1 and name H51)	6.00	2.00	1.00
assi (resi 1 and name H3')	(resi 2 and name H51)	3.80	2.00	0.70
assi (resi 1 and name H4')	(resi 1 and name H6)	3.80	2.00	0.70
assi (resi 1 and name H4')	(resi 1 and name H51)	6.00	2.00	1.00
assi (resi 1 and name H4')	(resi 2 and name H51)	5.00	2.00	1.00
assi (resi 1 and name H5')	(resi 1 and name H6)	2.50	0.70	0.50
assi (resi 1 and name H5')	(resi 1 and name H51)	5.00	2.00	1.00
assi (resi 1 and name H5')	(resi 2 and name H51)	5.00	2.00	1.00
assi (resi 1 and name H5'')	(resi 1 and name H6)	3.80	2.00	0.70
assi (resi 1 and name H5')	(resi 1 and name H51)	5.00	2.00	1.00
assi (resi 1 and name H5'')	(resi 2 and name H6)	6.00	2.00	1.00
assi (resi 1 and name H5'')	(resi 2 and name H51)	5.00	2.00	1.00
assi (resi 1 and name H6)	(resi 2 and name H5'')	6.00	2.00	1.00
assi (resi 1 and name H6)	(resi 2 and name H51)	3.80	2.00	0.70
assi (resi 2 and name H1')	(resi 2 and name H6)	3.80	2.00	0.70
assi (resi 2 and name H1')	(resi 2 and name H51)	5.00	2.00	1.00
assi (resi 2 and name H1')	(resi 3 and name H1')	5.00	2.00	1.00
assi (resi 2 and name H1')	(resi 3 and name H4')	6.00	2.00	1.00
assi (resi 2 and name H1')	(resi 3 and name H8)	3.80	2.00	0.70
assi (resi 2 and name H1')	(resi 34 and name H2)	5.00	2.00	1.00

assi (resi 2 and name H2')	(resi 2 and name H6)	2.50	0.70	0.50
assi (resi 2 and name H2')	(resi 2 and name H51)	5.00	2.00	1.00
assi (resi 2 and name H2')	(resi 3 and name H8)	3.80	2.00	0.70
assi (resi 2 and name H2'')	(resi 2 and name H6)	3.80	2.00	0.70
assi (resi 2 and name H2'')	(resi 2 and name H51)	5.00	2.00	1.00
assi (resi 2 and name H2'')	(resi 3 and name H2')	6.00	2.00	1.00
assi (resi 2 and name H2'')	(resi 3 and name H4')	6.00	2.00	1.00
assi (resi 2 and name H2'')	(resi 3 and name H8)	3.80	2.00	0.70
assi (resi 2 and name H3')	(resi 2 and name H6)	5.00	2.00	1.00
assi (resi 2 and name H4')	(resi 2 and name H6)	5.00	2.00	1.00
assi (resi 2 and name H4')	(resi 2 and name H51)	6.00	2.00	1.00
assi (resi 2 and name H5')	(resi 2 and name H6)	5.00	2.00	1.00
assi (resi 2 and name H5'')	(resi 2 and name H6)	3.80	2.00	0.70
assi (resi 2 and name H5'')	(resi 2 and name H51)	5.00	2.00	1.00
assi (resi 2 and name H5'')	(resi 3 and name H8)	6.00	2.00	1.00
assi (resi 2 and name H6)	(resi 3 and name H8)	5.00	2.00	0.70
assi (resi 2 and name H51)	(resi 34 and name H2)	6.00	2.00	1.00
assi (resi 3 and name H1')	(resi 3 and name H2)	5.00	2.00	1.00
assi (resi 3 and name H1')	(resi 3 and name H8)	3.80	2.00	0.70
assi (resi 3 and name H1')	(resi 4 and name H1')	6.00	2.00	1.00
assi (resi 3 and name H1')	(resi 4 and name H4')	6.00	2.00	1.00
assi (resi 3 and name H1')	(resi 4 and name H5'')	5.00	2.00	1.00
assi (resi 3 and name H1')	(resi 4 and name H8)	3.80	2.00	0.70
assi (resi 3 and name H1')	(resi 33 and name H2)	5.00	2.00	1.00
assi (resi 3 and name H2')	(resi 3 and name H8)	2.50	0.70	0.50
assi (resi 3 and name H2')	(resi 4 and name H5'')	5.00	2.00	1.00
assi (resi 3 and name H2')	(resi 4 and name H8)	3.80	2.00	0.70
assi (resi 3 and name H2'')	(resi 3 and name H8)	3.80	2.00	0.70
assi (resi 3 and name H2'')	(resi 4 and name H5'')	3.80	2.00	0.70
assi (resi 3 and name H2'')	(resi 4 and name H8)	2.50	0.70	0.50
assi (resi 3 and name H3')	(resi 3 and name H8)	3.80	2.00	0.70
assi (resi 3 and name H3')	(resi 4 and name H8)	5.00	2.00	1.00
assi (resi 3 and name H4')	(resi 3 and name H8)	5.00	2.00	1.00
assi (resi 3 and name H4')	(resi 4 and name H8)	6.00	2.00	1.00
assi (resi 3 and name H5')	(resi 3 and name H8)	5.00	2.00	1.00
assi (resi 3 and name H5'')	(resi 3 and name H8)	5.00	2.00	1.00
assi (resi 3 and name H5'')	(resi 4 and name H8)	6.00	2.00	1.00
assi (resi 3 and name H2)	(resi 4 and name H1')	5.00	2.00	1.00
assi (resi 3 and name H2)	(resi 4 and name H2)	3.80	2.00	0.70
assi (resi 3 and name H2)	(resi 33 and name H1')	5.00	2.00	1.00
assi (resi 3 and name H2)	(resi 33 and name H2)	3.80	2.00	0.70
assi (resi 3 and name H2)	(resi 33 and name H8)	5.00	2.00	1.00
assi (resi 3 and name H8)	(resi 4 and name H8)	5.00	2.00	1.00
assi (resi 4 and name H1')	(resi 4 and name H2)	5.00	2.00	1.00
assi (resi 4 and name H1')	(resi 4 and name H8)	3.80	2.00	0.70
assi (resi 4 and name H1')	(resi 5 and name H1')	6.00	2.00	1.00
assi (resi 4 and name H1')	(resi 5 and name H5'')	3.80	2.00	0.70
assi (resi 4 and name H1')	(resi 5 and name H6)	3.80	2.00	0.70
assi (resi 4 and name H1')	(resi 5 and name H51)	3.80	2.00	0.70

assi (resi 4 and name H1')	(resi 6 and name H51)	6.00	2.00	1.00
assi (resi 4 and name H2')	(resi 4 and name H8)	2.50	0.70	0.50
assi (resi 4 and name H2')	(resi 5 and name H6)	3.80	2.00	0.70
assi (resi 4 and name H2')	(resi 5 and name H51)	3.80	2.00	0.70
assi (resi 4 and name H2'')	(resi 4 and name H8)	3.80	2.00	0.70
assi (resi 4 and name H2'')	(resi 5 and name H2')	6.00	2.00	1.00
assi (resi 4 and name H2'')	(resi 5 and name H6)	3.80	2.00	0.70
assi (resi 4 and name H2'')	(resi 5 and name H51)	3.80	2.00	0.70
assi (resi 4 and name H2'')	(resi 6 and name H51)	5.00	2.00	1.00
assi (resi 4 and name H3')	(resi 4 and name H8)	3.80	2.00	0.70
assi (resi 4 and name H3')	(resi 5 and name H6)	5.00	2.00	1.00
assi (resi 4 and name H3')	(resi 5 and name H51)	3.80	2.00	0.70
assi (resi 4 and name H4')	(resi 4 and name H8)	5.00	2.00	1.00
assi (resi 4 and name H4')	(resi 5 and name H51)	5.00	2.00	1.00
assi (resi 4 and name H5')	(resi 4 and name H8)	5.00	2.00	1.00
assi (resi 4 and name H5'')	(resi 4 and name H8)	5.00	2.00	1.00
assi (resi 4 and name H2)	(resi 5 and name H1')	3.80	2.00	0.70
assi (resi 4 and name H2)	(resi 5 and name H4')	6.00	2.00	1.00
assi (resi 4 and name H2)	(resi 32 and name H1')	5.00	2.00	1.00
assi (resi 4 and name H8)	(resi 5 and name H6)	5.00	2.00	1.00
assi (resi 4 and name H8)	(resi 5 and name H51)	3.80	2.00	0.70
assi (resi 5 and name H1')	(resi 5 and name H6)	3.80	2.00	0.70
assi (resi 5 and name H1')	(resi 5 and name H51)	5.00	2.00	1.00
assi (resi 5 and name H1')	(resi 6 and name H1')	6.00	2.00	1.00
assi (resi 5 and name H1')	(resi 6 and name H5'')	5.00	2.00	1.00
assi (resi 5 and name H1')	(resi 6 and name H6)	3.80	2.00	0.70
assi (resi 5 and name H1')	(resi 6 and name H51)	3.80	2.00	0.70
assi (resi 5 and name H1')	(resi 30 and name H2)	6.00	2.00	1.00
assi (resi 5 and name H2')	(resi 5 and name H6)	2.50	0.70	0.50
assi (resi 5 and name H2')	(resi 5 and name H51)	5.00	2.00	1.00
assi (resi 5 and name H2')	(resi 6 and name H5'')	5.00	2.00	1.00
assi (resi 5 and name H2')	(resi 6 and name H6)	3.80	2.00	0.70
assi (resi 5 and name H2')	(resi 6 and name H51)	3.80	2.00	0.70
assi (resi 5 and name H2'')	(resi 5 and name H6)	3.80	2.00	0.70
assi (resi 5 and name H2'')	(resi 5 and name H51)	5.00	2.00	1.00
assi (resi 5 and name H2'')	(resi 6 and name H6)	3.80	2.00	0.70
assi (resi 5 and name H2'')	(resi 6 and name H51)	3.80	2.00	0.70
assi (resi 5 and name H3')	(resi 5 and name H6)	6.00	2.00	1.00
assi (resi 5 and name H3')	(resi 5 and name H51)	5.00	2.00	1.00
assi (resi 5 and name H3')	(resi 6 and name H51)	5.00	2.00	1.00
assi (resi 5 and name H4')	(resi 5 and name H6)	5.00	2.00	1.00
assi (resi 5 and name H4')	(resi 5 and name H51)	6.00	2.00	1.00
assi (resi 5 and name H5')	(resi 5 and name H6)	5.00	2.00	1.00
assi (resi 5 and name H5')	(resi 5 and name H51)	6.00	2.00	1.00
assi (resi 5 and name H5'')	(resi 5 and name H6)	5.00	2.00	1.00
assi (resi 5 and name H5'')	(resi 5 and name H51)	6.00	2.00	1.00
assi (resi 5 and name H6)	(resi 6 and name H6)	5.00	2.00	1.00
assi (resi 5 and name H6)	(resi 6 and name H51)	3.80	2.00	0.70
assi (resi 5 and name H51)	(resi 6 and name H6)	6.00	2.00	1.00
assi (resi 5 and name H51)	(resi 6 and name H51)	5.00	2.00	1.00

---

assi (resi 6 and name H1')	(resi 6 and name H6)	3.80	2.00	0.70
assi (resi 6 and name H1')	(resi 6 and name H51)	5.00	2.00	1.00
assi (resi 6 and name H1')	(resi 7 and name H1')	6.00	2.00	1.00
assi (resi 6 and name H1')	(resi 7 and name H6)	3.80	2.00	0.70
assi (resi 6 and name H1')	(resi 7 and name H51)	3.80	2.00	0.70
assi (resi 6 and name H1')	(resi 30 and name H2)	5.00	2.00	1.00
assi (resi 6 and name H2')	(resi 6 and name H6)	2.50	0.70	0.50
assi (resi 6 and name H2')	(resi 6 and name H51)	5.00	2.00	1.00
assi (resi 6 and name H2')	(resi 7 and name H6)	3.80	2.00	0.70
assi (resi 6 and name H2')	(resi 7 and name H51)	3.80	2.00	0.70
assi (resi 6 and name H2'')	(resi 6 and name H6)	3.80	2.00	0.70
assi (resi 6 and name H2'')	(resi 6 and name H51)	5.00	2.00	1.00
assi (resi 6 and name H2'')	(resi 7 and name H6)	3.80	2.00	0.70
assi (resi 6 and name H2'')	(resi 7 and name H51)	3.80	2.00	0.70
assi (resi 6 and name H3')	(resi 6 and name H6)	3.80	2.00	0.70
assi (resi 6 and name H3')	(resi 6 and name H51)	5.00	2.00	1.00
assi (resi 6 and name H3')	(resi 7 and name H6)	5.00	2.00	1.00
assi (resi 6 and name H4')	(resi 6 and name H6)	5.00	2.00	1.00
assi (resi 6 and name H4')	(resi 6 and name H51)	6.00	2.00	1.00
assi (resi 6 and name H4')	(resi 7 and name H6)	5.00	2.00	1.00
assi (resi 6 and name H4')	(resi 7 and name H51)	5.00	2.00	1.00
assi (resi 6 and name H5'')	(resi 6 and name H6)	3.80	2.00	0.70
assi (resi 6 and name H6)	(resi 7 and name H51)	3.80	2.00	0.70
assi (resi 6 and name H51)	(resi 7 and name H6)	6.00	2.00	1.00
assi (resi 6 and name H51)	(resi 7 and name H51)	5.00	2.00	1.00
assi (resi 7 and name H1')	(resi 7 and name H6)	3.80	2.00	0.70
assi (resi 7 and name H1')	(resi 7 and name H51)	5.00	2.00	1.00
assi (resi 7 and name H1')	(resi 8 and name H4)	5.00	2.00	1.00
assi (resi 7 and name H1')	(resi 8 and name H5)	3.80	2.00	0.70
assi (resi 7 and name H1')	(resi 29 and name H2)	5.00	2.00	1.00
assi (resi 7 and name H2')	(resi 7 and name H6)	3.80	2.00	0.70
assi (resi 7 and name H2')	(resi 7 and name H51)	5.00	2.00	1.00
assi (resi 7 and name H2')	(resi 8 and name H4)	5.00	2.00	1.00
assi (resi 7 and name H2')	(resi 8 and name H5)	3.80	2.00	1.00
assi (resi 7 and name H2'')	(resi 7 and name H6)	3.80	2.00	0.70
assi (resi 7 and name H2'')	(resi 7 and name H51)	5.00	2.00	1.00
assi (resi 7 and name H2'')	(resi 8 and name H4)	5.00	2.00	1.00
assi (resi 7 and name H2'')	(resi 8 and name H5)	3.80	2.00	0.70
assi (resi 7 and name H3')	(resi 7 and name H6)	3.80	2.00	0.70
assi (resi 7 and name H3')	(resi 7 and name H6)	6.00	2.00	1.00
assi (resi 7 and name H4')	(resi 7 and name H6)	5.00	2.00	1.00
assi (resi 7 and name H4')	(resi 7 and name H51)	6.00	2.00	1.00
assi (resi 7 and name H5')	(resi 7 and name H6)	5.00	2.00	1.00
assi (resi 7 and name H5'')	(resi 7 and name H6)	5.00	2.00	1.00
assi (resi 7 and name H5'')	(resi 7 and name H51)	6.00	2.00	1.00
assi (resi 7 and name H6)	(resi 8 and name H4)	5.00	2.00	1.00
assi (resi 7 and name H6)	(resi 8 and name H5)	5.00	2.00	1.00
assi (resi 7 and name H51)	(resi 8 and name H4)	5.00	2.00	1.00

[illegible]

assi (resi 9 and name H3')	(resi 10 and name H5)	5.00	2.00	1.00
assi (resi 9 and name H4')	(resi 9 and name H2)	6.00	2.00	1.00
assi (resi 9 and name H4')	(resi 9 and name H5)	5.00	2.00	1.00
assi (resi 9 and name H4')	(resi 10 and name H5)	6.00	2.00	1.00
assi (resi 9 and name H5")	(resi 9 and name H2)	6.00	2.00	1.00
assi (resi 9 and name H5")	(resi 9 and name H5)	5.00	2.00	1.00
assi (resi 9 and name H2)	(resi 10 and name H5")	6.00	2.00	1.00
assi (resi 9 and name H2)	(resi 10 and name H2)	6.00	2.00	1.00
assi (resi 9 and name H2)	(resi 10 and name H4)	6.00	2.00	1.00
assi (resi 9 and name H2)	(resi 10 and name H5)	6.00	2.00	1.00
assi (resi 9 and name H4)	(resi 10 and name H4)	3.80	2.00	0.70
assi (resi 9 and name H4)	(resi 10 and name H5)	6.00	2.00	1.00
assi (resi 9 and name H5)	(resi 10 and name H5")	6.00	2.00	1.00
assi (resi 9 and name H5)	(resi 10 and name H4)	5.00	2.00	1.00
assi (resi 9 and name H5)	(resi 10 and name H5)	5.00	2.00	1.00
assi (resi 10 and name H1')	(resi 10 and name H2)	3.80	2.00	0.70
assi (resi 10 and name H1')	(resi 10 and name H4)	6.00	2.00	1.00
assi (resi 10 and name H1')	(resi 10 and name H5)	5.00	2.00	1.00
assi (resi 10 and name H1')	(resi 11 and name H4')	5.00	2.00	1.00
assi (resi 10 and name H1')	(resi 11 and name H5')	5.00	2.00	1.00
assi (resi 10 and name H1')	(resi 11 and name H5")	5.00	2.00	1.00
assi (resi 10 and name H1')	(resi 11 and name H8)	6.00	2.00	1.00
assi (resi 10 and name H2')	(resi 10 and name H2)	5.00	2.00	1.00
assi (resi 10 and name H2')	(resi 10 and name H4)	5.00	2.00	1.00
assi (resi 10 and name H2')	(resi 10 and name H5)	3.80	2.00	0.70
assi (resi 10 and name H2')	(resi 11 and name H4')	6.00	2.00	1.00
assi (resi 10 and name H2')	(resi 11 and name H5")	6.00	2.00	1.00
assi (resi 10 and name H2')	(resi 11 and name H8)	5.00	2.00	1.00
assi (resi 10 and name H2")	(resi 10 and name H2)	5.00	2.00	1.00
assi (resi 10 and name H2")	(resi 10 and name H4)	5.00	2.00	1.00
assi (resi 10 and name H2")	(resi 10 and name H5)	3.80	2.00	0.70
assi (resi 10 and name H2")	(resi 11 and name H4')	6.00	2.00	1.00
assi (resi 10 and name H2")	(resi 11 and name H5")	6.00	2.00	1.00
assi (resi 10 and name H2")	(resi 11 and name H8)	5.00	2.00	1.00
assi (resi 10 and name H3')	(resi 10 and name H5)	5.00	2.00	1.00
assi (resi 10 and name H4')	(resi 10 and name H2)	6.00	2.00	1.00
assi (resi 10 and name H4')	(resi 10 and name H5)	6.00	2.00	1.00
assi (resi 10 and name H5")	(resi 10 and name H5)	5.00	2.00	1.00
assi (resi 10 and name H5)	(resi 11 and name H2)	6.00	2.00	1.00
assi (resi 10 and name H5)	(resi 11 and name H8)	6.00	2.00	1.00
assi (resi 11 and name H1')	(resi 11 and name H2)	5.00	2.00	1.00
assi (resi 11 and name H1')	(resi 11 and name H8)	3.80	2.00	0.70
assi (resi 11 and name H1')	(resi 12 and name H1')	5.00	2.00	1.00
assi (resi 11 and name H1')	(resi 12 and name H4')	6.00	2.00	1.00
assi (resi 11 and name H1')	(resi 12 and name H5")	5.00	2.00	1.00
assi (resi 11 and name H1')	(resi 12 and name H8)	3.80	2.00	0.70
assi (resi 11 and name H2')	(resi 11 and name H8)	2.50	0.70	0.50
assi (resi 11 and name H2')	(resi 12 and name H5")	5.00	2.00	1.00
assi (resi 11 and name H2')	(resi 12 and name H8)	3.80	2.00	1.00

---

assi (resi 11 and name H2")	(resi 11 and name H8)	3.80	2.00	0.70
assi (resi 11 and name H2")	(resi 12 and name H8)	3.80	2.00	0.70
assi (resi 11 and name H3')	(resi 11 and name H8)	5.00	2.00	1.00
assi (resi 11 and name H4')	(resi 11 and name H8)	6.00	2.00	1.00
assi (resi 11 and name H4')	(resi 12 and name H8)	6.00	2.00	1.00
assi (resi 11 and name H5')	(resi 11 and name H8)	6.00	2.00	1.00
assi (resi 11 and name H2)	(resi 12 and name H1')	6.00	2.00	1.00
assi (resi 11 and name H2)	(resi 12 and name H2)	5.00	2.00	1.00
assi (resi 11 and name H8)	(resi 12 and name H8)	5.00	2.00	1.00
assi (resi 12 and name H1')	(resi 12 and name H2)	5.00	2.00	1.00
assi (resi 12 and name H1')	(resi 12 and name H8)	3.80	2.00	0.70
assi (resi 12 and name H1')	(resi 13 and name H1')	5.00	2.00	1.00
assi (resi 12 and name H1')	(resi 13 and name H4')	5.00	2.00	1.00
assi (resi 12 and name H1')	(resi 13 and name H5")	5.00	2.00	1.00
assi (resi 12 and name H1')	(resi 13 and name H8)	3.80	2.00	0.70
assi (resi 12 and name H2')	(resi 12 and name H2)	6.00	2.00	1.00
assi (resi 12 and name H2')	(resi 12 and name H8)	2.50	0.70	0.50
assi (resi 12 and name H2')	(resi 13 and name H8)	3.80	2.00	0.70
assi (resi 12 and name H2")	(resi 12 and name H8)	3.80	2.00	0.70
assi (resi 12 and name H2")	(resi 13 and name H5")	3.80	2.00	0.70
assi (resi 12 and name H2")	(resi 13 and name H8)	2.50	0.50	0.70
assi (resi 12 and name H3')	(resi 12 and name H8)	5.00	2.00	1.00
assi (resi 12 and name H3')	(resi 13 and name H8)	6.00	2.00	1.00
assi (resi 12 and name H4')	(resi 12 and name H8)	5.00	2.00	1.00
assi (resi 12 and name H4')	(resi 13 and name H8)	6.00	2.00	1.00
assi (resi 12 and name H5")	(resi 12 and name H8)	5.00	2.00	1.00
assi (resi 12 and name H2)	(resi 13 and name H1')	5.00	2.00	1.00
assi (resi 12 and name H2)	(resi 13 and name H2)	3.80	2.00	0.70
assi (resi 13 and name H1')	(resi 13 and name H2)	5.00	2.00	1.00
assi (resi 13 and name H1')	(resi 13 and name H8)	3.80	2.00	0.70
assi (resi 13 and name H1')	(resi 14 and name H1')	6.00	2.00	1.00
assi (resi 13 and name H1')	(resi 14 and name H5")	3.80	2.00	0.70
assi (resi 13 and name H1')	(resi 14 and name H6)	3.80	2.00	0.70
assi (resi 13 and name H1')	(resi 14 and name H51)	5.00	2.00	0.70
assi (resi 13 and name H1')	(resi 15 and name H51)	6.00	2.00	1.00
assi (resi 13 and name H2')	(resi 13 and name H8)	3.80	2.00	0.70
assi (resi 13 and name H2')	(resi 14 and name H6)	3.80	2.00	0.70
assi (resi 13 and name H2')	(resi 14 and name H51)	3.80	2.00	0.70
assi (resi 13 and name H2")	(resi 13 and name H8)	3.80	2.00	0.70
assi (resi 13 and name H2")	(resi 14 and name H2')	5.00	2.00	1.00
assi (resi 13 and name H2")	(resi 14 and name H5")	3.80	2.00	0.70
assi (resi 13 and name H2")	(resi 14 and name H6)	3.80	2.00	0.70
assi (resi 13 and name H2")	(resi 14 and name H51)	3.80	2.00	0.70
assi (resi 13 and name H2")	(resi 15 and name H51)	5.00	2.00	1.00
assi (resi 13 and name H3')	(resi 13 and name H8)	3.80	2.00	0.70
assi (resi 13 and name H3')	(resi 14 and name H6)	5.00	2.00	1.00
assi (resi 13 and name H3')	(resi 14 and name H51)	3.80	2.00	1.00
assi (resi 13 and name H4')	(resi 13 and name H8)	5.00	2.00	1.00
assi (resi 13 and name H4')	(resi 14 and name H6)	6.00	2.00	1.00



assi (resi 13 and name H4')	(resi 14 and name H51)	5.00	2.00	1.00
assi (resi 13 and name H5')	(resi 13 and name H8)	5.00	2.00	1.00
assi (resi 13 and name H5'')	(resi 13 and name H8)	5.00	2.00	1.00
assi (resi 13 and name H5'')	(resi 14 and name H51)	5.00	2.00	1.00
assi (resi 13 and name H2)	(resi 14 and name H1')	5.00	2.00	1.00
assi (resi 13 and name H2)	(resi 14 and name H51)	6.00	2.00	1.00
assi (resi 13 and name H8)	(resi 14 and name H6)	5.00	2.00	1.00
assi (resi 13 and name H8)	(resi 14 and name H51)	3.80	2.00	0.70
assi (resi 14 and name H1')	(resi 14 and name H6)	3.80	2.00	0.70
assi (resi 14 and name H1')	(resi 14 and name H51)	5.00	2.00	1.00
assi (resi 14 and name H1')	(resi 15 and name H1')	5.00	2.00	1.00
assi (resi 14 and name H1')	(resi 15 and name H5'')	5.00	2.00	1.00
assi (resi 14 and name H1')	(resi 15 and name H6)	3.80	2.00	0.70
assi (resi 14 and name H1')	(resi 15 and name H51)	3.80	2.00	0.70
assi (resi 14 and name H2')	(resi 14 and name H6)	3.80	2.00	0.70
assi (resi 14 and name H2')	(resi 14 and name H51)	5.00	2.00	1.00
assi (resi 14 and name H2')	(resi 15 and name H5'')	5.00	2.00	1.00
assi (resi 14 and name H2')	(resi 15 and name H6)	3.80	2.00	0.70
assi (resi 14 and name H2')	(resi 15 and name H51)	3.80	2.00	0.70
assi (resi 14 and name H2'')	(resi 14 and name H6)	3.80	2.00	0.70
assi (resi 14 and name H2'')	(resi 14 and name H51)	6.00	2.00	1.00
assi (resi 14 and name H2'')	(resi 15 and name H2')	5.00	2.00	1.00
assi (resi 14 and name H2'')	(resi 15 and name H5'')	5.00	2.00	1.00
assi (resi 14 and name H2'')	(resi 15 and name H6)	3.80	2.00	0.70
assi (resi 14 and name H2'')	(resi 15 and name H51)	3.80	2.00	0.70
assi (resi 14 and name H4')	(resi 14 and name H6)	5.00	2.00	1.00
assi (resi 14 and name H4')	(resi 14 and name H51)	6.00	2.00	1.00
assi (resi 14 and name H4')	(resi 15 and name H6)	5.00	2.00	1.00
assi (resi 14 and name H4')	(resi 15 and name H51)	5.00	2.00	1.00
assi (resi 14 and name H5')	(resi 14 and name H6)	5.00	2.00	1.00
assi (resi 14 and name H5'')	(resi 14 and name H6)	5.00	2.00	1.00
assi (resi 14 and name H5'')	(resi 14 and name H51)	5.00	2.00	1.00
assi (resi 14 and name H6)	(resi 15 and name H6)	3.80	2.00	0.70
assi (resi 14 and name H6)	(resi 15 and name H51)	3.80	2.00	0.70
assi (resi 14 and name H51)	(resi 15 and name H6)	6.00	2.00	1.00
assi (resi 14 and name H51)	(resi 15 and name H51)	5.00	2.00	1.00
assi (resi 15 and name H1')	(resi 15 and name H6)	3.80	2.00	0.70
assi (resi 15 and name H1')	(resi 15 and name H51)	5.00	2.00	1.00
assi (resi 15 and name H1')	(resi 16 and name H1')	5.00	2.00	1.00
assi (resi 15 and name H1')	(resi 16 and name H4')	5.00	2.00	1.00
assi (resi 15 and name H1')	(resi 16 and name H5'')	5.00	2.00	1.00
assi (resi 15 and name H1')	(resi 16 and name H8)	3.80	2.00	0.70
assi (resi 15 and name H2')	(resi 15 and name H6)	2.50	0.70	0.50
assi (resi 15 and name H2')	(resi 15 and name H51)	5.00	2.00	1.00
assi (resi 15 and name H2')	(resi 16 and name H5'')	5.00	2.00	1.00
assi (resi 15 and name H2')	(resi 16 and name H8)	3.80	2.00	0.70
assi (resi 15 and name H2'')	(resi 15 and name H6)	3.80	2.00	0.70
assi (resi 15 and name H2'')	(resi 15 and name H51)	5.00	2.00	1.00
assi (resi 15 and name H2'')	(resi 16 and name H4')	5.00	2.00	1.00

assi (resi 15 and name H2")	(resi 16 and name H5")	3.80	2.00	0.70
assi (resi 15 and name H2")	(resi 16 and name H8)	3.80	2.00	0.70
assi (resi 15 and name H4')	(resi 15 and name H6)	5.00	2.00	1.00
assi (resi 15 and name H5')	(resi 15 and name H6)	5.00	2.00	1.00
assi (resi 15 and name H5')	(resi 15 and name H51)	6.00	2.00	1.00
assi (resi 15 and name H5")	(resi 15 and name H6)	5.00	2.00	1.00
assi (resi 15 and name H5")	(resi 15 and name H51)	6.00	2.00	1.00
assi (resi 15 and name H6)	(resi 16 and name H8)	5.00	2.00	1.00
assi (resi 16 and name H1')	(resi 16 and name H2)	5.00	2.00	1.00
assi (resi 16 and name H1')	(resi 16 and name H8)	3.80	2.00	0.70
assi (resi 16 and name H1')	(resi 17 and name H1')	5.00	2.00	1.00
assi (resi 16 and name H1')	(resi 17 and name H5')	5.00	2.00	1.00
assi (resi 16 and name H1')	(resi 17 and name H5")	5.00	2.00	1.00
assi (resi 16 and name H1')	(resi 17 and name H8)	3.80	2.00	0.70
assi (resi 16 and name H2')	(resi 16 and name H8)	2.50	0.70	0.50
assi (resi 16 and name H2')	(resi 17 and name H8)	3.80	2.00	0.70
assi (resi 16 and name H2")	(resi 16 and name H8)	3.80	2.00	0.70
assi (resi 16 and name H2")	(resi 17 and name H2')	5.00	2.00	1.00
assi (resi 16 and name H2")	(resi 17 and name H4')	6.00	2.00	1.00
assi (resi 16 and name H2")	(resi 17 and name H5')	5.00	2.00	1.00
assi (resi 16 and name H2")	(resi 17 and name H5")	5.00	2.00	1.00
assi (resi 16 and name H2")	(resi 17 and name H8)	3.80	2.00	0.70
assi (resi 16 and name H3')	(resi 16 and name H8)	3.80	2.00	0.70
assi (resi 16 and name H3')	(resi 17 and name H8)	5.00	2.00	1.00
assi (resi 16 and name H4')	(resi 16 and name H8)	5.00	2.00	1.00
assi (resi 16 and name H4')	(resi 17 and name H8)	6.00	2.00	1.00
assi (resi 16 and name H5')	(resi 16 and name H8)	5.00	2.00	1.00
assi (resi 16 and name H5")	(resi 16 and name H8)	5.00	2.00	1.00
assi (resi 16 and name H2)	(resi 17 and name H1')	5.00	2.00	1.00
assi (resi 16 and name H2)	(resi 17 and name H2)	3.80	2.00	0.70
assi (resi 16 and name H2)	(resi 17 and name H8)	6.00	2.00	1.00
assi (resi 17 and name H1')	(resi 17 and name H2)	5.00	2.00	1.00
assi (resi 17 and name H1')	(resi 17 and name H8)	3.80	2.00	0.70
assi (resi 17 and name H2')	(resi 17 and name H8)	2.50	0.70	0.50
assi (resi 17 and name H2")	(resi 17 and name H8)	3.80	2.00	0.70
assi (resi 17 and name H3')	(resi 17 and name H8)	5.00	2.00	1.00
assi (resi 17 and name H4')	(resi 17 and name H8)	5.00	2.00	1.00
assi (resi 17 and name H5')	(resi 17 and name H8)	5.00	2.00	1.00
assi (resi 17 and name H5")	(resi 17 and name H8)	5.00	2.00	1.00
assi (resi 18 and name H1')	(resi 18 and name H6)	3.80	2.00	0.70
assi (resi 18 and name H1')	(resi 18 and name H51)	5.00	2.00	1.00
assi (resi 18 and name H1')	(resi 19 and name H4')	6.00	2.00	1.00
assi (resi 18 and name H1')	(resi 19 and name H5")	3.80	2.00	0.70
assi (resi 18 and name H1')	(resi 19 and name H6)	3.80	2.00	0.70
assi (resi 18 and name H1')	(resi 19 and name H51)	5.00	2.00	1.00
assi (resi 18 and name H1')	(resi 17 and name H2)	6.00	2.00	1.00
assi (resi 18 and name H2')	(resi 18 and name H6)	2.50	0.70	0.50
assi (resi 18 and name H2')	(resi 18 and name H51)	5.00	2.00	1.00

---

assi (resi 18 and name H2')	(resi 19 and name H5")	5.00	2.00	1.00
assi (resi 18 and name H2')	(resi 19 and name H6)	3.80	2.00	0.70
assi (resi 18 and name H2')	(resi 19 and name H51)	3.80	2.00	0.70
assi (resi 18 and name H2')	(resi 17 and name H2)	6.00	2.00	1.00
assi (resi 18 and name H2")	(resi 18 and name H6)	3.80	2.00	0.70
assi (resi 18 and name H2")	(resi 18 and name H51)	6.00	2.00	1.00
assi (resi 18 and name H2")	(resi 19 and name H4')	6.00	2.00	1.00
assi (resi 18 and name H2")	(resi 19 and name H5")	3.80	2.00	0.70
assi (resi 18 and name H2")	(resi 19 and name H6)	3.80	2.00	0.70
assi (resi 18 and name H2")	(resi 19 and name H51)	3.80	2.00	0.70
assi (resi 18 and name H2")	(resi 17 and name H2)	6.00	2.00	1.00
assi (resi 18 and name H3')	(resi 18 and name H6)	5.00	2.00	1.00
assi (resi 18 and name H3')	(resi 18 and name H51)	6.00	2.00	1.00
assi (resi 18 and name H3')	(resi 19 and name H51)	3.80	2.00	0.70
assi (resi 18 and name H4')	(resi 18 and name H6)	3.80	2.00	0.70
assi (resi 18 and name H4')	(resi 18 and name H51)	6.00	2.00	1.00
assi (resi 18 and name H4')	(resi 19 and name H51)	5.00	2.00	1.00
assi (resi 18 and name H5')	(resi 18 and name H6)	2.50	0.70	0.50
assi (resi 18 and name H5')	(resi 18 and name H51)	5.00	2.00	1.00
assi (resi 18 and name H5')	(resi 19 and name H51)	5.00	2.00	1.00
assi (resi 18 and name H5")	(resi 18 and name H6)	3.80	2.00	0.70
assi (resi 18 and name H5')	(resi 18 and name H51)	5.00	2.00	1.00
assi (resi 18 and name H5")	(resi 19 and name H6)	6.00	2.00	1.00
assi (resi 18 and name H5")	(resi 19 and name H51)	5.00	2.00	1.00
assi (resi 18 and name H6)	(resi 19 and name H5")	6.00	2.00	1.00
assi (resi 18 and name H6)	(resi 19 and name H51)	3.80	2.00	0.70
assi (resi 19 and name H1')	(resi 19 and name H6)	3.80	2.00	0.70
assi (resi 19 and name H1')	(resi 19 and name H51)	5.00	2.00	1.00
assi (resi 19 and name H1')	(resi 20 and name H1')	5.00	2.00	1.00
assi (resi 19 and name H1')	(resi 20 and name H4')	6.00	2.00	1.00
assi (resi 19 and name H1')	(resi 20 and name H8)	3.80	2.00	0.70
assi (resi 19 and name H1')	(resi 17 and name H2)	5.00	2.00	1.00
assi (resi 19 and name H2')	(resi 19 and name H6)	2.50	0.70	0.50
assi (resi 19 and name H2')	(resi 19 and name H51)	5.00	2.00	1.00
assi (resi 19 and name H2')	(resi 20 and name H8)	3.80	2.00	0.70
assi (resi 19 and name H2")	(resi 19 and name H6)	3.80	2.00	0.70
assi (resi 19 and name H2")	(resi 19 and name H51)	5.00	2.00	1.00
assi (resi 19 and name H2")	(resi 20 and name H2')	6.00	2.00	1.00
assi (resi 19 and name H2")	(resi 20 and name H4')	6.00	2.00	1.00
assi (resi 19 and name H2")	(resi 20 and name H8)	3.80	2.00	0.70
assi (resi 19 and name H3')	(resi 19 and name H6)	5.00	2.00	1.00
assi (resi 19 and name H4')	(resi 19 and name H6)	5.00	2.00	1.00
assi (resi 19 and name H4')	(resi 19 and name H51)	6.00	2.00	1.00
assi (resi 19 and name H5')	(resi 19 and name H6)	5.00	2.00	1.00
assi (resi 19 and name H5")	(resi 19 and name H6)	3.80	2.00	0.70
assi (resi 19 and name H5")	(resi 19 and name H51)	5.00	2.00	1.00
assi (resi 19 and name H5")	(resi 20 and name H8)	6.00	2.00	1.00
assi (resi 19 and name H6)	(resi 20 and name H8)	5.00	2.00	0.70
assi (resi 19 and name H51)	(resi 17 and name H2)	6.00	2.00	1.00

---

assi (resi 20 and name H1')	(resi 20 and name H2)	5.00	2.00	1.00
assi (resi 20 and name H1')	(resi 20 and name H8)	3.80	2.00	0.70
assi (resi 20 and name H1')	(resi 21 and name H1')	6.00	2.00	1.00
assi (resi 20 and name H1')	(resi 21 and name H4')	6.00	2.00	1.00
assi (resi 20 and name H1')	(resi 21 and name H5")	5.00	2.00	1.00
assi (resi 20 and name H1')	(resi 21 and name H8)	3.80	2.00	0.70
assi (resi 20 and name H1')	(resi 16 and name H2)	5.00	2.00	1.00
assi (resi 20 and name H2')	(resi 20 and name H8)	2.50	0.70	0.50
assi (resi 20 and name H2')	(resi 21 and name H5")	5.00	2.00	1.00
assi (resi 20 and name H2')	(resi 21 and name H8)	3.80	2.00	0.70
assi (resi 20 and name H2")	(resi 20 and name H8)	3.80	2.00	0.70
assi (resi 20 and name H2")	(resi 21 and name H5")	3.80	2.00	0.70
assi (resi 20 and name H2")	(resi 21 and name H8)	2.50	0.70	0.50
assi (resi 20 and name H3')	(resi 20 and name H8)	3.80	2.00	0.70
assi (resi 20 and name H3')	(resi 21 and name H8)	5.00	2.00	1.00
assi (resi 20 and name H4')	(resi 20 and name H8)	5.00	2.00	1.00
assi (resi 20 and name H4')	(resi 21 and name H8)	6.00	2.00	1.00
assi (resi 20 and name H5')	(resi 20 and name H8)	5.00	2.00	1.00
assi (resi 20 and name H5")	(resi 20 and name H8)	5.00	2.00	1.00
assi (resi 20 and name H5")	(resi 21 and name H8)	6.00	2.00	1.00
assi (resi 20 and name H2)	(resi 21 and name H1')	5.00	2.00	1.00
assi (resi 20 and name H2)	(resi 21 and name H2)	3.80	2.00	0.70
assi (resi 20 and name H2)	(resi 16 and name H1')	5.00	2.00	1.00
assi (resi 20 and name H2)	(resi 16 and name H2)	3.80	2.00	0.70
assi (resi 20 and name H2)	(resi 16 and name H8)	5.00	2.00	1.00
assi (resi 20 and name H8)	(resi 21 and name H8)	5.00	2.00	1.00
assi (resi 21 and name H1')	(resi 21 and name H2)	5.00	2.00	1.00
assi (resi 21 and name H1')	(resi 21 and name H8)	3.80	2.00	0.70
assi (resi 21 and name H1')	(resi 22 and name H1')	6.00	2.00	1.00
assi (resi 21 and name H1')	(resi 22 and name H5")	3.80	2.00	0.70
assi (resi 21 and name H1')	(resi 22 and name H6)	3.80	2.00	0.70
assi (resi 21 and name H1')	(resi 22 and name H51)	3.80	2.00	0.70
assi (resi 21 and name H1')	(resi 23 and name H51)	6.00	2.00	1.00
assi (resi 21 and name H2')	(resi 21 and name H8)	2.50	0.70	0.50
assi (resi 21 and name H2')	(resi 22 and name H6)	3.80	2.00	0.70
assi (resi 21 and name H2')	(resi 22 and name H51)	3.80	2.00	0.70
assi (resi 21 and name H2")	(resi 21 and name H8)	3.80	2.00	0.70
assi (resi 21 and name H2")	(resi 22 and name H2')	6.00	2.00	1.00
assi (resi 21 and name H2")	(resi 22 and name H6)	3.80	2.00	0.70
assi (resi 21 and name H2")	(resi 22 and name H51)	3.80	2.00	0.70
assi (resi 21 and name H2")	(resi 23 and name H51)	5.00	2.00	1.00
assi (resi 21 and name H3')	(resi 21 and name H8)	3.80	2.00	0.70
assi (resi 21 and name H3')	(resi 22 and name H6)	5.00	2.00	1.00
assi (resi 21 and name H3')	(resi 22 and name H51)	3.80	2.00	0.70
assi (resi 21 and name H4')	(resi 21 and name H8)	5.00	2.00	1.00
assi (resi 21 and name H4')	(resi 22 and name H51)	5.00	2.00	1.00
assi (resi 21 and name H5')	(resi 21 and name H8)	5.00	2.00	1.00
assi (resi 21 and name H5")	(resi 21 and name H8)	5.00	2.00	1.00
assi (resi 21 and name H2)	(resi 22 and name H1')	3.80	2.00	0.70
assi (resi 21 and name H2)	(resi 22 and name H4')	6.00	2.00	1.00

assi (resi 21 and name H2)	(resi 15 and name H1')	5.00	2.00	1.00
assi (resi 21 and name H8)	(resi 22 and name H6)	5.00	2.00	1.00
assi (resi 21 and name H8)	(resi 22 and name H51)	3.80	2.00	0.70
assi (resi 22 and name H1')	(resi 22 and name H6)	3.80	2.00	0.70
assi (resi 22 and name H1')	(resi 22 and name H51)	5.00	2.00	1.00
assi (resi 22 and name H1')	(resi 23 and name H1')	6.00	2.00	1.00
assi (resi 22 and name H1')	(resi 23 and name H5")	5.00	2.00	1.00
assi (resi 22 and name H1')	(resi 23 and name H6)	3.80	2.00	0.70
assi (resi 22 and name H1')	(resi 23 and name H51)	3.80	2.00	0.70
assi (resi 22 and name H1')	(resi 13 and name H2)	6.00	2.00	1.00
assi (resi 22 and name H2')	(resi 22 and name H6)	2.50	0.70	0.50
assi (resi 22 and name H2')	(resi 22 and name H51)	5.00	2.00	1.00
assi (resi 22 and name H2')	(resi 23 and name H5")	5.00	2.00	1.00
assi (resi 22 and name H2')	(resi 23 and name H6)	3.80	2.00	0.70
assi (resi 22 and name H2')	(resi 23 and name H51)	3.80	2.00	0.70
assi (resi 22 and name H2")	(resi 22 and name H6)	3.80	2.00	0.70
assi (resi 22 and name H2")	(resi 22 and name H51)	5.00	2.00	1.00
assi (resi 22 and name H2")	(resi 23 and name H6)	3.80	2.00	0.70
assi (resi 22 and name H2")	(resi 23 and name H51)	3.80	2.00	0.70
assi (resi 22 and name H3')	(resi 22 and name H6)	6.00	2.00	1.00
assi (resi 22 and name H3')	(resi 22 and name H51)	5.00	2.00	1.00
assi (resi 22 and name H3')	(resi 23 and name H51)	5.00	2.00	1.00
assi (resi 22 and name H4')	(resi 22 and name H6)	5.00	2.00	1.00
assi (resi 22 and name H4')	(resi 22 and name H51)	6.00	2.00	1.00
assi (resi 22 and name H5')	(resi 22 and name H6)	5.00	2.00	1.00
assi (resi 22 and name H5')	(resi 22 and name H51)	6.00	2.00	1.00
assi (resi 22 and name H5")	(resi 22 and name H6)	5.00	2.00	1.00
assi (resi 22 and name H5")	(resi 22 and name H51)	6.00	2.00	1.00
assi (resi 22 and name H6)	(resi 23 and name H6)	5.00	2.00	1.00
assi (resi 22 and name H6)	(resi 23 and name H51)	3.80	2.00	0.70
assi (resi 22 and name H51)	(resi 23 and name H6)	6.00	2.00	1.00
assi (resi 22 and name H51)	(resi 23 and name H51)	5.00	2.00	1.00
assi (resi 23 and name H1')	(resi 23 and name H6)	3.80	2.00	0.70
assi (resi 23 and name H1')	(resi 23 and name H51)	5.00	2.00	1.00
assi (resi 23 and name H1')	(resi 24 and name H1')	6.00	2.00	1.00
assi (resi 23 and name H1')	(resi 24 and name H6)	3.80	2.00	0.70
assi (resi 23 and name H1')	(resi 24 and name H51)	3.80	2.00	0.70
assi (resi 23 and name H1')	(resi 13 and name H2)	5.00	2.00	1.00
assi (resi 23 and name H2')	(resi 23 and name H6)	2.50	0.70	0.50
assi (resi 23 and name H2')	(resi 23 and name H51)	5.00	2.00	1.00
assi (resi 23 and name H2')	(resi 24 and name H6)	3.80	2.00	0.70
assi (resi 23 and name H2')	(resi 24 and name H51)	3.80	2.00	0.70
assi (resi 23 and name H2")	(resi 23 and name H6)	3.80	2.00	0.70
assi (resi 23 and name H2")	(resi 23 and name H51)	5.00	2.00	1.00
assi (resi 23 and name H2")	(resi 24 and name H6)	3.80	2.00	0.70
assi (resi 23 and name H2")	(resi 24 and name H51)	3.80	2.00	0.70
assi (resi 23 and name H3')	(resi 23 and name H6)	3.80	2.00	0.70
assi (resi 23 and name H3')	(resi 23 and name H51)	5.00	2.00	1.00
assi (resi 23 and name H3')	(resi 24 and name H6)	5.00	2.00	1.00

[illegible]

---

assi (resi 25 and name H3')	(resi 26 and name H5)	5.00	2.00	1.00
assi (resi 25 and name H4')	(resi 25 and name H2)	6.00	2.00	1.00
assi (resi 25 and name H4')	(resi 25 and name H5)	5.00	2.00	1.00
assi (resi 25 and name H5')	(resi 25 and name H5)	5.00	2.00	1.00
assi (resi 25 and name H5'')	(resi 25 and name H2)	6.00	2.00	1.00
assi (resi 25 and name H5'')	(resi 25 and name H5)	5.00	2.00	1.00
assi (resi 25 and name H2)	(resi 26 and name H5'')	6.00	2.00	1.00
assi (resi 25 and name H2)	(resi 26 and name H4)	6.00	2.00	1.00
assi (resi 25 and name H2)	(resi 26 and name H5)	6.00	2.00	1.00
assi (resi 25 and name H4)	(resi 26 and name H4)	3.80	2.00	0.70
assi (resi 25 and name H4)	(resi 26 and name H5)	5.00	2.00	1.00
assi (resi 25 and name H4)	(resi 10 and name H4)	6.00	2.00	1.00
assi (resi 25 and name H4)	(resi 11 and name H2)	6.00	2.00	1.00
assi (resi 25 and name H5)	(resi 26 and name H4)	5.00	2.00	1.00
assi (resi 25 and name H5)	(resi 26 and name H5)	5.00	2.00	1.00
assi (resi 26 and name H1')	(resi 26 and name H2)	3.80	2.00	0.70
assi (resi 26 and name H1')	(resi 26 and name H4)	6.00	2.00	1.00
assi (resi 26 and name H1')	(resi 26 and name H5)	5.00	2.00	1.00
assi (resi 26 and name H1')	(resi 27 and name H4')	6.00	2.00	1.00
assi (resi 26 and name H1')	(resi 27 and name H5'')	6.00	2.00	1.00
assi (resi 26 and name H1')	(resi 27 and name H4)	5.00	2.00	1.00
assi (resi 26 and name H1')	(resi 27 and name H5)	5.00	2.00	1.00
assi (resi 26 and name H2')	(resi 26 and name H2)	5.00	2.00	1.00
assi (resi 26 and name H2')	(resi 26 and name H4)	5.00	2.00	1.00
assi (resi 26 and name H2')	(resi 26 and name H5)	3.80	2.00	0.70
assi (resi 26 and name H2')	(resi 27 and name H4)	5.00	2.00	1.00
assi (resi 26 and name H2')	(resi 27 and name H5)	5.00	2.00	1.00
assi (resi 26 and name H2'')	(resi 26 and name H2)	5.00	2.00	1.00
assi (resi 26 and name H2'')	(resi 26 and name H4)	5.00	2.00	1.00
assi (resi 26 and name H2'')	(resi 26 and name H5)	3.80	2.00	0.70
assi (resi 26 and name H2'')	(resi 27 and name H4)	5.00	2.00	1.00
assi (resi 26 and name H2'')	(resi 27 and name H5)	5.00	2.00	1.00
assi (resi 26 and name H3')	(resi 26 and name H5)	5.00	2.00	1.00
assi (resi 26 and name H3')	(resi 27 and name H5)	5.00	2.00	1.00
assi (resi 26 and name H4')	(resi 26 and name H2)	6.00	2.00	1.00
assi (resi 26 and name H4')	(resi 26 and name H5)	5.00	2.00	1.00
assi (resi 26 and name H4')	(resi 27 and name H5)	6.00	2.00	1.00
assi (resi 26 and name H5'')	(resi 26 and name H2)	6.00	2.00	1.00
assi (resi 26 and name H5'')	(resi 26 and name H5)	5.00	2.00	1.00
assi (resi 26 and name H2)	(resi 27 and name H5'')	6.00	2.00	1.00
assi (resi 26 and name H2)	(resi 27 and name H2)	6.00	2.00	1.00
assi (resi 26 and name H2)	(resi 27 and name H4)	6.00	2.00	1.00
assi (resi 26 and name H2)	(resi 27 and name H5)	6.00	2.00	1.00
assi (resi 26 and name H4)	(resi 27 and name H4)	3.80	2.00	0.70
assi (resi 26 and name H4)	(resi 27 and name H5)	6.00	2.00	1.00
assi (resi 26 and name H5)	(resi 27 and name H5'')	6.00	2.00	1.00
assi (resi 26 and name H5)	(resi 27 and name H4)	5.00	2.00	1.00
assi (resi 26 and name H5)	(resi 27 and name H5)	5.00	2.00	1.00
assi (resi 27 and name H1')	(resi 27 and name H2)	3.80	2.00	0.70

assi (resi 27 and name H1')	(resi 27 and name H4)	6.00	2.00	1.00
assi (resi 27 and name H1')	(resi 27 and name H5)	5.00	2.00	1.00
assi (resi 27 and name H1')	(resi 28 and name H4')	5.00	2.00	1.00
assi (resi 27 and name H1')	(resi 28 and name H5')	5.00	2.00	1.00
assi (resi 27 and name H1')	(resi 28 and name H5'')	5.00	2.00	1.00
assi (resi 27 and name H1')	(resi 28 and name H8)	6.00	2.00	1.00
assi (resi 27 and name H2')	(resi 27 and name H2)	5.00	2.00	1.00
assi (resi 27 and name H2')	(resi 27 and name H4)	5.00	2.00	1.00
assi (resi 27 and name H2')	(resi 27 and name H5)	3.80	2.00	0.70
assi (resi 27 and name H2')	(resi 28 and name H4')	6.00	2.00	1.00
assi (resi 27 and name H2')	(resi 28 and name H5'')	6.00	2.00	1.00
assi (resi 27 and name H2')	(resi 28 and name H8)	5.00	2.00	1.00
assi (resi 27 and name H2'')	(resi 27 and name H2)	5.00	2.00	1.00
assi (resi 27 and name H2'')	(resi 27 and name H4)	5.00	2.00	1.00
assi (resi 27 and name H2'')	(resi 27 and name H5)	3.80	2.00	0.70
assi (resi 27 and name H2'')	(resi 28 and name H4')	6.00	2.00	1.00
assi (resi 27 and name H2'')	(resi 28 and name H5'')	6.00	2.00	1.00
assi (resi 27 and name H2'')	(resi 28 and name H8)	5.00	2.00	1.00
assi (resi 27 and name H3')	(resi 27 and name H5)	5.00	2.00	1.00
assi (resi 27 and name H4')	(resi 27 and name H2)	6.00	2.00	1.00
assi (resi 27 and name H4')	(resi 27 and name H5)	6.00	2.00	1.00
assi (resi 27 and name H5'')	(resi 27 and name H5)	5.00	2.00	1.00
assi (resi 27 and name H5)	(resi 28 and name H2)	6.00	2.00	1.00
assi (resi 27 and name H5)	(resi 28 and name H8)	6.00	2.00	1.00
assi (resi 28 and name H1')	(resi 28 and name H2)	5.00	2.00	1.00
assi (resi 28 and name H1')	(resi 28 and name H8)	3.80	2.00	0.70
assi (resi 28 and name H1')	(resi 29 and name H1')	5.00	2.00	1.00
assi (resi 28 and name H1')	(resi 29 and name H4')	6.00	2.00	1.00
assi (resi 28 and name H1')	(resi 29 and name H5'')	5.00	2.00	1.00
assi (resi 28 and name H1')	(resi 29 and name H8)	3.80	2.00	0.70
assi (resi 28 and name H2')	(resi 28 and name H8)	2.50	0.70	0.50
assi (resi 28 and name H2')	(resi 29 and name H5'')	5.00	2.00	1.00
assi (resi 28 and name H2')	(resi 29 and name H8)	3.80	2.00	1.00
assi (resi 28 and name H2'')	(resi 28 and name H8)	3.80	2.00	0.70
assi (resi 28 and name H2'')	(resi 29 and name H8)	3.80	2.00	0.70
assi (resi 28 and name H3')	(resi 28 and name H8)	5.00	2.00	1.00
assi (resi 28 and name H4')	(resi 28 and name H8)	6.00	2.00	1.00
assi (resi 28 and name H4')	(resi 29 and name H8)	6.00	2.00	1.00
assi (resi 28 and name H5')	(resi 28 and name H8)	6.00	2.00	1.00
assi (resi 28 and name H2)	(resi 29 and name H1')	6.00	2.00	1.00
assi (resi 28 and name H2)	(resi 29 and name H2)	5.00	2.00	1.00
assi (resi 28 and name H8)	(resi 29 and name H8)	5.00	2.00	1.00
assi (resi 29 and name H1')	(resi 29 and name H2)	5.00	2.00	1.00
assi (resi 29 and name H1')	(resi 29 and name H8)	3.80	2.00	0.70
assi (resi 29 and name H1')	(resi 30 and name H1')	5.00	2.00	1.00
assi (resi 29 and name H1')	(resi 30 and name H4')	5.00	2.00	1.00
assi (resi 29 and name H1')	(resi 30 and name H5'')	5.00	2.00	1.00
assi (resi 29 and name H1')	(resi 30 and name H8)	3.80	2.00	0.70
assi (resi 29 and name H2')	(resi 29 and name H2)	6.00	2.00	1.00



assi (resi 29 and name H2')	(resi 29 and name H8)	2.50	0.70	0.50
assi (resi 29 and name H2')	(resi 30 and name H8)	3.80	2.00	0.70
assi (resi 29 and name H2'')	(resi 29 and name H8)	3.80	2.00	0.70
assi (resi 29 and name H2'')	(resi 30 and name H5'')	5.00	2.00	1.00
assi (resi 29 and name H2'')	(resi 30 and name H8)	2.50	0.50	0.70
assi (resi 29 and name H3')	(resi 29 and name H8)	5.00	2.00	1.00
assi (resi 29 and name H3')	(resi 30 and name H8)	6.00	2.00	1.00
assi (resi 29 and name H4')	(resi 29 and name H8)	5.00	2.00	1.00
assi (resi 29 and name H4')	(resi 30 and name H8)	6.00	2.00	1.00
assi (resi 29 and name H5'')	(resi 29 and name H8)	5.00	2.00	1.00
assi (resi 29 and name H2)	(resi 30 and name H1')	5.00	2.00	1.00
assi (resi 29 and name H2)	(resi 30 and name H2)	3.80	2.00	0.70
assi (resi 30 and name H1')	(resi 30 and name H2)	5.00	2.00	1.00
assi (resi 30 and name H1')	(resi 30 and name H8)	3.80	2.00	0.70
assi (resi 30 and name H1')	(resi 31 and name H1')	6.00	2.00	1.00
assi (resi 30 and name H1')	(resi 31 and name H5'')	5.00	2.00	1.00
assi (resi 30 and name H1')	(resi 31 and name H6)	3.80	2.00	0.70
assi (resi 30 and name H1')	(resi 31 and name H51)	5.00	2.00	0.70
assi (resi 30 and name H1')	(resi 32 and name H51)	6.00	2.00	1.00
assi (resi 30 and name H2')	(resi 30 and name H8)	3.80	2.00	0.70
assi (resi 30 and name H2')	(resi 31 and name H6)	3.80	2.00	0.70
assi (resi 30 and name H2')	(resi 31 and name H51)	3.80	2.00	0.70
assi (resi 30 and name H2'')	(resi 30 and name H8)	3.80	2.00	0.70
assi (resi 30 and name H2'')	(resi 31 and name H2')	5.00	2.00	1.00
assi (resi 30 and name H2'')	(resi 31 and name H5'')	3.80	2.00	0.70
assi (resi 30 and name H2'')	(resi 31 and name H6)	3.80	2.00	0.70
assi (resi 30 and name H2'')	(resi 31 and name H51)	3.80	2.00	0.70
assi (resi 30 and name H2'')	(resi 32 and name H51)	5.00	2.00	1.00
assi (resi 30 and name H3')	(resi 30 and name H8)	3.80	2.00	0.70
assi (resi 30 and name H3')	(resi 31 and name H6)	5.00	2.00	1.00
assi (resi 30 and name H3')	(resi 31 and name H51)	3.80	2.00	1.00
assi (resi 30 and name H4')	(resi 30 and name H8)	5.00	2.00	1.00
assi (resi 30 and name H4')	(resi 31 and name H6)	6.00	2.00	1.00
assi (resi 30 and name H4')	(resi 31 and name H51)	5.00	2.00	1.00
assi (resi 30 and name H5')	(resi 30 and name H8)	5.00	2.00	1.00
assi (resi 30 and name H5'')	(resi 30 and name H8)	5.00	2.00	1.00
assi (resi 30 and name H5'')	(resi 31 and name H51)	5.00	2.00	1.00
assi (resi 30 and name H2)	(resi 31 and name H1')	5.00	2.00	1.00
assi (resi 30 and name H2)	(resi 31 and name H51)	6.00	2.00	1.00
assi (resi 30 and name H8)	(resi 31 and name H6)	5.00	2.00	1.00
assi (resi 30 and name H8)	(resi 31 and name H51)	3.80	2.00	0.70
assi (resi 31 and name H1')	(resi 31 and name H6)	3.80	2.00	0.70
assi (resi 31 and name H1')	(resi 31 and name H51)	5.00	2.00	1.00
assi (resi 31 and name H1')	(resi 32 and name H1')	5.00	2.00	1.00
assi (resi 31 and name H1')	(resi 32 and name H5'')	5.00	2.00	1.00
assi (resi 31 and name H1')	(resi 32 and name H6)	3.80	2.00	0.70
assi (resi 31 and name H1')	(resi 32 and name H51)	3.80	2.00	0.70
assi (resi 31 and name H2')	(resi 31 and name H6)	3.80	2.00	0.70
assi (resi 31 and name H2')	(resi 31 and name H51)	5.00	2.00	1.00

assi (resi 31 and name H2')	(resi 32 and name H5")	5.00	2.00	1.00
assi (resi 31 and name H2')	(resi 32 and name H6)	3.80	2.00	0.70
assi (resi 31 and name H2')	(resi 32 and name H51)	3.80	2.00	0.70
assi (resi 31 and name H2")	(resi 31 and name H6)	3.80	2.00	0.70
assi (resi 31 and name H2")	(resi 31 and name H51)	6.00	2.00	1.00
assi (resi 31 and name H2")	(resi 32 and name H2')	5.00	2.00	1.00
assi (resi 31 and name H2")	(resi 32 and name H5")	5.00	2.00	1.00
assi (resi 31 and name H2")	(resi 32 and name H6)	3.80	2.00	0.70
assi (resi 31 and name H2")	(resi 32 and name H51)	3.80	2.00	0.70
assi (resi 31 and name H4')	(resi 31 and name H6)	5.00	2.00	1.00
assi (resi 31 and name H4')	(resi 31 and name H51)	6.00	2.00	1.00
assi (resi 31 and name H4')	(resi 32 and name H6)	5.00	2.00	1.00
assi (resi 31 and name H4')	(resi 32 and name H51)	5.00	2.00	1.00
assi (resi 31 and name H5')	(resi 31 and name H6)	5.00	2.00	1.00
assi (resi 31 and name H5")	(resi 31 and name H6)	5.00	2.00	1.00
assi (resi 31 and name H5")	(resi 31 and name H51)	5.00	2.00	1.00
assi (resi 31 and name H6)	(resi 32 and name H6)	3.80	2.00	0.70
assi (resi 31 and name H6)	(resi 32 and name H51)	3.80	2.00	0.70
assi (resi 31 and name H51)	(resi 32 and name H6)	6.00	2.00	1.00
assi (resi 31 and name H51)	(resi 32 and name H51)	5.00	2.00	1.00
assi (resi 32 and name H1')	(resi 32 and name H6)	3.80	2.00	0.70
assi (resi 32 and name H1')	(resi 32 and name H51)	5.00	2.00	1.00
assi (resi 32 and name H1')	(resi 33 and name H1')	5.00	2.00	1.00
assi (resi 32 and name H1')	(resi 33 and name H4')	5.00	2.00	1.00
assi (resi 32 and name H1')	(resi 33 and name H5")	5.00	2.00	1.00
assi (resi 32 and name H1')	(resi 33 and name H8)	3.80	2.00	0.70
assi (resi 32 and name H2')	(resi 32 and name H6)	2.50	0.70	0.50
assi (resi 32 and name H2')	(resi 32 and name H51)	5.00	2.00	1.00
assi (resi 32 and name H2')	(resi 33 and name H5")	5.00	2.00	1.00
assi (resi 32 and name H2')	(resi 33 and name H8)	3.80	2.00	0.70
assi (resi 32 and name H2")	(resi 32 and name H6)	3.80	2.00	0.70
assi (resi 32 and name H2")	(resi 32 and name H51)	5.00	2.00	1.00
assi (resi 32 and name H2")	(resi 33 and name H4')	5.00	2.00	1.00
assi (resi 32 and name H2")	(resi 33 and name H5")	3.80	2.00	0.70
assi (resi 32 and name H2")	(resi 33 and name H8)	3.80	2.00	0.70
assi (resi 32 and name H4')	(resi 32 and name H6)	5.00	2.00	1.00
assi (resi 32 and name H5')	(resi 32 and name H6)	5.00	2.00	1.00
assi (resi 32 and name H5')	(resi 32 and name H51)	6.00	2.00	1.00
assi (resi 32 and name H5")	(resi 32 and name H6)	5.00	2.00	1.00
assi (resi 32 and name H5")	(resi 32 and name H51)	6.00	2.00	1.00
assi (resi 32 and name H6)	(resi 33 and name H8)	5.00	2.00	1.00
assi (resi 33 and name H1')	(resi 33 and name H2)	5.00	2.00	1.00
assi (resi 33 and name H1')	(resi 33 and name H8)	3.80	2.00	0.70
assi (resi 33 and name H1')	(resi 34 and name H1')	5.00	2.00	1.00
assi (resi 33 and name H1')	(resi 34 and name H5')	5.00	2.00	1.00
assi (resi 33 and name H1')	(resi 34 and name H5")	5.00	2.00	1.00
assi (resi 33 and name H1')	(resi 34 and name H8)	3.80	2.00	0.70
assi (resi 33 and name H2')	(resi 33 and name H8)	2.50	0.70	0.50
assi (resi 33 and name H2')	(resi 34 and name H8)	3.80	2.00	0.70

assi (resi 33 and name H2")	(resi 33 and name H8)	3.80	2.00	0.70
assi (resi 33 and name H2")	(resi 34 and name H2')	5.00	2.00	1.00
assi (resi 33 and name H2")	(resi 34 and name H4')	6.00	2.00	1.00
assi (resi 33 and name H2")	(resi 34 and name H5')	5.00	2.00	1.00
assi (resi 33 and name H2")	(resi 34 and name H5")	5.00	2.00	1.00
assi (resi 33 and name H2")	(resi 34 and name H8)	3.80	2.00	0.70
assi (resi 33 and name H3')	(resi 33 and name H8)	3.80	2.00	0.70
assi (resi 33 and name H3')	(resi 34 and name H8)	5.00	2.00	1.00
assi (resi 33 and name H4')	(resi 33 and name H8)	5.00	2.00	1.00
assi (resi 33 and name H4')	(resi 34 and name H8)	6.00	2.00	1.00
assi (resi 33 and name H5')	(resi 33 and name H8)	5.00	2.00	1.00
assi (resi 33 and name H5")	(resi 33 and name H8)	5.00	2.00	1.00
assi (resi 33 and name H2)	(resi 34 and name H1')	5.00	2.00	1.00
assi (resi 33 and name H2)	(resi 34 and name H2)	3.80	2.00	0.70
assi (resi 33 and name H2)	(resi 34 and name H8)	6.00	2.00	1.00
assi (resi 34 and name H1')	(resi 34 and name H2)	5.00	2.00	1.00
assi (resi 34 and name H1')	(resi 34 and name H8)	3.80	2.00	0.70
assi (resi 34 and name H2')	(resi 34 and name H8)	2.50	0.70	0.50
assi (resi 34 and name H2")	(resi 34 and name H8)	3.80	2.00	0.70
assi (resi 34 and name H3')	(resi 34 and name H8)	5.00	2.00	1.00
assi (resi 34 and name H4')	(resi 34 and name H8)	5.00	2.00	1.00
assi (resi 34 and name H5')	(resi 34 and name H8)	5.00	2.00	1.00
assi (resi 34 and name H5")	(resi 34 and name H8)	5.00	2.00	1.00

H-bond restraints verified by 26 interstrand correlations (mainly between adenine-H2 and H1' on the opposite strand).

assi (resi 1 and name H3)	(resi 34 and name N1)	1.90	0.10	0.10
assi (resi 1 and name N3)	(resi 34 and name N1)	2.90	0.10	0.10
assi (resi 1 and name O4)	(resi 34 and name H61)	1.90	0.10	0.10
assi (resi 1 and name O4)	(resi 34 and name N6)	2.90	0.10	0.10
assi (resi 2 and name H3)	(resi 33 and name N1)	1.90	0.10	0.10
assi (resi 2 and name N3)	(resi 33 and name N1)	2.90	0.10	0.10
assi (resi 2 and name O4)	(resi 33 and name H61)	1.90	0.10	0.10
assi (resi 2 and name O4)	(resi 33 and name N6)	2.90	0.10	0.10
assi (resi 3 and name N1)	(resi 32 and name H3)	1.90	0.10	0.10
assi (resi 3 and name N1)	(resi 32 and name N3)	2.90	0.10	0.10
assi (resi 3 and name H61)	(resi 32 and name O4)	1.90	0.10	0.10
assi (resi 3 and name N6)	(resi 32 and name O4)	2.90	0.10	0.10
assi (resi 4 and name N1)	(resi 31 and name H3)	1.90	0.10	0.10
assi (resi 4 and name N1)	(resi 31 and name N3)	2.90	0.10	0.10
assi (resi 4 and name H61)	(resi 31 and name O4)	1.90	0.10	0.10
assi (resi 4 and name N6)	(resi 31 and name O4)	2.90	0.10	0.10
assi (resi 5 and name H3)	(resi 30 and name N1)	1.90	0.10	0.10
assi (resi 5 and name N3)	(resi 30 and name N1)	2.90	0.10	0.10

---

assi (resi 5 and name O4)	(resi 30 and name H61)	1.90	0.10	0.10
assi (resi 5 and name O4)	(resi 30 and name N6)	2.90	0.10	0.10
assi (resi 6 and name H3)	(resi 29 and name N1)	1.90	0.10	0.10
assi (resi 6 and name N3)	(resi 29 and name N1)	2.90	0.10	0.10
assi (resi 6 and name O4)	(resi 29 and name H61)	1.90	0.10	0.10
assi (resi 6 and name O4)	(resi 29 and name N6)	2.90	0.10	0.10
assi (resi 7 and name H3)	(resi 28 and name N1)	1.90	0.10	0.10
assi (resi 7 and name N3)	(resi 28 and name N1)	2.90	0.10	0.10
assi (resi 7 and name O4)	(resi 28 and name H61)	1.90	0.10	0.10
assi (resi 7 and name O4)	(resi 28 and name N6)	2.90	0.10	0.10
assi (resi 11 and name N1)	(resi 24 and name H3)	1.90	0.10	0.10
assi (resi 11 and name N1)	(resi 24 and name N3)	2.90	0.10	0.10
assi (resi 11 and name H61)	(resi 24 and name O4)	1.90	0.10	0.10
assi (resi 11 and name N6)	(resi 24 and name O4)	2.90	0.10	0.10
assi (resi 12 and name N1)	(resi 23 and name H3)	1.90	0.10	0.10
assi (resi 12 and name N1)	(resi 23 and name N3)	2.90	0.10	0.10
assi (resi 12 and name H61)	(resi 23 and name O4)	1.90	0.10	0.10
assi (resi 12 and name N6)	(resi 23 and name O4)	2.90	0.10	0.10
assi (resi 13 and name N1)	(resi 22 and name H3)	1.90	0.10	0.10
assi (resi 13 and name N1)	(resi 22 and name N3)	2.90	0.10	0.10
assi (resi 13 and name H61)	(resi 22 and name O4)	1.90	0.10	0.10
assi (resi 13 and name N6)	(resi 22 and name O4)	2.90	0.10	0.10
assi (resi 14 and name H3)	(resi 21 and name N1)	1.90	0.10	0.10
assi (resi 14 and name N3)	(resi 21 and name N1)	2.90	0.10	0.10
assi (resi 14 and name O4)	(resi 21 and name H61)	1.90	0.10	0.10
assi (resi 14 and name O4)	(resi 21 and name N6)	2.90	0.10	0.10
assi (resi 15 and name H3)	(resi 20 and name N1)	1.90	0.10	0.10
assi (resi 15 and name N3)	(resi 20 and name N1)	2.90	0.10	0.10
assi (resi 15 and name O4)	(resi 20 and name H61)	1.90	0.10	0.10
assi (resi 15 and name O4)	(resi 20 and name N6)	2.90	0.10	0.10
assi (resi 16 and name N1)	(resi 19 and name H3)	1.90	0.10	0.10
assi (resi 16 and name N1)	(resi 19 and name N3)	2.90	0.10	0.10
assi (resi 16 and name H61)	(resi 19 and name O4)	1.90	0.10	0.10
assi (resi 16 and name N6)	(resi 19 and name O4)	2.90	0.10	0.10
assi (resi 17 and name N1)	(resi 18 and name H3)	1.90	0.10	0.10
assi (resi 17 and name N1)	(resi 18 and name N3)	2.90	0.10	0.10
assi (resi 17 and name H61)	(resi 18 and name O4)	1.90	0.10	0.10
assi (resi 17 and name N6)	(resi 18 and name O4)	2.90	0.10	0.10

Imidazole-Imidazole restraints were taken from DFT calculations of a 1-methylimidazole-silver-1-methylimidazole basepair with cisoid methyl groups as necessary for a Watson.Crick base pair surrogate.<sup>[195]</sup>

assi (resi 8 and name N1)	(resi 27	and name N1)	8.48	0.10	0.10
assi (resi 8 and name C2)	(resi 27	and name C2)	5.89	0.10	0.10
assi (resi 8 and name N3)	(resi 27	and name N3)	4.27	0.10	0.10
assi (resi 8 and name C4)	(resi 27	and name C4)	5.89	0.10	0.10
assi (resi 8 and name C5)	(resi 27	and name C5)	8.51	0.10	0.10
assi (resi 8 and name C1')	(resi 27	and name C1')	10.80	0.10	0.10
assi (resi 9 and name N1)	(resi 26	and name N1)	8.48	0.10	0.10
assi (resi 9 and name C2)	(resi 26	and name C2)	5.89	0.10	0.10
assi (resi 9 and name N3)	(resi 26	and name N3)	4.27	0.10	0.10
assi (resi 9 and name C4)	(resi 26	and name C4)	5.89	0.10	0.10
assi (resi 9 and name C5)	(resi 26	and name C5)	8.51	0.10	0.10
assi (resi 9 and name C1')	(resi 26	and name C1')	10.80	0.10	0.10
assi (resi 10 and name N1)	(resi 25	and name N1)	8.48	0.10	0.10
assi (resi 10 and name C2)	(resi 25	and name C2)	5.89	0.10	0.10
assi (resi 10 and name N3)	(resi 25	and name N3)	4.27	0.10	0.10
assi (resi 10 and name C4)	(resi 25	and name C4)	5.89	0.10	0.10
assi (resi 10 and name C5)	(resi 25	and name C5)	8.51	0.10	0.10
assi (resi 10 and name C1')	(resi 25	and name C1')	10.80	0.10	0.10

Phosphate-sugar-backbone dihedral restraints based on a 1D [<sup>31</sup>P]-NMR spectrum acquired at 400 MHz frequency at 298 K (100 % D<sub>2</sub>O, 120mM NaClO<sub>4</sub>) and cover the B-DNA range. Exact values were taken from the dihedral angle restraint file of the Dickerson-Drew-Dodecamer in the example folder dna\_refi of XPLOR NIH 2.15.0, which represents a perfect B-DNA duplex. Error boundaries of  $\pm 20^\circ$  were used for all residues.

assign	( resid n-1 and name O3')			
	( resid n and name P)			
	( resid n and name O5')			
	( resid n and name C5')	-70	{* $\alpha$ *}	
assign	( resid n and name P)			
	( resid n and name O5')			
	( resid n and name C5')			
	( resid n and name C4')	180	{* $\beta$ *}	
assign	( resid n and name O5')			
	( resid n and name C5')			
	( resid n and name C4')			
	( resid n and name C3')	60	{* $\gamma$ *}	
assign	( resid n and name O5')			
	( resid n and name C5')			
	( resid n and name C4')			
	( resid n+1 and name C3')	-170	{* $\epsilon$ *}	

```

assign  ( resid n    and name C3' )
        ( resid n    and name O3' )
        ( resid n+1 and name P   )
        ( resid n+1 and name O5' )      -85      { *  $\zeta$  * }

```

Sugar pucker restraints based on a [ $^1\text{H}$ ,  $^1\text{H}$ ]-TOCSY spectrum acquired at 700 MHz frequency at 298 K (100 %  $\text{D}_2\text{O}$ , 120 mM  $\text{NaClO}_4$ ). Helical B-type DNA is usually 2'-endo and gives strong H1'-H2' and H1'-H3' crosspeak in TOCSY experiment. Exact values were taken from the dihedral angle restraint file of the Dickerson-Drew-Dodecamer in the example folder dna\_refi of XPLOR NIH 2.15.0, which represents a perfect B-DNA duplex. Error boundaries of  $\pm 20^\circ$  were used for all residues, except for Im8, Im9, Im10, Im25, Im26 and Im27 which were left unrestrained.

```

assign  ( resid n    and name C5' )
        ( resid n    and name C4' )
        ( resid n    and name C3' )
        ( resid n    and name O3' )      140      { *  $\delta$  * }

```

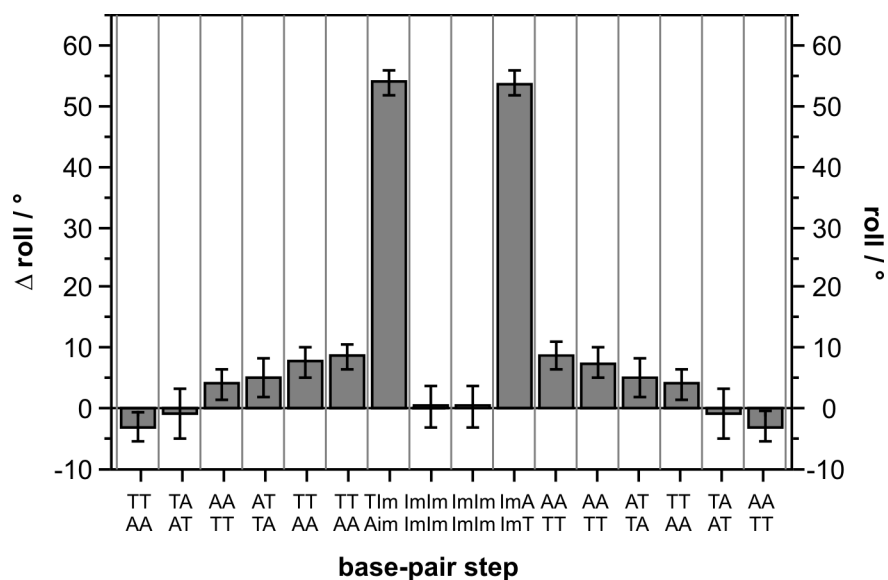
The torsion angle  $\chi$  defines the orientation of the base to the sugar around the glycosidic bond.  $\chi$  was restrained to *anti* orientation for all residues, with error boundaries of  $\pm 20^\circ$ . Im8, Im9, Im10, Im25, Im26 and Im27 were left unrestrained.

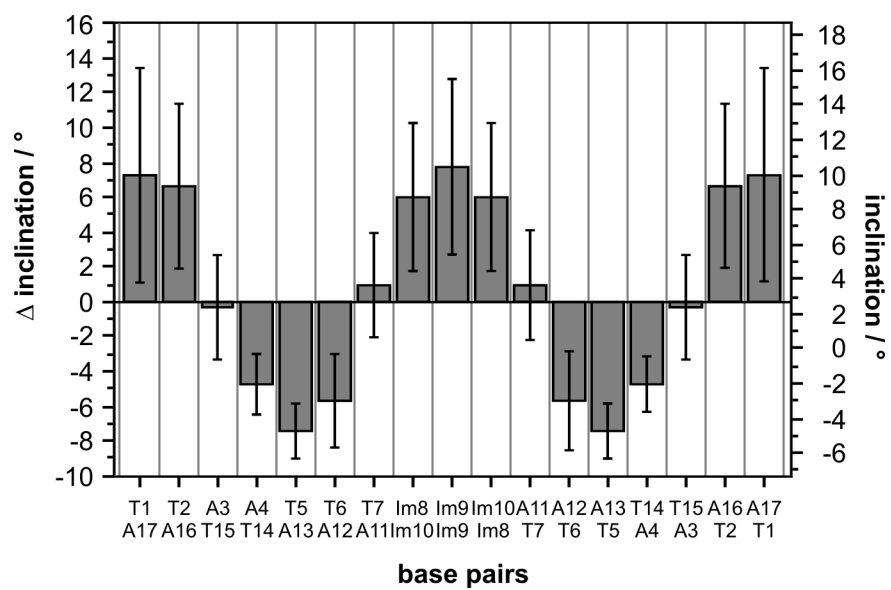
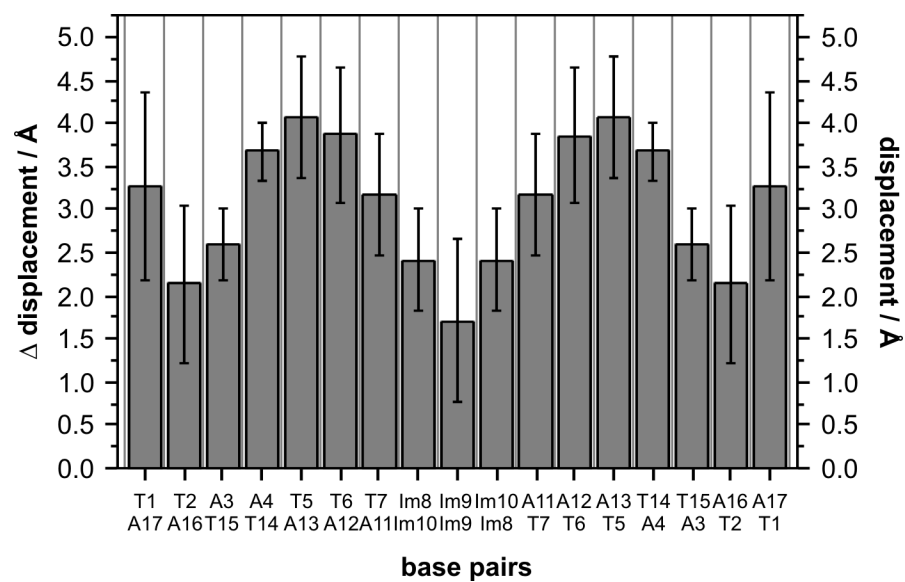
```

assign  ( resid n    and name O4' )
        ( resid n    and name C1' )
        ( resid n    and name N9 )
        ( resid n    and name C4 )      -120      { *  $\chi$  of purines* }

assign  ( resid n    and name O4' )
        ( resid n    and name C1' )
        ( resid n    and name N1 )
        ( resid n    and name C4 )      -120      { *  $\chi$  of pyrimidines* }

```

Tilt  $\tau$ 

inclination  $\eta$ global displacement



---

**Appendix 19** Glycosidic angle  $\chi / ^\circ$  of the DNA duplex structure as derived with the programme 3DNA.<sup>[240]</sup>


---

	strand A	strand B
	Glycosidic angle $\chi / ^\circ$	
<b>T1</b>	-121±5	-121±5
<b>T2</b>	-109±3	-109±2
<b>A3</b>	-124±5	-124±4
<b>A4</b>	-111±3	-111±3
<b>T5</b>	-116±4	-116±4
<b>T6</b>	-116±4	-116±5
<b>T7</b>	-109±4	-110±4
<b>Im8</b>	63±5	63±5
<b>Im9</b>	65±3	65±3
<b>Im10</b>	64±7	65±7
<b>A11</b>	-104±4	-104±4
<b>A12</b>	-124±2	-124±2
<b>A13</b>	-112±3	-112±3
<b>T14</b>	-111±5	-111±5
<b>T15</b>	-119±4	-119±4
<b>A16</b>	-116±6	-116±6
<b>A17</b>	-122±3	-122±3

---



## 8 Literature

- [1] G. E. Moore, *Electronics* **1965**, 38, 114.
- [2] G. M. Whitesides, J. P. Mathias and C. T. Seto, *Science* **1991**, 254, 1312.
- [3] J. D. Watson and F. H. C. Crick, *Nature* **1953**, 171, 737.
- [4] M. Chastain and I. Tinoco, Jr., *Prog. Nucleic Acid Res. Mol. Biol.* **1991**, 41, 131.
- [5] W. Saenger, *Principles of Nucleic Acid Structure*, Springer Verlag, New York, **1984**, p
- [6] R. Koradi, M. Billeter and K. Wüthrich, *J. Mol. Graph.* **1996**, 14, 29.
- [7] A. C. Dock-Bregeon, B. Chevrier, A. Podjarny, J. Johnson, J. S. de Bear, G. R. Gough, P. T. Gilham and D. Moras, *J. Mol. Biol.* **1989**, 209, 459.
- [8] A. H. J. Wang, G. J. Quigley, F. J. Kolpak, J. L. Crawford, J. H. van Boom, G. van der Marel and A. Rich, *Nature* **1979**, 282, 680.
- [9] C. M. Niemeyer, *Angew. Chem., Int. Ed.* **2001**, 40, 4128.
- [10] N. C. Seeman, *Nature* **2003**, 421, 427.
- [11] H. Dietz, S. M. Douglas and W. M. Shih, *Science* **2009**, 325, 725.
- [12] S. M. Douglas, H. Dietz, T. Liedl, B. Hogberg, F. Graf and W. M. Shih, *Nature* **2009**, 459, 414.
- [13] P. W. K. Rothmund, *Nature* **2006**, 440, 297.
- [14] S. L. Beaucage and M. H. Caruthers, *Tetrahedron Lett.* **1981**, 22, 1859.
- [15] C. B. Reese, *Org. Biomol. Chem.* **2005**, 3, 3851.
- [16] K. Keren, R. S. Berman and E. Braun, *Nano Lett.* **2004**, 4, 323.
- [17] S. Jäger, G. Rasched, H. Kornreich-Leshem, M. Engeser, O. Thum and M. Famulok, *J. Am. Chem. Soc.* **2005**, 127, 15071.
- [18] S. Buchini and C. J. Leumann, *Curr. Opin. Chem. Biol.* **2003**, 7, 717.
- [19] J. Micklefield, *Curr. Med. Chem.* **2001**, 8, 1157.
- [20] A. Ray and B. Norden, *FASEB J.* **2000**, 14, 1041.
- [21] A. Eschenmoser, *Science* **1999**, 284, 2118.
- [22] A. Eschenmoser, *Chimia* **2005**, 59, 836.
- [23] C. J. Leumann, *Chimia* **2005**, 59, 776.
- [24] P. E. Nielsen, M. Egholm, R. H. Berg and O. Buchardt, *Science* **1991**, 254, 1497.
- [25] A. T. Vasella, *Chimia* **2005**, 59, 785.
- [26] L. L. Zhang, A. Peritz and E. Meggers, *J. Am. Chem. Soc.* **2005**, 127, 4174.
- [27] I. Hirao, *Curr. Opin. Chem. Biol.* **2006**, 10, 622.
- [28] E. T. Kool, *Acc. Chem. Res.* **2002**, 35, 936.
- [29] J. A. Piccirilli, T. Krauch, S. E. Moroney and S. A. Benner, *Nature* **1990**, 343, 33.
- [30] C. Switzer, S. E. Moroney and S. A. Benner, *J. Am. Chem. Soc.* **1989**, 111, 8322.
- [31] M. J. Lutz, J. Horlacher and S. A. Benner, *Bioorg. Med. Chem. Lett.* **1998**, 8, 1149.
- [32] J. D. Bain, C. Switzer, A. R. Chamberlin and S. A. Benner, *Nature* **1992**, 356, 537.
- [33] A. K. Ogawa, Y. Q. Wu, D. L. McMinn, J. Q. Liu, P. G. Schultz and F. E. Romesberg, *J. Am. Chem. Soc.* **2000**, 122, 3274.
- [34] E. T. Kool and H. O. Sintim, *Chem. Commun.* **2006**, 3665.
- [35] J. Hunziker and G. Mathis, *Chimia* **2005**, 59, 780.
- [36] K. Tanaka and M. Shionoya, *J. Org. Chem.* **1999**, 64, 5002.

- [37] G. H. Clever, C. Kaul and T. Carell, *Angew. Chem., Int. Ed.* **2007**, *46*, 6226.
- [38] W. He, R. M. Franzini and C. Achim, *Prog. Inorg. Chem.* **2007**, *55*, 545.
- [39] J. Müller, *Eur. J. Inorg. Chem.* **2008**, 3749.
- [40] M. Shionoya and K. Tanaka, *Curr. Opin. Chem. Biol.* **2004**, *8*, 592.
- [41] K. Tanaka and M. Shionoya, *Coord. Chem. Rev.* **2007**, *251*, 2732.
- [42] H. Weizman and Y. Tor, *Chem. Commun.* **2001**, 453.
- [43] E. Meggers, P. L. Holland, W. B. Tolman, F. E. Romesberg and P. G. Schultz, *J. Am. Chem. Soc.* **2000**, *122*, 10714.
- [44] S. Atwell, E. Meggers, G. Spraggon and P. G. Schultz, *J. Am. Chem. Soc.* **2001**, *123*, 12364.
- [45] D. Böhme, N. Düpre, D. A. Megger and J. Müller, *Inorg. Chem.* **2007**, *46*, 10114.
- [46] G. H. Clever and T. Carell, *Angew. Chem., Int. Ed.* **2007**, *46*, 250.
- [47] G. H. Clever, K. Polborn and T. Carell, *Angew. Chem., Int. Ed.* **2005**, *44*, 7204.
- [48] G. H. Clever, Y. Sörtl, H. Burks, W. Spahl and T. Carell, *Chem. Eur. J.* **2006**, *12*, 8708.
- [49] B. D. Heuberger, D. Shin and C. Switzer, *Org. Lett.* **2008**, *10*, 1091.
- [50] A. Ono, S. Cao, H. Togashi, M. Tashiro, T. Fujimoto, T. Machinami, S. Oda, Y. Miyake, I. Okamoto and Y. Tanaka, *Chem. Commun.* **2008**, 4825.
- [51] F.-A. Polonius and J. Müller, *Angew. Chem., Int. Ed.* **2007**, *46*, 5602.
- [52] C. Switzer and D. Shin, *Chem. Commun.* **2005**, 1342.
- [53] C. Switzer, S. Sinha, P. H. Kim and B. D. Heuberger, *Angew. Chem., Int. Ed.* **2005**, *44*, 1529.
- [54] K. Tanaka, G. H. Clever, Y. Takezawa, Y. Yamada, C. Kaul, M. Shionoya and T. Carell, *Nature Nanotechnology* **2006**, *1*, 190.
- [55] K. Tanaka, A. Tengeiji, T. Kato, N. Toyama and M. Shionoya, *Science* **2003**, *299*, 1212.
- [56] K. Tanaka, Y. Yamada and M. Shionoya, *J. Am. Chem. Soc.* **2002**, *124*, 8802.
- [57] Y. Tanaka, S. Oda, H. Yamaguchi, Y. Kondo, C. Kojima and A. Ono, *J. Am. Chem. Soc.* **2007**, *129*, 244.
- [58] H. Weizman and Y. Tor, *J. Am. Chem. Soc.* **2001**, *123*, 3375.
- [59] S. D. Wettig, D. O. Wood, P. Aich and J. S. Lee, *J. Inorg. Biochem.* **2005**, *99*, 2093.
- [60] L. Zhang and E. Meggers, *J. Am. Chem. Soc.* **2005**, *127*, 74.
- [61] N. Zimmermann, E. Meggers and P. G. Schultz, *J. Am. Chem. Soc.* **2002**, *124*, 13684.
- [62] N. Zimmermann, E. Meggers and P. G. Schultz, *Bioorg. Chem.* **2004**, *32*, 13.
- [63] M. K. Schlegel, L. Zhang, N. Pagano and E. Meggers, *Org. Biomol. Chem.* **2009**, *7*, 476.
- [64] R. M. Franzini, R. M. Watson, G. K. Patra, R. M. Breece, D. L. Tierney, M. P. Hendrich and C. Achim, *Inorg. Chem.* **2006**, *45*, 9798.
- [65] B. P. Gilmartin, K. Ohr, R. L. McLaughlin, R. Koerner and M. E. Williams, *J. Am. Chem. Soc.* **2005**, *127*, 9546.
- [66] A. Küsel, J. Zhang, M. Alvarino Gil, A. C. Stückl, W. Meyer-Klaucke, F. Meyer and U. Diedrichsen, *Eur. J. Inorg. Chem.* **2005**, 4317.
- [67] K. Ohr, R. L. McLaughlin and M. E. Williams, *Inorg. Chem.* **2007**, *46*, 965.
- [68] D.-L. Popescu, T. J. Parolin and C. Achim, *J. Am. Chem. Soc.* **2003**, *125*, 6354.

- [69] R. M. Watson, Y. A. Skorik, G. K. Patra and C. Achim, *J. Am. Chem. Soc.* **2005**, *127*, 14628.
- [70] D. D. Eley and D. I. Spivey, *Trans. Faraday Soc.* **1962**, *58*, 411.
- [71] C. J. Murphy, M. R. Arkin, Y. Jenkins, N. D. Ghatlia, S. H. Bossmann, N. J. Turro and J. K. Barton, *Science* **1993**, *262*, 1025.
- [72] Y. A. Berlin, A. L. Burin and M. A. Ratner, *Superlattices and Microstructures* **2000**, *28*, 241.
- [73] Y. A. Berlin, A. L. Burin and M. A. Ratner, *J. Am. Chem. Soc.* **2001**, *123*, 260.
- [74] N. J. Turro and J. K. Barton, *J. Biol. Inorg. Chem.* **1998**, *3*, 201.
- [75] A. Y. Kasumov, M. Kociak, S. Gueron, B. Reulet, V. T. Volkov, D. V. Klinov and H. Bouchiat, *Science* **2001**, *291*, 280.
- [76] H. W. Fink, *Cell. Mol. Life Sci.* **2001**, *58*, 1.
- [77] H. W. Fink and C. Schonenberger, *Nature* **1999**, *398*, 407.
- [78] D. Porath, A. Bezryadin, S. de Vries and C. Dekker, *Nature* **2000**, *403*, 635.
- [79] D. N. Beratan, S. Priyadarshy and S. M. Risser, *Chem. Biol.* **1997**, *4*, 3.
- [80] P. J. de Pablo, F. Moreno-Herrero, J. Colchero, J. Gomez-Herrero, P. Herrero, A. M. Baro, P. Ordejon, J. M. Soler and E. Artacho, *Phys. Rev. Lett.* **2000**, *85*, 4992.
- [81] S. Priyadarshy, S. M. Risser and D. N. Beratan, *J. Phys. Chem.* **1996**, *100*, 17678.
- [82] B. Giese, *Annu. Rev. Biochem.* **2002**, *71*, 51.
- [83] H. A. Wagenknecht, *Angew. Chem., Int. Ed.* **2003**, *42*, 2454.
- [84] C. J. Burrows and J. G. Muller, *Chem. Rev.* **1998**, *98*, 1109.
- [85] S. Kawanishi, Y. Hiraku and S. Oikawa, *Mutat. Res.* **2001**, *488*, 65.
- [86] P. O'Neill and E. M. Fielden, *Adv. Radiation Biol.* **1993**, *17*, 53.
- [87] D. Wang, D. A. Kreutzer and J. M. Essigmann, *Mutat. Res.* **1998**, *400*, 99.
- [88] T. Carell, C. Behrens and J. Gierlich, *Org. Biomol. Chem.* **2003**, *1*, 2221.
- [89] J. Richter, *Physica E* **2003**, *16*, 157.
- [90] H. A. Wagenknecht, *Nat. Prod. Rep.* **2006**, *23*, 973.
- [91] H. A. Becerril, R. M. Stoltenberg, D. R. Wheeler, R. C. Davis, J. N. Harb and A. T. Woolley, *J. Am. Chem. Soc.* **2005**, *127*, 2828.
- [92] L. Berti, A. Alessandrini and P. Facci, *J. Am. Chem. Soc.* **2005**, *127*, 11216.
- [93] E. Braun, Y. Eichen, U. Sivan and G. Ben-Yoseph, *Nature* **1998**, *391*, 775.
- [94] M. Mertig, L. C. Ciacchi, R. Seidel, W. Pompe and A. De Vita, *Nano Lett.* **2002**, *2*, 841.
- [95] R. Möller, A. Csaki, J. M. Kohler and W. Fritzsche, *Langmuir* **2001**, *17*, 5426.
- [96] C. F. Monson and A. T. Woolley, *Nano Lett.* **2003**, *3*, 359.
- [97] T. Nishinaka, A. Takano, Y. Doi, M. Hashimoto, A. Nakamura, Y. Matsushita, J. Kumaki and E. Yashima, *J. Am. Chem. Soc.* **2005**, *127*, 8120.
- [98] J. Richter, M. Mertig, W. Pompe, I. Mönch and H. K. Schackert, *Appl. Phys. Lett.* **2001**, *78*, 536.
- [99] H. Yan, S. H. Park, G. Finkelstein, J. H. Reif and T. LaBean, *Science* **2003**, *301*, 1882.
- [100] G. A. Burley, J. Gierlich, M. R. Mofid, H. Nir, S. Tal, Y. Eichen and T. Carell, *J. Am. Chem. Soc.* **2006**, *128*, 1398.
- [101] M. Fischler, U. Simon, H. Nir, Y. Eichen, G. A. Burley, J. Gierlich, P. M. E. Gramlich and T. Carell, *Small* **2007**, *3*, 1049.

- [102] P. Aich, S. L. Labiuk, L. W. Tari, L. J. T. Delbaere, W. J. Roesler, K. J. Falk, R. P. Steer and J. S. Lee, *J. Mol. Biol.* **1999**, 294, 477.
- [103] P. Aich, R. J. S. Skinner, S. D. Wettig, R. P. Steer and J. S. Lee, *J. Biomol. Struct. Dyn.* **2002**, 20, 93.
- [104] A. Rakitin, P. Aich, C. Papadopoulos, Y. Kobzar, A. S. Vedeneev, J. S. Lee and J. M. Xu, *Phys. Rev. Lett.* **2001**, 86, 3670.
- [105] M. Fuentes-Cabrera, B. G. Sumpter, J. E. Šponer, J. Šponer, L. Petit and J. C. Wells, *J. Phys. Chem. B* **2007**, 111, 870.
- [106] M. C. Erat and R. K. O. Sigel, *Chimia* **2005**, 59, 817.
- [107] K. Wüthrich, *NMR of Proteins and Nucleic Acids*, John Wiley & Sons, New York, **1986**.
- [108] B. Fürtig, C. Richter, J. Wöhnert and H. Schwalbe, *ChemBioChem* **2003**, 4, 936.
- [109] E. V. Puglisi and J. D. Puglisi in *Nuclear magnetic resonance spectroscopy of RNA*, Vol. Eds.: R. W. Simons and M. Grunberg-Manago), Cold Spring Harbor Laboratory Press, Cold Spring Harbor, **1998**, pp. 117.
- [110] D. J. Patel, S. A. Kozlowski, A. Nordheim and A. Rich, *Proc. Natl. Acad. Sci. U. S. A.* **1982**, 79, 1413.
- [111] P. B. Moore in *The RNA folding problem*, Vol. Eds.: R. F. Gesteland, T. R. Cech and J. F. Atkins), Cold Spring Harbor Press, Cold Spring Harbor, **1999**, pp. 381.
- [112] A. T. Brünger, P. D. Adams, G. M. Clore, W. L. DeLano, P. Gros, R. W. Grosse-Kunstleve, J.-S. Jiang, J. Kuszewski, M. Nilges, N. S. Pannu, R. J. Read, L. M. Rice, T. Simonson and G. L. Warren, *Acta Crystallogr., Sect. D: Biol. Crystallogr.* **1998**, D54, 905.
- [113] P. Güntert, C. Mumenthaler and K. Wüthrich, *J. Mol. Biol.* **1997**, 273, 283.
- [114] C. D. Schwieters, J. J. Kuszewski, N. Tjandra and G. M. Clore, *J. Magn. Reson.* **2003**, 160, 65.
- [115] W. J. Metzler, C. Wang, D. B. Kitchen, R. M. Levy and A. Pardi, *J. Mol. Biol.* **1990**, 214, 711.
- [116] S. Gallo, M. Furler and R. K. O. Sigel, *Chimia* **2005**, 59, 812.
- [117] E. Freisinger and R. K. O. Sigel, *Coord. Chem. Rev.* **2007**, 251, 1834.
- [118] R. K. O. Sigel and A. M. Pyle, *Chem. Rev.* **2007**, 107, 97.
- [119] B. Lippert, *Cisplatin: Chemistry and Biochemistry of a Leading Anticancer Drug*, VCHA and Wiley-VCH, , Zürich, Weinheim, **1999**.
- [120] P. M. Gordon and J. A. Piccirilli, *Nat. Struct. Biol.* **2001**, 8, 893.
- [121] S.-O. Shan, A. V. Kravchuk, J. A. Piccirilli and D. Herschlag, *Biochemistry* **2001**, 40, 5161.
- [122] M. C. Erat and R. K. O. Sigel, *J. Biol. Inorg. Chem.* **2008**, 13, 1025.
- [123] M. C. Erat, O. Zerbe, T. Fox and R. K. O. Sigel, *ChemBioChem* **2007**, 8, 306.
- [124] R. L. Gonzalez, Jr. and I. Tinoco Jr., *J. Mol. Biol.* **1999**, 289, 1267.
- [125] F. H.-T. Allain and G. Varani, *Nucleic Acids Res.* **1995**, 23, 341.
- [126] S. E. Butcher, F. H. T. Allain and J. Feigon, *Biochemistry* **2000**, 39, 2174.
- [127] G. Colmenarejo and I. Tinoco Jr., *J. Mol. Biol.* **1999**, 290, 119.
- [128] J. H. Davis, T. R. Foster, M. Tonelli and S. E. Butcher, *RNA* **2007**, 13, 76.
- [129] J. S. Kieft and I. Tinoco, Jr., *Structure* **1997**, 5, 713.
- [130] H. Robinson and A. H. J. Wang, *Nucleic Acids Res.* **1996**, 24, 676.

- [131] S. Rüdisser and I. Tinoco, Jr., *J. Mol. Biol.* **2000**, 295, 1211.
- [132] M. Schmitz and I. Tinoco Jr., *RNA* **2000**, 6, 1212.
- [133] M. C. Erat and R. K. O. Sigel, *Inorg. Chem.* **2007**, 46, 11224.
- [134] R. K. O. Sigel, *Eur. J. Inorg. Chem.* **2005**, 12, 2281.
- [135] R. K. O. Sigel, D. G. Sashital, D. L. Abramovitz, A. G. Palmer III, S. E. Butcher and A. M. Pyle, *Nat. Struct. Mol. Biol.* **2004**, 11, 187.
- [136] S. Basu, A. A. Szewczak, M. Cocco and S. A. Strobel, *J. Am. Chem. Soc.* **2000**, 122, 3240.
- [137] N. V. Hud, P. Schultze and J. Feigon, *J. Am. Chem. Soc.* **1998**, 120, 6403.
- [138] S. Katz, *Biochim. Biophys. Acta* **1963**, 68, 240.
- [139] Y. Miyake and A. Ono, *Tetrahedron Lett.* **2005**, 46, 2441.
- [140] Y. Miyake, H. Togashi, M. Tashiro, H. Yamaguchi, S. Oda, M. Kudo, Y. Tanaka, Y. Kondo, R. Sawa, T. Fujimoto, T. Machinami and A. Ono, *J. Am. Chem. Soc.* **2006**, 128, 2172.
- [141] A. Ono and H. Togashi, *Angew. Chem., Int. Ed.* **2004**, 43, 4300.
- [142] W. Brüning, E. Freisinger, M. Sabat, R. K. O. Sigel and B. Lippert, *Chem. Eur. J.* **2002**, 8, 4681.
- [143] W. Brüning, R. K. O. Sigel, E. Freisinger and B. Lippert, *Angew. Chem., Int. Ed.* **2001**, 40, 3397.
- [144] B. Lippert, P. Amo-Ochoa, W. Brüning, E. Freisinger, M. S. Luth, S. Meier, C. Meiser, S. Metzger, H. Rauter, A. Schreiber, R. K. O. Sigel and H. Witkowski, *Pure Appl. Chem.* **1998**, 70, 977.
- [145] J. Müller, F.-A. Polonius and M. Roitzsch, *Inorg. Chim. Acta* **2005**, 358, 1225.
- [146] J. A. R. Navarro and B. Lippert, *Coord. Chem. Rev.* **1999**, 186, 653.
- [147] L. D. Kosturko, C. Folzer and R. F. Stewart, *Biochemistry* **1974**, 13, 3949.
- [148] Z. Kuklenyik and L. G. Marzilli, *Inorg. Chem.* **1996**, 35, 5654.
- [149] E. Ennifar, P. Walter and P. Dumas, *Nucleic Acids Res.* **2003**, 31, 2671.
- [150] R. K. O. Sigel, E. Freisinger and B. Lippert, *J. Biol. Inorg. Chem.* **2000**, 5, 287.
- [151] R. K. O. Sigel and A. M. Pyle, *Met. Ions Biol. Syst.* **2003**, 40, 477.
- [152] J. F. Milligan, D. R. Groebe, G. W. Witherell and O. C. Uhlenbeck, *Nucleic Acids Res.* **1987**, 15, 8783.
- [153] L. Hartvig and J. Christiansen, *EMBO J.* **1996**, 15, 4767.
- [154] D. A. Mead, E. Szczesnaskorupa and B. Kemper, *Protein Eng.* **1986**, 1, 67.
- [155] H. Song and C. Kang, *Genes Cells* **2001**, 6, 291.
- [156] T. A. Steitz, *Curr. Opin. Chem. Biol.* **2009**, 19, 683.
- [157] A. Bagno and G. Saielli, *J. Am. Chem. Soc.* **2007**, 129, 11360.
- [158] W. Eimer, J. R. Williamson, S. G. Boxer and R. Pecora, *Biochemistry* **1990**, 29, 799.
- [159] J. Lapham, J. P. Rife, P. B. Moore and D. M. Crothers, *J. Biomol. NMR* **1997**, 10, 255.
- [160] V. A. Bloomfield, D. M. Crothers and I. Tinoco, *Nucleic Acids Structures, Properties, and Functions*, University Science Books, Sausalito, CA, USA, **2003**.
- [161] M. Sarkar, S. Sigurdsson, S. Tomac, S. Sen, E. Rozners, B. Sjöberg, R. Strömberg and A. Gräslund, *Biochemistry* **1996**, 35, 4678.
- [162] T. Pan and T. R. Sosnick, *Nat. Struct. Biol.* **1997**, 4, 931.
- [163] S. Stampfl, A. Lempradl, G. Koehler and R. Schroeder, *ChemBioChem* **2007**, 8, 1137

- [164] G. M. T. Cheetham, D. Jeruzalmi and T. A. Steitz, *Nature* **1999**, 399, 80.
- [165] G. M. T. Cheetham and T. A. Steitz, *Science* **1999**, 286, 2305.
- [166] K. J. Durniak, S. Bailey and T. A. Steitz, *Science* **2008**, 322, 553.
- [167] D. Jeruzalmi and T. A. Steitz, *EMBO J.* **1998**, 17, 4101.
- [168] W. P. Kennedy, J. R. Momand and Y. W. Yin, *J. Mol. Biol.* **2007**, 370, 256.
- [169] R. Sousa, Y. J. Chung, J. P. Rose and B. C. Wang, *Nature* **1993**, 364, 593.
- [170] T. H. Tahirov, D. Temiakov, M. Anikin, V. Patlan, W. T. McAllister, D. G. Vassilyev and S. Yokoyama, *Nature* **2002**, 420, 43.
- [171] D. Temiakov, V. Patlan, M. Anikin, W. T. McAllister, S. Yokoyama and D. G. Vassilyev, *Cell* **2004**, 116, 381.
- [172] Y. W. Yin and T. A. Steitz, *Science* **2002**, 298, 1387.
- [173] Y. W. Yin and T. A. Steitz, *Cell* **2004**, 116, 393.
- [174] A. J. Carpousis and J. D. Gralla, *Biochemistry* **1980**, 19, 3245.
- [175] C. T. Martin, D. K. Muller and J. E. Coleman, *Biochemistry* **1988**, 27, 3966.
- [176] T. A. Steitz, *Nature* **1998**, 391, 231.
- [177] T. A. Steitz, *Curr. Opin. Chem. Biol.* **2004**, 14, 4.
- [178] G. Bonner, D. Patra, E. M. Lafer and R. Sousa, *EMBO J.* **1992**, 11, 3767.
- [179] C. M. Joyce, *Proc. Natl. Acad. Sci. U. S. A.* **1997**, 94, 1619.
- [180] C. M. Joyce and T. A. Steitz, *J. Bacteriol.* **1995**, 177, 6321.
- [181] Y. Huang, F. Eckstein, R. Padilla and R. Sousa, *Biochemistry* **1997**, 36, 8231.
- [182] R. Padilla and R. Sousa, *Nucleic Acids Res.* **1999**, 27, 1561.
- [183] R. Sousa and R. Padilla, *EMBO J.* **1995**, 14, 4609.
- [184] S. O. Gudima, D. A. Kostyuk, O. I. Grishchenko, V. L. Tunitskaya, L. V. Memelova and S. N. Kochetkov, *FEBS Lett.* **1998**, 439, 302.
- [185] D. A. Kostyuk, S. M. Dragan, D. L. Lyakhov, V. O. Rechinsky, V. L. Tunitskaya, B. K. Chernov and S. N. Kochetkov, *FEBS Lett.* **1995**, 369, 165.
- [186] Y. Huang, A. Beaudry, J. McSwiggen and R. Sousa, *Biochemistry* **1997**, 36, 13718.
- [187] J. Cabello-Villegas and E. P. Nikonowicz, *Nucleic Acids Res.* **2000**, 28, e74.
- [188] L. Hemmingsen, K. N. Sas and E. Danielsen, *Chem. Rev.* **2004**, 104, 4027.
- [189] O. Iranzo, P. W. Thulstrup, S. B. Ryu, L. Hemmingsen and V. L. Pecoraro, *Chem. Eur. J.* **2007**, 13, 9178.
- [190] N. Selevsek, S. Rival, A. Tholey, E. Heinzle, U. Heinz, L. Hemmingsen and H. W. Adolph, *J. Biol. Chem.* **2009**, 284, 16419.
- [191] L. Hemmingsen, *personal communication*.
- [192] M. Barcelo, *personal communication*.
- [193] S. Johannsen, S. Paulus, N. Düpre, J. Müller and R. K. O. Sigel, *J. Inorg. Biochem.* **2008**, 102, 1141.
- [194] M. K. Schlegel, L.-O. Essen and E. Meggers, *J. Am. Chem. Soc.* **2008**, 130, 8158.
- [195] J. Müller, D. Böhme, P. Lax, M. Morell Cerdà and M. Roitzsch, *Chem. Eur. J.* **2005**, 11, 6246.
- [196] S. Johannsen, N. Megger, D. Böhme, R. K. O. Sigel and J. Müller, *Nat. Chem.* **2010**, 2, 229.



- [197] S. Johannsen, D. Böhme, N. Düpre, J. Müller and R. K. O. Sigel, *Abstracts Book of the 4th EuCheMS Conf. on Nitrogen Ligands* (Garmisch-Partenkirchen, Germany) **2008**, p. 132.
- [198] S. Johannsen, D. Böhme, N. Düpre, J. Müller and R. K. O. Sigel, *Abstracts Book of the 9th Eur. Biol. Inorg. Chem. Conf. (EuroBIC-9)* (Wroclaw, Poland) **2008**, p. 207.
- [199] B. Knobloch, H. Sigel, A. Okruszek and R. K. O. Sigel, *Org. Biomol. Chem.* **2006**, *4*, 1085.
- [200] B. Lippert, *Prog. Inorg. Chem.* **2005**, *54*, 385.
- [201] J. Catalán, R. M. Claramunt, J. Elguero, J. Laynez, M. Menéndez, F. Anvia, J. H. Quian, M. Taagepera and R. W. Taft, *J. Am. Chem. Soc.* **1988**, *110*, 4105.
- [202] H. Walba and R. Ruiz-Velasco Jr., *J. Org. Chem.* **1969**, *34*, 3315.
- [203] D. Banerjee, T. A. Kaden and H. Sigel, *Inorg. Chem.* **1981**, *20*, 2586.
- [204] C. P. Da Costa, D. Krajewska, A. Okruszek, W. J. Stec and H. Sigel, *J. Biol. Inorg. Chem.* **2002**, *7*, 405.
- [205] L.-N. Ji, N. A. Corfù and H. Sigel, *Dalton Trans.* **1991**, 1367.
- [206] L.-N. Ji, N. A. Corfù and H. Sigel, *Inorg. Chim. Acta* **1993**, *206*, 215.
- [207] L. E. Kapinos and H. Sigel, *Inorg. Chim. Acta* **2002**, *337*, 131.
- [208] L. E. Kapinos, B. Song and H. Sigel, *Inorg. Chim. Acta* **1998**, *280*, 50.
- [209] L. E. Kapinos, B. Song and H. Sigel, *Chem.--Eur. J.* **1999**, *5*, 1794.
- [210] S. S. Massoud and H. Sigel, *Inorg. Chem.* **1988**, *27*, 1447.
- [211] A. Mucha, B. Knobloch, M. Jezowska-Bojczuk, H. Kozłowski and R. K. O. Sigel, *Chem. Eur. J.* **2008**, *14*, 6663.
- [212] A. Saha, N. Saha, L. N. Ji, J. Zhao, F. Gregan, S. A. A. Sajadi, B. Song and H. Sigel, *J. Biol. Inorg. Chem.* **1996**, *1*, 231.
- [213] H. Sigel, A. D. Zuberbühler and O. Yamauchi, *Anal. Chim. Acta* **1991**, *255*, 63.
- [214] B. Song and H. Sigel, *Inorg. Chem.* **1998**, *37*, 2066.
- [215] B. Song, J. Zhao, R. Griesser, C. Meiser, H. Sigel and B. Lippert, *Chem. Eur. J.* **1999**, *5*, 2374.
- [216] H. Sigel, B. P. Operschall and R. Griesser, *Chem. Soc. Rev.* **2009**, *38*, 2465.
- [217] R. K. O. Sigel, B. Song and H. Sigel, *J. Am. Chem. Soc.* **1997**, *119*, 744.
- [218] R. B. Martin, *Science* **1963**, *139*, 1198.
- [219] E. M. Bianchi, S. A. A. Sajadi, B. Song and H. Sigel, *Chem. Eur. J.* **2003**, *9*, 881.
- [220] R. Tribolet and H. Sigel, *Eur. J. Biochem.* **1987**, *163*, 353.
- [221] P. Acharya, S. Acharya, P. Cheruku, N. V. Amirkhanov, A. Foldesi and J. Chattopadhyaya, *J. Am. Chem. Soc.* **2003**, *125*, 9948.
- [222] K. Chin, K. A. Sharp, B. Honig and A. M. Pyle, *Nat. Struct. Biol.* **1999**, *6*, 1055.
- [223] P. C. Bevilacqua, T. S. Brown, S.-i. Nakano and R. Yajima, *Biopolymers* **2004**, *73*, 90.
- [224] B. Lippert, *Chem. Biodiversity* **2008**, *5*, 1455.
- [225] E. M. Moody, J. T. J. Lecomte and P. C. Bevilacqua, *RNA* **2005**, *11*, 157.
- [226] G. J. Narlikar and D. Herschlag, *Annu. Rev. Biochem.* **1997**, *66*, 19.
- [227] G. Varani, F. Aboul-ela and F. H. T. Allain, *Prog. Nucl. Magn. Reson. Spectrosc.* **1996**, *29*, 51.
- [228] Y. Tanaka and A. Ono, *Dalton Trans.* **2008**, 4965.
- [229] H. Sigel and D. B. McCormick, *Acc. Chem. Res.* **1970**, *3*, 201.

- [230] K. Zangger and I. M. Armitage, *Met. Based Drugs* **1999**, 6, 239.
- [231] G. A. Bowmaker, R. K. Harris, B. Assadollahzadeh, D. C. Apperly, P. Hodgkinson and P. Amornsakchai, *Magn. Reson. Chem.* **2004**, 42, 819.
- [232] G. C. van Stein, G. van Koten, K. Vrieze, C. Brevard and A. L. Spek, *J. Am. Chem. Soc.* **1984**, 106, 4486.
- [233] G. C. van Stein, G. van Koten, K. Vrieze, A. L. Spek, E. A. Klop and C. Brevard, *Inorg. Chem.* **1985**, 24, 1367.
- [234] S. S. Narula, R. K. Mehra, D. R. Winge and I. M. Armitage, *J. Am. Chem. Soc.* **1991**, 113, 9354.
- [235] C. Brevard, G. C. van Stein and G. van Koten, *J. Am. Chem. Soc.* **1981**, 103, 6746.
- [236] G. C. van Stein, H. van der Poel, G. van Koten, A. L. Spek, A. J. M. Duisenberg and P. S. Pregosin, *Chem. Commun.* **1980**, 1016.
- [237] G. C. van Stein, G. van Koten and C. Brevard, *J. Organomet. Chem.* **1982**, 226, C27.
- [238] G. C. van Stein, G. van Koten, B. Debok, L. C. Taylor, K. Vrieze and C. Brevard, *Inorg. Chim. Acta* **1984**, 89, 29.
- [239] G. C. van Stein, G. van Koten, K. Vrieze and C. Brevard, *Inorg. Chem.* **1984**, 23, 4269.
- [240] X.-J. Lu and W. K. Olson, *Nucleic Acids Res.* **2003**, 31, 5108.
- [241] R. Chandrasekaran and S. Arnott, *J. Biomol. Struct. Dyn.* **1996**, 13, 1015.
- [242] X. Liu, G.-C. Guo, M.-L. Fu, X.-H. Liu, M.-S. Wang and J.-S. Huang, *Inorg. Chem.* **2006**, 45, 3679.
- [243] S. S. Mallajosyula and S. K. Pati, *Angew. Chem., Int. Ed.* **2009**, 48, 4977.
- [244] S. Johannsen, M. M. T. Korth, J. Schnabl and R. K. O. Sigel, *Chimia* **2009**, 63, 146.
- [245] I. Hirao, M. Kimoto, T. Mitsui, T. Fujiwara, R. Kawai, A. Sato, Y. Harada and S. Yokoyama, *Nat. Methods* **2006**, 3, 729.
- [246] G. T. Hwang and F. E. Romesberg, *Nucleic Acids Res.* **2006**, 34, 2037.
- [247] T. W. Kim, L. G. Briebe, T. Ellenberger and E. T. Kool, *J. Biol. Chem.* **2006**, 281, 2289.
- [248] T. W. Kim, J. C. Delaney, J. M. Essigmann and E. T. Kool, *Proc. Natl. Acad. Sci. U. S. A.* **2005**, 102, 15803.
- [249] A. M. Leconte, S. Matsuda and F. E. Romesberg, *J. Am. Chem. Soc.* **2006**, 128, 6780.
- [250] S. Matsuda, A. A. Henry and F. E. Romesberg, *J. Am. Chem. Soc.* **2006**, 128, 6369.
- [251] T. Mitsui, M. Kimoto, Y. Harada, S. Yokoyama and I. Hirao, *J. Am. Chem. Soc.* **2005**, 127, 8652.
- [252] M. A. O'Neill and J. K. Barton in *DNA-mediated charge transport chemistry and biology*, Vol. 236 Springer-Verlag Berlin, Berlin, **2004**, pp. 67.
- [253] P. Davanloo, A. H. Rosenberg, J. J. Dunn and F. W. Studier, *Proc. Natl. Acad. Sci. U. S. A.* **1984**, 81, 2035.
- [254] D. E. Draper and T. C. Gluick, *Methods Enzymol.* **1995**, 259, 281.
- [255] L. A. Marky and K. J. Breslauer, *Biopolymers* **1987**, 26, 1601.
- [256] L. Hemmingsen, R. Bauer, M. J. Bjerrum, M. Zeppezauer, H. W. Adolph, G. Formicka and E. Cedergrenzeppezauer, *Biochemistry* **1995**, 34, 7145.
- [257] P. K. Glasoe and F. A. Long, *J. Phys. Chem.* **1960**, 64, 188.
- [258] R. Lumry, E. L. Smith and R. R. Glantz, *J. Am. Chem. Soc.* **1951**, 73, 5933.

- 
- [259] C. F. Guerra, J. W. Handgraaf, E. J. Baerends and F. M. Bickelhaupt, *J. Comput. Chem.* **2004**, *25*, 189.
- [260] R. Stefl, H. Wu, S. Ravindranathan, V. Sklenář and J. Feigon, *Proc. Natl. Acad. Sci. U. S. A.* **2004**, *101*, 1177.



# Curriculum Vitae

## Personal data:

Name	SILKE JOHANNSEN
Date and Place of Birth	18 <sup>th</sup> November 1980 in Zittau, Gemany
Nationality	German
Marital status	single, one son, one daughter

## Education

1987 – 1991	Primary school in Wurzen
1992 – 1999	Grammar school/high school, Magnus-Gottfried-Lichtwer-Gymnasium Wurzen
June 1999	Abitur (leaving certificate)
October 1999 – October 2004	Studies of Chemistry at the Westfälische Wilhelms-Universität Münster, Germany
Febuary 2004 – October 2004	Diploma thesis with Prof. Dr. Monika Schönhoff at the Institute of Physical Chemistry, Westfälische Wilhelms-Universität Münster, Germany Subject: <i>"Natriumbeweglichkeit in Polyelektrolytkomplexen"</i>
October 18, 2004	Diploma degree in Chemistry from the Westfälische Wilhelms-Universität Münster, Germany
April 2006 – 2010	PhD thesis with Prof. Dr. Roland K. O. Sigel at the Institute of Inorganic Chemistry, University of Zürich, Switzerland Subject: <i>"A study on nucleic acids with metal-mediated base pairs"</i>
June 2010	Dissertation at the University of Zürich, Switzerland

## Awards

April 2007	Poster prize at the 2nd Annual Dorothy Crowfoot Hodgkin Symposium, University of Zürich, <i>“Incorporation of Ag<sup>+</sup> ions into DNA by the aid of artificial nucleotides”</i> .
September 2008	Poster prize at the Fall Meeting of the Swiss Chemical Society, University of Zürich, <i>“NMR investigation of an oligonucleotide containing metal-mediated base pairs”</i> .
September 2009	Poster prize at the ISABC 10 - International Symposium on Applied Bioinorganic Chemistry, Debrecen, <i>“NMR characterisation of an oligonucleotide containing metal-mediated base pairs”</i> .

## Internships and other activities:

July – September 1999	WRC World Resources Company GmbH, Wurzen Germany, internship
September 2000	WRC World Resources Company GmbH, Wurzen Germany, internship
September 16 – 27, 2002	Forschungszentrum Jülich, Germany, course on <i>Neutron Scattering</i>
October 2000 – January 2004	Student assistant at the "Dekanat des Fachbereichs Chemie und Pharmazie", Westfälische Wilhelms-Universität Münster, Germany
November 2003 – March 2004	Student assistant at the Institute of Physical Chemistry, Westfälische Wilhelms-Universität Münster, Germany
October 2 - 6, 2006	NCCR Practical Course: Advanced NMR Methods for structural studies of biomolecular complexes and membrane proteins, ETH Zürich, Switzerland
May 5 – 9, 2008	Management Training Week for Life Science Researchers, Berlin, Germany
November 2008 – June 2009	Communication Skills for Leaders, University Zürich, Switzerland

## Scientific Teaching Experience

October 2006– December 2007	Teaching assistant in the Laboratory Course in Chemistry for Medical and Dental students at the University of Zürich, Switzerland
October 2006 – December 2007	Teaching assistant in the Laboratory Course in Chemistry for Veterinary Medical students at the University of Zürich, Switzerland
October – December 2007	Teaching assistant in the Laboratory Course in Chemistry for Medical and Dental students at the University of Zürich, Switzerland
October – December 2007	Teaching assistant in the Laboratory Course in Chemistry for Veterinary Medical students at the University of Zürich, Switzerland

## List of Publication

*Using in vitro transcription to construct scaffolds for one-dimensional arrays of mercuric ions*

Silke Johannsen, Susann Paulus, Nicole Düpre, Jens Müller, Roland K. O. Sigel, *J. Inorg. Biochem.*, **2008**, 102, 1141-1151.

*Exploring metal ion coordination to nucleic acids by NMR*

Silke Johannsen, Maximiliane M. T. Korth, Joachim Schnabl, Roland K. O. Sigel, *Chimia*, **2009**, 63, 146-152.

*Solution structure of a DNA double helix with consecutive metal-mediated base pairs*

Silke Johannsen, Nicole Megger, Dominik Böhme, Roland K. O. Sigel, Jens Müller, *Nature Chem.* **2010**, 2, 229-234.

*Synthesis and acid-base properties of an imidazole-containing nucleotide analogue, 1-(2'-deoxy- $\beta$ -D-ribofuranosyl)imidazole 5'-monophosphate (*dImMP*<sup>2-</sup>)*

Silke Johannsen, Nicole Megger, Jens Müller, Roland K. O. Sigel, in preparation.

*The hairpin structure of an oligonucleotide containing artificial imidazole nucleobases is strongly influenced by pH*

Silke Johannsen, Nicole Megger, Dominik Böhme, Jens Müller, Roland K. O. Sigel, in preparation.

## Conference Contribution

### Oral presentations:

*NMR investigations of metal-modified oligonucleotides"*

Silke Johannsen, Roland K. O. Sigel

Lecture at the 1<sup>st</sup> International Symposium on Chemical and Molecular Sciences, November 1, 2007, Zürich, Switzerland.

*Structural characterization of a metal-modified DNA*

Silke Johannsen, Roland K. O. Sigel

Lecture at the COST D39-WG2 Meeting: Metallo-Drug Design and Action, April 28-29, 2009, Zürich, Switzerland.

*Formation and structure of metal-modified nucleic acid*

Silke Johannsen, Roland K. O. Sigel

Lecture at the COST D39 Conference: Metallo-Drug Design and Action, September 24-25, 2009, Debrecen, Hungary.

### Poster presentations:

*NMR investigation of a  $Ag^+$  ion binding oligonucleotide containing artificial imidazole nucleosides*

Silke Johannsen, Dominik Böhme, Jens Müller and Roland K. O. Sigel

ESF-COST High-Level Research Conference, Inorganic Chemistry – Metal-Nucleic Acid Interactions, November 12-17, 2006, Athens, Greece.

*Incorporation of  $Ag^+$  ions into DNA by the aid of artificial nucleotides*

Silke Johannsen, Dominik Böhme, Jens Müller and Roland K. O. Sigel

2<sup>nd</sup> Annual Dorothy Crowfoot Hodgkin Symposium, April 27, 2007, Zürich, Switzerland.



*Characterisation of Ag(I) ion binding oligonucleotide containing artificial imidazole nucleosides*

Silke Johannsen, Dominik Böhme, Jens Müller and Roland K. O. Sigel

ICBIC XIII – International Conference of Biological Inorganic Chemistry, July 15-20, Vienna, Austria.

*Structure conversion of an oligonucleotide containing artificial imidazole nucleosides in the presence of Ag(I) ions*

Silke Johannsen, Dominik Böhme, Jens Müller and Roland K. O. Sigel

Fall Meeting of the Swiss Chemical Society, September 12, 2007, Lausanne, Switzerland.

*Structural interconversion of an oligonucleotide containing artificial nucleobases upon addition of Ag<sup>+</sup>*

Silke Johannsen, Dominik Böhme, Nicole Düpre, Jens Müller and Roland K. O. Sigel

4th EuCheMS Conference on Nitrogen Ligands, August 24-28, Garmisch-Partenkirchen, Germany.

*The influence of pH on the loop-structure of an oligonucleotide containing artificial nucleobases*

Silke Johannsen, Dominik Böhme, Nicole Düpre, Jens Müller and Roland K. O. Sigel

EUROBIC 9 - European Biological Inorganic Chemistry Conference, September 2-6, 2008, Wroclaw, Poland.

*NMR investigation of an oligonucleotide containing metal-mediated base pairs*

Silke Johannsen, Dominik Böhme, Nicole Düpre, Jens Müller and Roland K. O. Sigel

Fall Meeting of the Swiss Chemical Society, September 11, 2008, Zürich, Switzerland.

*NMR characterisation of an oligonucleotide containing metal-mediated base pairs*

Silke Johannsen, Nicole Megger, Dominik Böhme, Jens Müller and Roland K. O. Sigel

ISABC 10 - International Symposium on Applied Bioinorganic Chemistry, September 25-28, 2009, Debrecen, Hungary.